Distribution Agreement

In presenting this thesis or dissertation as a partial fulfillment of the requirements for an advanced degree from Emory University, I hereby grant to Emory University and its agents the non-exclusive license to archive, make accessible, and display my thesis or dissertation in whole or in part in all forms of media, now or hereafter known, including display on the world wide web. I understand that I may select some access restrictions as part of the online submission of this thesis or dissertation. I retain all ownership rights to the copyright of the thesis or dissertation. I also retain the right to use in future works (such as articles or books) all or part of this thesis or dissertation.

Signature:

_____ _____

Chester Jeffery Joyner Date

Immunology and Pathogenesis of Acute and Relapsing Malaria

By
Chester J. Joyner
Doctor of Philosophy

Graduate Division of Biological and Biomedical Sciences
Immunology and Molecular Pathogenesis

Mary R. Galinski, Ph.D, Advisor

Tracey J. Lamb, Ph.D, Committee Member

Frances Eun-Hyung Lee, M.D, Committee Member

Alberto Moreno, M.D, Committee Member

Rabindra Tirouvanziam, Ph.D, Committee Member

Accepted:

Lisa A. Tedesco, Ph.D
Dean of the James T. Laney School of Graduate Studies

Date

Immunology and Pathogenesis of Acute and Relapsing Malaria

By

Chester Jeffery Joyner

B.S., Georgia Southern University, 2011

Advisor: Mary R. Galinski, Ph.D.

An abstract of a dissertation submitted to the Faculty of the James T. Laney School of Graduate Studies of Emory University in partial fulfillment of the requirements for the degree of Doctor of Philosophy in Biological and Biomedical Science

2017

Abstract

Immunology and Pathogenesis of Acute and Relapsing Malaria

By Chester Jeffery Joyner

Malaria is a global public health problem that causes significant mortality and morbidity each year. The two predominate malaria parasites that infect humans are *Plasmodium falciparum* and *Plasmodium vivax*. Over the past 40 years, malaria research has predominately focused on *P. falciparum* since this parasite causes the most malaria-related mortality. Although necessary, this focus has stifled progress on understanding the biology, epidemiology, and pathogenesis of *P. vivax*. These gaps of knowledge are now major obstacles towards malaria eradication.

The studies carried out in this dissertation aimed to improve our understanding of the immunology and pathogenesis of acute and relapsing vivax malaria by capitalizing upon the rhesus macaque – *Plasmodium cynomolgi* model of *P. vivax* infection. An initial study performed a detailed characterization of the development of disease, especially during acute infections and relapses, after infecting a cohort of rhesus macaques with *P. cynomolgi*. The collection of such data for this animal model of malaria was unprecedented and now provides the most comprehensive characterization of pathogenesis to date. Two major results from this initial study were that there was insufficient compensation by the bone marrow for anemia during acute infection and that relapses did not necessarily result in the development of illness.

Insufficient erythropoiesis has been previously reported in individuals infected with *P. vivax*, but the underlying mechanisms that govern this process have been unclear. Here, these mechanisms were explored using bone marrow aspirates collected throughout the rhesus macaque infections. The results of this study led to the conclusion that monocyte-driven inflammation may disrupt transcriptional networks that are critical for erythropoiesis during acute infections, ultimately resulting in insufficient erythropoiesis. Specifically, GATA1 and GATA2, which are two master regulators of erythroid differentiation in the marrow, were suggested to be dysfunctional. Future studies are now warranted to identify the molecules that may antagonize these proteins during acute malaria.

Relapses have been suggested to be responsible for a significant portion of vivax malaria disease burden, and thus, the lack of illness during relapses caused by *P. cynomolgi* was unexpected. A follow-up study was designed to address the question whether other infection scenarios (i.e. homologous reinfections or heterologous infections) could be responsible for more clinical cases of vivax malaria than previously realized. Samples from these infections were also used to characterize the immune responses that were important for conferring clinical protection in each of these infections. This study suggested that heterologous infections may be responsible for a greater portion of clinical vivax malaria in endemic areas than previously recognized and also demonstrated that a memory B-cell response was critical for suppressing parasite growth to prevent the development of illness during relapses and homologous reinfections.

Overall, the studies in this dissertation support use of the rhesus macaque – *P. cynomolgi* infection model of vivax malaria to answer burning questions at the forefront of vivax malaria research. These investigations have advanced the field in understanding clinical aspects of the infections, pathogenesis, and immunity.

Immunology and Pathogenesis of Acute and Relapsing Malaria

By

Chester Jeffery Joyner

B.S., Georgia Southern University, 2011

Advisor: Mary R. Galinski, Ph.D.

A dissertation submitted to the Faculty of the James T. Laney School of Graduate Studies of Emory University in partial fulfillment of the requirements for the degree of Doctor of Philosophy in Biological and Biomedical Science

Acknowledgements

I would like to thank:

- my parents and family members for unconditional love and support throughout this journey; I couldn't have done it without each of you

- my invaluable and supportive friends that have been there when I needed them and have stuck with me even when I was never available due to experiments

- the faculty and staff at Georgia Southern University that ignited and fostered my passion for biomedical research

- Dr. Dana Nayduch for introducing me to and encouraging my love of parasitology, training me as a young scientist, and continuing to support me throughout all of my scientific endeavors

- the faculty and staff at Yerkes National Primate Research Center for their hours of discussions, work, and support whenever carrying out many of the experiments in this dissertation

- the faculty, staff, students, and post-docs at the Malaria Host-Pathogen Interaction Center for constructive scientific discussions

- my labmates that have provided continuous support, stimulating scientific discussion, and assistance to carry out this work

- my dissertation committee for their guidance, support, and advice that has allowed me to develop into the young scientist I am today

- Mary Galinski for being a mentor, friend, and partner for all of my current and future endeavors

Table of Contents

List of Tables and Figures

Chapter I

Introduction to Vivax Malaria: Relapses, Pathogenesis, and Nonhuman Primate Models

Chester J. Joyner

Introduction

Malaria is responsible for significant morbidity, mortality, and socioeconomic hardships in about 100 countries [1]. The causative agents of the disease are parasitic protozoans of the genus *Plasmodium*, and there are five species that infect humans: *Plasmodium falciparum*, *P. vivax*, *P. malariae*, *P. ovale*, and *P. knowlesi*. *Plasmodium falciparum* predominates in sub-Saharan Africa and is responsible for the majority of global malaria mortality each year [1]. Outside of Africa, *Plasmodium vivax* is the most prevalent parasite and causes significant morbidity [2, 3].

Plasmodium sp. have complex life-cycles that involve a vertebrate and invertebrate host. Human malaria parasites are transmitted via the bite of a female Anopheline mosquito. The infectious form of the parasites are known as sporozoites and are deposited into the dermis during a blood meal. Sporozoites then migrate to capillary venules where they traverse the endothelium and enter the circulation. The sporozoites are carried in the bloodstream to the liver where they exit the circulation, invade a host hepatocyte, and undergo replication and development. After multiplying in the liver, the parasites, now known as merozoites, are released back into the blood where they invade red blood cells (RBCs). After invading an RBC, the parasites go through distinct morphological changes that result in the production of new merozoites that lyse the RBC and then re-invade a new RBC. These cyclical rounds of multiplication in the blood are known as the asexual cycle. During the asexual cycle, some parasites undergo gametocytogenesis and develop into gametocytes that are taken up by a mosquito during a blood meal; this step completes the life-cycle.

There is a wealth of knowledge that has been acquired in the past century on malaria. This information, however, is skewed towards *P. falciparum* [4-6]. This is largely due to neglecting *P. vivax* research over the past 20 years due to the misconception that this parasite causes a benign infection [7, 8]. Now, it is widely accepted that *P. vivax* like *P. falciparum* can cause severe disease [3, 9]. Nonetheless, the focus on *P. falciparum* has led to breakthroughs that have had monumental effects on lowering falciparum malaria mortality rates [1]. For example, the increase of malaria

control programs has helped to decrease the number of deaths caused by *P. falciparum* over the past decade [10]. Renewed research on *P. vivax* will undoubtedly lead to similar breakthroughs.

Plasmodium vivax research is now revitalized after years of advocacy and publications highlighting the significant burden this parasite causes [2]. Furthermore, it is now recognized that large gaps of knowledge on *P. vivax* will ultimately make this parasite as difficult, if not more difficult, to eliminate than *P. falciparum* [11]. Two major areas that remain at the forefront of vivax malaria research are understanding the immunology and pathogenesis of *P. vivax* infections, particularly relapses.

***Plasmodium vivax* Relapses**

The first evidence for malaria to recur after treatment can be traced as far back as ancient Rome. However, the first convincing account that *P. vivax* could cause recurrent infections using a different mechanism than persisting in the blood was first assembled in 1902 by Kortweg [12]. Kortweg was a physician in the Netherlands and followed the epidemiology of *P. vivax* in a small village. His studies tracked *P. vivax* cases and provided convincing evidence that the outbreaks of *P. vivax* during the early spring of each year must be due to the acquisition of the parasite 8-9 months earlier since there were not new mosquitoes present that could transmit the infection [13, 14]. Supporting evidence of Kortweg's theory was obtained during the first World War I when soldiers would have recurrent vivax malaria despite treatment with quinine that should cure the infection. These recurrent infections would occur 2-10 months after administration of treatment, which intuitively seemed too long for blood-stage forms to persist. Together, these studies provided a body of evidence that *P. vivax* may persist in a site outside of the blood.

Further characterization of the latency of *P. vivax* was carried-out after the English physician Julius Wagner-Jauregg discovered that malaria could be used to treat the general paralysis and dementia caused by neurosyphilis [15, 16]. This treatment was termed malaria chemotherapy and was widely adopted to treat these patients. Due to these experiments, a wealth

of knowledge was obtained regarding the pathogenesis and infections of human malaria parasites in their natural host. *Plasmodium vivax* was commonly used in malaria chemotherapy, and thus, a wealth of data was collected on "strains" of *P. vivax* that were isolated from patients [17, 18]. Collectively, the malaria chemotherapy studies established that isolates of different geographical origin produced different relapse periodicities, which is defined as the time between a primary infection and a relapse. From the data, it appeared that isolates from temperate areas (e.g. Chesson strain) would cause relapses within 1-2 months whereas other strains from northern climates (e.g. North Korea strain) would consistently not relapse for 4-6 months [17]. Even now, it is still unclear how this difference in latency is advantageous to the parasite or how the process is regulated.

The wealth of information obtained on *P. vivax* from the malaria chemotherapy studies in addition to the discovery that *Plasmodium gallinaceum* has an exo-erythrocytic cycle suggested that primate malarias must also possess a pre-erythrocytic stage. The discovery of a hepatic protozoan known as hepatocystis by Garnham in African monkeys was a key insight [18]. After this discovery, the pre-erythrocytic site for *Plasmodium* development in primates was determined to be the liver [19, 20]. This was first demonstrated using nonhuman primates (NHPs) and then in an inmate infected with *P. vivax* who underwent liver-biopsies during the first 8 or so days after the infection was initiated [21]. This work, however, did not identify a persistent exo-erythrocytic form that could explain the latency phenomenon.

The discovery of a persistent, uninucleate liver-stage form in the livers of monkeys infected with *P. cynomolgi*, a simian malaria parasite that can infect macaques and possesses all of the key biological features of *P. vivax*, was the first identification of a form that could potentially be responsible for the latency phenomenon. These forms were termed hypnozoites and were subsequently demonstrated to be present in a chimpanzee infected with *P. vivax* [20, 22-25]. Thus, it was concluded that these forms must be responsible for *P. vivax* recurrences that occurred months after an initial infection. The term relapse was introduced to distinguish that these infections

occurred due to the activation of hypnozoites that resided in the liver, thus, distinguishing this mechanism from a recrudescence, which is due to the replication of persistent blood-stage forms.

Since these historical studies, there has been minimal progress in understanding the biology of relapses caused by *P. vivax* and the hypnozoites that cause them. Direct studies on the hypnozoite have been inhibited by technological limitations such as the low-infectivity of primary hepatocyte cultures by sporozoites, the difficulty of obtaining consistent sources and amounts of *P. vivax* sporozoites, etc. [26]. However, there have been recent breakthroughs in these areas that are facilitating the investigation of hypnozoites using *P. cynomolgi*, a sister species of *P. vivax*, such as the development of new liver-stage culture systems [27]. Using these cultures, the first transcriptome of hepatocytes containing hypnozoites was recently published [28]. Other breakthroughs are currently in development, and this area of research will likely continue to build as new advancements are made.

In contrast, the understanding of relapse biology is moving at a much slower pace. Progress in this area is largely inhibited by the difficulty of obtaining samples from malaria patients that are "bona fide" relapses [26]. In endemic areas, relapses occur simultaneously with new infections and recrudescences, which make it difficult to distinguish a true relapse from other infection types. A biomarker that identifies relapses, or at least provides some confidence that a sample was taken during a relapse, would be an invaluable tool for the research community.

Even without a biomarker, there are studies that have moved the field's understanding of relapses forward although they are few in number. The area that has received the most attention in relapse biology is understanding the parasite genotypes that compose a relapse versus other infections [29-31]. The goal of this work is to understand the clonality of relapse infections and harness genetic tools to determine if a blood-stage infection is the result of a relapse, new infection, or potentially a recrudescence. Such studies have demonstrated that most relapses in adults are composed of multiple parasite variants based on microsatellite markers [32]. However, it is unclear

if the complexity of parasite genotypes during a relapse translate into a negative impact on patients since the samples used in these studies are almost exclusively from symptomatic individuals.

The pathogenesis of relapse infections remains poorly understood. This gap in knowledge is largely due to the bias towards collecting samples from symptomatic patients and also the inability to know that an infection is a relapse in endemic areas except in unique circumstances like large-scale mass drug administration studies or travelers that become infected and can be followed [33-37]. However, it is widely thought that relapses must be responsible for a large amount of morbidity since previous epidemiological studies have suggested that anywhere from 80-96% of *P. vivax* blood-stage infections are due to relapses at least in areas with high endemicity [35, 36]. Although such conclusions appear logical, they do not take into account the information available from the malaria chemotherapy studies that suggest that not all relapses cause disease [38]. For example, it was noted that relapses after an initial blood-stage infection would be more mild if the blood-stage parasitemia was allowed to persist [38-40]. Overall, it is clear that more research is needed on relapses to understand if these infections result in disease and identify the parasite or host factors that may influence clinical presentation.

To fully understand relapse biology, direct study of these infections in comparison to an initial attack will be critical. Specifically, studies should aim to understand the pathophysiology of relapses and determine how they are similar or different than an initial infection. The host response, particularly the immune response, should be a focused area of research since these studies could help provide guidance to design vaccines to prevent relapses. Indeed, such a vaccine would be invaluable to eliminate *P. vivax* since it would likely reduce transmission back to the mosquito. To carry out these critical studies on relapses, animal models will be required due to the limitations of studies with malaria patients discussed above. Since rodent malaria parasites do not form hypnozoites, other models will be required. Specifically, NHP models have the ability to fill this niche, and in addition to their historical roles in understanding relapses and *P. vivax*, these models

will predictably remain critical for answering outstanding questions related to relapse biology.

Vivax Malaria Pathogenesis

The blood-stage of the *Plasmodium* life-cycle is responsible for clinical illness. Similar to falciparum malaria, vivax malaria disease severity ranges from asymptomatic to severe [3]. In fact, most *P. vivax* infections, like *P. falciparum*, are asymptomatic with minimal symptomology. Common symptoms of mild malaria include low-grade fever, malaise, rigor, headache, emesis, etc. that typically resolve without the need for treatment. However, some infections progress to severe disease that can develop into life-threatening syndromes [3, 4, 7, 41]. The specific host, parasite, and infection characteristics that influence the progression to severe disease are poorly understood.

Vivax malaria pathogenesis research has been largely neglected due to the misconception that this parasite causes a benign disease [8, 42-45]. Careful review of the data from individuals that underwent malaria chemotherapy, however, provides clear evidence of the ability of this parasite to cause severe illness. In fact, mortality rates of up to 10% could be seen with the Madagascar strain of *P. vivax* during treatment [4]. It can be argued that the malaria chemotherapy studies were not the norm, and given the pre-existing syphilis infection, severe illness and mortality could have been due to the coinfection. However, other more recent studies also demonstrate that *P. vivax* can result in death even without pre-existing infections and/or comorbidities [46].

Severe malaria caused by *Plasmodium vivax* is characterized by many of the same clinical signs and symptoms as *P. falciparum*. The most common complication due to *P. vivax* is the development of anemia [41]. Anemia characterizes most of the severe vivax malaria cases and is a notable aspect of disease burden in Brazil and Papua New Guinea [47].The definition of severe malarial anemia caused by *P. vivax* is a hemoglobin value < 5 g/dl or hematocrit < 15% in children less than 12 years of age and a hemoglobin value < 7 g/dl or hematocrit < 20% in adults [48]. Severe anemia caused by *P. vivax* is typically limited to children in endemic areas who have not developed substantial immunity, but adults that are chronically infected can also develop anemia at in high transmission settings like PNG [41].

The underlying mechanisms that contribute to the development and maintenance of anemia caused by *P. vivax* require further study. However, it is clear that both disruption of normal bone marrow function and removal of uninfected RBCs play a role [41]. It is clear from autopsy studies on patients that died of vivax malaria that the bone marrow is affected, and dyserythropoiesis commonly reported [49-51]. Furthermore, individuals that are anemic during acute vivax malaria do not replenish RBCs that are lost despite normal physiological responses to compensate for the anemia such as increased erythropoietin levels [52]. Thus, it is likely that *P. vivax* infection has a potent effect on erythropoiesis. It is clear from studies with *P. falciparum* and rodent malaria models that inflammation in the marrow has adverse consequences on erythropoiesis [53-58]. Recently, studies suggested that *P. vivax* may also alter or disrupt compensatory erythropoiesis by invading young reticulocytes in the bone marrow and destroying them before they can be released into the circulation to compensate for the loss of RBCs [59, 60]. More research is needed, however, to evaluate if such events happen *in vivo*.

The removal of uninfected RBCs by the host, known as the bystander effect is the second major process involved in the development of anemia caused by *P. vivax*. Modelling hematological data collected from *P. vivax* malaria chemotherapy patients has suggested that as many as 35 uninfected RBCs are removed for every single infected RBC [61]. This number is about 3-4 fold higher than the estimates for *P. falciparum*, suggesting that whatever processes are involved are more potently induced by *P. vivax* than *P. falciparum* [62, 63]. There are a variety of mechanisms that have been described that may lead to the removal of the uninfected RBCs; these include 'anti-self' antibodies, complement, and phagocytosis by splenic macrophages [64-66]. However, direct *in vivo* evidence is still needed to validate these mechanisms, which are largely based on working with serum samples and *in vitro* experiments.

Thrombocytopenia, or low platelet counts, is another common complication of *P. vivax* infection, but its distinct etiologies are unknown [67-70]. Multiple processes including the phagocytosis of platelets [71], binding of platelets to parasites [72], and perhaps even production

of platelets by the megakaryocytes in the bone marrow may be altered [50, 73]. It is unclear if this condition is potentially lethal or just a proxy for severe malarial anemia since both of these complications typically occur hand-in-hand. Evidence from field studies suggest that thrombocytopenia is only a useful metric for predicting mortality when combined with the presence of severe anemia [74]. Therefore, these two processes may be interrelated. Since the bone marrow environment is also where megakaryocytes reside, and these cells are dysplastic in vivax malaria autopsy patients, it would not be surprising that thrombocytopenia and anemia are intricately linked [50, 51, 75, 76]. More research is needed to understand the role, if any, of thrombocytopenia in vivax malaria pathogenesis.

Some of the most deadly manifestations of vivax malaria include metabolic acidosis followed by respiratory distress and acute kidney injury that leads to renal failure [3, 44, 77, 78]. Acute kidney injury has been observed post-mortem and attributed to a large number of severe vivax malaria cases, particularly in India [79]. Respiratory complications are also prevalent in vivax malaria patients, and autopsy studies provide evidence that there is edema consistent with lung pathology [80]. Parasite byproducts such as hemozoin, the byproduct the parasite produces as it consumes hemoglobin within an RBC, and infected RBCs have been observed in the lung and kidney [79, 81, 82]. Additional studies, however, are needed to confirm if parasite burden in the tissues actually correlates with pathology since most patients who have succumbed and are assessed in autopsy studies have received anti-malarial treatment prior to their passing. Notably, renal impairment and lung complications appear to be more influenced by geographic location than anemia. This suggests that other factors are involved in these presentations, and whether such factors are due to the host, parasite, comorbidities, etc. remains unknown.

Although the pathophysiology of vivax malaria is more understood now than ever, there is still much to learn about the mechanisms that govern the development of anemia, kidney injury, lung pathology, etc. Furthermore, the pathogenesis of relapses in contrast to initial infections remains an area that is poorly explored. Indeed, 80-96% of *P. vivax* blood-stage infections in PNG

and Southeastern Asia are thought to be due to relapses based on modelling of epidemiological data [6, 11, 35, 36]. A logical conclusion from such information would be that relapses are then responsible for significant disease. However, this is an assumption that requires empirical testing.

In fact, data from malaria chemotherapy studies suggest that not all relapses cause disease. In fact, Boyd and Kitchen reported that relapses had significantly reduced parasitemia and were afebrile if the initial infection was allowed to persist for 48 days [83-86]. Additionally, challenges with the same strain of *P. vivax* did not result in a clinical episode [85, 86]. Collectively, these experiments suggest that non-sterilizing immunity can be obtained after a single-infection, and that this immunity is capable of ameliorating disease. Such data complicates current dogma that relapses cause disease and suggests that other factors may influence relapse pathogenesis. These factors and the host responses need to be further explored to appropriately assess the contribution of relapses to disease burden.

Unlike the days of malaria chemotherapy where 'humans were the experimental animals due to the lack of ethical restrictions, we are currently unable to perform experiments directly testing the ability of relapses to cause disease and/or explore mechanisms of vivax malaria pathophysiology in humans. However, NHP models of malaria can be used to explore and empirically test questions related to malaria relapses with respect to pathophysiology and immunity.

NHP Malaria Model Systems

Non-human primate model systems have been instrumental in malaria research for decades whether for furthering basic understanding of *Plasmodium* biology, malaria pathogenesis, or preclinical investigations pertinent to developing new interventions [17, 87, 88]. Recently, NHPs were critical for the development of an *in vitro*, primary hepatocyte culture system that supported the cultivation of *P. cynomolgi* liver-stage forms (LSFs) for approximately 40 days and provided the first tangible evidence that hypnozoites existed and were capable of activating and multiplying to generate merozoites [27, 89].

Various NHP-simian and human malaria parasite combinations can be used to study *Plasmodium* biology. Many strains of the parasites that infect NHPs are available and can be used to address scientific questions relating to relapses and pathogenesis. Different strains of *P. cynomolgi* and *P. vivax* that possess distinctive relapse patterns can be utilized to study the consequences of frequent versus infrequent relapses on the host immune system. A suitable mouse model is not currently available to study such phenomena. Indeed, humanized mice containing human hepatocytes have been demonstrated to support *P. falciparum* liver-stage growth [90-92]. These models also appear to have some utility for *P. vivax* because they appear to support the development of hypnozoites [92]. However, these mice lack intact immune systems and, thus, are deficient when addressing immunobiological questions, whether for *P. falciparum* or other primate malaria species [91].

Vivax malaria - NHP models

While NHP models have been used occasionally to supplement fundamental *P. falciparum* research findings from culture systems and for pre-clinical studies, *P. vivax* research over the last few decades would have been virtually impossible without NHP models; *i.e.*, small New World *Aotus* and *Saimiri* monkeys [87]. Unlike *P. falciparum*, a long-term *in vitro* culture system for *P. vivax* does not currently exist due to the need for a regular supply of reticulocytes or other unknown factors [93]. In the meantime, NHP models have been critical for generating *P. vivax* material for in-depth analyses and NHP experimental studies continue to complement and expand upon blood-stage analyses that are now possible with small clinical samples attained from human infections [94, 95].

To investigate relapses, *Aotus* or *Saimiri* species can be infected with NHP-adapted *P. vivax* strains via mosquito inoculation or syringe injection of sporozoites into a blood vessel [87, 96]. Similar to human infections, relapsing, recrudescing or chronic infection profiles can be observed in these models provided the animals are splenectomized to interfere with an overly robust

removal of infected erythrocytes. Blood-stage parasitemias, which begin to develop within 8-10 days, can be curatively treated without destroying the hypnozoites. PCR testing can confirm the absence of blood-stage parasites, and thus, any subsequent blood-stage infections can be confirmed as relapses and not recrudescences. This experimental strategy is currently the only reliable means to study vivax relapses, with the caveats that these animals are small (typically about 1 kilogram), parasitemia is typically low or moderate (1-2%), and only small blood volumes can be taken (6 milliliters/kilogram/month). One strain in particular was developed at the Centers for Disease Control and Prevention (CDC) for studying relapses, called the Brazil VII strain, as it shows multiple relapse patterns over a period of several months similar to that observed previously in humans with "tropical strains" (unpublished data).

Simian parasite - NHP models for vivax malaria

Simian malaria parasite-NHP models are powerful systems to investigate relapses compared to the small New World NHPs. Simian malaria parasites productively infect Old World monkeys, including rhesus macaques (*Macaca mulatta*) and long-tailed macaques (*Macaca fascicularis*), which possess similar genetic composition and physiology to humans [97-99] The macaques are much larger than New World monkeys, which allows for greater blood or bone marrow draws (10 milliliters/kilogram/month with most animals weighing between 6-10 kilograms; or 6 milliliters/kilogram/month if they are anemic.) for isolation of parasite material and host cells for immunity studies. Additionally, more biologically suitable reagents exist for experimentation with these NHP species.

Plasmodium cynomolgi is a "sister species" of *P. vivax.* These closely related parasites share similar biology such as the formation of hypnozoites in the liver and caveloae vesicle complexes in the infected erythrocytes [100, 101]. Tens of millions of *P. cynomolgi* sporozoites can be generated in a specified, experimental time-frame compared to *P. vivax* sporozoites which are more difficult to generate ([102]; unpublished data). They can then be used to experimentally

to infect macaques and lead to productive blood-stage parasitemias [103] The same experimental approach to study relapses (see above) can then be employed to ensure that true relapses are studied. Two other simian malaria species that could be useful for studying hypnozoites or relapse mechanisms are *P. fieldi* and, especially, *P. simiovale* [104-106].

As with *P. vivax*, many *P. cynomolgi* isolates exist that have their own infection and relapse characteristics. The number and frequency of relapses in rhesus infected with different strains of *P. cynomolgi* can be predicted with greater accuracy than typically possible with New World monkey-adapted *P. vivax* isolates although *P. vivax* Brazil VII has so far been uniquely dependable in this regard (unpublished data). In rhesus, variables such as the sporozoite inoculum can be altered to produce consistent infection patterns even though inter-individual variability between animals as well as inherent properties of the strain being used in the study can influence infection kinetics [107].

Plasmodium cynomolgi can be genetically manipulated more easily than *P. vivax*, though *P. vivax* transfection has been accomplished through a collaboration between the CDC and Yerkes, with transient transfection of trophozoites demonstrated in *Saimiri boliviensis* [108]. In recent years, these investigators also developed *P. cynomolgi* parasites with integrated transgenes, including a *red fluorescent protein* (*rfp*) gene [100]. Transient mCherry and green fluorescent protein-expressing *P. cynomolgi* parasites have also been reported and used to purify *P. cynomolgi* LSFs from NHP primary hepatocyte cultures using fluorescence-activated cell sorting [109]. Technical hurdles such as achieving better yields of purified parasites for downstream experiments still remain. Nonetheless, these are monumental breakthroughs given the challenges working with these parasites.

Summary

Combining NHP models of malaria with modern day biological approaches has the potential to make rapid progress towards understanding the immunology and pathogenesis of acute

and relapsing malaria caused by *P. vivax*. Such investigations are in dire need to understand *P. vivax* epidemiology, pathogenesis, and immunity in an era where malaria eradication is a priority. Specifically, the *P. cynomolgi* – rhesus macaque model of vivax malaria is ideally suited for such endeavors. The studies carried out in this dissertation utilized this NHP – simian malaria parasite model to study the immunology and pathogenesis of acute and relapsing malaria caused by *P. vivax*.

References

1. Organization WH: *World Malaria Report 2016.*2016.
2. Howes RE, Battle KE, Mendis KN, Smith DL, Cibulskis RE, Baird JK, et al. Global Epidemiology of *Plasmodium vivax*. Am J Trop Med Hyg 2016.
3. Anstey NM, Douglas NM, Poespoprodjo JR, Price RN. *Plasmodium vivax*: clinical spectrum, risk factors and pathogenesis. Adv Parasitol 2012; 80:151-201.
4. Baird JK. Evidence and implications of mortality associated with acute *Plasmodium vivax* malaria. Clin Microbiol Rev 2013; 26:36-57.
5. Galinski MR, Barnwell JW. Plasmodium vivax: who cares? Malar J 2008; 7 Suppl 1:S9.
6. Mueller I, Galinski MR, Baird JK, Carlton JM, Kochar DK, Alonso PL, et al. Key gaps in the knowledge of *Plasmodium vivax*, a neglected human malaria parasite. Lancet Infect Dis 2009; 9:555-566.
7. Price RN, Tjitra E, Guerra CA, Yeung S, White NJ, Anstey NM. Vivax malaria: neglected and not benign. Am J Trop Med Hyg 2007; 77:79-87.
8. Baird JK. Pernicious and Threatening *Plasmodium vivax* as Reality. Am J Trop Med Hyg 2014.
9. Lacerda MV, Mourão MP, Alexandre MA, Siqueira AM, Magalhães BM, Martinez-Espinosa FE, et al. Understanding the clinical spectrum of complicated *Plasmodium vivax* malaria: a systematic review on the contributions of the Brazilian literature. Malaria Journal 2012; 11:1-18.
10. Daily JP. Malaria 2017: Update on the Clinical Literature and Management. Curr Infect Dis Rep 2017; 19:28.
11. Bassat Q, Velarde M, Mueller I, Lin J, Leslie T, Wongsrichanalai C, et al. Key Knowledge Gaps for *Plasmodium vivax* Control and Elimination. Am J Trop Med Hyg 2016; 95:62-71.
12. White NJ, Imwong M. Relapse. Adv Parasitol 2012; 80:113-150.
13. Swellengrebel N, De Buck A, Schoute E, Kraan M. Investigations on the Transmission of Malaria in some Villages north of Amsterdam. Quarterly Bulletin of the Health Organisation League of Nations 1936; 5.
14. Winckel CW. Long latency in *Plasmodium vivax* infections in a temperate zone. Doc Med Geogr Trop 1955; 7:292-298.
15. Tsay CJ. Julius Wagner-Jauregg and the legacy of malarial therapy for the treatment of general paresis of the insane. Yale J Biol Med 2013; 86:245-254.
16. White NJ. Determinants of relapse periodicity in *Plasmodium vivax* malaria. Malaria Journal 2011; 10:297.
17. Coatney GR, Collins, W.E., Warren M., Contacos, P.G.: *Primate Malarias.* Washington DC: U. S. Dept. of Health, Education and Welfare; 1971.
18. Garnham PC. Exoerthrocytic schizogony in *Plasmodium kochi* Laveran; a preliminary note. Trans R Soc Trop Med Hyg 1947; 40:719-722.
19. Shortt HE, Garnham PC. Pre-erythrocytic stage in mammalian malaria parasites. Nature 1948; 161:126.
20. Shortt HE, Garnham PCC. Demonstration of a persisting exo-erythrocytic cycle in *Plasmodium cynomolgi* and its bearing on the production of relapses. Brit Med J 1948; 1.
21. Shortt HE, Garnham PCC, Covell G, Shute PG. The pre-erythrocytic stage of human malaria, *Plasmodium vivax*. Brit Med J 1948; 1.
22. Shortt HE, Garnham PCC. The pre-erythrocytic development of *Plasmodium cynomolgi* and Plasmodium vivax. Trans R Soc Trop Med Hyg 1948; 41.
23. Krotoski WA. Discovery of the hypnozoite and a new theory of malarial relapse. Trans R Soc Trop Med Hyg 1985; 79:1-11.

24. Krotoski WA, Collins WE, Bray RS, Garnham PC, Cogswell FB, Gwadz RW, et al. Demonstration of hypnozoites in sporozoite-transmitted *Plasmodium vivax* infection. Am J Trop Med Hyg 1982; 31:1291-1293.
25. Krotoski WA, Garnham PC, Bray RS, Krotoski DM, Killick-Kendrick R, Draper CC, et al. Observations on early and late post-sporozoite tissue stages in primate malaria. I. Discovery of a new latent form of *Plasmodium cynomolgi* (the hypnozoite), and failure to detect hepatic forms within the first 24 hours after infection. Am J Trop Med Hyg 1982; 31:24-35.
26. Joyner CJ, Barnwell JW, Galinski MR. No More Monkeying Around: Primate Malaria Model Systems are Key to Understanding *Plasmodium vivax* Liver-Stage Biology, Hypnozoites, and Relapses. Frontiers in Microbiology 2015; 6.
27. Dembele L, Franetich JF, Lorthiois A, Gego A, Zeeman AM, Kocken CH, et al. Persistence and activation of malaria hypnozoites in long-term primary hepatocyte cultures. Nat Med 2014; 20:307-312.
28. Cubi R, Vembar SS, Biton A, Franetich JF, Bordessoulles M, Sossau D, et al. Laser capture microdissection enables transcriptomic analysis of dividing and quiescent liver stages of *Plasmodium* relapsing species. Cellular Microbiology 2017; 19:e12735.
29. Imwong M, Boel ME, Pagornrat W, Pimanpanarak M, McGready R, Day NP, et al. The first *Plasmodium vivax* relapses of life are usually genetically homologous. J Infect Dis 2012; 205:680-683.
30. de Souza AM, de Araujo FC, Fontes CJ, Carvalho LH, de Brito CF, de Sousa TN. Multiple-clone infections of *Plasmodium vivax*: definition of a panel of markers for molecular epidemiology. Malar J 2015; 14:330.
31. Imwong M, Snounou G, Pukrittayakamee S, Tanomsing N, Kim JR, Nandy A, et al. Relapses of *Plasmodium vivax* infection usually result from activation of heterologous hypnozoites. J Infect Dis 2007; 195:927-933.
32. Imwong M, Snounou G, Pukrittayakamee S, Tanomsing N, Kim JR, Nandy A, et al. Relapses of *Plasmodium vivax* infection usually result from activation of heterologous hypnozoites. J Infect Dis 2007; 195.
33. Bright AT, Manary MJ, Tewhey R, Arango EM, Wang T, Schork NJ, et al. A High Resolution Case Study of a Patient with Recurrent Plasmodium vivax Infections Shows That Relapses Were Caused by Meiotic Siblings. PLoS Negl Trop Dis 2014; 8:e2882.
34. Robinson LJ, Wampfler R, Betuela I, Karl S, White MT, Li Wai Suen CS, et al. Strategies for understanding and reducing the *Plasmodium vivax* and *Plasmodium ovale* hypnozoite reservoir in Papua New Guinean children: a randomised placebo-controlled trial and mathematical model. PLoS Med 2015; 12:e1001891.
35. White MT, Karl S, Battle KE, Hay SI, Mueller I, Ghani AC. Modelling the contribution of the hypnozoite reservoir to *Plasmodium vivax* transmission. Elife 2014; 3.
36. Adekunle AI, Pinkevych M, McGready R, Luxemburger C, White LJ, Nosten F, et al. Modeling the Dynamics of *Plasmodium vivax* Infection and Hypnozoite Reactivation *In Vivo*. PLoS Negl Trop Dis 2015; 9:e0003595.
37. Maneerattanasak S, Gosi P, Krudsood S, Chimma P, Tongshoob J, Mahakunkijcharoen Y, et al. Molecular and immunological analyses of confirmed *Plasmodium vivax* relapse episodes. Malaria Journal 2017; 16:228.
38. Boyd MF. A review of studies on immunity to vivax malaria. J Natl Malar Soc 1947; 6.
39. Boyd MF. On strains or races of the malaria parasites. Am J Trop Med 1940; 20.
40. Boyd MF, Matthews CB. Further observations on the duration of immunity to the homologous strain of *Plasmodium vivax*. Am J Trop Med Hyg 1939; 19.
41. Douglas NM, Anstey NM, Buffet PA, Poespoprodjo JR, Yeo TW, White NJ, et al. The anaemia of *Plasmodium vivax* malaria. Malaria Journal 2012; 11:1-14.

42. Kevin Baird J. Malaria caused by *Plasmodium vivax*: recurrent, difficult to treat, disabling, and threatening to life--the infectious bite preempts these hazards. Pathog Glob Health 2013; 107:475-479.
43. Mueller I, Galinski MR, Baird JK, Carlton JM, Kochar DK, Alonso PL, et al. Key gaps in the knowledge of *Plasmodium vivax*, a neglected human malaria parasite. Lancet Infect Dis 2009; 9.
44. Baird JK. Severe and fatal vivax malaria challenges 'benign tertian malaria' dogma. Ann Trop Paediatr 2009; 29.
45. Baird JK. Neglect of *Plasmodium vivax* malaria. Trends Parasitol 2007; 23.
46. Lacerda MV, Fragoso SC, Alecrim MG, Alexandre MA, Magalhaes BM, Siqueira AM, et al. Postmortem characterization of patients with clinical diagnosis of *Plasmodium vivax* malaria: to what extent does this parasite kill? Clin Infect Dis 2012; 55:e67-74.
47. Douglas NM, Anstey NM, Buffet PA, Poespoprodjo JR, Yeo TW, White NJ, et al. The anaemia of *Plasmodium vivax* malaria. Malar J 2012; 11:135.
48. Organization WH: *Management of severe malaria - A practical handbook.* Third edn. World Health Organization: World Health Organization; 2013.
49. Baro B, Deroost K, Raiol T, Brito M, Almeida ACG, de Menezes-Neto A, et al. *Plasmodium vivax* gametocytes in the bone marrow of an acute malaria patient and changes in the erythroid miRNA profile. PLOS Neglected Tropical Diseases 2017; 11:e0005365.
50. Abdalla SH. Hematopoiesis in human malaria. Blood Cells 1990; 16:401-416; discussion 417-409.
51. Wickramasinghe SN, Looareesuwan S, Nagachinta B, White NJ. Dyserythropoiesis and ineffective erythropoiesis in *Plasmodium vivax* malaria. Br J Haematol 1989; 72:91-99.
52. Price RN, Douglas NM, Anstey NM. New developments in *Plasmodium vivax* malaria: severe disease and the rise of chloroquine resistance. Curr Opin Infect Dis 2009; 22.
53. Thuma PE, van Dijk J, Bucala R, Debebe Z, Nekhai S, Kuddo T, et al. Distinct clinical and immunologic profiles in severe malarial anemia and cerebral malaria in Zambia. J Infect Dis 2011; 203.
54. Perkins DJ, Were T, Davenport GC, Kempaiah P, Hittner JB, Ong'echa JM. Severe malarial anemia: innate immunity and pathogenesis. Int J Biol Sci 2011; 7:1427-1442.
55. Thawani N, Tam M, Stevenson MM. STAT6-mediated suppression of erythropoiesis in an experimental model of malarial anemia. Haematologica 2009; 94:195-204.
56. Lamikanra AA, Brown D, Potocnik A, Casals-Pascual C, Langhorne J, Roberts DJ. Malarial anemia: of mice and men. Blood 2007; 110.
57. Casals-Pascual C, Kai O, Cheung JO, Williams S, Lowe B, Nyanoti M, et al. Suppression of erythropoiesis in malarial anemia is associated with hemozoin in vitro and in vivo. Blood 2006; 108:2569-2577.
58. Chang KH, Stevenson MM. Malarial anaemia: mechanisms and implications of insufficient erythropoiesis during blood-stage malaria. Int J Parasitol 2004; 34:1501-1516.
59. Malleret B, Li A, Zhang R, Tan KSW, Suwanarusk R, Claser C, et al. *Plasmodium vivax*: restricted tropism and rapid remodeling of CD71-positive reticulocytes. Blood 2015; 125:1314-1324.
60. Ru YX, Mao BY, Zhang FK, Pang TX, Zhao SX, Liu JH, et al. Invasion of erythroblasts by *Pasmodium vivax*: a new mechanism contributing to malarial anemia. Ultrastruct Pathol 2009; 33.
61. Collins WE, Jeffery GM, Roberts JM. A retrospective examination of reinfection of humans with *Plasmodium vivax*. Am J Trop Med Hyg 2004; 70.

62. Jakeman GN, Saul A, Hogarth WL, Collins WE. Anaemia of acute malaria infections in non-immune patients primarily results from destruction of uninfected erythrocytes. Parasitology 1999; 119.
63. Price RN, Simpson JA, Nosten F, Luxemburger C, Hkirjaroen L, ter Kuile F, et al. Factors contributing to anemia after uncomplicated falciparum malaria. Am J Trop Med Hyg 2001; 65:614-622.
64. Fernandez-Arias C, Rivera-Correa J, Gallego-Delgado J, Rudlaff R, Fernandez C, Roussel C, et al. Anti-Self Phosphatidylserine Antibodies Recognize Uninfected Erythrocytes Promoting Malarial Anemia. Cell Host Microbe 2016; 19:194-203.
65. Sherman IW, Prudhomme J. Phosphatidylserine expression on the surface of malaria-parasitized erythrocytes. Parasitol Today 1996; 12:122; author reply 122.
66. Biryukov S, Stoute JA. Complement activation in malaria: friend or foe? Trends Mol Med 2014.
67. Gupta NK, Bansal SB, Jain UC, Sahare K. Study of thrombocytopenia in patients of malaria. Trop Parasitol 2013; 3:58-61.
68. Kochar DK, Das A, Kochar A, Middha S, Acharya J, Tanwar GS, et al. Thrombocytopenia in *Plasmodium falciparum, Plasmodium vivax* and mixed infection malaria: A study from Bikaner (Northwestern India). Platelets 2010; 21.
69. Lacerda MV, Mourao MP, Coelho HC, Santos JB. Thrombocytopenia in malaria: who cares? Mem Inst Oswaldo Cruz 2011; 106.
70. Lacerda MVG: Clinical manifestations and pathogenesis of malarial thrombocytopenia. In *PhD Thesis.* Tropical Medicine Department: University of Brasília; 2007
71. Coelho HC, Lopes SC, Pimentel JP, Nogueira PA, Costa FT, Siqueira AM, et al. Thrombocytopenia in *Plasmodium vivax* Malaria Is Related to Platelets Phagocytosis. PLoS One 2013; 8:e63410.
72. Kelton JG, Keystone J, Moore J, Denomme G, Tozman E, Glynn M, et al. Immune-mediated thrombocytopenia of malaria. J Clin Invest 1983; 71:832-836.
73. Wickramasinghe SN, Abdalla SH. Blood and bone marrow changes in malaria. Baillieres Best Pract Res Clin Haematol 2000; 13:277-299.
74. Hanson J, Phu NH, Hasan MU, Charunwatthana P, Plewes K, Maude RJ, et al. The clinical implications of thrombocytopenia in adults with severe falciparum malaria: a retrospective analysis. BMC Med 2015; 13:97.
75. Wickramasinghe SN, Abdalla SH. Blood and bone marrow changes in malaria. Baillieres Best Pract Res Clin Haematol 2000; 13.
76. Knuttgen HJ. THE BONE-MARROW OF NON-IMMUNE EUROPEANS IN ACUTE MALARIA INFECTION - A TOPICAL REVIEW. Annals of Tropical Medicine and Parasitology 1987; 81:567-576.
77. Alexandre MA, Ferreira CO, Siqueira AM, Magalhaes BL, Mourao MPG, Lacerda MVG, et al. Severe *Plasmodium vivax* Malaria, Brazilian Amazon. Emerg Infect Dis 2010; 16.
78. Andrade BB, Reis-Filho A, Souza-Neto SM, Clarencio J, Camargo LM, Barral A, et al. Severe *Plasmodium vivax* malaria exhibits marked inflammatory imbalance. Malar J 2010; 9.
79. Das BS. Renal failure in malaria. J Vector Borne Dis 2008; 45:83-97.
80. Anstey NM, Handojo T, Pain MCF, Kenangalem E, Tjitra E, Price RN, et al. Lung injury in vivax malaria: pathophysiological evidence for pulmonary vascular sequestration and posttreatment alveolar-capillary inflammation. J Infect Dis 2007; 195.
81. Tan LK, Yacoub S, Scott S, Bhagani S, Jacobs M. Acute lung injury and other serious complications of *Plasmodium vivax* malaria. Lancet Infect Dis 2008; 8.

82. Anstey NM, Handojo T, Pain MC, Kenangalem E, Tjitra E, Price RN, et al. Lung injury in vivax malaria: pathophysiological evidence for pulmonary vascular sequestration and posttreatment alveolar-capillary inflammation. J Infect Dis 2007; 195.
83. Boyd MF, Kitchen SF. Renewed clinical activity in naturally induced vivax malaria. Am J Trop Med 1944; s1-24.
84. Boyd MF, Matthews CB. Further observations on the duration of immunity to the homologous strain of *Plasmodium vivax*. Am J Trop Med 1939; s1-19.
85. Boyd MF, Kitchen SF. On the efficiency of the homologous properties of acquired immunity to *Plasmodium vivax*. Am J Trop Med 1936; s1-16.
86. Boyd MF, Stratman-Thomas WK, Kitchen SF. On the duration of acquired homologous immunity to *Plasmodium vivax*. Am J Trop Med 1936; s1-16.
87. Galinski MR, Barnwell JW: Non-human Primate Models for Human Malaria Research. In *Nonhuman Primates in Biomedical Research: Diseases.* Elsevier, Inc.; 2012: 299-323
88. Beignon AS, Le Grand R, Chapon C. In vivo imaging in NHP models of malaria: Challenges, progress and outlooks. Parasitol Int 2013.
89. Barnwell JW, Galinski MR. Malarial liver parasites awaken in culture. Nat Med 2014; 20:237-239.
90. Vaughan AM, Mikolajczak SA, Wilson EM, Grompe M, Kaushansky A, Camargo N, et al. Complete *Plasmodium falciparum* liver-stage development in liver-chimeric mice. J Clin Invest 2012; 122:3618-3628.
91. Kaushansky A, Mikolajczak SA, Vignali M, Kappe SH. Of men in mice: the success and promise of humanized mouse models for human malaria parasite infections. Cell Microbiol 2014.
92. Mikolajczak SA, Vaughan AM, Kangwanrangsan N, Roobsoong W, Fishbaugher M, Yimamnuaychok N, et al. *Plasmodium vivax* liver stage development and hypnozoite persistence in human liver-chimeric mice. Cell Host Microbe 2015; 17:526-535.
93. Noulin F, Borlon C, Van Den Abbeele J, D'Alessandro U, Erhart A. 1912-2012: a century of research on *Plasmodium vivax* in vitro culture. Trends Parasitol 2013.
94. Mary RG, Rabindra MT, Alberto M: *Plasmodium vivax* vaccine surrogate markers of protection: dawning of a new era. In *Malaria Vaccine Development: Over 40 Years of Trials and Tribulations.* Future Medicine Ltd; 2014: 28-47
95. Russell B, Suwanarusk R, Malleret B, Costa FT, Snounou G, Kevin Baird J, et al. Human ex vivo studies on asexual *Plasmodium vivax*: the best way forward. Int J Parasitol 2012; 42:1063-1070.
96. Galinski MR, Meyer EV, Barnwell JW. *Plasmodium vivax*: Modern Strategies to Study a Persistent Parasite's Life Cycle. Adv Parasitol 2013; 81:1-26.
97. Gardner MB, Luciw PA. Macaque models of human infectious disease. Ilar j 2008; 49:220-255.
98. Messaoudi I, Estep R, Robinson B, Wong SW. Nonhuman primate models of human immunology. Antioxid Redox Signal 2011; 14:261-273.
99. Zimin AV, Cornish AS, Maudhoo MD, Gibbs RM, Zhang X, Pandey S, et al. A new rhesus macaque assembly and annotation for next-generation sequencing analyses. Biology Direct In Press.
100. Akinyi S, Hanssen E, Meyer EV, Jiang J, Korir CC, Singh B, et al. A 95 kDa protein of *Plasmodium vivax* and *P. cynomolgi* visualized by three-dimensional tomography in the caveola-vesicle complexes (Schuffner's dots) of infected erythrocytes is a member of the PHIST family. Mol Microbiol 2012; 84:816-831.
101. Tachibana S, Sullivan SA, Kawai S, Nakamura S, Kim HR, Goto N, et al. *Plasmodium cynomolgi* genome sequences provide insight into *Plasmodium vivax* and the monkey malaria clade. Nat Genet 2012; 44:1051-1055.

102. Rosenberg R, Rungsiwongse J. The number of sporozoites produced by individual malaria oocysts. Am J Trop Med Hyg 1991; 45:574-577.
103. Collins WE, Warren M, Galland GG. Studies on infections with the Berok strain of *Plasmodium cynomolgi* in monkeys and mosquitoes. J Parasitol 1999; 85:268-272.
104. Cogswell FB, Collins WE, Krotoski WA, Lowrie RC. Hypnozoites of *Plasmodium simiovale*. The American Journal of Tropical Medicine and Hygiene 1991; 45:211-213.
105. Collins WE, Contacos PG. Observations on the relapse activity of *Plasmodium simiovale* in the rhesus monkey. J Parasitol 1974; 60:343.
106. Held JR, Contacos PG, Coatney GR. Studies of the exoerythrocytic stages of simian malaria. I. *Plasmodium fieldi*. J Parasitol 1967; 53:225-232.
107. Schmidt LH. Compatibility of relapse patterns of *Plasmodium cynomolgi* infections in rhesus monkeys with continuous cyclical development and hypnozoite concepts of relapse. Am J Trop Med Hyg 1986; 35:1077-1099.
108. Pfahler JM, Galinski MR, Barnwell JW, Lanzer M. Transient transfection of *Plasmodium vivax* blood stage parasites. Mol Biochem Parasitol 2006; 149:99-101.
109. Voorberg-van der Wel A, Zeeman A-M, van Amsterdam SM, van den Berg A, Klooster EJ, Iwanaga S, et al. Transgenic Fluorescent *Plasmodium cynomolgi* Liver Stages Enable Live Imaging and Purification of Malaria Hypnozoite-Forms. PLoS ONE 2013; 8:e54888.

Chapter II

Plasmodium cynomolgi infections in rhesus macaques display clinical and parasitological features pertinent to modeling vivax malaria pathology and relapse infections

Chester J. Joyner[1,5], Alberto Moreno[1,3,5], Esmeralda V.S. Meyer[1,5], Monica Cabrera-Mora[1,5], the MaHPIC Consortium[5], Jessica C. Kissinger[4,5] John W. Barnwell[1,2,5], and Mary R. Galinski[1,3,5*]

ASSOCIATIONS/AFFILIATIONS

[1]International Center for Malaria Research, Education and Development, Emory Vaccine Center, Yerkes National Primate Research Center, Emory University, Atlanta, GA, USA

[2]Malaria Branch, Division of Parasitic Diseases and Malaria, Centers for Disease Control and Prevention, Atlanta, GA, USA

[3]Division of Infectious Diseases, Department of Medicine, Emory University, Atlanta, GA, USA

[4]Department of Genetics, Institute of Bioinformatics, Center for Tropical and Emerging Global Diseases, University of Georgia, Athens, GA, USA

[5]Malaria Host–Pathogen Interaction Center; http://systemsbiology.emory.edu

Published in *Malaria Journal*, 2016, 15:451.

Abstract

Background: *Plasmodium vivax* infections in humans or in New World monkeys pose research challenges that necessitate the use of alternative model systems. *Plasmodium cynomolg*i is a closely related species that shares genetic and biological characteristics with *P. vivax*, including relapses. Here, we evaluate the hematological dynamics and clinical presentation of sporozoite-initiated *P. cynomolgi* infections in *Macaca mulatta* (rhesus macaques) over a 100-day period.

Methods: Five *M. mulatta* were inoculated with 2,000 *P. cynomolgi* B strain sporozoites. Parasitological and hematological data were collected daily to study the clinical presentations of primary infections and relapses. Peripheral blood and bone marrow aspirates were collected at specific time points during infection for future and retrospective systems biology analyses.

Results: Patent infections were observed between days 10 to 12, and the acute, primary infection consisted of parasitemias ranging from 269,962 to 1,214,842 parasites/µl (4.42% to 19.5% parasitemia). All animals presented with anemia, ranging from moderate (7-10 g/dl) to severe (< 7 g/dl), based on peripheral hemoglobin concentrations. Minimum hemoglobin levels coincided with the clearance of parasites and peripheral reticulocytosis was evident at this time. Mild thrombocytopenia (<150,000 platelets/µl) was observed in all animals, but unlike hemoglobin, platelets were lowest whenever peripheral parasitemia peaked. The animal conditions were classified as non-severe, severe, or lethal (in one case) based upon their clinical presentation. The lethal phenotype presented uniquely with an exceptionally high parasitemia (19.5%) and lack of a modest reticulocyte release, which was observed in the other animals prior to acute manifestations. One or two relapses were observed in the four surviving animals, and these were characterized by significantly lower parasitemias and minimal changes in clinical parameters compared to pre-infection values.

Conclusions: Rhesus macaque infections initiated by *P. cynomolgi* B strain sporozoites recapitulated pathology of human malaria, including anemia and thrombocytopenia, with inter-individual differences in disease severity. Importantly, this study provides an in-depth assessment of clinical and parasitological data, and shows that unlike the primary infections, the relapses did not cause clinical malaria. Notably, this body of research has provided experimental plans, large accessible datasets, and blood and bone marrow samples pertinent for ongoing and iterative systems biology investigations.

Background

Malaria represents a constant burden and public health challenge in approximately 100 countries worldwide [1]. *Plasmodium falciparum* is responsible for the largest number of cases and malaria-associated deaths, with extensive research efforts focused on understanding the basic biology and associated pathogenesis of this parasite species. *Plasmodium vivax* has also been recognized as a major contributor to the global burden of malaria, and numerous recent reports indicate infections can result in complications with lethal outcomes [2-5]. Still, by comparison, neglect of *P. vivax* is apparent, greatly due to the challenges associated with studying this species, which include the lack of a long-term *in vitro* culture system or a rodent model that can support the entire life-cycle and re-create critical aspects of *P. vivax* infections and disease as observed in humans [6-9].

Plasmodium vivax, as well as *P. ovale,* differ from the three other human malaria-causing species (*P. falciparum*, *P. malariae* and *P. knowlesi*) because they can develop dormant liver-stage forms, known as hypnozoites [10]. Hypnozoites can activate and multiply, causing relapsing blood-stage infections days, months, or years after the primary infection. Relapses may result in clinical disease and, importantly, provide the chance for gametocytes to encounter Anopheline mosquito vectors and ensure transmission. New insights are needed to treat this liver-stage reservoir to ensure the elimination of relapses and blood-stage infections containing infectious gametocytes. Virtually nothing is known about the biology of relapse infections despite the fact that relapses are thought to be responsible for as high as 96% of vivax infections in different parts of the world [11]. It is currently unclear how relapses are similar or different from primary infections, from a parasitological and clinical perspective, and the relative contribution of relapses to clinical malaria has been uncertain.

Understanding the course of primary and relapse infections, and specific mechanisms that result in vivax malaria pathogenesis, disease severity and recovery, are important goals. In

particular, the identification of mechanisms that function in the peripheral blood and bone marrow resulting in the onset and recovery of malarial anemia [12, 13] and thrombocytopenia [14] may aid the search for novel interventions and therapeutic strategies to manage and/or alleviate these common complications. Headway has been made with the study of specimens isolated from human patients living in endemic areas [15, 16]; however, these studies are mostly restricted to one or a few small blood samples at the time of illness and treatment. Furthermore, the analysis and interpretation of these studies can be affected by uncontrollable variables such as diet, medications, transmission characteristics, coinfections, and other maladies. These factors can confound associations of clinical signs and symptoms. Non-human primate animal models can eliminate a number of these concerns, with experimental plans allowing for the study of specific biological, immunological or pathological processes in a controlled, prospective and manipulable environment.

Non-human primate models have contributed to the broad understanding of malaria biology, pathogenesis and immunity with regards to liver-stage and blood-stage infections, and they have also been instrumental for screening vaccine and drug candidates or specific formulations [17-21]. *Plasmodium vivax* can be studied directly in New World monkey species such as squirrel (*Saimiri boliviensis*) and owl (*Aotus* sp.) monkeys, and these models have been important, for example, in testing vaccine and drug candidates with parasite challenge infections [22, 23] and, recently, to identify and characterize blood-stage proteomes of *P. vivax* infected erythrocytes [24, 25]. However due to the small size of these animals (~1 kg), which limits the amount of blood (or bone marrow) available for sampling, and the lack of validated reagents available to evaluate host physiological and immunological responses, they are not ideal for extensive hypothesis testing in relation to malaria pathogenesis, immune responses and recovery processes.

Plasmodium cynomolgi is a simian malaria parasite of Old World macaques that is genetically closely related to *P. vivax* [26, 27] and shares many biological similarities to the human parasite including the preferential invasion of reticulocytes [28, 29], development of unique

infected red blood cell (RBC) structures called caveola-vesicle complexes [30, 31], and critically, the ability to form hypnozoites that can reactivate and cause relapse infections [10, 18, 32, 33]. Macaques are closely related to humans, and a large variety of cross reactive reagents for assessing host responses have been developed since these monkeys are model organisms for infectious diseases [34]. Young adult macaques (~5 kg or greater) can support longitudinal *Plasmodium* infection studies that require repeated sampling within a short time frame. *Macaca mulatta* (rhesus monkey) and *Macaca fascicularis* genome sequences [35, 36] and the genome sequence of several strains of *P. cynomolgi* [26], have been characterized in recent years, enabling basic as well as systems biology studies of host-parasite interactions.

Here, comprehensive analyses of sporozoite-initiated, longitudinal infections of *P. cynomolgi* in rhesus macaques are presented with the long-term goal of using this model for systems biology investigations to better understand human malaria pathogenesis, particularly as it pertains to pathophysiological complications observed in sick patients and with regards to the impact of relapses on both the health of individuals and transmission [37]. Previous studies have utilized the *P. cynomolgi* – macaque model to understand the parasite's basic biology and parasite kinetics, including the study of hypnozoites and relapses [20, 33, 38]. However, an extensive characterization of the clinical and hematological perturbations that occur during the infections has not been reported, particularly on a daily basis.

Methods

Experimental Design. The basic experimental design of this study is shown in Figure 1A. The sampling strategy included a single pre-infection and six subsequent blood and bone marrow aspirate specimen collections during the infection at major infection or pathology presentation time points. The criteria for the collection of samples are described in Table 1 and adhered strictly to Institutional Animal Care and Use Committee (IACUC) approved volume limits of 10ml/kg/month or 6.6 ml/kg/month if an animal was anemic. Adjustments were made as to when samples were acquired based on each animal's parasitological and hematological kinetics. Clinical signs and symptoms observed by trained veterinary staff were also taken into consideration daily. All samples collected for an experimental period satisfied at least one or more of the pre-defined clinical criteria (Table 1). As expected, some individuals required pharmacological and/or clinical support during the acute, primary infection. Blood and bone marrow aspirate specimens were acquired prior to such clinical interventions.

Table 1. Criteria for the collection of samples at different experimental periods

Experimental Period	Criteria*
Pre-Infection	Normal motor activity and appetite. Hematological parameters within normal range
Acute Primary	Prostration, lethargy, low appetite. Moderate to severe anemia, thrombocytopenia, tachypnea, hyperparasitemia, impaired consciousness, hyperpyrexia, azotemia, hyponatremia, hyperkalemia and clinical evidence of activated coagulation (e.g. petechiae).
Post Peak	Moderate anemia, reticulocytemia, control of parasitemia.
Relapse	Low parasitemia
Inter-Relapse	Hematological parameters within normal range, no parasitemia
Final	Hematological parameters within normal range

*The specific criteria and observations at sample collection points were recorded for each animal based on the clinical assessments made by veterinary staff and investigators.

In addition to collecting samples for analysis at major points during the infections, this study was also designed to collect clinical data on a daily basis. The aim of these collections was to develop highly-resolved clinical kinetics. To achieve this goal, the animals were accessed daily without sedation for attaining up to 100 µl of blood through standardized ear-prick procedures, similar to the collection of blood from a human finger-prick. This blood was used to perform complete blood counts (CBCs) as well as enumerate reticulocytes and parasites during the infection.

Animal Use. Five healthy, male malaria-naïve *M. mulatta* (RFa14, RIc14, RMe14, RSb14, and RFv13) born and raised at the Yerkes National Primate Research Center (YNPRC), an Association for Assessment and Accreditation of Laboratory Animal Care (AAALAC) International –Certified institution, were assigned to this study. The animals were socially housed in pairs at YNPRC during the experiment, and all housing was in compliance with Animal Welfare Act regulations as well as the Guide for the Care and Use of Laboratory Animals. Males were designated to eliminate confounding factors studying anemia that could be attributed to loss of blood during the female menstrual cycle. An additional rhesus monkey was assigned at the Centers for Disease Control and Prevention (CDC) and utilized for the generation of sporozoites. Standard procedures for monitoring the clinical conditions of the animals, collecting biological samples (venous blood and bone marrow aspirates), and performing mosquito feedings on infected animals to generate infectious salivary gland sporozoites were approved by Emory University's or the CDC's IACUC and followed accordingly. All nonhuman primates used in this study were provided regular environmental enrichment opportunities consisting of daily feeding enrichment, provision of manipulanda, and physical enrichment. Subjects were regularly monitored for any behavioral signs of distress by YNPRC behavior management personnel. Animals were trained using positive reinforcement to allow blood collections from the ear without sedation.

Parasite Selection. Plasmodium cynomolgi B strain was selected for infections because the relapse pattern of this strain had been characterized previously [32], providing confidence that relapse

infections would be observed within the 100-day experimental infection period, based on an inoculum size of 2,000 freshly dissected salivary gland sporozoites. This strain was also selected because of the availability of its reference genome [26], needed for retrospective system biology studies on the samples that were collected and stored for such purposes.

Sporozoite Generation and Inoculation. To generate sporozoites, a donor rhesus macaque was infected with blood-stage parasites that were reconstituted from *P. cynomolgi* B strain ring-stage cryopreserved stocks maintained by the Malaria Branch at the CDC. Prior to the start of this study, the identity of these parasites was verified by Illumina 454 sequencing and comparison to the reported genome sequence of Tachibana et. al. [26]. Laboratory bred *Anopheles dirus, An. gambiae and An. stephensi* mosquitoes were fed on the donor monkey using standard, IACUC-approved procedures after observance of male and female gametocytes in the blood. Successful infection of the mosquitoes was confirmed within a 7-day period post feeding via midgut dissections to monitor oocyst development and the progression of the infections with sporozoites detected in the salivary glands on days 11 and 12 after mosquitoes fed on infected blood. The salivary glands were freshly dissected from the infected mosquitoes and immediately processed by repeated passage through a 26G needle 10 times to release sporozoites in RPMI-1640 culture media supplemented with 10% fetal calf serum (FCS) on ice. The processed salivary gland and other mosquito debris were allowed to settle by gravity and the sporozoites in the supernatant were washed once by centrifugation at 1000 ×*g* in sterile culture medium with 10% FCS. Sporozoite concentrations were determined by counting in a Neubauer hemocytometer chamber using a light microscope at 400X magnification. Isolated sporozoites were resuspended in sterile RPMI 1640 with 10% FCS, and the macaque cohort infections were initiated by the intravenous inoculation of 2,000 sporozoites per animal.

Clinical Monitoring. Blood samples were collected daily from the monkey cohort from day -1 to 100 into EDTA-coated capillary tubes using standardized IACUC-approved ear-prick procedures.

These samples were used to perform complete blood counts (CBCs) using an automatic cell analyzer (Beckman AcT-diff; Coulter Corporation) and reticulocyte enumeration using new methylene blue staining of thin blood smears. Clinical data were reviewed with parasitological data daily to monitor the clinical conditions of the animals and determine when specimens should be collected based on the criteria noted in Table 1.

Parasite Enumeration. Parasitemia counts (parasites/µl) were determined daily via microscopy readings of thick and thin blood films stained with a modified Wrights-Giemsa using enumeration protocols recommended by the World Health Organization [39]. Briefly, the number of infected RBCs (iRBC) observed on thick blood smears per 500 leukocytes was recorded, and the parasitemia determined by multiplying the percentage of parasites out of the total number of leukocytes with the leukocyte concentration obtained from the CBC. When parasitemia readings were at or greater than 1%, thin blood smear counts were obtained by counting the number of infected RBCs out of a total of 1,000 to 2,000 RBCs. The percentage of infected RBCs was then calculated, and the RBC concentration from the CBC was used to determine the parasitemia (parasites/µl). The percent of iRBCs (or percent parasitemia) was also calculated by dividing the number of parasites by the RBC count and multiplying by 100. To ensure accuracy, two expert microscopists independently determined the parasitemias each day. If a significant discrepancy was observed (e.g. ≥ 2 standard deviations of the mean) and/or if unexpectedly low or high parasitemia readings were reported, a third, independent senior expert microscopist was designated to provide an additional parasitemia reading. All three parasitemia counts were compared, and the definitive parasitemia was typically based on the average of the two counts that were the closest together. In other cases, primarily while verifying the presence of relapses with low parasitemias or after sub-curative blood-stage treatment, the third microscopist's counts were used as the decisive readings. For relapse verification, the third microscopist counted the number of parasites per 2,000 WBCs, which quadrupled the level of sensitivity of the assay.

Specimen Collections. Peripheral blood and bone marrow aspirate samples were collected prior to infection and during the infections (Fig. 1A) for immediate analyses and projected future multi-omic studies (e.g. transcriptomics, proteomic, lipidomics, metabolomics and immunological profiling) to be performed and integrated with the clinical and parasitological data described here. The animals were anesthetized with ketamine, and blood and bone marrow aspirates were collected from the femoral vein and iliac crest, respectively. Venous and capillary blood samples were collected in EDTA using either BD vacutainer or capillary tubes, respectively, for hematological assays, e.g. CBCs and reticulocyte enumeration, and for parasite enumeration. Blood for clinical chemistry analyses was collected in lithium heparin tubes.

Clinical Definitions. Clinical definitions were based on reference values for rhesus macaques as defined at the YNPRC and other available literature [40]. The normal range of hemoglobin concentration for male rhesus macaques is 12-14 g/deciliter (dl) and anemia can be similarly defined in humans. Here, anemia was defined as severe (<7 g/dl), moderate (7-10 g/dl), or mild (10-11 g/dl), based on the hemoglobin nadir, or the lowest level, during the primary infection and relapses. Anemia was further classified as normocytic (63.7 – 86.9 femtoliters (fl), microcytic (<63.7 fl) or macrocytic (>86.9 fl) based on the mean corpuscular volume (MCV). Thrombocytopenia was defined as having a platelet count below 150,000 platelets/µl during either the primary or relapse infections, and severe thrombocytopenia was defined as having a platelet count of <50,000 platelets/µl.

Therapeutic Interventions. The WHO criteria for the management of severe malaria were utilized as a guide to determine when animals were progressing towards severe disease and necessitated clinical and/or therapeutic intervention to ward off terminally severe outcomes [41]. Animals that developed clinical complications associated with severe malaria during the acute infection periods were administered a sub-curative antimalarial treatment of 1 mg/kg of artemether. Additionally, severe anemia (< 7 g/dl) was treated with IV fluid support and whole blood transfusion, also guided by YNPRC veterinarian recommendations and IACUC-approved procedures. After collecting the

specimens for the post peak infection point (Figure 1A), blood-stage infections were cured with artemether administered at 4 mg/kg on the first day of treatment and 2 mg/kg/day for seven days thereafter. This ensured that subsequent blood-stage parasitemias detected in the animals were the result of relapses from the activation of hypnozoites, and not recrudescences of sub-patent, persisting blood-stage forms. Curative blood-stage treatment with artemether was also administered using this same regimen after each relapse, and a curative course of chloroquine (15 mg/kg/day for 3 days administered intramuscularly) and primaquine (1 mg/kg/day for 7 days administered orally) was administered at the end of the entire experiment to treat the blood stages and the hypnozoites, respectively.

Statistical Analysis. Nonparametric statistical approaches were used to assess statistical significance. A Friedman test was performed followed by Dunn's Multiple Comparison post-hoc analysis to identify significant changes in clinical parameters from pre-infection values over time and between pre-, primary, and relapse infection values. Spearman's nonparametric correlation analysis was performed on clinical parameters using clinical values obtained from the defined experimental periods to ensure that different sample types (i.e. venous blood collected at major infection points versus capillary blood collected daily) did not influence associations. A Wilcoxon matched-pairs rank sums test was performed to compare the primary and relapse infection parasitemias. Both Graphpad Prism Version 6 and JMP Version 12 were used for statistical analysis.

Data management and release. All samples were tracked with barcodes and a Laboratory Management Information System (LIMS). Data that were manually generated, e.g. clinical assessments, parasitemias, animal handing, treatment, diet, snacks and procedures were entered into the LIMS or electronic spreadsheets with double-data entry to increase accuracy. Data fields were constrained with limits or populated with pull-down lists of allowable values to further increase accuracy. All data were then transferred to internal repositories for validation and integration with other data. Standard Operating Procedures (SOPs) for all methods were collected

and archived. Data derived from blood and bone marrow samples were associated with the appropriate animal and experimental metadata via a barcode. All data associated with this study (clinical, experimental, SOPs and data dictionary to define all terms) were backed-up locally as well as off-site. The dataset supporting the conclusions of this article is included with the article as Supplementary File 1 and is also being made available via the freely accessible database, PlasmoDB [42] (http://PlasmoDB.org), as no archival repositories exist for these types of data. This experiment is known in the deposited files as MaHPIC Experiment 4 (E04).

Results

Primary and relapsing parasitological profiles of *Plasmodium cynomolgi* B strain in *M. mulatta* during a 100-day experimental infection.

Intravenous inoculation of approximately 2,000 freshly isolated salivary gland sporozoites produced patent infections within 10 to 12 days (mean ± SE = 11.2 ± 0.37) consistent with previous literature (Figure 1B; [17, 32]). The maximum parasitemias during the primary infections ranged from 269,962 to 1,214,842 parasites/μl (4.42% – 19.5% iRBC) between days 18 to 20 post-inoculation (Figure 1B). RFa14, RMe14 and RFv13 required sub-curative treatment with artemether (1 mg/kg) as noted due to clinical complications (see Table 2). These interventions were implemented to avoid negative outcomes, including possible death. RFa14 and RMe14 developed recrudescent infections 48-72 hours later, as anticipated based on prior experience with subcurative artemether treatments of *P. cynomolgi* and *P. coatneyi* in rhesus macaques at the CDC and the YNPRC [43]. RFv13 subsequently, despite the treatment, developed severe clinical complications, which required this animal to be euthanized, per IACUC guidelines and protocols (Figure 1B). In summary, this animal presented with acute renal failure. RSb14 and RIc14 did not require sub-curative treatment. These animals were able to control their primary parasitemia, presumably through an immune mechanism, resulting in an approximate 10-fold reduction in parasite levels from about 300,000 parasites/μl down to 4,000 to 8,000 parasites/μl between days 18 to 23 post-inoculation (Figure 1B). This reduction in parasitemia was then followed by a rise again to nearly peak parasitemia levels, which is characteristic of most *P. cynomolgi* infections (Figure 1B; [17]).

To distinguish relapses from possible recrudescences of persisting low-level blood-stage parasitemias, RIc14, RSb14, RFa14 and RMe14 received curative blood-stage treatment with artemether after their primary parasitemia and illness. Artemether was administered uniformly on day 26 at 4 mg/kg, and then 2 mg/kg/day for seven days thereafter (Figure 1B). During the 100-day experiment, RIc14 and RSb14 experienced two relapses, whereas RFa14 and RMe14 had a

single relapse (Figure 1B). RIc14 and RSb14 experienced their first relapse within 19 and 26 days (day 51 and day 58 post-inoculation), respectively, after completion of curative blood-stage treatment on day 32 (Figure 1B). Contrastingly, RFa14 and RMe14 remained negative by microscopy during this period (Figure 1B). Curative antimalarial treatment for blood-stages was administered to all animals on Day 63, and relapse infections were detected as early as 10 days after the completion of this second curative blood-stage treatment. All animals relapsed prior to the end of the 100-day study, after the second round of curative blood-stage treatment; RIc14 on day 83 and RSb14 on day 88, with RFa14 and RMe14 relapsing for the first times on day 95 and day 80, respectively.

The peak parasitemia for the first relapse infections ranged from 846 to 11,584 parasites/µl, which was strikingly lower than the primary infection (Figure 1C). Since the animals as a group experienced either one or more relapses, this comparison was performed using the maximum parasitemia for the first relapse noted for each individual. This result was not statistically significant ($p = 0.0625$) however, based on the four of five animals remaining in the study. A follow-up study will expand on these numbers. Contrary to a previous report stating that relapse parasitemias decrease with subsequent relapses [19], a large difference in parasitemia was not observed between the first and second relapses for RSb14 and RIc14 (Figure 1B).

Different degrees of anemia were observed during the primary blood-stage infections.

The primary *P. cynomolgi* B strain blood-stage infection resulted in anemia in the entire cohort (Figure 2A and 2B). Similar to anemia in humans with malaria, inter-individual differences in anemia severity were evident and ranged from moderate (7-10 g/dl) to severe (< 7 g/dl) (Figure 2B; Table 2). The anemia was normocytic (defined as 63.7 - 86.9 fl) based on MCV values (Figure 2C). Although parasitemia and hemoglobin concentration were negatively correlated (Spearman $\rho = -0.7288$, $p < 0.0001$), a statistically significant decrease in hemoglobin concentration compared to pre-infection values did not coincide with the peak of parasitemia during the acute, primary phase of the infection ($p > 0.05$; Figures 2A and 2B). Rather, the hemoglobin concentrations were

significantly lower than pre-infection values approximately 4 to 7 days after the recognized peak of parasitemia, a period that we have termed here as the "post-peak of parasitemia" (Figure 2A and 2B). During this period, the macaques were either controlling the infections naturally leading to decreases in parasite numbers or recovering from the infections after the administration of a sub-curative dose of artemether. Importantly, anemia to some degree was observed irrespective of the administration of sub-curative treatment (Figure 2B).

Reticulocytes were enumerated to monitor the clinical situation, the animals' attempts to recover from anemia, and as a peripheral indicator of erythropoiesis in the bone marrow. Under homeostatic conditions, reticulocyte release will coincide with decreases in peripheral hemoglobin concentration to compensate for the loss of RBCs in the periphery. Thus, reticulocyte concentrations should increase during the acute, primary infection period and begin to return to pre-infection levels after the peak of parasitemia. Contrary to this hypothesis, the reticulocyte concentrations did not increase from pre-infection levels until the post-peak parasitemic phase when the animals were beginning to show signs of recovery (Figure 2D and 2E). Curiously, there was a small increase in reticulocyte concentrations between approximately days 8 and 15 post-inoculation for all animals except RFv13 (the animal with the most severe disease), followed by an immediate decrease back to pre-infection levels whenever parasitemia began to increase exponentially (Figure 2E).

Thrombocytopenia developed during the primary blood-stage infections.

Thrombocytopenia, a clinical condition that is the result of reduced number of platelets in the blood, is a common hematological finding during malaria, but its specific role in pathogenesis has been highly debated [14, 44-48]. Indeed, thrombocytopenia (<150,000 platelets/μl) was observed in all macaques (Figure 3A and 3B). Despite the decrease below a clinically relevant threshold, the drop in platelet concentration was not statistically significant from pre-infection values ($p > 0.05$), and furthermore, severe thrombocytopenia (<50,000 platelets/μl) was not observed (Figure 3A and 3B). Thrombocytopenia was most pronounced at day 20, near the peak of

parasitemia, where the peripheral platelet concentrations were approximately 38% of the baseline levels (Figures 3B and 3C). The recovery of platelets coincided with a decrease in parasitemia between days 20 and 26, irrespective of the administration of sub-curative blood-stage treatment or self-control of the infections (Figure 3B). Notably, platelet concentration in the periphery increased to higher than pre-infection values before stabilizing (Figures 3B and 3C).

Thrombocytopenia is thought to be the result of a variety of mechanisms including the binding of platelets to infected RBCs, removal of platelets by phagocytic cells, and sequestration of the platelets in the microvasculature and organs [14, 16, 37]. Here, a decrease in mean platelet volume (MPV) was noted whenever platelet concentrations were beginning to return to pre-infection levels, between days 20 and 30 post-inoculation (Figure 3D). Alterations in MPV could indicate that platelet production by megakaryocytes in the bone marrow was disrupted, providing another mechanism that could potentially contribute to thrombocytopenia. In addition to impaired production of platelets, a lower MPV could be caused by low platelet concentrations. However, the current data do not support this explanation, because as platelet concentrations returned to pre-infection levels the MPV decreased (Figure 3D). Furthermore, MPV and platelet concentration were inversely correlated (Spearman $\rho = -0.3785$, $p < 0.0358$) (Figure 3D). To further evaluate the hypothesis that megakaryocyte function could be compromised during *cynomolgi* malaria, the dynamics of reticulocyte release and platelet recovery were examined. If platelet and/or reticulocyte production were compromised due to altered bone marrow physiology, then the recovery of these cell types in the periphery may overlap. Indeed, the increase of platelet concentrations after the primary blood-stage infections coincided with increases in peripheral reticulocyte concentrations (Figure 3E).

Relapses did not result in significant changes in clinical parameters.

One of the primary goals of this study was to better understand the clinical aspects of relapses compared to primary blood-stage infections. Analyses focused on the first relapses, with comparisons across the four animals that survived the primary infection. Importantly, significant

changes were not observed in parasite burden (Figure 1B), hemoglobin (Figure 2B), reticulocyte (Figure 2E), or platelet concentrations (Figure 3B) during the second relapses compared to the first. Relapses did not result in the same changes in clinical parameters as the primary infections and did not differ significantly from pre-infection values (Figures 4B, 4C, and 4D). In fact, most clinical values did not significantly change from pre-infection values (Figures 2B, 2E, and 3B).

RMe14, the macaque with the highest parasitemia during a relapse, was the only animal that developed minor alterations in hemoglobin, platelet, and reticulocyte concentrations during relapses (Figures 2B, 2E, 3B). Specifically, the hemoglobin level for this animal dropped from 14 g/dl, recorded 7

days before the peak of the relapse parasitemia, to 11 g/dl, making it mildly anemic (Figure 2B). Unlike during the period of the primary blood-stage infection, the drop in hemoglobin concentration resulted in an increase in the peripheral reticulocyte concentration, suggesting that the mechanism(s) that prevented the compensatory release of reticulocytes to compensate for alterations in hemoglobin concentration during the primary infection did not occur during relapse infections, likely due to the controlled parasite burden (Figure 2E). Platelet concentration also dropped sporadically during relapses for this animal (Figure 3B).

Clinical presentations ranged from non-severe to lethal.

A variety of clinical phenotypes were observed in this study, which could be distinguished as non-severe, severe, and lethal (Table 2). RIc14 and RSb14 were able to control the primary infection without sub-curative blood-stage treatment and displayed mild thrombocytopenia and moderate levels of anemia. Thus, these two animals were classified as non-severe. Contrastingly, RFa14, RMe14 and RFv13 required sub-curative treatment during the primary blood-stage infection due to a variety of adverse clinical signs. RFa14 presented with a unique phenotype characterized by a drop in hemoglobin to approximately 11.2 g/dl and platelet concentration to approximately 125,000 platelets/µl in the peripheral blood early during the primary infection, and uniquely, petechiae were noticed on the trunk of this animal.

This profile was consistent with that reported with a *P. coatneyi* infection in a rhesus macaque, where the animal progressed to very severe disease complications due to disseminated intravascular coagulopathy [49]. Due to the poor prognosis associated with these indications, RFa14 was sub-curatively treated and classified as severe. Contrastingly, RMe14 and RFv13 developed severe anemia (<7 g/dl) during the primary infection (Figure 2B). In response to this presentation, sub-curative blood-stage treatment was administered and whole blood-transfusions performed for both of these animals. RMe14 recovered and was categorized as having a severe clinical phenotype, but RFv13 succumbed to the infection as noted above despite this intervention, resulting in the additional classification as a lethal clinical phenotype.

Parasitemia and the lack of an increase in reticulocytes during the initial phase of the primary infection distinguish the lethal clinical phenotype.

The contribution of parasite burden to each clinical phenotype was evaluated. The peak parasitemia in the non-severe animals was 273,509 and 305,636 (mean = 289,573) parasites/µl whereas the two severe animals that survived had parasitemias of 309,365 and 379,140 (mean = 344,452) parasites/µl during the primary infection (Figures 1B and 5A). Using this measure, the parasitemia was not strikingly different between the non-severe and severe clinical phenotypes. Next, the peripheral parasitemias were analyzed as a percentage, or the number of infected RBCs out of the total RBCs. Using this approach, there was possibly a minor difference between the two phenotypes. Specifically, the non-severe animals had parasitemias of 4% and 5% whereas the severe animals had parasitemias of 6.3% and 7.8%, prior to administration of the sub-curative blood-stage treatments (Figure 5B). The animal that succumbed to the infection developed a maximum parasitemia of approximately 1,200,000 parasites/µl and showed a 19.5 % parasitemia prior to clinical intervention, which was approximately four fold higher than observed in the surviving animals (Figure 5A and 5B).

Unexpectedly, one other clinical feature in addition to parasite burden was identified that distinguished the lethal from the non-severe and severe phenotypes. Even though the hemoglobin

concentrations and platelet kinetics for the non-severe, severe, and lethal phenotypes were all similar during the primary blood-stage infections (Figures 5C and 5D), the reticulocyte kinetics for the lethal infection (RFv13) was not the same as for the other two phenotypes (Figure 5E). Specifically, as noted above, the peripheral reticulocyte concentrations in this animal did not show a modest increase during the patent blood-stage infection between days 10 to 15 post-inoculation, in comparison to the other animals where a modest, short-term increase was evident (Figure 5E). This difference in reticulocyte kinetics could indicate that this and possibly other early host responses may influence and be a predictor of clinical complications and the potential course of the disease state or recovery processes.

Discussion

This 100-day experiment was designed to study the clinical and parasitological attributes of the primary blood-stage and relapse infections caused by *P. cynomolgi* in rhesus macaques and set the stage for future, comprehensive studies using this model to understand the underlying mechanisms of immunity, pathogenesis and disease. Highly resolved kinetics of core hematological parameters were developed after inoculation with infectious B strain sporozoites, and specifically, reticulocyte, platelet, hemoglobin, MPV, and MCV dynamics are presented here. This study expands upon previous rhesus infection studies with the *P. cynomolgi* B strain, which primarily monitored parasitological data but did not assess clinical parameters on a daily basis [17, 32]. The compiled clinical and parasitological datasets generated here provide a glimpse into the daily dynamics of malaria beyond what is typically feasible in humans. It is anticipated that the data generated in this experiment (all of which are being shared publicly – see Methods & Supplementary File 1) will aid the development and testing of hypotheses by the research community whether for clinical studies or continued investigations using *P. cynomolgi* as a model.

Anemia ranged from mild to severe during the primary infections in this study and appears to be the result of multiple processes. First, it is noteworthy that hemoglobin decreased to the lowest levels after parasitemia was reduced, whether from the natural control of the infection by the macaque or drug treatment. This data demonstrates that the loss of RBCs due to parasitism is not the sole reason for anemia in this model. Indeed, other non-human primate malaria models [43], rodent malaria models [50], and humans [51, 52] show a similar kinetic where anemia is worse after the peripheral parasitemia has decreased. This phenomenon is attributed to the simultaneous removal of iRBCs and uninfected RBCs [53, 54], which has also been modelled mathematically to arrive at similar conclusions [51]. Secondly, the normal, timely replenishment of circulating RBCs by the release of reticulocytes from the bone marrow was disrupted, as shown previously with *P. coatneyi* infection of rhesus macaques [43]. Thus, the disruption of compensatory bone marrow

mechanisms with the effective release and/or production of reticulocytes from the bone marrow is likewise apparent in the *P. cynomolgi* – rhesus macaque model during the acute, primary infection. For each of these species, which model *P. falciparum* and *P. vivax*, respectively, the disruption of normal bone marrow physiology could be potentially due to ongoing immunological responses against the parasite or parasite byproducts such as hemozoin that are released as the parasites multiply in the blood [50, 55-57]. In agreement as shown here, there was an initial increase of reticulocytes early during the primary infections and these cells returned to baseline levels when the parasitemia was increasing exponentially in the blood. This supports the view that the disruption of the normal compensatory mechanisms is dependent on parasite levels. Future studies will be needed to better understand the host-pathogen interactions that occur during the primary infection and how they contribute to malarial anemia in this model.

The relative contribution of thrombocytopenia to disease outcome during malaria remains controversial and also not well understood [14, 44, 47]. In this study, all animals developed mild thrombocytopenia irrespective of their clinical presentations, and thus, thrombocytopenia was not viewed as an indicator of disease severity or outcome. Prior evidence suggests that thrombocytopenia could be due to removal of platelets by splenic macrophages during infection [16], whereas other models suggest that platelets form clumps with iRBCs [58] or become sequestered in the microvasculature by adhering to activated endothelial cells [59]. Interestingly, published experiments with the *P. cynomolgi* B strain have demonstrated that thrombocytopenia occurs in both spleen-intact and splenectomized macaques, suggesting that there are other contributing factors in the development of this complication aside from processes associated with this organ [60]. In agreement, the data from this study indicates that platelet production may have been impaired since the MPV was decreased as the number of platelets rebounded after the peak of parasitemia. Previous studies with malaria patients have reported changes in MPV during malaria [61, 62]. The alteration in MPV may indicate disruption of megakaryocyte function, and thus, platelet production. In further support of this hypothesis, both reticulocytes and platelets

returned to pre-infection levels together, and since both of these cell types originate from the bone marrow, the simultaneous return to normal levels could be explained by the restoration of normal bone marrow physiology. Overall, these data suggest that the disruption of normal bone marrow physiology during acute malaria may also lead to impaired platelet production and contribute to thrombocytopenia. Future studies should explore this hypothesis further and aim to understand if thrombocytopenia is in part just a bystander effect of bone marrow dysfunction.

It is important to recognize that macaques infected with *P. cynomolgi* presented with inter-individual differences in disease severity, similar to humans. In RFv13, a very high parasitemia (19.5% parasitemia), appeared to contribute to the lethality since this parasitemia clearly distinguished this animal from the two non-severe (RSb14 and RIc14) and two severe (RMe14 and RFa14) clinical presentations. These phenotypes did not clearly stratify away from each other based on parasitological profiles alone, indicating that while parasitemia may play a role in severe disease, it is not solely responsible for the observed differences in clinical presentation and other pathological processes may come into play. This is reminiscent of human malaria where individuals can progress to severe malaria regardless of parasitemia [63-65]. Curiously, unlike the four surviving macaques, RFv13 did not show a modest increase in reticulocytes during the beginning of the primary infection. In future studies, it would be useful to evaluate this finding and other potential indicators of the progression of infections and how these early responses to blood-stage infections influence pathogenesis and clinical presentation.

Schmidt [32] demonstrated that relapse frequencies in the rhesus macaque differ based on the number of *P. cynomolgi* B strain sporozoites inoculated, and based on this evidence, some investigators have used 1×106 sporozoites to generate early, frequent and uniform relapse patterns across individuals for screening anti-hypnozoite drugs [19]. In contrast, only about 2,000 sporozoites were inoculated in the current study, aiming for primary infections followed by more natural patterns of relapse. While this is still higher than what is suspected to be naturally injected by a mosquito [66, 67], 2,000 sporozoites best ensured at least one or two relapses in all animals

during the course of this study. In fact, the average number of relapses observed was 1.5. This number may have been higher if the animals had not been cured as a group after the fifth specimen collection. Nevertheless, the observed relapse patterns reported here are similar to what would be expected with *P. vivax* infections with tropical strains of this parasite [7, 68, 69]. A follow-up iterative experiment was designed to monitor the natural relapse patterns, without such treatment plans, and to monitor gametocytes during the relapse periods more carefully.

Understanding, preventing and treating relapses caused by *P. vivax*, and also *P. ovale*, remain key challenges in today's malaria eradication efforts, especially if asymptomatic carriers remain infectious to mosquitoes. Critically, the relative impact of primary versus relapse clinical malaria presentations has remained undefined in a controlled, experimental model system and direct evidence from human studies is not available because of the challenges distinguishing the two in human cases without a well-controlled study design [70-73]. Here, each *bona fide* relapse, subsequent to blood-stage treatment and in the absence of re-infections, resulted in significantly lower parasitemias compared to the primary infections and minimal, if any, changes in clinical parameters to indicate illness. This suggests that immunity, or potentially other undefined mechanisms, during the primary infection, led to controlled relapses characterized by reduced parasitemias and lack of clinical complications. Whenever minor alterations in clinical parameters were observed during a relapse (e.g. minor drop in hemoglobin levels from 14 to 11 g/dl), as was the case for RMe14, these alterations resolved in a controlled, non-pathological manner, without the need for clinical support. The lack of clinical illness during relapses was not necessarily expected, especially in animals that only experienced a single primary blood-stage infection, since previous reports have concluded, through mathematical and statistical modelling of data collected from holoendemic areas that relapses are responsible for up to 96% of blood-stage *P. vivax* infections [11, 74]. Thus, this experiment draws light to the question "What percentage of relapses actually cause clinical malaria?" Relapses have been a major concern due to their role in causing possible repeated bouts of illness and because they can be a source of infectious gametocytes to

maintain transmission. The data presented here supports the hypothesis that relapses may not necessarily be the main cause of clinical vivax or ovale malaria cases. This warrants further study to understand the clinical outcome of primary infections compared to relapses, in addition to transmissibility questions, caused by homologous or heterologous strains as would also be anticipated in malaria endemic regions [73, 75, 76].

In a previous study, rhesus infected with *P. cynomolgi* were treated soon after infected RBCs were detected, and the parasitemia of the first relapses appeared to be higher than subsequent relapses [19]. The clinical status of the macaques during relapses was not presented, however, so it is unknown if the clinical profile of the relapses differed from the primary infections. In contrast, the parasitemia in the current study was allowed to persist during the primary infections, since a goal was to understand the course of the clinical presentations. Interestingly, with this approach, the first and second relapses had similar parasitological and clinical attributes, and the difference in parasitemia between the primary infection and relapses was substantial. This data highlights the point that the timing of the experimental treatment of blood-stage infections may affect the later presentation of relapses, and could in turn influence whether the relapse parasitemia and illness are suppressed, or not. Future studies should evaluate if the timing of blood-stage treatment affects the development of immunity against the parasite.

As shown by this research team and others using this model system, relapse infections can be definitively produced under controlled experimental conditions [19, 32], in the absence of new sporozoite-initiated infections, and they can be distinguished from blood-stage recrudescences through the administration of curative blood-stage treatments. This creates a clear ‘window’ of time after the administration of curative treatment of blood-stage infections, during which time the activation of hypnozoites and appearance of relapse parasites can be anticipated and studied. While a challenging prospect, it is during this period that the identification of blood-based, metabolic biomarkers of liver-stage forms may one day become a reality, paving the way towards diagnostic tools and curative liver-stage treatments [77].

Conclusions

The *P. cynomolgi* – rhesus macaque model is invaluable for malaria research, particularly with regards to the direct study of both primary and relapse infections and pathophysiological mechanisms. This study uniquely provides a day-to-day clinical perspective in hematological changes during longitudinal infections, and sets the stage for systems biology investigations based on data from a few individuals [78, 79]. Here, all five subjects showed different degrees of clinical severity. It is anticipated that future analyses (immunological, biochemical, etc.) using the blood and bone marrow specimens collected from this experiment, with the integration of such data with the fundamental information presented here, will lead to the identification of possible mechanisms and an improved understanding of anemia, thrombocytopenia, and relapses. Notably, the current data has provided insight into relapse biology by demonstrating that *bona fide* relapses did not result in signs of clinical malaria. This was not necessarily expected and is important to consider when assessing both the clinical and epidemiological impact of relapses caused by *P. vivax* and *P. ovale*.

Funding

This project was funded in part by Federal funds from the US National Institute of Allergy and Infectious Diseases, National Institutes of Health, Department of Health and Human Services under contract # HHSN272201200031C (PI: Mary Galinski), which supports the Malaria Host–Pathogen Interaction Center (MaHPIC), as well as the Office of Research Infrastructure Programs/OD P51OD011132.

Authors' Contributions

Conceived and designed the experiments: MRG, AM, EVSM, JWB and members of the MaHPIC Consortium. Performed the experiments: CJ, MCM, and members of the MaHPIC consortium. Managed and deposited the data and metadata: JCK and members of the MaHPIC consortium. Performed data analysis and generated the figures: CJ. Interpreted the data analysis: CJ, AM, JWB, MRG. Wrote the paper: CJ, MRG. Provided expert knowledge, viewpoints and manuscript contributions: AM, JWB, JCK, and members of the MaHPIC consortium.

Acknowledgements

The authors acknowledge faculty and staff of Yerkes National Primate Research Center, especially the Animal Resources and Veterinary Departments, for their assistance. A special thanks is given to veterinarian Jennifer S. Wood for her consultations regarding the clinical presentations of the animals.

MaHPIC Consortium: Amy Kong, Chris Ibegbu, Dalia Arafat, Dean Jones, Douglas P. Nace, Eberhard O. Voit, Jan Pohl, Jay Humphrey, Jeremy DeBarry, JoAnn Sullivan, Juan B. Gutierrez, Kevin J Lee, Luis L. Fonseca, Mark Styczynski, Mustafa Nural, Sarah T. Pruett, Stacey A. Lapp, Suman Pakala, Tracey J. Lamb, Tyrone Williams, Karan Uppal, ViLinh Tran, Weiwei Yin, Yi Yan

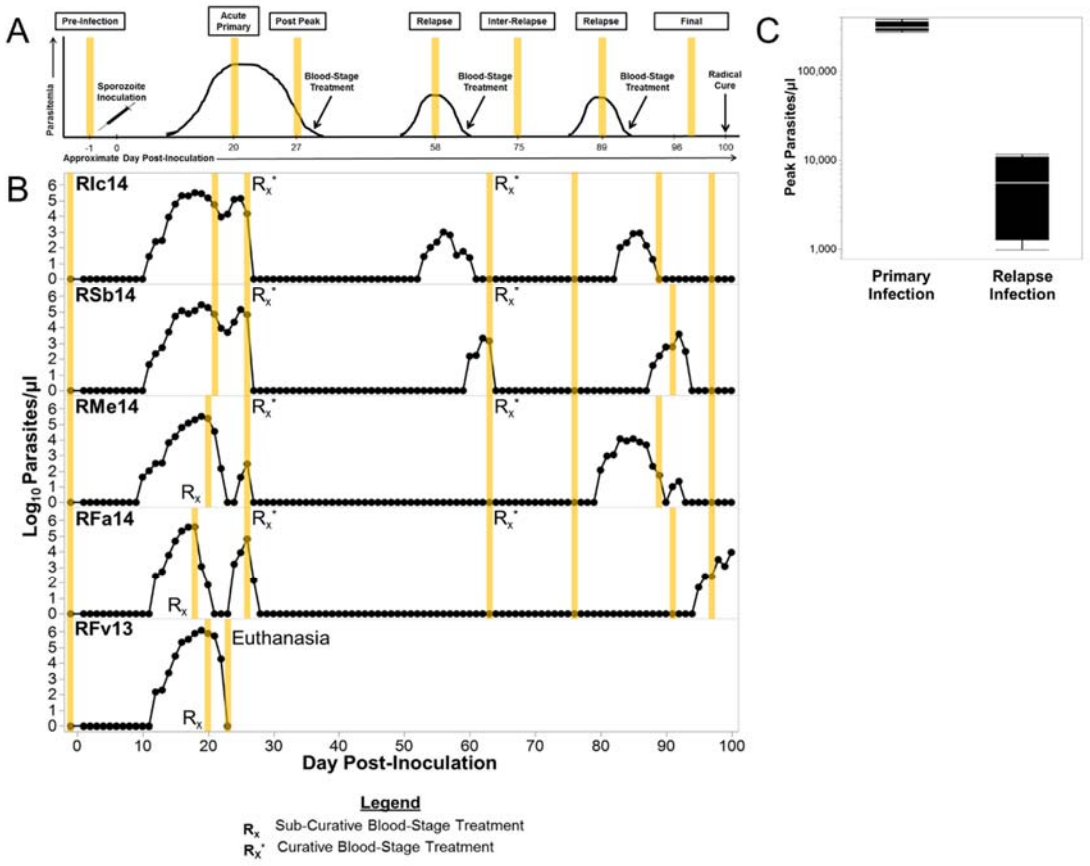

Figure 1. Study design, parasitemias, and treatment regimens of rhesus macaques infected with *P. cynomolgi* sporozoites. (A) Longitudinal study design to collect whole blood and bone marrow aspirates for current and retrospective analyses at critical infection points as indicated (yellow). (B) Log_{10} parasitemia and treatment regimens for the five rhesus macaques infected with 2,000 *P. cynomolgi* B strain sporozoites on Day 0 are shown. Whole blood and bone marrow aspirate sample collections are marked in yellow for each animal and correspond with critical infection points depicted in Panel A and summarized in Table 1. Sub-curative and curative blood-stage treatments were administered as needed based on the clinical complications that occurred during the primary infection and to ensure *bona fide* relapses. (C) The mean of the peak parasitemias for the primary and first relapses of RIc14, RSb14, RMe14, and RFa14 are shown. Statistical significance was assessed by a Wilcoxon-Matched pairs sign rank test; p-values less than 0.05 were considered significant.

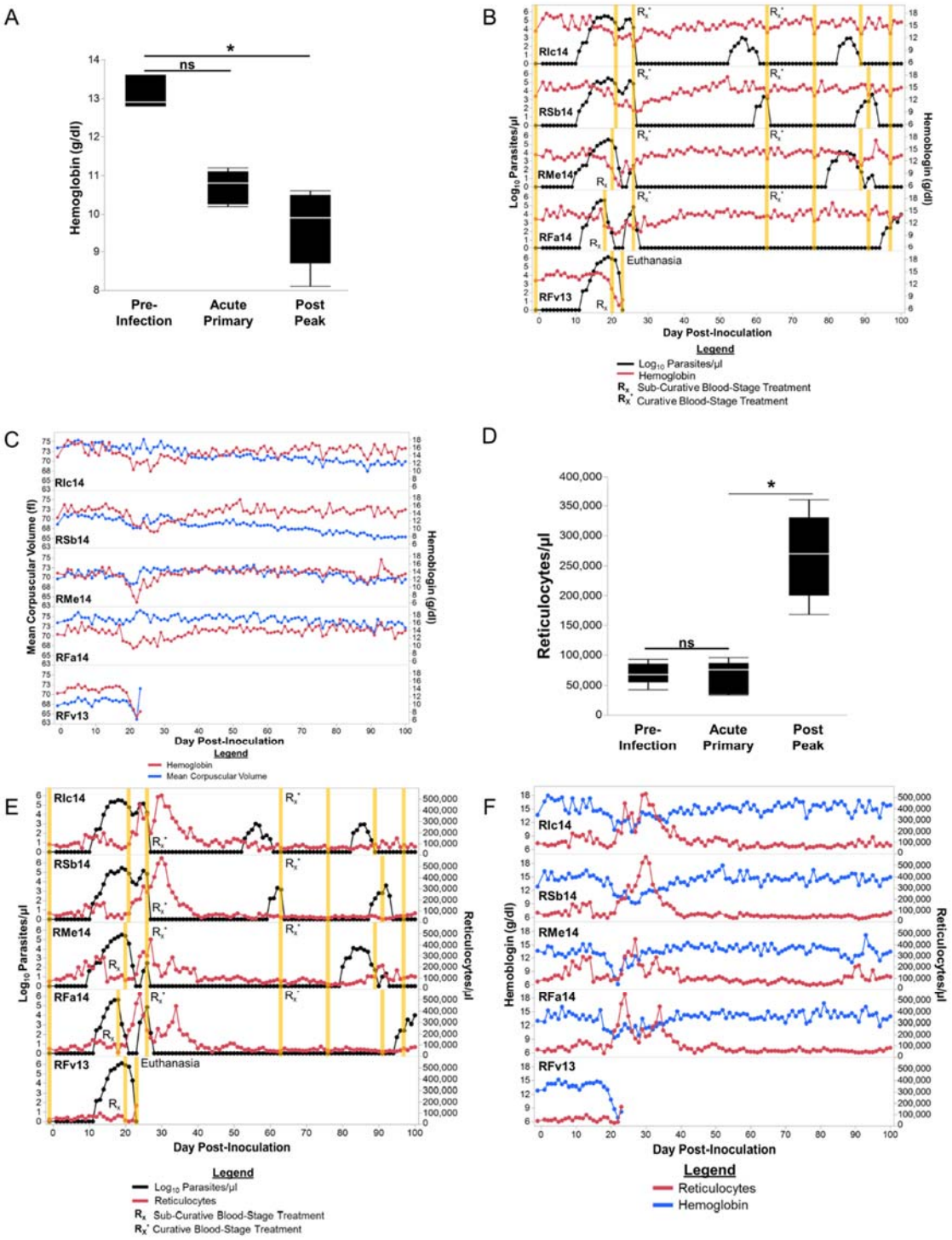

Figure 2. *Plasmodium cynomolgi* B strain infection in rhesus macaques induces moderate to severe anemia. (A) Hemoglobin concentrations of five rhesus macaques are shown prior to infection, during the acute primary, and after the peak of parasitemia. (B) Hemoglobin kinetics in

relation to parasitemia and the relationship between hemoglobin and MCV (C) for up to 100 days after inoculation are shown. (D) Reticulocyte concentrations of five rhesus macaques are indicated prior to infection, during the acute primary, and after the peak of parasitemia. (E) Reticulocyte dynamics in relation to parasitemia for up to 100 days after inoculation are depicted, and the relationship between hemoglobin and reticulocyte concentrations are shown in Panel F. Orange bars (B and E) indicate when peripheral blood and bone marrow aspirates were collected for retrospective systems biology analysis. Statistical analysis was performed by a Friedman's Test with Dunn's multiple comparison post-hoc for Panels A and D; *= $p < 0.05$, ns = not significant.

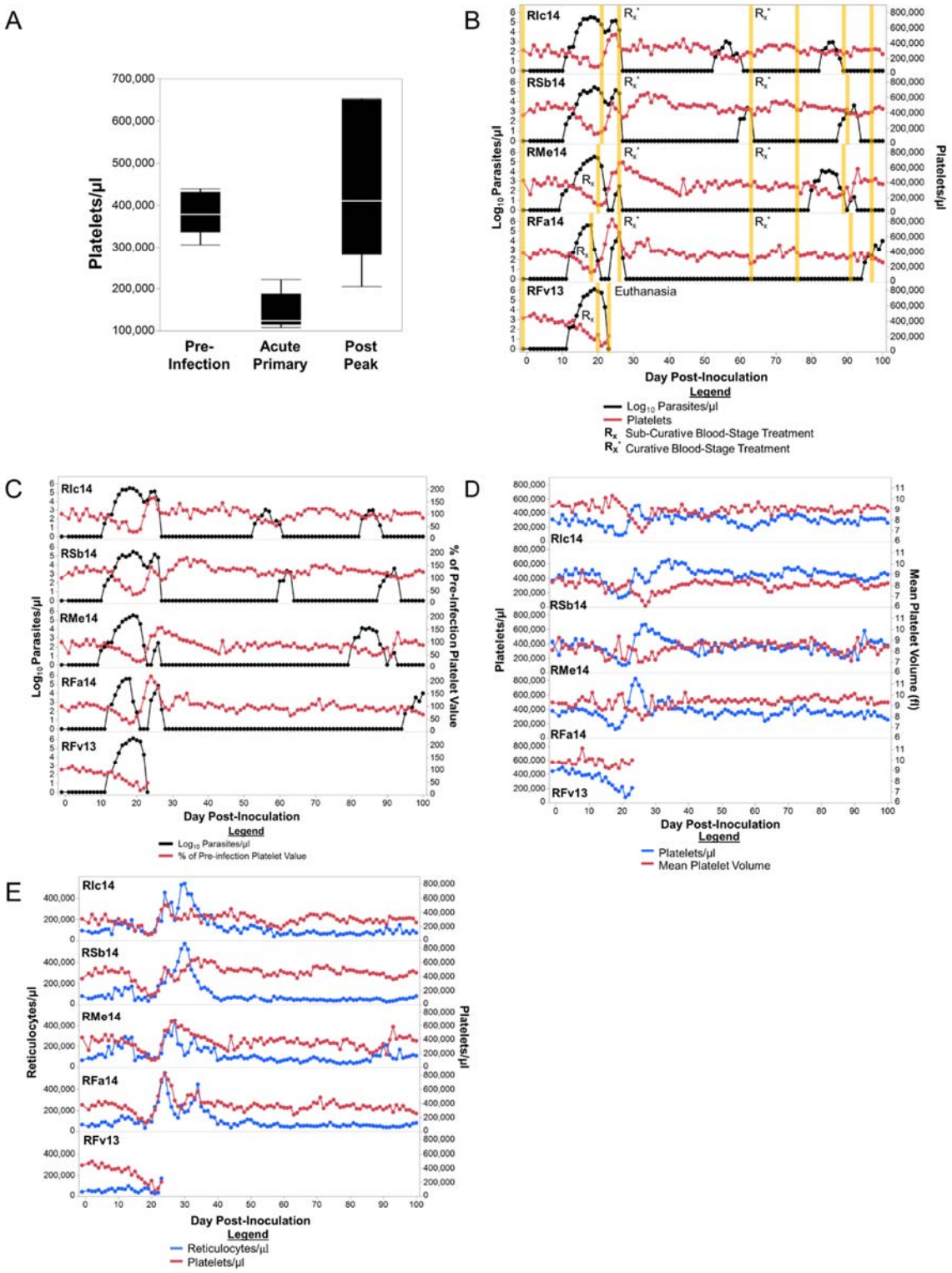

Figure 3. *Plasmodium cynomolgi* B strain infection results in thrombocytopenia during the primary infection. The mean platelet concentration (A) before infection, during the acute primary,

and post peak of parasitemia are shown. (B) Platelet concentrations in relation to parasitemia (B), pre-infection values (C), MPV (D), and reticulocyte numbers (E) are indicated for five macaques for up to 100 days after inoculation. Statistical analysis was performed by a Friedman's Test with Dunn's multiple comparison post-hoc for Panel A and no statistical significance was found.

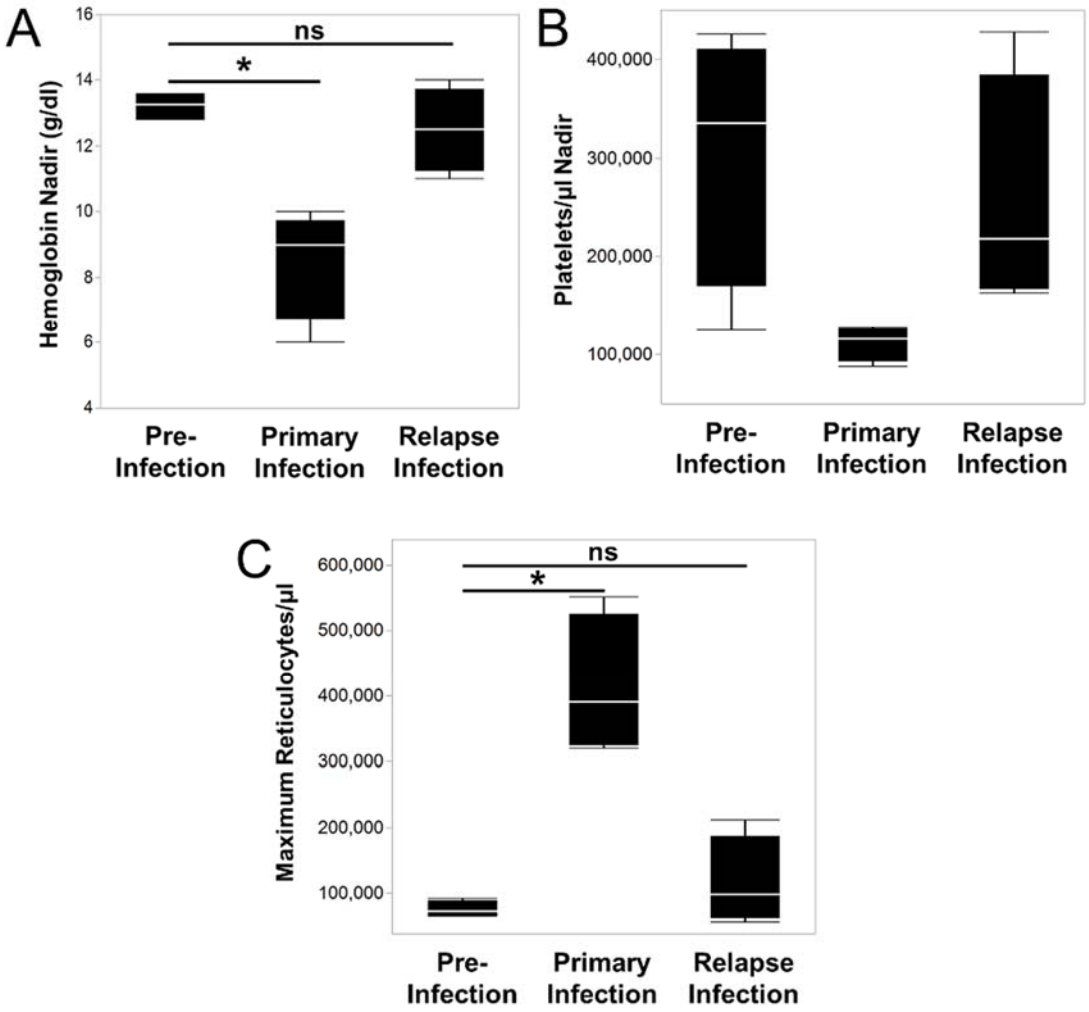

Figure 4. Homologous relapses induce minimal, if any, changes in clinical parameters from pre-infection values. The mean hemoglobin concentration (A), platelet nadir (B), and maximum number of reticulocytes (C) for RMe14, RFa14, RIc14, and RSb14 prior to infection, during the primary infection, and for relapses are shown. Statistical significance was assessed by a Friedman's Test with Dunn's multiple comparison post-hoc analysis. P-values less than 0.05 were considered significant; *= $p < 0.05$, ns = not significant.

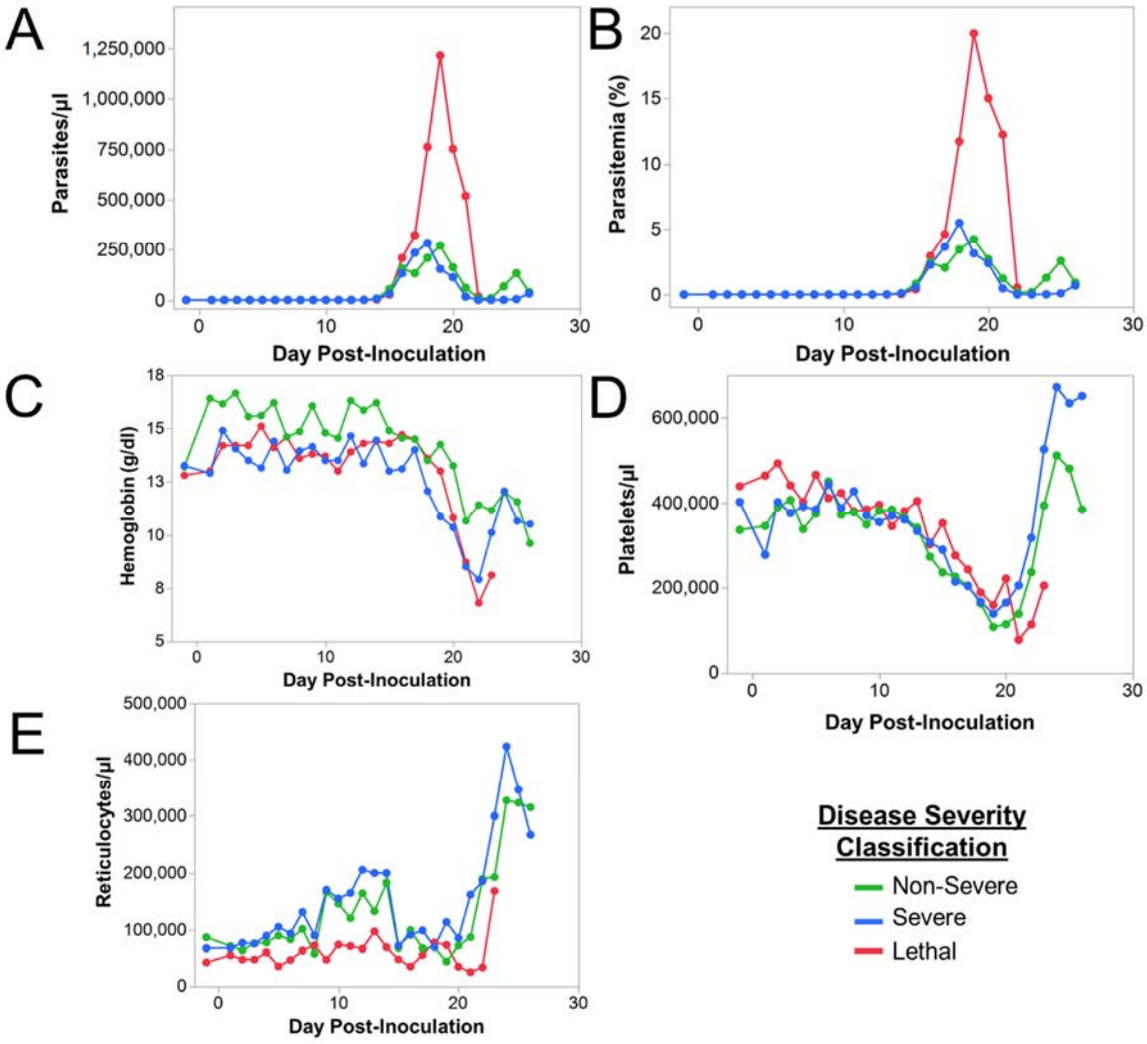

Figure 5. Higher parasitemia and less reticulocytes during early infection distinguish the lethal cynomolgi malaria infection. Parasitemia (A and B), hemoglobin kinetic (C), reticulocyte concentration (D), and platelet concentration (E) are shown comparing the three different cynomolgi infection clinical phenotypes. The average of the two non-severe and two severe animals were used for each point on the graph; since the lethal phenotype is unique, a single animal's values were used.

Table 2. Clinical summary and phenotype classification of rhesus macaques infected with *Plasmodium cynomolgi* B Strain					
	RSb14	**RIc14**	**RFa14**	**RMe14**	**RFv13**
Anemia **Degree**	Yes Moderate	Yes Moderate	Yes Moderate	Yes Severe	Yes Severe
Thrombocytopenia	Yes	Yes	Yes	Yes	Yes
Unique Sign	None	None	Petechiae	None	None
Sub-Curative Treatment	No	No	Yes	Yes	Yes
Additional Clinical Interventions	None	None	None	Blood Transfusion	Blood Transfusion
Clinical Phenotype Classification	**Non-Severe**		**Severe**		**Lethal**

References

1. WHO: *World Malaria Report.*2015.
2. Baird JK: Severe and fatal vivax malaria challenges 'benign tertian malaria' dogma. *Ann Trop Paediatr* 2009, 29.
3. Baird JK: Pernicious and Threatening *Plasmodium vivax* as Reality. *Am J Trop Med Hyg* 2014.
4. Price RN, Tjitra E, Guerra CA, Yeung S, White NJ, Anstey NM: Vivax malaria: neglected and not benign. *Am J Trop Med Hyg* 2007, 77.
5. Anstey NM, Douglas NM, Poespoprodjo JR, Price RN: *Plasmodium vivax*: clinical spectrum, risk factors and pathogenesis. *Adv Parasitol* 2012, 80:151-201.
6. Mueller I, Galinski MR, Baird JK, Carlton JM, Kochar DK, Alonso PL, del Portillo HA: Key gaps in the knowledge of *Plasmodium vivax*, a neglected human malaria parasite. *Lancet Infect Dis* 2009, 9:555-566.
7. Joyner CJ, Barnwell JW, Galinski MR: No More Monkeying Around: Primate Malaria Model Systems are Key to Understanding *Plasmodium vivax* Liver-Stage Biology, Hypnozoites, and Relapses. *Frontiers in Microbiology* 2015, 6.
8. Galinski MR, Meyer EV, Barnwell JW: *Plasmodium vivax*: Modern Strategies to Study a Persistent Parasite's Life Cycle. *Adv Parasitol* 2013, 81:1-26.
9. Noulin F, Borlon C, Van Den Abbeele J, D'Alessandro U, Erhart A: 1912-2012: a century of research on *Plasmodium vivax in vitro* culture. *Trends Parasitol* 2013.
10. Krotoski WA, Collins WE, Bray RS, Garnham PC, Cogswell FB, Gwadz RW, Killick-Kendrick R, Wolf R, Sinden R, Koontz LC, Stanfill PS: Demonstration of hypnozoites in sporozoite-transmitted *Plasmodium vivax* infection. *Am J Trop Med Hyg* 1982, 31:1291-1293.
11. Adekunle AI, Pinkevych M, McGready R, Luxemburger C, White LJ, Nosten F, Cromer D, Davenport MP: Modeling the Dynamics of *Plasmodium vivax* Infection and Hypnozoite Reactivation *In Vivo*. *PLoS Negl Trop Dis* 2015, 9:e0003595.
12. Perkins DJ, Were T, Davenport GC, Kempaiah P, Hittner JB, Ong'echa JM: Severe malarial anemia: innate immunity and pathogenesis. *Int J Biol Sci* 2011, 7:1427-1442.
13. Lamikanra AA, Brown D, Potocnik A, Casals-Pascual C, Langhorne J, Roberts DJ: Malarial anemia: of mice and men. *Blood* 2007, 110:18-28.
14. Lacerda MV, Mourao MP, Coelho HC, Santos JB: Thrombocytopenia in malaria: who cares? *Mem Inst Oswaldo Cruz* 2011, 106.
15. Castro-Gomes T, Mourao LC, Melo GC, Monteiro WM, Lacerda MV, Braga EM: Potential immune mechanisms associated with anemia in *Plasmodium vivax* malaria: a puzzling question. *Infect Immun* 2014, 82:3990-4000.
16. Coelho HC, Lopes SC, Pimentel JP, Nogueira PA, Costa FT, Siqueira AM, Melo GC, Monteiro WM, Malheiro A, Lacerda MV: Thrombocytopenia in *Plasmodium vivax* Malaria Is Related to Platelets Phagocytosis. *PLoS One* 2013, 8:e63410.
17. Coatney GR, Collins, W.E., Warren M., Contacos, P.G.: *Primate Malarias.* Washington DC: U. S. Dept. of Health, Education and Welfare; 1971.
18. Krotoski WA, Garnham PC, Bray RS, Krotoski DM, Killick-Kendrick R, Draper CC, Targett GA, Guy MW: Observations on early and late post-sporozoite tissue stages in primate malaria. I. Discovery of a new latent form of *Plasmodium cynomolgi* (the hypnozoite), and failure to detect hepatic forms within the first 24 hours after infection. *Am J Trop Med Hyg* 1982, 31:24-35.
19. Deye GA, Gettayacamin M, Hansukjariya P, Im-erbsin R, Sattabongkot J, Rothstein Y, Macareo L, Fracisco S, Bennett K, Magill AJ, Ohrt C: Use of a rhesus *Plasmodium*

cynomolgi model to screen for anti-hypnozoite activity of pharmaceutical substances. *Am J Trop Med Hyg* 2012, 86:931-935.

20. Dembele L, Gego A, Zeeman A-M, Franetich J-F, Silvie O, Rametti A, Le Grand R, Dereuddre-Bosquet N, Sauerwein R, van Gemert G-J, et al: Towards an *In Vitro* Model of *Plasmodium* Hypnozoites Suitable for Drug Discovery. *PLoS ONE* 2011, 6:e18162.
21. Galinski M, Barnwell, JW. : In *Nonhuman Primate Models for Human Malaria Research.* Edited by Christian R. Abee ST, and Timothy Morris London: Academic Press.; 2012: 299-323
22. Douglas AD, Baldeviano GC, Lucas CM, Lugo-Roman LA, Crosnier C, Bartholdson SJ, Diouf A, Miura K, Lambert LE, Ventocilla JA, et al: A PfRH5-based vaccine is efficacious against heterologous strain blood-stage *Plasmodium falciparum* infection in aotus monkeys. *Cell Host Microbe* 2015, 17:130-139.
23. Yadava A, Hall CE, Sullivan JS, Nace D, Williams T, Collins WE, Ockenhouse CF, Barnwell JW: Protective Efficacy of a *Plasmodium vivax* Circumsporozoite Protein-Based Vaccine in *Aotus nancymaae* Is Associated with Antibodies to the Repeat Region. *PLoS Negl Trop Dis* 2014, 8:e3268.
24. Anderson DC, Lapp SA, Akinyi S, Meyer EV, Barnwell JW, Korir-Morrison C, Galinski MR: *Plasmodium vivax* trophozoite-stage proteomes. *J Proteomics* 2015, 115:157-176.
25. Moreno-Perez DA, Degano R, Ibarrola N, Muro A, Patarroyo MA: Determining the *Plasmodium vivax* VCG-1 strain blood stage proteome. *J Proteomics* 2014, 113c:268-280.
26. Tachibana S, Sullivan SA, Kawai S, Nakamura S, Kim HR, Goto N, Arisue N, Palacpac NM, Honma H, Yagi M, et al: *Plasmodium cynomolgi* genome sequences provide insight into *Plasmodium vivax* and the monkey malaria clade. *Nat Genet* 2012, 44:1051-1055.
27. Waters AP, Higgins DG, McCutchan TF: Evolutionary relatedness of some primate models of *Plasmodium*. *Mol Biol Evol* 1993, 10:914-923.
28. Warren M, Skinner JC, Guinn E: Biology of the Simian Malarias of Southeast Asia. I. Host Cell Preferences of Young Trophozoites of Four Species of *Plasmodium*. *The Journal of Parasitology* 1966, 52:14-16.
29. Okenu DM, Meyer EV, Puckett TC, Rosas-Acosta G, Barnwell JW, Galinski MR: The reticulocyte binding proteins of *Plasmodium cynomolgi*: a model system for studies of *P. vivax*. *Mol Biochem Parasitol* 2005, 143:116-120.
30. Akinyi S, Hanssen E, Meyer EV, Jiang J, Korir CC, Singh B, Lapp S, Barnwell JW, Tilley L, Galinski MR: A 95 kDa protein of *Plasmodium vivax* and *P. cynomolgi* visualized by three-dimensional tomography in the caveola-vesicle complexes (Schuffner's dots) of infected erythrocytes is a member of the PHIST family. *Mol Microbiol* 2012, 84:816-831.
31. Aikawa M, Miller LH, Rabbege J: Caveola--vesicle complexes in the plasmalemma of erythrocytes infected by *Plasmodium vivax* and *P cynomolgi*. Unique structures related to Schuffner's dots. *Am J Pathol* 1975, 79:285-300.
32. Schmidt LH: Compatibility of relapse patterns of *Plasmodium cynomolgi* infections in rhesus monkeys with continuous cyclical development and hypnozoite concepts of relapse. *Am J Trop Med Hyg* 1986, 35:1077-1099.
33. Dembele L, Franetich JF, Lorthiois A, Gego A, Zeeman AM, Kocken CH, Le Grand R, Dereuddre-Bosquet N, van Gemert GJ, Sauerwein R, et al: Persistence and activation of malaria hypnozoites in long-term primary hepatocyte cultures. *Nat Med* 2014, 20:307-312.
34. Sestak K, Scheiners C, Wu XW, Hollemweguer E: Identification of anti-human CD antibodies reactive with rhesus macaque peripheral blood cells. *Veterinary Immunology and Immunopathology* 2007, 119:21-26.
35. Gibbs RA, Rogers J, Katze MG, Bumgarner R, Weinstock GM, Mardis ER, Remington KA, Strausberg RL, Venter JC, Wilson RK, et al: Evolutionary and biomedical insights from the rhesus macaque genome. *Science* 2007, 316:222-234.

36. Yan G, Zhang G, Fang X, Zhang Y, Li C, Ling F, Cooper DN, Li Q, Li Y, van Gool AJ, et al: Genome sequencing and comparison of two nonhuman primate animal models, the cynomolgus and Chinese rhesus macaques. *Nat Biotechnol* 2011, 29:1019-1023.
37. Anstey NM, Russell B, Yeo TW, Price RN: The pathophysiology of vivax malaria. *Trends Parasitol* 2009, 25.
38. Shortt HE, Garnham PCC: The pre-erythrocytic development of *Plasmodium cynomolgi* and *Plasmodium vivax*. *Transactions of the Royal Society of Tropical Medicine and Hygiene* 1948, 41:785-795.
39. Organization WH: *Basic Malaria Microscopy.* Second Edition edn: World Health Organization; 2010.
40. Smucny DA, Allison DB, Ingram DK, Roth GS, Kemnitz JW, Kohama SG, Lane MA, Black A: Changes in blood chemistry and hematology variables during aging in captive rhesus macaques (*Macaca mulatta*). J Med Primatol 30:161-173, 2001. *J Med Primatol* 2004, 33:48-54.
41. Organization WH: *Management of severe malaria - A practical handbook.* Third edn. World Health Organization: World Health Organization; 2013.
42. Aurrecoechea C, Brestelli J, Brunk BP, Dommer J, Fischer S, Gajria B, Gao X, Gingle A, Grant G, Harb OS, et al: PlasmoDB: a functional genomic database for malaria parasites. *Nucleic Acids Research* 2009, 37:D539-D543.
43. Moreno A, Cabrera-Mora M, Garcia A, Orkin J, Strobert E, Barnwell JW, Galinski MR: *Plasmodium coatneyi* in rhesus macaques replicates the multisystemic dysfunction of severe malaria in humans. *Infect Immun* 2013, 81:1889-1904.
44. Hanson J, Phu NH, Hasan MU, Charunwatthana P, Plewes K, Maude RJ, Prapansilp P, Kingston HW, Mishra SK, Mohanty S, et al: The clinical implications of thrombocytopenia in adults with severe falciparum malaria: a retrospective analysis. *BMC Med* 2015, 13:97.
45. Lacerda MVG: Clinical manifestations and pathogenesis of malarial thrombocytopenia. In *PhD Thesis.* Tropical Medicine Department: University of Brasília; 2007
46. Martinez-Salazar EL, Tobon-Castano A: Platelet profile is associated with clinical complications in patients with vivax and falciparum malaria in Colombia. *Rev Soc Bras Med Trop* 2014, 47:341-349.
47. Rodriguez-Morales AJ, Giselle-Badillo A, Manrique-Castano S, Yepes MC: Anemia and thrombocytopenia in *Plasmodium vivax* malaria is not unusual in patients from endemic and non-endemic settings. *Travel Med Infect Dis* 2014, 12:549-550.
48. Silva SBR: Evaluation of frequency and factors associated to thrombocytopenia caused by *Plasmodium vivax*. In *Master Dissertation.* 2009
49. Moreno A, Garcia A, Cabrera-Mora M, Strobert E, Galinski MR: Disseminated intravascular coagulation complicated by peripheral gangrene in a rhesus macaque (*Macaca mulatta*) experimentally infected with *Plasmodium coatneyi*. *Am J Trop Med Hyg* 2007, 76:648-654.
50. Lamikanra AA, Brown D, Potocnik A, Casals-Pascual C, Langhorne J, Roberts DJ: Malarial anemia: of mice and men. *Blood* 2007, 110.
51. Jakeman GN, Saul A, Hogarth WL, Collins WE: Anaemia of acute malaria infections in non-immune patients primarily results from destruction of uninfected erythrocytes. *Parasitology* 1999, 119.
52. Collins WE, Jeffery GM, Roberts JM: A retrospective examination of anemia during infection of humans with *Plasmodium vivax*. *Am J Trop Med Hyg* 2003, 68.
53. Evans KJ, Hansen DS, van Rooijen N, Buckingham LA, Schofield L: Severe malarial anemia of low parasite burden in rodent models results from accelerated clearance of uninfected erythrocytes. *Blood* 2006, 107:1192-1199.

54. Price RN, Simpson JA, Nosten F, Luxemburger C, Hkirijaroen L, ter Kuile F, Chongsuphajaisiddhi T, White NJ: Factors contributing to anemia after uncomplicated falciparum malaria. *Am J Trop Med Hyg* 2001, 65.
55. Lamikanra AA, Merryweather-Clarke AT, Tipping AJ, Roberts DJ: Distinct Mechanisms of Inadequate Erythropoiesis Induced by Tumor Necrosis Factor Alpha or Malarial Pigment. *PLoS ONE* 2015, 10:e0119836.
56. Lamikanra AA, Theron M, Kooij TW, Roberts DJ: Hemozoin (malarial pigment) directly promotes apoptosis of erythroid precursors. *PLoS One* 2009, 4:e8446.
57. Casals-Pascual C, Kai O, Cheung JO, Williams S, Lowe B, Nyanoti M, Williams TN, Maitland K, Molyneux M, Newton CR, et al: Suppression of erythropoiesis in malarial anemia is associated with hemozoin *in vitro* and *in vivo*. *Blood* 2006, 108:2569-2577.
58. Pain A, Ferguson DJP, Kai O, Urban BC, Lowe B, Marsh K, Roberts DJ: Platelet-mediated clumping of *Plasmodium falciparum*-infected erythrocytes is a common adhesive phenotype and is associated with severe malaria. *Proceedings of the National Academy of Sciences* 2001, 98:1805-1810.
59. Skudowitz RB, Katz J, Lurie A, Levin J, Metz J: Mechanisms of thrombocytopenia in malignant tertian malaria. *Br Med J* 1973, 2:515-518.
60. Sodeman Jr WA, Jeffery GM: Primary malarial thrombocytopenia in the rhesus monkey. *Transactions of the Royal Society of Tropical Medicine and Hygiene* 1966, 60:70-74.
61. Leal-Santos FA, Silva SB, Crepaldi NP, Nery AF, Martin TO, Alves-Junior ER, Fontes CJ: Altered platelet indices as potential markers of severe and complicated malaria caused by *Plasmodium vivax*: a cross-sectional descriptive study. *Malaria Journal* 2013, 12:1-6.
62. Coelho HCC, Lopes SCP, Pimentel JPD, Nogueira PA, Costa FTM, Siqueira AM, Melo GC, Monteiro WM, Malheiro A, Lacerda MVG: Thrombocytopenia in *Plasmodium vivax* malaria is related to platelets phagocytosis. *PLoS ONE* 2013, 8:e63410.
63. Naing C, Whittaker MA, Nyunt Wai V, Mak JW: Is *Plasmodium vivax* malaria a severe malaria?: A Systematic Review and Meta-Analysis. *PLoS Negl Trop Dis* 2014, 8:e3071.
64. Quispe AM, Pozo E, Guerrero E, Durand S, Baldeviano GC, Edgel KA, Graf PC, Lescano AG: *Plasmodium vivax* Hospitalizations in a Monoendemic Malaria Region: Severe Vivax Malaria? *Am J Trop Med Hyg* 2014.
65. Arévalo-Herrera M, Lopez-Perez M, Medina L, Moreno A, Gutierrez JB, Herrera S: Clinical profile of *Plasmodium falciparum* and *Plasmodium vivax* infections in low and unstable malaria transmission settings of Colombia. *Malaria Journal* 2015, 14:154.
66. Beier JC, Davis JR, Vaughan JA, Noden BH, Beier MS: Quantitation of *Plasmodium falciparum* sporozoites transmitted *in vitro* by experimentally infected *Anopheles gambiae* and *Anopheles stephensi*. *Am J Trop Med Hyg* 1991, 44:564-570.
67. Medica DL, Sinnis P: Quantitative Dynamics of *Plasmodium yoelii* Sporozoite Transmission by Infected Anopheline Mosquitoes. *Infection and Immunity* 2005, 73:4363-4369.
68. Collins WE: Primate Malarias. *Advances in veterinary science and comparative medicine* 1974, 18:1-23.
69. Lombardini ED, Gettayacamin M, Turner GD, Brown AE: A Review of *Plasmodium coatneyi*-Macaque Models of Severe Malaria. *Vet Pathol* 2015, 52:998-1011.
70. Robinson LJ, Wampfler R, Betuela I, Karl S, White MT, Li Wai Suen CS, Hofmann NE, Kinboro B, Waltmann A, Brewster J, et al: Strategies for understanding and reducing the *Plasmodium vivax* and *Plasmodium ovale* hypnozoite reservoir in Papua New Guinean children: a randomised placebo-controlled trial and mathematical model. *PLoS Med* 2015, 12:e1001891.
71. Bright AT, Manary MJ, Tewhey R, Arango EM, Wang T, Schork NJ, Yanow SK, Winzeler EA: A High Resolution Case Study of a Patient with Recurrent *Plasmodium vivax*

Infections Shows That Relapses Were Caused by Meiotic Siblings. *PLoS Negl Trop Dis* 2014, 8:e2882.

72. Bright AT, Alenazi T, Shokoples S, Tarning J, Paganotti GM, White NJ, Houston S, Winzeler EA, Yanow SK: Genetic analysis of primaquine tolerance in a patient with relapsing vivax malaria. *Emerg Infect Dis* 2013, 19:802-805.
73. Imwong M, Boel ME, Pagornrat W, Pimanpanarak M, McGready R, Day NP, Nosten F, White NJ: The first *Plasmodium vivax* relapses of life are usually genetically homologous. *J Infect Dis* 2012, 205:680-683.
74. White MT, Karl S, Battle KE, Hay SI, Mueller I, Ghani AC: Modelling the contribution of the hypnozoite reservoir to *Plasmodium vivax* transmission. *Elife* 2014, 3.
75. White NJ, Imwong M: Relapse. *Adv Parasitol* 2012, 80:113-150.
76. Imwong M, Snounou G, Pukrittayakamee S, Tanomsing N, Kim JR, Nandy A, Guthmann JP, Nosten F, Carlton J, Looareesuwan S, et al: Relapses of *Plasmodium vivax* infection usually result from activation of heterologous hypnozoites. *J Infect Dis* 2007, 195.
77. Salinas JL, Kissinger JC, Jones DP, Galinski MR: Metabolomics in the fight against malaria. *Mem Inst Oswaldo Cruz* 2014, 109:589-597.
78. Chen R, Mias GI, Li-Pook-Than J, Jiang L, Lam HY, Chen R, Miriami E, Karczewski KJ, Hariharan M, Dewey FE, et al: Personal omics profiling reveals dynamic molecular and medical phenotypes. *Cell* 2012, 148:1293-1307.
79. Li S, Todor A, Luo R: Blood transcriptomics and metabolomics for personalized medicine. *Computational and Structural Biotechnology Journal* 2016, 14:1-7.

Chapter III

Severe and complicated cynomolgi malaria in a rhesus macaque resulted in similar histopathological changes as those seen in human malaria

Chester J. Joyner[1], the MaHPIC Consortium[1], Jennifer S. Wood[5], Alberto Moreno[1, 2, 3], Anapatricia Garcia[4,] and Mary R. Galinski[1,2, 3*]

[1]Malaria Host–Pathogen Interaction Center

[2]Emory Vaccine Center, Yerkes National Primate Research Center, Emory University, Atlanta, GA, USA

[3]Division of Infectious Diseases, Department of Medicine, Emory University, Atlanta, GA, USA

[4]Division of Pathology, Yerkes National Primate Research Center, Emory University, Atlanta, GA, USA

[5]Division of Animal Resources, Yerkes National Primate Research Center, Emory University, Atlanta, GA, USA

[*] corresponding author

Published in *Am. J. Trop. Med. Hyg.*, 2017, 97(2).

Abstract

Histopathological data collected from patients with severe malaria have been instrumental for studying malaria pathogenesis. Animal models of malaria are critical to complement such studies. Here, the histopathological changes observed in a rhesus macaque with severe and complicated *Plasmodium cynomolgi* malaria are reported. The animal presented with thrombocytopenia, severe anemia, and hyperparasitemia during the acute infection. The macaque was given sub-curative anti-malarial treatment, fluid support, and a blood transfusion to treat the clinical complications, but at the time of transfusion, kidney function was compromised. These interventions did not restore kidney function, and the animal was euthanized due to irreversible renal failure. Gross pathological and histological examinations revealed that the lungs, kidneys, liver, spleen and bone marrow exhibited abnormalities similar to those described in malaria patients. Overall, this case report illustrates the similarities in the pathophysiological complications that can occur in human malaria and cynomolgi malaria in rhesus macaques.

Introduction

Clinical malaria presents with a variety of signs and symptoms that range from asymptomatic to life-threatening, but the factors and mechanisms that result in this spectrum of disease severity are largely unknown.[1-4] Tissues collected at autopsy from humans who have succumbed to falciparum malaria have been informative for studies on severe and complicated malaria pathogenesis as well as parasite biology.[5-7] Nonhuman primate (NHP) and rodent malaria models have complemented these studies by enabling investigations of mechanisms that cannot be directly studied using patient samples or post-mortem tissues.[8-10] Similarly, studies using tissues collected from vivax malaria patients have provided insight into vivax malaria pathophysiology.[2, 11, 12] Complementary studies using animal models would greatly enhance the ability to study vivax malaria pathogenesis. However, rodent models of vivax malaria do not exist, and NHP models of vivax malaria have been underutilized.[13, 14]

The *Plasmodium cynomolgi* – rhesus macaque model of *P. vivax* infection mimics the hematological changes and clinical presentations observed in vivax malaria patients.[15] Additionally, *P. cynomolgi* shares many biological characteristics with *P. vivax* including genetic make-up [16], infected red blood cell (RBC) structures such as caveola vesicle complexes [17, 18], preferential invasion of reticulocytes [19], and formation of hypnozoites [20, 21]. These factors make this model system ideal for studying vivax malaria and determining if and which pathophysiological mechanisms are shared between vivax malaria in humans and cynomolgi malaria in rhesus macaques.

In this case report, the histopathological changes associated with severe and complicated cynomolgi malaria in a rhesus monkey are described for the first time to our knowledge.

Methods

Experimental Design. A case of severe and complicated malaria in an animal from a cohort of five *Macaca mulatta* (Indian rhesus macaques) experimentally infected with *P. cynomolgi* M/B strain[22] is presented here. A detailed description of the experimental procedures, animal housing, enrichment activities, clinical interventions, hematological parameters and clinical outcomes has been reported previously.[15]

Animal Use. This study was approved by Emory University's Institutional Animal Care and Use Committee. All endpoints, including humane euthanasia, were documented and approved. Regular consulting with Yerkes National Primate Research Center veterinarians and staff was done throughout the experiment.

Blood Chemistry. Blood was collected in a heparinized tube at the time of transfusion and analyzed using a Liasys serum chemistry automated analyzer.

Gross Pathology and Histological Analysis. Complete postmortem evaluation of this rhesus macaque was performed after IACUC approved-humane euthanasia. Organs from this animal were collected shortly after gross pathological examination. Sections of main organ tissues were collected and fixed in 10% buffered formalin and processed for routine histological evaluation following hematoxylin and eosin staining. [23] In addition, selected organ sections were stained with Masson's Trichrome blue or Pearl's iron stain using standard methodologies.[23]

Transmission Electron Microscopy. Selected tissue sections collected at the time of necropsy were processed for transmission electron microscopy (TEM) as previously described and evaluated using a JEM 1210 electron microscope.[24]

Data Deposition. Serum blood chemistry profiles are publicly available on PlasmoDB.[25]

Results

Clinical Presentation. The hematological and parasitological data related to this animal was previously presented in Joyner et al. but is summarized below.[15] A group of five rhesus macaques were experimentally infected with 2,000 freshly isolated *P. cynomolgi* M/B strain sporozoites via intravenous injection on Day 0, and the infection reached patency 12 days post-inoculation (PI). On day 19 PI, one animal presented with hyperparasitemia, 1,214,842 parasites/µl or 19.95%, and thrombocytopenia (<150,000 platelets/µl).[15] A sub-curative, blood-stage treatment using artemether (dose: 1 mg/kg) was subsequently administered intramuscularly on day 21 PI to reduce parasitemia. On day 22 PI, the parasitemia decreased after administration of artemether; however, hemoglobin dropped to 6.8 g/dl. The animal was given a whole blood transfusion to treat severe anemia, and at the time of transfusion, the serum chemistry profile was determined. Liver dysfunction was evident based on elevated serum aspartate aminotransferase (AST) and alanine aminotransferase (ALT) concentrations (Table 1). Kidney dysfunction was also apparent based on elevated serum blood urea nitrogen (BUN), creatinine, potassium, and decreased sodium concentrations (Table 1). On day 23 PI, the animal's condition had not improved despite veterinary interventions and supportive care (Table 1), and humane euthanasia was performed by intravascular pentobarbital overdose.

Physical Examination. The animal weighed 6.27 kg at the time of necropsy, and the physical appearance was fair. The mucous membranes were pale and had a yellow tint (data not shown).

Gross Pathology. Hepatosplenomegaly was evident with the spleen weighing 26.4 g, approximately eight times the normal weight, and the liver weighing 207.4 g, about double the normal weight. Both had a bronze discoloration (Figure 1A and data not shown). The lungs were pale and discolored with a green tint (Figure 3A). The kidneys were enlarged, swollen, and also discolored (Figure 5A). Upon sectioning, the kidneys were wet and congested in the medullary regions. Fluid was present in the abdomen. The alimentary canal, heart, skull, brain, bone marrow, joints, lymph nodes, pelvic organs, urinary bladder, and adrenals appeared normal (data not shown).

Histopathology. The spleen contained many macrophages with brown-black pigment, but negative for iron stain. This finding, consistent with the presence of hemozoin, was confirmed by TEM (Figure 1B-C). Interestingly, a macrophage containing hemozoin also appears to have phagocytosed an uninfected RBC (Figure 1E). Other splenic structures such as lymphoid follicles and periarteriolar lymphatic sheaths appeared morphologically normal (Figure 1B).

The bone marrow was moderately hypercellular (Figure 2A). Myeloid and erythroid cell lineages were present, although erythroid precursors were markedly increased (Figure 2A). Intriguingly, megakaryocytes were enlarged, dysplastic, and possessed multiple misshapen nuclei (Figures 2C and 2D). Hemozoin was scattered throughout the marrow and appeared to be contained within macrophages (Figure 2B).

The lungs showed signs of edema and interstitial pneumonia (Figure 3B). Multifocal areas of type II cell hyperplasia were observed, and some areas of the alveolar walls appeared mildly thickened with fibrin (Figures 3C and 3F). TEM revealed that the pulmonary interstitium contained filamentous structures consistent with fibrin deposition (Figures 3F and 3G). The alveolar walls had macrophages containing an electron-dense crystalloid material, consistent with hemozoin (Figures 3C and 3D).

The liver contained multiple areas of inflammatory infiltrates composed of plasma cells and lymphocytes; this was particularly evident in the portal areas (Figure 4C). The hepatocytes were vacuolated and occasionally appeared eosinophilic (Figure 4A). The sinusoids were lined by hemozoin-containing macrophages, likely Kupffer cells (Figures 4A and 4B). There was mild hemosiderosis, but most pigment was negative for iron stain (Figure 4B).

The kidneys contained many large hypercellular glomeruli, and the renal interstitium was edematous (Figures 5C and 5E). Interestingly, there were multiple areas with leukocyte infiltrates consisting of plasma cells, lymphocytes, and eosinophils (Figure 5F). The cuboidal epithelium lining renal tubules was eosinophilic and vacuolated (Figure 5C). Many tubules contained cellular and granular casts (Figure 5B) and were lined by cuboidal epithelium that appeared to be

undergoing necrosis or apoptosis based on the pyknotic and karyorrhectic morphology of the nuclei (Figure 5C). Mineralization was evident in some tubules (Figure 4D).

Discussion

A case of a rhesus macaque with severe cynomolgi malaria that became complicated by renal failure due to acute tubular necrosis was presented here. This animal's renal function did not improve after anti-malarial treatment, intravenous fluid therapy, and blood transfusion, likely due to the severity of the renal dysfunction. Indeed, serum concentrations of creatinine similar to this animal's levels have been associated with poor outcomes in humans.[26] Leukocyte infiltrates composed of plasma cells, eosinophils, and lymphocytes were identified in the kidney, suggesting that these cells may be involved in renal complications.

Hepatic dysfunction was also evident based on hepatomegaly and elevated AST and ALT levels. Interestingly, the liver appeared mostly normal despite evidence of inflammation and leukocyte infiltrates. Hepatocyte degeneration was not observed, as reported in vivax malaria, raising the question whether this finding in humans may be due to other comorbidities in endemic areas.[11]

Respiratory distress is common during complicated vivax malaria, and signs of mild respiratory distress including edema, interstitial pneumonia, type II cell hyperplasia, and fibrin deposition were observed here.[2, 12] Parasites were not observed in the lung tissue, unlike previous reports from malaria patients.[11] This may be because the animal was sub-curatively treated 48 h prior to necropsy. Future studies using the rhesus macaque model could be designed to forego treatment to determine if *P. cynomolgi* predominates in the lungs compared to other organs, as speculated with *P. vivax*.

Macrophages containing hemozoin were abundant in the spleen, and one macrophage observed by TEM had internalized an uninfected RBC. This finding provides supporting evidence that phagocytosis of uninfected RBCs occurs in vivo. [27-29] Future studies can explore this further using ex vivo samples from carefully timed splenectomies or terminal studies to understand mechanisms relating to the removal of uninfected RBCs.

Alterations in bone marrow morphology were strikingly similar to that reported in humans.[30-32] Myeloid and erythroid cell lineages were markedly increased, hemozoin-containing macrophages were evident throughout the marrow in close proximity to the erythroid series, and megakaryocytes possessed aberrant morphology. This rhesus macaque model enabling multiple bone marrow draws is particularly well-suited for in-depth studies of bone marrow dysfunction and anemia during malaria.

Collectively, the histopathological changes observed here are remarkably similar to severe and complicated malaria in humans. This report supports the use of NHP models to explore malaria pathogenesis and to complement clinical or post-mortem studies with human tissues.

Acknowledgements

The author's would like to thank Dr. John W. Barnwell for helpful discussions and insights related to this case report. Special thanks are also extended to the Yerkes National Primate Research Center veterinary and animal research services staff for their continued support, assistance, and helpful discussions.

Financial Support

This project was funded, in part, by Federal funds awarded from the US National Institute of Allergy and Infectious Diseases, National Institutes of Health, Department of Health and Human Services under contract # HHSN272201200031C (PI: Mary Galinski), which supports the Malaria Host–Pathogen Interaction Center (MaHPIC). Additional support from federal funds were provided by the Office of Research Infrastructure Programs/OD P51OD011132.

Table 1. Blood chemistry values of a rhesus macaque with severe and complicated cynomolgi malaria at the time of clinical intervention and 24 h after.			
Analyte	**Reference Range**	**Before Clinical Intervention**	**24h After Clinical Intervention**
Total Protein	7.8-9.6	5.6	5.9
Albumin	3.1-5.3	2.7	3
Globulin	1.5-7	2.9	2.9
A/G	1-100	0.9	1
AST-GOT	14-30 u/l	57	72
ALT-SGPT	14-30 u/l	152	114
Alkaline Phosphatase	100-277	228	385
GGTP	14-75	40	68
Bilirubin	0-3.7	0.3	0.2
BUN	8-30 mg/dl	180	171
Creatinine	0.8-2.3 mg/dl	8.3	8.6
B/C	1-25	21.8	22.3
Phosphorus	3.5-6.5	6.8	9.1
Glucose	84-131 mg/dl	93	77
Calcium	9.8-11.8 mg/dl	8.7	8.7
Magnesium	0.3-5	2	2.3
Sodium	142-160	130	134
Potassium	4.1-5.3	5.7	5.5
Chloride	97-113	93	99
Cholesterol	97-186	163	177
Triglycerides	0-800	560	605
Amylase	88-400	379	477
CPK	2-1500	299	558
NA/K		22	24

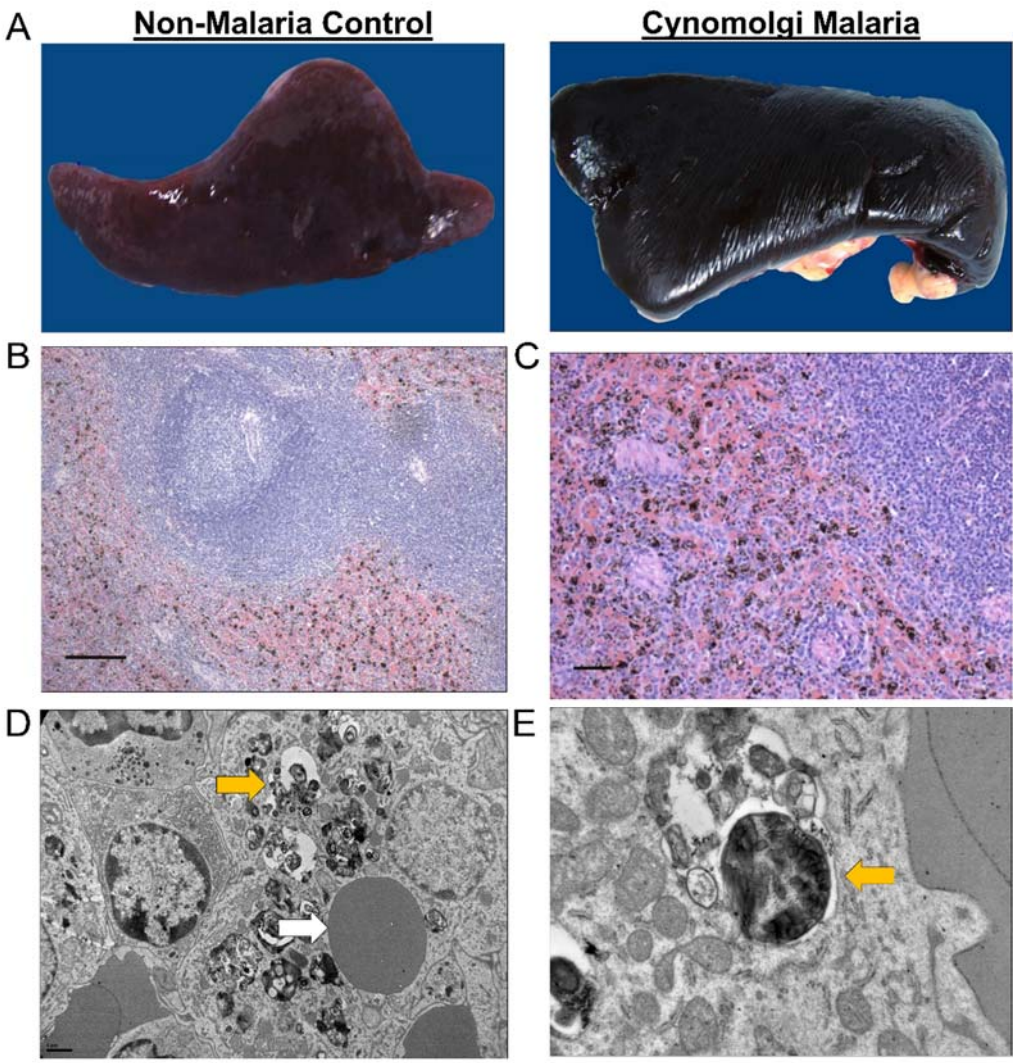

Figure 1. Erythrophagocytosis and hemozoin-containing phagocytes in the spleen during severe and complicated cynomolgi malaria. (A) Comparison of spleens collected at necropsy from a rhesus macaque with severe and complicated cynomolgi malaria and a rhesus euthanized for reasons other than malaria. (B and C) Hematoxylin and eosin tissue sections of the spleen from the rhesus with severe and complicated cynomolgi malaria. Notice diffuse deposition of a brown-black pigment consistent with hemozoin. (D) Transmission electron micrograph of a spleen depicting a macrophage containing an uninfected red blood cell and hemozoin crystals; yellow arrow= hemozoin, white arrow = uninfected red blood cell. (E) Higher magnification of E showing hemozoin contained within a vacuole inside a macrophage; yellow arrow = hemozoin.

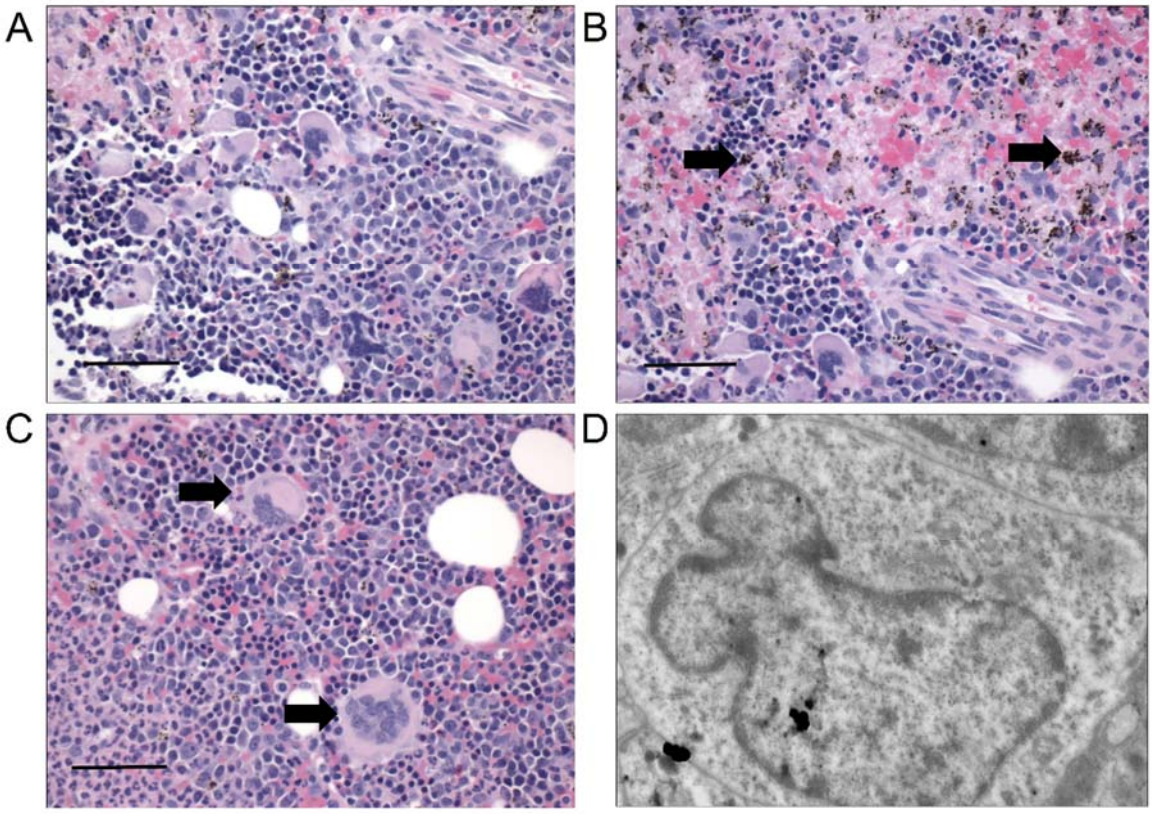

Figure 2. Sections of bone marrow during severe and complicated cynomolgi malaria. (A, B, C) Hematoxylin and eosin stained bone marrow sections from a rhesus macaque with severe and complicated cynomolgi malaria depicting expansion of erythroid precursors and dysplastic megakaryocytes. Panel B: black arrows = hemozoin; Panel C: black arrows = megakaryocytes. (D) Transmission electron micrograph of a megakaryocyte from Panel C with an immature, indented nucleus and decreased nucleus to cytoplasm ratio.

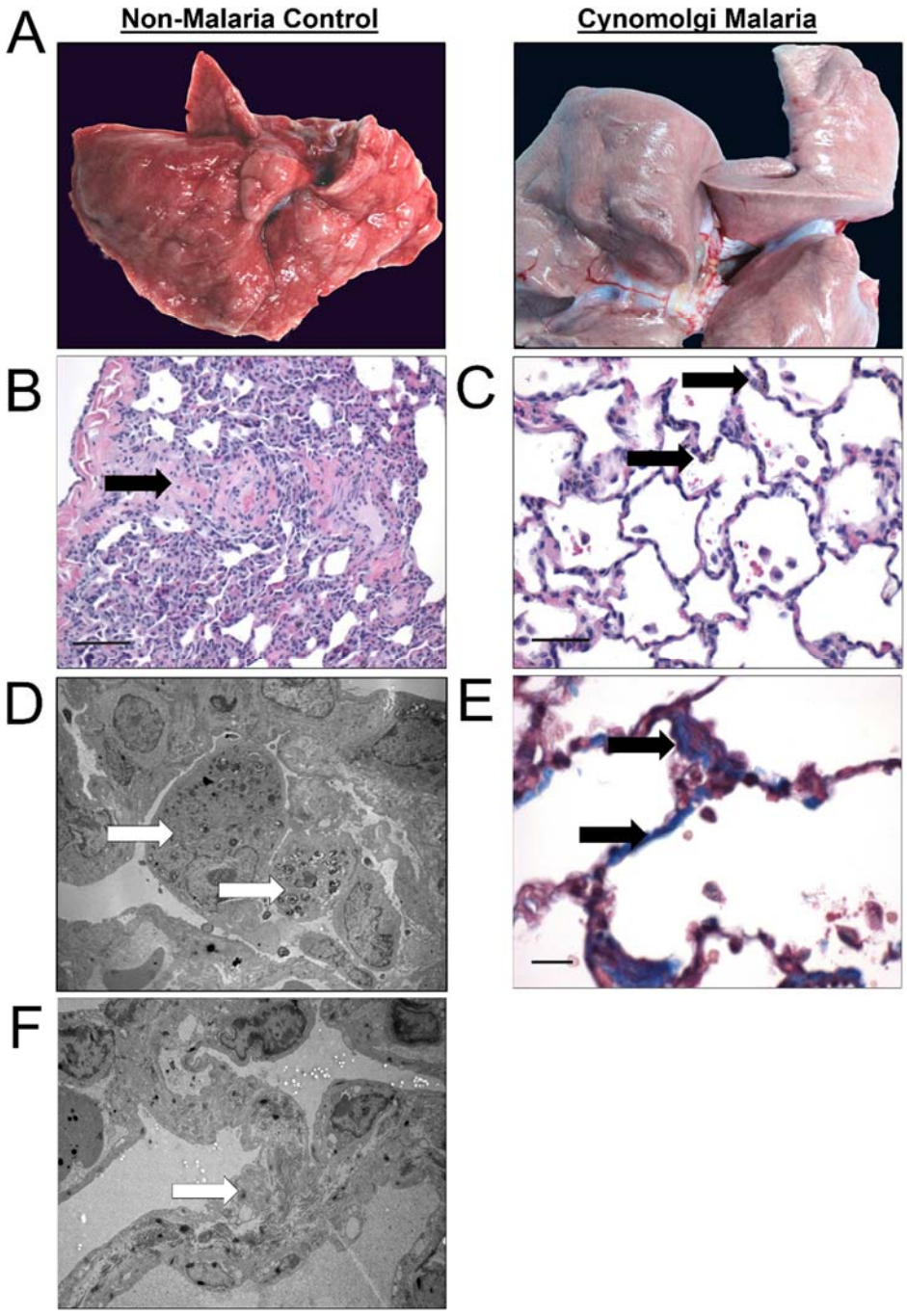

Figure 3. Pulmonary lesions during severe and complicated cynomolgi malaria. (A) Comparison of a lung collected at necropsy from the rhesus macaque with severe and complicated cynomolgi malaria and a rhesus euthanized for reasons other than malaria. (B, C) Digital micrographs of

sections from Panel A stained with hematoxylin and eosin. Black arrows indicate eosinophilic material in the parenchyma (B) and type II cell hyperplasia and alveolar macrophages (C). (D, F) Transmission electron micrographs from the infected lung in Panel A depicting a macrophage-containing hemozoin (D) and fibrils contained within Type II cells (F). (E) Lung tissue section stained with Masson's trichrome blue staining. Arrows indicate increased deposition of collagen within the interstitium in the lung.

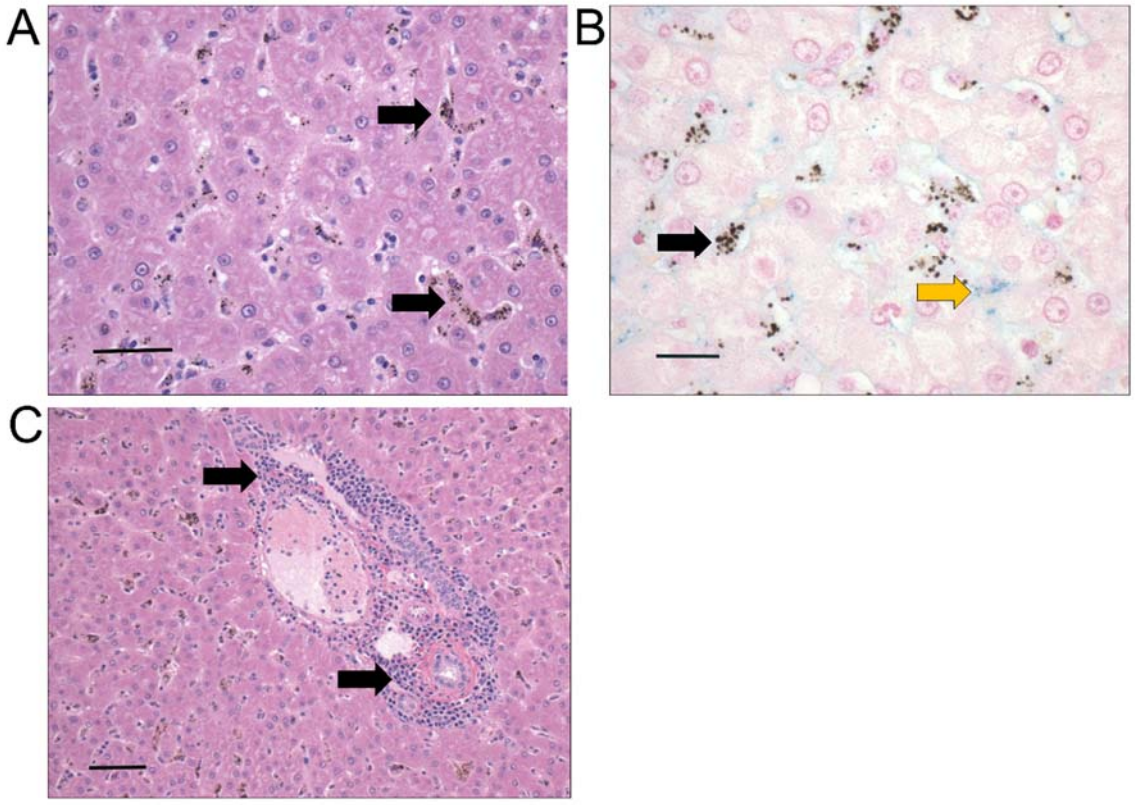

Figure 4. Liver section depicting leukocyte infiltrates and hemozoin-laden macrophages lining the sinusoids during severe and complicated cynomolgi malaria. (A, C) Hematoxylin and eosin stain of liver sections during severe and complicated cynomolgi malaria. (B) Liver section stained with Pearl's iron stain depicting blue stain of iron deposits. Panel A: black arrows = hemozoin in phagocytic cells lining the liver sinusoids. Panel B: black arrows = hemozoin; yellow arrow = iron deposits. Panel C: black arrows = lymphoplasmacytic infiltration within portal area.

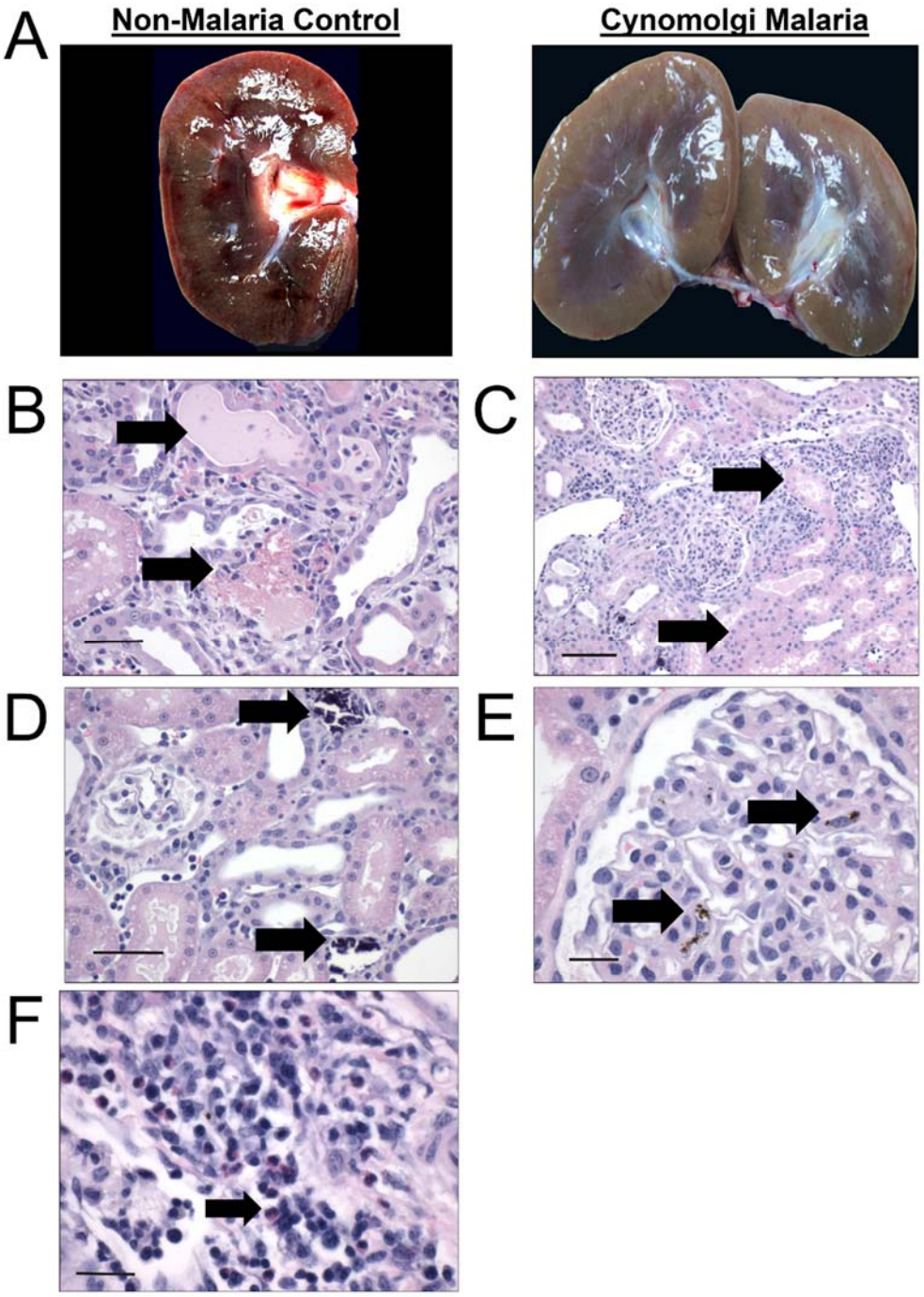

Figure 5. Gross and histological findings in the kidney during severe and complicated cynomolgi malaria. (A) Comparison of a kidney collected at necropsy from the rhesus macaque with severe and complicated cynomolgi malaria and a rhesus euthanized for reasons other than malaria. (B-F) Hematoxylin and eosin kidney sections during severe and complicated cynomolgi malaria. Panel

B: black arrows = cellular and hyaline casts; Panel C: black arrows = tubules lined with necrotic epithelium; Panel D: black arrows = mineralization in the kidney tubules; Panel E: black arrow = hemozoin in the glomerulus; Panel F: black arrow: inflammatory infiltration of plasma cells, lymphocytes and eosinophils in the interstitium.

References

1. Laishram DD, Sutton PL, Nanda N, Sharma VL, Sobti RC, Carlton JM, et al. The complexities of malaria disease manifestations with a focus on asymptomatic malaria. Malaria Journal 2012; 11:1-15.
2. Anstey NM, Russell B, Yeo TW, Price RN. The pathophysiology of vivax malaria. Trends Parasitol 2009; 25.
3. Anstey NM, Douglas NM, Poespoprodjo JR, Price RN. *Plasmodium vivax*: clinical spectrum, risk factors and pathogenesis. Adv Parasitol 2012; 80:151-201.
4. Wassmer SC, Taylor TE, Rathod PK, Mishra SK, Mohanty S, Arevalo-Herrera M, et al. Investigating the Pathogenesis of Severe Malaria: A Multidisciplinary and Cross-Geographical Approach. Am J Trop Med Hyg 2015; 93:42-56.
5. Joice R, Nilsson SK, Montgomery J, Dankwa S, Egan E, Morahan B, et al. *Plasmodium falciparum* transmission stages accumulate in the human bone marrow. Science Translational Medicine 2014; 6:244re245-244re245.
6. Hochman SE, Madaline TF, Wassmer SC, Mbale E, Choi N, Seydel KB, et al. Fatal Pediatric Cerebral Malaria Is Associated with Intravascular Monocytes and Platelets That Are Increased with HIV Coinfection. mBio 2015; 6.
7. Casals-Pascual C, Kai O, Cheung JO, Williams S, Lowe B, Nyanoti M, et al. Suppression of erythropoiesis in malarial anemia is associated with hemozoin in vitro and in vivo. Blood 2006; 108:2569-2577.
8. Lombardini ED, Gettayacamin M, Turner GD, Brown AE. A Review of *Plasmodium coatneyi*-Macaque Models of Severe Malaria. Vet Pathol 2015; 52:998-1011.
9. Lamikanra AA, Brown D, Potocnik A, Casals-Pascual C, Langhorne J, Roberts DJ. Malarial anemia: of mice and men. Blood 2007; 110:18-28.
10. Langhorne J, Buffet P, Galinski M, Good M, Harty J, Leroy D, et al. The relevance of non-human primate and rodent malaria models for humans. Malar J 2011; 10:23.
11. Lacerda MV, Fragoso SC, Alecrim MG, Alexandre MA, Magalhaes BM, Siqueira AM, et al. Postmortem characterization of patients with clinical diagnosis of *Plasmodium vivax* malaria: to what extent does this parasite kill? Clin Infect Dis 2012; 55:e67-74.
12. Valecha N, Pinto RG, Turner GD, Kumar A, Rodrigues S, Dubhashi NG, et al. Histopathology of fatal respiratory distress caused by *Plasmodium vivax* malaria. Am J Trop Med Hyg 2009; 81:758-762.
13. Joyner CJ, Barnwell JW, Galinski MR. No More Monkeying Around: Primate Malaria Model Systems are Key to Understanding *Plasmodium vivax* Liver-Stage Biology, Hypnozoites, and Relapses. Frontiers in Microbiology 2015; 6.
14. Galinski MR, Barnwell JW: Chapter 5 - Nonhuman Primate Models for Human Malaria Research**.** In *Nonhuman Primates in Biomedical Research (Second Edition).* Edited by Morris CRAMT. Boston: Academic Press; 2012: 299-323
15. Joyner C, Moreno A, Meyer EVS, Cabrera-Mora M, Kissinger JC, Barnwell JW, et al. *Plasmodium cynomolgi* infections in rhesus macaques display clinical and parasitological features pertinent to modelling vivax malaria pathology and relapse infections. Malaria Journal 2016; 15:1-18.
16. Tachibana S, Sullivan SA, Kawai S, Nakamura S, Kim HR, Goto N, et al. *Plasmodium cynomolgi* genome sequences provide insight into *Plasmodium vivax* and the monkey malaria clade. Nat Genet 2012; 44:1051-1055.
17. Aikawa M, Miller LH, Rabbege J. Caveola--vesicle complexes in the plasmalemma of erythrocytes infected by *Plasmodium vivax* and *P. cynomolgi*. Unique structures related to Schuffner's dots. Am J Pathol 1975; 79:285-300.
18. Akinyi S, Hanssen E, Meyer EV, Jiang J, Korir CC, Singh B, et al. A 95 kDa protein of *Plasmodium vivax* and *P. cynomolgi* visualized by three-dimensional tomography in the

caveola-vesicle complexes (Schuffner's dots) of infected erythrocytes is a member of the PHIST family. Mol Microbiol 2012; 84:816-831.
19. Warren M, Skinner JC, Guinn E. Biology of the Simian Malarias of Southeast Asia. I. Host Cell Preferences of Young Trophozoites of Four Species of Plasmodium. The Journal of Parasitology 1966; 52:14-16.
20. Krotoski WA, Garnham PC, Bray RS, Krotoski DM, Killick-Kendrick R, Draper CC, et al. Observations on early and late post-sporozoite tissue stages in primate malaria. I. Discovery of a new latent form of *Plasmodium cynomolgi* (the hypnozoite), and failure to detect hepatic forms within the first 24 hours after infection. Am J Trop Med Hyg 1982; 31:24-35.
21. Dembele L, Franetich JF, Lorthiois A, Gego A, Zeeman AM, Kocken CH, et al. Persistence and activation of malaria hypnozoites in long-term primary hepatocyte cultures. Nat Med 2014; 20:307-312.
22. Sutton PL, Luo Z, Divis PC, Friedrich VK, Conway DJ, Singh B, et al. Characterizing the genetic diversity of the monkey malaria parasite *Plasmodium cynomolgi*. Infect Genet Evol 2016; 40:243-252.
23. Sheehan D.C. HBB: *Theory and Practice of Histotechnology.* Second Edition edn. St. Luois, Toront, London: The C.V. Mosby Company.
24. Hayat M: *Basic Techniques for Transmission Electron Microscopy.* Elsevier, Inc.; 1986.
25. Aurrecoechea C, Brestelli J, Brunk BP, Dommer J, Fischer S, Gajria B, et al. PlasmoDB: a functional genomic database for malaria parasites. Nucleic Acids Research 2009; 37:D539-D543.
26. Sheiban AK. Prognosis of malaria associated severe acute renal failure in children. Ren Fail 1999; 21:63-66.
27. Fonseca LL, Alezi HS, Moreno A, Barnwell JW, Galinski MR, Voit EO. Quantifying the removal of red blood cells in Macaca mulatta during a *Plasmodium coatneyi* infection. Malaria Journal 2016; 15:1-15.
28. Jakeman GN, Saul A, Hogarth WL, Collins WE. Anaemia of acute malaria infections in non-immune patients primarily results from destruction of uninfected erythrocytes. Parasitology 1999; 119.
29. Fernandez-Arias C, Rivera-Correa J, Gallego-Delgado J, Rudlaff R, Fernandez C, Roussel C, et al. Anti-Self Phosphatidylserine Antibodies Recognize Uninfected Erythrocytes Promoting Malarial Anemia. Cell Host Microbe 2016; 19:194-203.
30. Abdalla SH. Hematopoiesis in human malaria. Blood Cells 1990; 16:401-416; discussion 417-409.
31. Wickramasinghe SN, Abdalla SH. Blood and bone marrow changes in malaria. Baillieres Best Pract Res Clin Haematol 2000; 13:277-299.
32. Knuttgen HJ. The bone marrow of non-immune Europeans in acute malaria infection: a topical review. Ann Trop Med Parasitol 1987; 81:567-576.

Chapter IV

Integrative analysis implicates monocytes in inefficient erythropoiesis during acute *Plasmodium cynomolgi* malaria in rhesus macaques

Yan Tang[1,2§], Chester J. Joyner[2§], Monica Cabrera-Mora[2], Celia L. Saney[2], Stacey A. Lapp[2], Mustafa V. Nural[2], Suman B. Pakala[2], Jeremy D. DeBarry[2], Stephanie Soderberg[2], the MaHPIC Consortium[2], Jessica C. Kissinger[2,3], Tracey J. Lamb[2,4], Mary R. Galinski[2,5], Mark P. Styczynski[1,2*]

[§]These authors contributed equally to this work

[1]School of Chemical & Biomolecular Engineering, Georgia Institute of Technology, Atlanta, Georgia, USA

[2]Malaria Host–Pathogen Interaction Center, Emory Vaccine Center, Yerkes National Primate Research Center, Emory University, Atlanta, GA, US

[3]Department of Genetics, Institute of Bioinformatics, Center for Tropical and Emerging Global Diseases, University of Georgia

[4]Department of Pathology, University of Utah, Salt Lake City, UT, USA

[5]Division of Infectious Diseases, Department of Medicine, Emory University, Atlanta, GA, USA

Published in *Malar. J.*, 2017, 16:34.

Abstract

Background: Mild to severe anemia is a common complication of malaria that is caused in part by inefficient erythropoiesis in the bone marrow. This study utilized systems biology to evaluate the transcriptional, cellular subset, and cytokine changes in the bone marrow during *P. cynomolgi* infection of rhesus macaques, a model of *Plasmodium vivax* malaria, that may underlie inefficient erythropoiesis.

Results: An appropriate erythropoietic response did not occur to compensate for anemia during acute cynomolgi malaria despite an increase in erythropoietin levels. During this period, there were significant perturbations in the bone marrow transcriptome. In contrast, relapses did not induce anemia and minimal changes in the transcriptome were detected. The differentially expressed genes during acute infection were primarily related to ongoing inflammatory responses with significant contributions from Type I and Type II Interferon transcriptional signatures. These were associated with increased frequency of intermediate and non-classical monocytes. Recruitment and/or expansion of these populations was correlated with a decrease in the erythroid progenitor population during acute infection, suggesting that monocyte-associated inflammation contributed to anemia. The decrease in erythroid progenitors was associated with downregulation of genes regulated by GATA1 and GATA2, two master regulators of erythropoiesis, providing a potential molecular basis for these findings.

Conclusions: These data suggest that malarial anemia may be driven by monocyte-associated suppression of GATA1/GATA2 in erythroid progenitors resulting in inefficient erythropoiesis during acute infection.

Background

Plasmodium vivax infections cause substantial morbidity with an estimated 8.5 million infections each year and can result in severe disease [1]. Anemia may occur during primary or relapse infections caused by *P. vivax* and may be due, in part, to bone marrow (BM) dysfunction as evidenced by post-mortem examinations of malaria patients [2]. This dysfunction leads to dyserythropoiesis and inefficient erythropoietic output to compensate for the loss of red blood cells (RBCs) from parasitism as well as immune-mediated removal of uninfected RBCs [3-6]. The underlying mechanisms and characteristics of BM dysfunction in humans remain poorly understood [2, 7, 8] due to the difficulties and ethical restrictions in obtaining longitudinal bone marrow samples from patients. Animal models can overcome this obstacle and be used to investigate mechanisms related to the development and recovery of BM dysfunction during malaria.

Nonhuman primate (NHP) macaque models are optimal for anemia studies in that they show very similar hematopoietic responses and erythropoietic processes as humans, and BM aspirates can be collected at multiple time points during longitudinal malaria studies [9, 10]. Although rodent models of malaria demonstrate overarching similarities in the development of anemia, differences in the hematopoietic responses between rodents and humans impose limitations on the extrapolation of some conclusions [11, 12]. For example, there are notable differences in the transcriptional programs that underlie erythropoiesis in mice compared to humans and different physiological mechanisms to deal with anemia [13].

The *Macaca mulatta* - *P. cynomolgi* model system recapitulates critical aspects of *P. vivax* infection in patients, including BM dysfunction and inefficient erythropoiesis during acute infections [10, 14, 15]. Importantly, *P. cynomolgi* also produces hypnozoites in the liver of rhesus macaques, enabling the study of relapse infections that occur with *P. vivax* in patients [9, 15, 16]. There has been extensive study of malaria-induced anemia in *P. falciparum*, in particular in the study of severe malarial anemia. Comparatively, much less is known about the pathogenesis of anemia during *P. vivax* infection, even though it is increasingly generally recognized that *P. vivax* also causes substantial anemia [17]. For example, P. vivax causes a greater removal of uninfected red blood cells than P. falciparum [18]. Furthermore, the effect of relapse infections on the bone marrow in comparison to an initial infection has not been thoroughly characterized even though relapses are speculated to potentially drive anemia in areas of high endemicity with frequent relapses [19].

Here, a malaria systems biology study is presented that used BM samples from a cohort of *M. mulatta* infected for about 100 days with *P. cynomolgi* M/B strain [9] as a model of vivax malaria. The main goal was to perform integrative analyses and identify potentially dysfunctional BM mechanisms that may contribute to anemia during acute vivax malaria and relapses. Multiple data types were generated, analyzed, and integrated (i.e. transcriptome, immune profiling, and clinical data). In this paper, we first present analysis of the transcriptome during the infection, focusing on large-scale changes via pathway analysis and highlighting the inflammation in the marrow during acute infection. We then explore what cell types may be responsible for these changes in the marrow and validate the upregulation of the immune pathways identified via transcriptional profiling by measuring systemic cytokine levels. Finally, we examine the consequence of all of these changes on erythroid progenitors, which pinpoints that there is likely disruption of GATA1/GATA2, which are known master regulators of erythroid differentiation.

Collectively, this is the first systems biology study to our knowledge using NHP models of *P. vivax* infection to study BM dysfunction and anemia.

Methods

Animals. Samples from a cohort of male rhesus macaques (*M. mulatta*) born and raised at the Yerkes National Primate Research Center (YNPRC), an AAALAC international certified institution, were used in this study. All male animals were used to avoid anemia related to the female menstrual cycle, which could confound interpretation of results. The animals were socially housed in pairs during the experiment, and all housing was in compliance with the Animal Welfare Act and Regulations, as well as the Guide for the Care and Use of Laboratory Animals. Details related to the animal's daily care have been reported in Joyner et al. [9].

Experimental Design. Bone marrow aspirates collected from four *M. mulatta* prior to infection and during *P. cynomolgi* M/B strain infections initiated by sporozoite inoculation were analyzed. The experimental design and clinical outcomes were described and analyzed previously [9]. Clinical parameters are discussed in this manuscript as relevant.

BM Collection and Processing. Seven BM aspirate specimens were collected in EDTA from each animal in the course of the 100-day experiment at pre-defined time points for simultaneous flow cytometry and RNA-Seq analysis as indicated in Figure 1A. Flow cytometry samples were processed as described below. For RNA-Seq analysis, BM mononuclear cells (MNCs) were isolated via Lymphoprep (Stem Cell Technologies) following the manufacturer's protocol. BM

MNCs were immediately placed into RLT buffer (Qiagen) after isolation, vortexed, and stored at -80ºC for RNA-Seq analysis.

Library preparation for RNA-Seq. RNA was extracted from BM MNCs using a Qiagen RNeasy Mini-Plus kit according to the manufacturer's instruction. After extraction, the quality of each sample was evaluated with a Bioanalyzer. An RNA Integrity Number [20] greater than eight, signifying good RNA quality, was recorded for all samples prior to library preparation. Approximately 1 μg of total RNA per sample type was reverse transcribed into double-stranded cDNA, with Illumina TruSeq Stranded mRNA Sample Prep kits used to generate strand-specific libraries. For quality control, total RNA for each library contained approximately 1% spike-in RNAs of known concentration and GC proportions (ERCC Spike-In Control, Life Technologies) [21]. Sequencing was done on an Illumina HiSeq 2000 at the YNPRC Genomics Core. Each library averaged approximately 50 million 100 bp paired-end reads.

Gene expression quantification. A whole-transcriptome profile of BM MNCs was generated by RNA-Seq, and over 50 million reads per sample were aligned jointly to concatenated host and parasite genomes (i.e. MacaM assembly, Version 4.0, GenBank accession number PRJNA214746 ID: 214746 and *P. cynomolgi* B/M strain PlasmoDB release-9.3) using Tophat2 with default parameters [22, 23]. Reads mapping to multiple genomic locations were excluded from analysis to ensure high-confidence mapping. Gene expression (read counts) were inferred at the level of annotated genes using HTSeq v0.5.4 [24]. Data reliability was assessed by several steps of quality control: linear correlation of spike-in control abundance with known concentration; confirmation of strand-specificity of controls as 99.9%; and confirmation of absence of 3' bias in the controls with RSeqC software [25]. Gene expression was normalized to library size with the R package DESeq (version1.10.1;[26]), used with default parameters.

RNA-Seq Data Processing. For macaque RNA-Seq, features with an FPKM value (Fragments Per Kilobase of transcript per Million mapped reads) below 5 were excluded from analysis. Gene

expression data were log2 transformed. A large variance in gene expression was observed among animals (Additional File 1B); Supervised Normalization of Microarrays (SNM) [27] was used to remove the variance associated with this animal effect. The full SNM model included longitudinal time point as the biological effect and animal as an adjustable effect. SNM-transformed RNA-Seq data was used for all analysis except for the initial hierarchical clustering analysis (Additional File 1A). All expression data were z-score normalized before integrative analysis.

Differential Expression Analysis (DEA). DEA was performed using analysis of variance in JMP Genomics. Differences in gene expression levels across all genes among time points were tested. Benjamini-Hochberg false discovery rates (FDR) [28] were used for multiple hypothesis correction, with FDR ≤ 0.05 used as the significance threshold.

Weighted Gene Co-expression Network Analysis. Genes identified as differentially expressed during the acute infection were used for WGCNA with default parameters. The soft thresholding power parameter of WGCNA was set to six to obtain networks of approximately scale-free topology, as is standard practice, and the eigengene of each coexpression gene module was used to study associations with immunological traits.

Flow Cytometry. Two-hundred microliters of BM aspirate to be used for flow cytometry was collected at the same time as RNA-Seq specimens. Bone marrow was initially washed with 2 mL of wash buffer (PBS + 2% Fetal Bovine Serum (FBS)) by centrifugation at 400 × *g* for 5 min. After centrifugation, the supernatant was aspirated and discarded. The remaining cell pellet was suspended in PBS to the original volume followed by staining with antibodies as indicated in Table 1. The cells were stained with the antibody cocktails for 30 min at room temperature in the dark. After staining, the sample was placed into 2 mL of BD FACS Lysing solution (BD Biosciences), incubated for 10 min in the dark at room temperature, and the remaining cells pelleted by centrifugation at 400 × *g* for 5 min. The cells were then washed in 3 mL of wash

buffer by centrifugation at 400 × *g* for 5 min. The supernatant was discarded and cells resuspended in a 2% paraformaldehyde and PBS solution (v/v) and analyzed using a BD LSR-II flow cytometer within 24 h using a standardized acquisition template. Daily calibration using BD CST beads was performed to ensure direct comparability of each acquisition.

Table 1. Flow cytometry panel for determining the frequency of immune and erythroid cells in macaque bone marrow aspirate.

Name	**Fluorochrome**	**Clone**
CD3	PerCp-Cy5.5	SP34-2
CD45	FITC	DO58-1283
CD41a	PE	HIP8
CD71	APC	LOl.1
CD11b	PE-Cy7	ICRF44
CD34	PE-CF594	563
CD44	APC-H7	G44.26
CD16	ALEXAFLUOR 700	3G8
CD14	PB	M5E2
CD20	V-500	L27

Fluorescence-Activated Cell Sorting (FACS). Bone marrow MNCs were isolated as described above. Residual RBCs were lysed with 1-2 mL of ACK Lysing solution (Life Technologies) followed by washing with excess sterile PBS. BM MNCs were then enumerated using a Countess II cell counter (Life Technologies) and two million BM MNCs were stained with the fluorescently conjugated antibodies in Table 2 as described above followed by re-suspension in incomplete RPMI 1640 without FBS and phenol red for FACS. Populations of interest were sorted under optimal conditions using a FACS Aria II cell sorter (Beckman). After sorting, the purity of each population was confirmed to be ≥95% and populations were adhered to slides

using a Cytospin followed by staining using Wrights-Giemsa to determine the composition of the target populations.

Table 2. Cell sorting panel for erythroid progenitor populations in rhesus macaque bone marrow.

Name	**Fluorochrome**	**Clone**
CD45	FITC	DO58-1283
CD41a	PE	HIP8
CD71	APC	LOl.1
CD34	PE-CF594	563

Multiplex Cytokine Assay. A custom-made multiplex cytokine assay was designed and purchased from Affymetrix. The manufacturer's suggested protocol was followed using plasma collected from blood specimens obtained on EDTA. Data was analyzed using the ProcartaPlex Software.

Erythropoietin ELISA. Erythropoietin levels were determined by using a Quantikine IVD ELISA assay for human erythropoietin using the manufacturer's suggested protocol. All samples were randomized prior to performing the ELISA.

Other Statistical Analysis. Limma was used for assessing significant changes in cytokine concentrations and cell population between infection points [29, 30]. The Benjamini-Hochberg correction was used to control the FDR. FDR ≤ 0.05 was used as the significance threshold. A linear mixed-effect model with a Tukey-Kramer HSD post-hoc analysis was used to determine statistical significance of alterations in hematological parameters using JMP 13 Pro. A paired t-test was used to evaluate if the changes in EPO levels and GATA1/GATA2 target gene expression were changed across infection stages. For the GATA1/GATA2 target gene analysis,

SNM-transformed data was used. Each gene was averaged across the four animals and the significance test performed on the averaged values.

Data Release. Clinical data used in this analysis are publicly available in Plasmo DB and described in Joyner et al. [31]. The BM transcriptome data has been publicly deposited in GEO (Accession number GSE94273).

Results

Insufficient compensation for anemia during acute cynomolgi malaria in rhesus macaques

The parasitological and hematological data utilized in this analysis was published previously, discussed, and made publicly available in Joyner et al. [31]. Briefly, five rhesus macaques were infected with *P. cynomolgi* M/B strain sporozoites and followed for up to 100 days. One macaque developed severe disease and irreversible kidney failure that required euthanasia; thus, this animal was removed from the current analysis [32]. Seven BM samples were collected longitudinally from each macaque, and these samples were classified into the following infection points for analysis in this manuscript: prior to inoculation (pre-infection), during acute primary infection, after the peak of parasitemia (i.e. post-peak), before and between relapses (i.e. inter-relapses), and during relapses (Figure 1A).

The rhesus macaques infected with *P. cynomolgi* M/B strain developed varying levels of anemia during the primary infection (Figure 1B; [31]). Despite the significant decrease in hemoglobin levels during acute infections, the circulating reticulocytes did not increase significantly until after the peak of parasitemia or after sub-curative blood-stage treatment had been administered (Figure 1B). These results suggested that the BM was not appropriately responding to the anemia during acute infections but was restored after the peak of parasitemia. Interestingly, relapses did not result in changes in hemoglobin levels or peripheral reticulocyte counts (Figure 1B).

To assess whether each animal was appropriately compensating for anemia, the reticulocyte production index (RPI) was calculated as previously described [33]. The RPI adjusts for alterations in reticulocyte maturation time in an anemic individual and provides a metric to assess if an appropriate compensatory response is being made by the BM to combat anemia. An RPI value of under 2 when hemoglobin levels are decreasing suggests that the BM is not mounting an appropriate compensatory response for anemia whereas an RPI of greater than 3 when hemoglobin is decreasing indicates an appropriate compensatory response. In support of the hemoglobin and reticulocyte data, there was not an appropriate compensatory response by the BM during acute infections (Figure 1B). However, an appropriate response was mounted after the peak of parasitemia and treatment, though hemoglobin levels continued to decrease (Figure 1B).

Erythropoietin (EPO) is critical for inducing erythropoiesis during normal RBC turnover and pathological conditions. Thus, the lack of response by the BM during acute infection could have been due to EPO not being upregulated. In contrast to this hypothesis, EPO levels were significantly increased during acute infection (Figure 1C).

Collectively, these analyses demonstrated that there was not an appropriate compensatory response by the BM in the face of the developing anemia early during acute infections.

Acute malaria, but not relapses, leads to substantial changes in the bone marrow transcriptome.

The next goals of this study were to analyze the transcriptional changes in the BM that may account for the lack of compensatory response by the BM during acute infection and to determine if relapses induced changes in the BM since anemia was not observed during relapses. RNA-Seq was performed using BM MNCs from the four rhesus macaques infected with *P. cynomolgi* at the time points indicated in Figure 1A and classified for downstream analysis as described above.

Hierarchical clustering was performed with the R mixOmics package [34] to determine the similarity and/or differences in the BM transcriptome among the animals for each infection point. Using this approach, the acute infection measurements clustered together, but no other infection points clustered with a discernable pattern, suggesting that factors other than the BM transcriptome were influencing the grouping of these stages (Additional File 1A). After determining that 26.7% of the gene expression variance was attributable to each individual, the variance associated with each individual was removed using a supervised normalization of microarray (SNM) transformation (Additional File 1B).

After transformation, 42.3% of the variance of the dataset was now attributable to the infection point (Additional File 1C). Hierarchical clustering of the data after accounting for the variance attributable to individual animals maintained clustering of the acute infection stage (Figure 2A). However, this also led to a more robust clustering of the other infection stages, although the clusters were not completely correlated with infection points (Figure 2A). This suggested that acute malaria caused significant and coherent changes in the BM transcriptome, but there did not appear to be unique changes during relapses, post-peak, or inter-relapse infection periods.

Since hierarchical clustering indicated that transcriptional profiles at post-peak and inter-relapse infection points were generally similar to pre-infection profiles, similarities and differences were formally evaluated between each infection point. The number of differentially expressed genes (DEGs) between infection points was determined using analysis of variance (ANOVA). Compared to pre-infection, 1266 genes were differentially expressed during acute infection, 315 after the peak of parasitemia, and only 201 genes during relapses (Figure 2B). For relapses, 75 of these genes were in common with acute infection (Figure 2C). During acute infection, 1148 of the DEGs were upregulated whereas 118 were downregulated compared to pre-infection. Relapses showed much less variance in gene expression even for genes with large absolute upregulation

and high significance during acute infection. Thus, while acute infection caused significant perturbations in the BM transcriptome, relapses had a small effect.

Pathways and processes altered in the bone marrow during acute malaria

Gene ontology analysis was employed to understand the pathways and processes altered during acute infection. Approximately 37 biological processes were significantly changed in the BM during acute infection (Additional File 2). The identified pathways could largely be consolidated into biological processes related to cellular stress (e.g. response to endoplasmic reticulum stress), increases in transcription (e.g. RNA processing), and ongoing immune responses in the BM (e.g. Type I IFN, IFNγ, cell response to cytokine signaling, etc.). The pathways and processes of the other infection points were also analyzed but none were significantly enriched; this is likely due to the low number of differentially expressed genes during these infection stages.

Pathway analysis using MetaCore (Thomson Reuters) and Molecular Signatures Database (MSigDB) [35, 36] identified additional molecular pathways that were increased during acute infection (Figure 3). The pathways identified were similar between both databases and were skewed towards upregulation (Figure 3A-D). This is likely due to the low number of down-regulated DEGs during acute infection (Figure 2B). Full lists of pathways identified in each database are provided in Additional Files 3-6.

The enriched pathways and gene sets from both databases highlighted the ongoing immune response in the BM during acute infection; in particular, pathways involved in cytokine signaling were overrepresented (Figures 3A-B). The most predominant cytokine signatures to emerge from the analysis of acute infection in both databases were Type I (i.e. IFN-α/β) and Type II interferon (i.e. IFN-γ), which were identified by both databases (Figures 3A-B). A heatmap of DEGs identified in these pathways shows upregulation during acute infection but not other infection points (Figure 3E-F). Although the related pathway was identified, changes in expression of the

ifnα and *ifnβ1* genes themselves were not captured by RNA-Seq during acute infection because the genes did not pass the FPKM threshold. *ifnγ* expression, on the other hand, was detectable and significantly increased ($p < 0.001$) during acute infection and after the peak of parasitemia ($p < 0.05$) (Figure 3G). To ensure that gene expression was indicative of the protein levels, the concentrations of IFNγ and IFNα in the plasma were measured via multiplex assay. Consistent with the transcriptional data, IFNγ levels were increased ($p=0.008$; Figure 3I) and IFNα levels did not change during acute infection although a significant decrease was detected after the peak of parasitemia (Figure 3H).

Other cytokine signatures identified as transcriptionally upregulated in the BM during acute infection included IL-10 and IL-27, which are known to have effects on the BM during acute malaria, and genes involved in the IL-3 signaling pathway (Figure 3B) [37, 38]. Interestingly, the IL-5 signaling pathway was the only cytokine signaling pathway identified as being downregulated during acute infection, which could be due to the skewing towards a Th1 response (Figure 3D).

This analysis also revealed the enrichment of pathways associated with pathogen recognition receptors (PRRs) that are important for sensing intracellular and extracellular microbial components as well as host danger molecules. Specifically, the analysis highlighted the importance of engagement of Toll-like Receptors, NOD-Like receptors and RIG-I/MDA5 (Figure 3A-B).

Intermediate and non-classical monocytes may negatively impact the erythroid lineage during acute malaria

Bone marrow is made up of a heterogeneous population of cells that together yield the transcriptional profiles measured here. Weighted Gene Set Co-expression Network Analysis (WGCNA) was employed to investigate which cells types in the BM may be responsible for the

observed changes in the BM transcriptome during acute malaria [39]. WGCNA was performed using DEGs identified during the acute infection and flow cytometry data collected at each infection point. The gating strategy for the cellular subsets used in WGCNA analysis is shown in Additional File 7. The populations included in the analysis were as follows: classical monocytes, intermediate monocytes, non-classical monocytes, B-cells, T-cells, granulocytes and a mixed population of erythroid progenitors (Additional File 8). Samples from other infection points were not included in this analysis to allow the acute infection to drive the formation of the coexpression modules.

The dominant modes of variance of each module were used to evaluate the association of the modules with cellular subsets. WGCNA identified four coexpression gene modules (Figure 4A). The modules colored turquoise and blue were composed of 490 and 335 DEGs, respectively, and were positively correlated with the number of intermediate and non-classical monocytes ($p<0.05$) in the BM. The turquoise module was negatively correlated with B cell numbers ($r=-0.52$, $p=0.01$). However, unlike monocytes, this was a negative correlation and is likely related to the disruption of the BM environment where B-cells develop. Other immune cell types identified by flow cytometry were not correlated with any of these co-expression modules. These results suggest that changes in the BM transcriptome during acute malaria were primarily related to monocytes.

To determine whether there was a link between the identified co-expression modules and suppression of the erythroid progenitor population, the relationship of the co-expression modules with the erythroid progenitor population was examined. All four co-expression modules were correlated with a drop in erythroid progenitors ($p < 0.05$ in all cases). Since only the turquoise and blue modules were associated with immune cells (monocytes), this suggested that the correlation of the yellow and brown co-expression modules represented non-immunological or diffuse immunological pathways.

Intermediate and non-classical monocytes are associated with pathways upregulated during acute malaria in the bone marrow

To test the hypothesis that monocytes were a major driving force of the transcriptome changes in the BM, pathway enrichment analysis was first performed on the genes in each module [35, 36]. The MSigDB database was used for this analysis; results obtained with this database were comparable to those obtained using MetaCore (Figure 4A-D). The turquoise module was enriched with pathways involved in the immune response (and interferon signaling pathways), general cellular response pathways (e.g. unfolded protein response), and RNA metabolism (Figure 4B). The blue module was enriched in pathways related to the immune response, including cytokine signaling by IFNγ, activation of NF-κB, and the IL-2 pathway (Figure 4C). Each of these pathways are known to be involved in monocyte activation [40]. Thus, the activation status of the intermediate and non-classical monocyte populations in the BM during acute infection likely influenced the BM transcriptome. Indeed, the intermediate and non-classical monocyte populations were expanded in the marrow during acute infection, but these differences did not reach statistical significance likely due to the sample size (Additional File 9).

The blue module was also enriched for the PRR pathways activated through NOD like receptors (NLRs) and RIG-I like receptors (RLRs) (Figure 4C). This suggests that these pathways, which were originally identified by DEG analysis, may be active in intermediate and non-classical monocytes in the BM in response to *Plasmodium* infection.

To validate the transcriptomic signatures related to cytokine signaling and identify the cytokines that may negatively impact the erythroid progenitors, WGCNA analysis was repeated using the flow cytometry, transcriptomics and cytokine data. Seventeen of 45 cytokine concentrations were found to be positively correlated with the turquoise and blue modules. Transitively, these cytokines were thus also negatively associated with the erythroid progenitor population (Figure 5). Although negatively correlated with the erythroid population in the BM, these cytokines were

positively associated with the frequency of non-classical and intermediate monocytes (Figure 5). IFNγ was correlated with the blue, brown, and turquoise modules, and IFN signaling was enriched in the turquoise and blue modules, which provided confirmatory support for the transcriptome analysis and the validity of the WGCNA approach (Figure 4B and 4C).

The brown module did not correlate with particular immune cell types, and this is likely due to the diverse set of pathways represented in this module (Figure 4D). The yellow module highlighted IFN signaling pathways (Figure 4E) but was not correlated with protein levels of IFN. Interestingly, a signature driven by erythropoietin (EPO) was also enriched in the yellow module (Additional File 10).Although an EPO signature is to be expected given that EPO plays an important role to increase BM output of RBCs during anemia, this signaling was inversely correlated in this study with the erythroid progenitors, suggesting that despite the elevated EPO levels in the plasma and signaling in the BM, an appropriate compensatory response could not be made. Indeed, these data are consistent with previous literature showing that malaria induces an EPO-independent anemia [41].

Transcriptional networks related to erythropoiesis are disrupted in the bone marrow during acute malaria

Given insufficient compensation for anemia during acute malaria, the transcriptome data was then mined to determine if transcriptional networks related to erythropoiesis were disrupted during acute *P. cynomolgi* infections. Correlation analysis (CA) was performed using the erythroid population frequencies determined by flow cytometry and BM MNC gene expression to identify genes that may be related to the decrease in erythroid progenitors observed in the BM (Figure 6B). Samples from pre-infection, acute primary, and post-peak were utilized for this analysis to determine changes that occurred before, during, and after the onset of anemia.

547 genes from the same RNA-Seq dataset utilized in the previous analyses were identified as significantly positively correlated (Spearman's correlation coefficient >0.6; p-value<0.05) at FDR<0.2 with the frequency of the erythroid progenitor population in the BM (Additional File 11). After identifying the related genes, the iRegulon pipeline was utilized to explore what transcription factors may be influencing the genes that were positively correlated with the change in erythroid progenitor cell frequencies during acute infection. iRegulon identified multiple transcription factors including CCAAT/Enhancer Binding Protein (CEBPD), GATA Binding Proteins (GATA1/GATA2) and TEA Domain Transcription Factor 4 (TEAD4) as being correlated with erythroid progenitor cell frequencies (Figure 6A).

This analysis focused on GATA1 and GATA2 because these proteins are master regulators of erythropoiesis, had the largest number of target genes identified in the dataset, and had two of the highest NES scores, which are a metric of statistical significance in the iRegulon pipeline (Figure 6A) [42, 43]. First, the expression of GATA1 and GATA2 was examined directly to understand if the gene expression of these proteins were changed during infection, as this could account for the insufficient erythropoietic response in the periphery. GATA2 gene expression did not change throughout the initial infection (Figure 6D). In contrast, GATA1 gene expression was not changed during acute infection but was significantly increased after the peak of parasitemia when erythropoiesis was restored (Figure 6C). Thus, GATA1/GATA2 gene expression was not upregulated during acute infection as would otherwise be predicted based on these proteins being critical for erythropoiesis.

Next, the genes regulated by GATA1 and GATA2 were examined to identify whether the genes regulated by these proteins were upregulated even though transcription of GATA1/GATA2 was not altered significantly during acute infection. The target genes of GATA1 and GATA2 were predicted to be downregulated during acute infection, when there was a small but significant decrease (p=0.045) in the frequency of the erythroid progenitor population in the BM (Figure

6B). Consistent with this hypothesis, the genes regulated by GATA1 and GATA2 were downregulated during acute infection, but upregulated post-peak (Figures 6 E-F) when the erythroid progenitor population in the BM was restored to pre-infection levels and an increase in peripheral reticulocytes was observed, indicating restored erythropoiesis. Indeed, the expansion of other cell types in the marrow during acute infection could drive the decrease in percentage of erythroid progenitors in the marrow during acute infection.

Discussion

The development of malarial anemia is multi-factorial, and it is clear that the loss and sustained reduction of RBCs during an infection is not due to parasitism alone. Bone marrow suppression and the removal of uninfected RBCs contribute to the development of anemia. In the rhesus macaque – *P. cynomolgi* model, both processes are shown to be involved based on hemoglobin and reticulocyte kinetics described here and in Joyner et al. [31]. Interestingly, inefficient erythropoiesis appears to contribute to the development of anemia early during a blood-stage infection; appropriate compensation for the anemia is observed after the peak of parasitemia and the administration of blood-stage treatment (Figure 1). Furthermore, there were few changes in the BM transcriptome after the peak of parasitemia, suggesting restored function of the BM (Figure 2). Therefore, it is clear that there are multiple phases in the longitudinal development of malarial anemia in macaques infected with *P. cynomolgi* that are likely governed through different mechanisms.

Predictions from field studies have suggested that relapses are responsible for most *P. vivax* blood-stage infections and potentially most clinical illness [44-46]. Therefore, the initial hypothesis of this study was that both *P. cynomolgi* acute primary infections and relapses would cause alterations in the BM transcriptomes since anemia would be an expected complication in both cases. However, unlike the acute infections, relapses did not result in significant changes in the BM transcriptomes. Although unexpected, this finding is in agreement with the conclusions in

Joyner *et al*., which demonstrated that *P. cynomolgi* relapses are not associated with the development of anemia, even when peripheral parasitemia is detectable [9].

The lack of anemia and changes in the BM transcriptome during *P. cynomolgi* relapses is likely due to the significant decrease in parasite burden during relapses in comparison to the initial infection (Figure 1). This decrease is likely due to immunity developed after an initial infection that prevents the parasite from reaching levels similar to those during the acute primary infection. Lower levels of parasite replication may allow the BM to maintain its normal compensatory functions during relapses, unlike acute infection where inefficient erythropoietic output is linked to higher parasite densities [9]. There is evidence from malaria chemotherapy studies that relapses do not necessarily result in disease and can result in asymptomatic infections [47-49]. Taken together, this evidence suggests that there is a threshold of parasite burden that disrupts erythropoietic output, likely through ongoing inflammation that is triggered by innate immune responses to growing asexual parasitemia prior to the development of effective anti-parasite immunity.

During acute infection, many biological pathways and processes in the BM were upregulated, including pathways related to cellular metabolism and transcription. Such pathways are likely representative of the ongoing host response against the parasite both in the periphery and potentially in the BM since both *P. vivax* and *P. falciparum* iRBCs can readily be found in the BM [50, 51]. Many of the upregulated pathways in the BM were related to inflammation and largely composed of cytokine signaling pathways. This agrees with previously published work demonstrating that cytokines, including IL-10 and IL-27, are important in BM responses during rodent malaria and/or in malaria patients [52, 53]. The current data suggest that these cytokines may also be involved in the BM of NHPs with malaria.

Here, Type I and Type II IFN signaling pathways were identified as potentially key cytokines involved in malarial anemia. However, despite an enrichment in transcriptional

pathways involved in Type I IFN signaling in the BM, IFNα protein levels in the plasma were not increased (Figure 3H). (*ifnα* gene expression in the BM was not reliably quantified.) In stark contrast, the Type II IFN signature was accompanied by an increase in *ifnγ* gene expression in the BM and IFNγ concentration in the plasma, and the erythroid progenitor population was negatively correlated with IFNγ (Figures 3G, 2I and 4). These data suggest that Type II IFNs may negatively impact the erythroid progenitor population through direct or indirect mechanisms during acute infection. Indeed, IFNγ can directly cause apoptosis of erythroid progenitors *in vitro* and it has been previously implicated in malarial anemia in rodent malaria models [12, 54, 55].

Type I IFNs can work in concert with IFNγ to suppress erythropoiesis [56-58], and therefore it is possible that Type I IFNs may initiate the disruption of erythropoiesis earlier during infection. The reasons why Type I IFN transcripts were too low to be quantified could be because they are more tightly regulated than IFNγ and the sampling regimen missed the point at which these proteins are synthesized and released into the plasma. Alternatively, these proteins may act predominantly at local levels and may have only been present in the BM. There are also may be other intermediary molecules that are unmeasured here but have a role in the phenomena we have observed. Regardless, recent studies demonstrate Type I IFNs to be important during early blood-stage malaria, and the results presented here suggest these cytokines should be explored further in relation to malaria anemia [59-61].

This study's results also suggested that monocytes were largely responsible for changes in the BM transcriptome during acute infection (Figures 3 and 4). It has previously been shown that macrophages and monocytes in the BM produce inflammatory cytokines in response to parasite byproducts such as hemozoin. It has been hypothesized that this process drives the dyserythropoiesis observed during malarial anemia [62]. Although most of these conclusions were drawn from *in vitro* experiments, the analysis here supports a model where monocytes in the BM negatively influence the erythroid lineage *in vivo* via cytokine production during acute

malaria [62]. It is interesting to speculate that these signatures may be coming from BM-resident monocytes and/or macrophages, but more work will be required to explore this possibility in future studies.

Although intermediate and non-classical monocytes are thought to be important for parasite control in the periphery [63], this analysis from the BM implicated these monocytes as potentially being responsible for the decrease in the erythroid progenitors. WGCNA analysis associated these monocyte subsets with an increase of pro-inflammatory cytokines such as IFNγ, MIP1-α/β and TNFα in the plasma, which would not necessarily be expected of these monocytes, as these subsets are not considered to be classically pro-inflammatory. Indeed, many of these cytokines are known to negatively impact erythroid progenitors, directly or indirectly [12, 62]. It is interesting to speculate that these monocytes may play a dual role in controlling parasite growth through cytokine production, etc. in the peripheral blood but also contribute to the development of anemia through these same processes. Future work could assess this directly using this NHP model of *P. vivax* infection.

Previous evidence has suggested that the disruption of erythropoiesis may be due to dysregulation of transcription factors that control erythropoiesis [64]. In this study, it was shown that GATA1 and GATA2, two master regulators of erythropoiesis, may not function appropriately during acute malaria. Genes regulated by GATA1 and GATA2 were downregulated during acute infection, but upregulated whenever appropriate erythropoietic output was restored. Indeed, some of the cytokines (e.g. TNFα, IFNγ) that were upregulated are known to antagonize GATA1 and, thus, disrupt terminal erythroid differentiation [65, 66], providing a potential mechanism for what was observed. Although both GATA1 and GATA2 were identified, GATA1 may be more central in the process, based on *gata2* gene expression not being upregulated when erythropoietic output was restored (Figure 5G). Future studies should examine the factors that

influence the function of GATA1/2 during malaria since it is clear that a variety of intermediate molecules besides those described here could also affect each protein's function [12, 67, 68].

Although this study provides the basis for future investigations related to malarial anemia using NHPs, there are limitations. First, the number of NHPs presented in this study is smaller than initially designed because one macaque from the cohort developed severe disease during the acute infection period and required euthanasia [9]. This decrease in the cohort size may limit the generalizability of the results, but other studies using *in vitro* systems, rodent malaria models, and samples from malaria patients have arrived at conclusions similar to those in this study [12, 62]. This suggests that studies with NHPs, which in comparison to studies using patient samples or rodent models will be restricted to small sample size, have the potential to produce generalizable results.

A second limitation of this study is that the transcriptomic profiling of the BM by RNA-Seq was performed on BM MNCs. This sample type is composed of multiple cellular lineages, and thus it is difficult to pinpoint the specific cell type in the BM that was responsible for changes in the transcriptome. The changes that we have identified are thus necessarily correlative rather than describing definitive and direct mechanisms in specific cell types. Although such uncertainty is in some ways a weakness, this approach also has its advantages. Most importantly, it enabled an unbiased survey of the major changes in the BM during acute malaria and relapse infections in macaques. In contrast, an initial focus on a singular cell type would likely have missed some critical transcriptional changes in the BM, and thus the insights derived from those changes. Future studies can target specific cellular lineages to better understand the role of each individual cell type in the BM during infection.

Conclusion

This NHP cohort study has direct implications for understanding *P. vivax* malaria and possibly other *Plasmodium* species. Insights have been gained into BM dysfunction and inflammatory processes during the acute stage of the disease caused by *P. cynomolgi* in rhesus macaques. Specifically, monocytes were implicated as a critical cell type involved in inflammation in the BM during acute malaria in macaques. Furthermore, monocytes were associated with a decrease in erythroid progenitors in the BM, suggesting monocyte-driven inflammation could suppress erythropoiesis *in vivo*. While erythroid progenitors were decreasing, GATA1 and GATA2 transcriptional networks, which are critical for terminal erythroid differentiation, were disrupted. This study provides an explanation for inefficient erythropoiesis during acute malaria in primates and paves the way for future investigations that can assess the role of specific cell types and pathways in this context. Such studies will be critical for new experimental directions aimed at identifying targets of possible interventions for malaria anemia. This study also shows for the first time that malaria relapses, shown earlier not to be associated with clinical illness in this model, do not cause similar perturbations of the BM as observed during primary acute infections.

Funding

This project has been funded in whole or in part with Federal funds from the National Institute of Allergy and Infectious Diseases; National Institutes of Health, Department of Health and Human Services [Contract No. HHSN272201200031C] and the National Center for Research Resources [ORIP/OD P51OD011132].

Author's Contributions

All authors read and approved this manuscript. M.R.G, T.J.L, and M.S. conceived and designed the experiments; C.J.J., M.C., S.L., and S.S. conducted the experiments; Y.T. and C.J.J. performed data analysis and prepared figures; C.J.J. and Y.T. wrote the paper; M.S., T.J.L., and M.R.G. provided experimental oversight, analytical guidance, and edited the paper; S.B.P., M.V.N., J.D.B, and J.C.K. managed the data and deposited it into republic repositories.

Acknowledgements

The authors would like to provide special thanks to Chris Ibegbu for consulting on antibodies for flow cytometry experiments, and Tiger Li for data analysis. The authors would also like to thank Children's Healthcare of Atlanta and Emory University's Pediatric Flow Cytometry Core and the Yerkes National Primate Research Center Flow Cytometry cores for allowing the use of their facilities and state-of-the-art instrumentation. We would also like to thank the Yerkes National Primate Research Center's Genomics Core for sequencing services.

References

1. WHO: *World Malaria Report 2016.*2016.
2. Abdalla SH. Hematopoiesis in human malaria. Blood Cells 1990; 16:401-416; discussion 417-409.
3. Fernandez-Arias C, Rivera-Correa J, Gallego-Delgado J, Rudlaff R, Fernandez C, Roussel C, et al. Anti-self phosphatidylserine antibodies recognize uninfected erythrocytes promoting malarial anemia. Cell Host Microbe 2016; 19:194-203.
4. Jakeman GN, Saul A, Hogarth WL, Collins WE. Anaemia of acute malaria infections in non-immune patients primarily results from destruction of uninfected erythrocytes. Parasitology 1999; 119 (Pt 2):127-133.
5. Collins WE, Jeffery GM, Roberts JM. A retrospective examination of anemia during infection of humans with *Plasmodium vivax*. Am J Trop Med Hyg 2003; 68:410-412.
6. Fonseca LL, Alezi HS, Moreno A, Barnwell JW, Galinski MR, Voit EO. Quantifying the removal of red blood cells in *Macaca mulatta* during a *Plasmodium coatneyi* infection. Malaria Journal 2016; 15:1-15.
7. Wickramasinghe SN, Abdalla SH. Blood and bone marrow changes in malaria. Baillieres Best Pract Res Clin Haematol 2000; 13.
8. Knuttgen HJ. The bone marrow of non-immune Europeans in acute malaria infection: a topical review. Ann Trop Med Parasitol 1987; 81:567-576.
9. Joyner C, Moreno A, Meyer EV, Cabrera-Mora M, Ma HC, Kissinger JC, et al. *Plasmodium cynomolgi* infections in rhesus macaques display clinical and parasitological features pertinent to modelling vivax malaria pathology and relapse infections. Malar J 2016; 15:451.
10. Joyner C, Barnwell JW, Galinski MR. No more monkeying around: primate malaria model systems are key to understanding *Plasmodium vivax* liver-stage biology, hypnozoites, and relapses. Front Microbiol 2015; 6:145.
11. Parekh C, Crooks GM. Critical differences in hematopoiesis and lymphoid development between humans and mice. J Clin Immunol 2013; 33:711-715.
12. Lamikanra AA, Brown D, Potocnik A, Casals-Pascual C, Langhorne J, Roberts DJ. Malarial anemia: of mice and men. Blood 2007; 110.
13. An X, Schulz VP, Mohandas N, Gallagher PG. Human and murine erythropoiesis. Curr Opin Hematol 2015; 22:206-211.
14. Barnwell JW, Galinski MR, DeSimone SG, Perler F, Ingravallo P. *Plasmodium vivax*, *P. cynomolgi*, and *P. knowlesi*: identification of homologue proteins associated with the surface of merozoites. Exp Parasitol 1999; 91:238-249.

15. Joyner CJ, Barnwell JW, Galinski MR. No More Monkeying Around: Primate Malaria Model Systems are Key to Understanding *Plasmodium vivax* Liver-Stage Biology, Hypnozoites, and Relapses. Frontiers in Microbiology 2015; 6.
16. Schmidt LH. Compatibility of relapse patterns of *Plasmodium cynomolgi* infections in rhesus monkeys with continuous cyclical development and hypnozoite concepts of relapse. Am J Trop Med Hyg 1986; 35:1077-1099.
17. Baird JK. Pernicious and Threatening *Plasmodium vivax* as Reality. Am J Trop Med Hyg 2014.
18. Jakeman GN, Saul A, Hogarth WL, Collins WE. Anaemia of acute malaria infections in non-immune patients primarily results from destruction of uninfected erythrocytes. Parasitology 1999; 119.
19. Douglas NM, Anstey NM, Buffet PA, Poespoprodjo JR, Yeo TW, White NJ, et al. The anaemia of *Plasmodium vivax* malaria. Malaria Journal 2012; 11:1-14.
20. Schroeder A, Mueller O, Stocker S, Salowsky R, Leiber M, Gassmann M, et al. The RIN: an RNA integrity number for assigning integrity values to RNA measurements. BMC Mol Biol 2006; 7:3.

21. Devonshire AS, Elaswarapu R, Foy CA. Evaluation of external RNA controls for the standardisation of gene expression biomarker measurements. BMC Genomics 2010; 11:662.
22. Trapnell C, Roberts A, Goff L, Pertea G, Kim D, Kelley DR, et al. Differential gene and transcript expression analysis of RNA-seq experiments with TopHat and Cufflinks. Nat Protoc 2012; 7:562-578.
23. Kim D, Pertea G, Trapnell C, Pimentel H, Kelley R, Salzberg SL. TopHat2: accurate alignment of transcriptomes in the presence of insertions, deletions and gene fusions. Genome Biology 2013; 14.
24. Anders S, Pyl PT, Huber W. HTSeq--a Python framework to work with high-throughput sequencing data. Bioinformatics 2015; 31:166-169.
25. Wang L, Wang S, Li W. RSeQC: quality control of RNA-seq experiments. Bioinformatics 2012; 28:2184-2185.
26. Anders S, Huber W. Differential expression analysis for sequence count data. Genome Biology 2010; 11:R106.
27. Mecham BH, Nelson PS, Storey JD. Supervised normalization of microarrays. Bioinformatics 2010; 26:1308-1315.
28. Benjamini Y, Hochberg Y. Controlling the False Discovery Rate - a Practical and Powerful Approach to Multiple Testing. Journal of the Royal Statistical Society Series B-Methodological 1995; 57:289-300.
29. Phipson B, Lee S, Majewski IJ, Alexander WS, Smyth GK. Robust hyperparameter estimation protects against hypervariable genes and improves power to detect differential expression. 2016:946-963.
30. Ritchie ME, Phipson B, Wu D, Hu Y, Law CW, Shi W, et al. limma powers differential expression analyses for RNA-sequencing and microarray studies. Nucleic Acids Res 2015; 43:e47.
31. Joyner C, Moreno A, Meyer EVS, Cabrera-Mora M, Kissinger JC, Barnwell JW, et al. *Plasmodium cynomolgi* infections in rhesus macaques display clinical and parasitological features pertinent to modelling vivax malaria pathology and relapse infections. Malaria Journal 2016; 15:1-18.
32. J. Joyner C, Consortium TM, Wood JS, Moreno A, Garcia A, Galinski MR. Case Report: Severe and Complicated Cynomolgi Malaria in a Rhesus Macaque Resulted in Similar Histopathological Changes as Those Seen in Human Malaria. The American Journal of Tropical Medicine and Hygiene 2017; 97:548-555.
33. Hillman RS. Characteristics of marrow production and reticulocyte maturation in normal man in response to anemia. The Journal of Clinical Investigation 1969; 48:443-453.
34. Le Cao KA, Gonzalez I, Dejean S. integrOmics: an R package to unravel relationships between two omics datasets. Bioinformatics 2009; 25:2855-2856.
35. Subramanian A, Tamayo P, Mootha VK, Mukherjee S, Ebert BL, Gillette MA, et al. Gene set enrichment analysis: a knowledge-based approach for interpreting genome-wide expression profiles. Proc Natl Acad Sci U S A 2005; 102:15545-15550.
36. Mootha VK, Lindgren CM, Eriksson KF, Subramanian A, Sihag S, Lehar J, et al. PGC-1alpha-responsive genes involved in oxidative phosphorylation are coordinately downregulated in human diabetes. Nat Genet 2003; 34:267-273.
37. Nussenblatt V, Mukasa G, Metzger A, Ndeezi G, Garrett E, Semba RD. Anemia and interleukin-10, tumor necrosis factor alpha, and erythropoietin levels among children with acute, uncomplicated Plasmodium falciparum malaria. Clin Diagn Lab Immunol 2001; 8:1164-1170.
38. Furusawa J, Mizoguchi I, Chiba Y, Hisada M, Kobayashi F, Yoshida H, et al. Promotion of Expansion and Differentiation of Hematopoietic Stem Cells by Interleukin-27 into Myeloid Progenitors to Control Infection in Emergency Myelopoiesis. PLoS Pathog 2016; 12:e1005507.
39. Langfelder P, Horvath S. WGCNA: an R package for weighted correlation network analysis. BMC Bioinformatics 2008; 9:559.

40. Martinez FO, Gordon S. The M1 and M2 paradigm of macrophage activation: time for reassessment. F1000Prime Reports 2014; 6:13.
41. Moreno A, Cabrera-Mora M, Garcia A, Orkin J, Strobert E, Barnwell JW, et al. *Plasmodium coatneyi* in rhesus macaques replicates the multisystemic dysfunction of severe malaria in humans. Infect Immun 2013; 81:1889-1904.
42. Skorokhod OA, Caione L, Marrocco T, Migliardi G, Barrera V, Arese P, et al. Inhibition of erythropoiesis in malaria anemia: role of hemozoin and hemozoin-generated 4-hydroxynonenal. Blood 2010; 116:4328-4337.
43. Suzuki M, Shimizu R, Yamamoto M. Transcriptional regulation by GATA1 and GATA2 during erythropoiesis. Int J Hematol 2011; 93:150-155.
44. Adekunle AI, Pinkevych M, McGready R, Luxemburger C, White LJ, Nosten F, et al. Modeling the Dynamics of *Plasmodium vivax* Infection and Hypnozoite Reactivation In Vivo. PLoS Negl Trop Dis 2015; 9:e0003595.
45. Betuela I, Rosanas-Urgell A, Kiniboro B, Stanisic DI, Samol L, de Lazzari E, et al. Relapses contribute significantly to the risk of *Plasmodium vivax* infection and disease in Papua New Guinean children 1-5 years of age. J Infect Dis 2012; 206:1771-1780.
46. Howes RE, Battle KE, Mendis KN, Smith DL, Cibulskis RE, Baird JK, et al. Global Epidemiology of *Plasmodium vivax*. Am J Trop Med Hyg 2016.
47. White NJ, Imwong M. Relapse. Adv Parasitol 2012; 80:113-150.
48. Boyd MF. A review of studies on immunity to vivax malaria. J Natl Malar Soc 1947; 6.
49. Boyd MF, Matthews CB. Further observations on the duration of immunity to the homologous strain of *Plasmodium vivax*. Am J Trop Med 1939; s1-19.
50. Malleret B, Li A, Zhang R, Tan KSW, Suwanarusk R, Claser C, et al. *Plasmodium vivax*: restricted tropism and rapid remodeling of CD71-positive reticulocytes. Blood 2015; 125:1314-1324.
51. Joice R, Nilsson SK, Montgomery J, Dankwa S, Egan E, Morahan B, et al. *Plasmodium falciparum* transmission stages accumulate in the human bone marrow. Sci Transl Med 2014; 6:244re245.
52. Casals-Pascual C, Kai O, Cheung JO, Williams S, Lowe B, Nyanoti M, et al. Suppression of erythropoiesis in malarial anemia is associated with hemozoin in vitro and in vivo. Blood 2006; 108:2569-2577.
53. Furusawa J-i, Mizoguchi I, Chiba Y, Hisada M, Kobayashi F, Yoshida H, et al. Promotion of Expansion and Differentiation of Hematopoietic Stem Cells by Interleukin-27 into Myeloid Progenitors to Control Infection in Emergency Myelopoiesis. PLOS Pathogens 2016; 12:e1005507.
54. de Bruin AM, Voermans C, Nolte MA. Impact of interferon-γ on hematopoiesis. Blood 2014; 124:2479-2486.
55. Thawani N, Tam M, Stevenson MM. STAT6-mediated suppression of erythropoiesis in an experimental model of malarial anemia. Haematologica 2009; 94:195-204.
56. Means RT, Jr., Krantz SB. Inhibition of human erythroid colony-forming units by gamma interferon can be corrected by recombinant human erythropoietin. Blood 1991; 78:2564-2567.
57. Means RT, Jr., Krantz SB. Inhibition of human erythroid colony-forming units by interferons alpha and beta: differing mechanisms despite shared receptor. Exp Hematol 1996; 24:204-208.
58. Tarumi T, Sawada K, Sato N, Kobayashi S, Takano H, Yasukouchi T, et al. Interferon-alpha-induced apoptosis in human erythroid progenitors. Exp Hematol 1995; 23:1310-1318.
59. Montes de Oca M, Kumar R, Rivera FL, Amante FH, Sheel M, Faleiro RJ, et al. Type I Interferons Regulate Immune Responses in Humans with Blood-Stage *Plasmodium falciparum* Infection. Cell Rep 2016; 17:399-412.
60. Zander RA, Guthmiller JJ, Graham AC, Pope RL, Burke BE, Carr DJ, et al. Type I Interferons Induce T Regulatory 1 Responses and Restrict Humoral Immunity during Experimental Malaria. PLoS Pathog 2016; 12:e1005945.

61. Sebina I, James KR, Soon MS, Fogg LG, Best SE, Labastida Rivera F, et al. IFNAR1-Signalling Obstructs ICOS-mediated Humoral Immunity during Non-lethal Blood-Stage *Plasmodium* Infection. PLoS Pathog 2016; 12:e1005999.
62. Perkins DJ, Were T, Davenport GC, Kempaiah P, Hittner JB, Ong'echa JM. Severe malarial anemia: innate immunity and pathogenesis. Int J Biol Sci 2011; 7:1427-1442.
63. Nockher WA, Scherberich JE. Expanded CD14+ CD16+Monocyte Subpopulation in Patients with Acute and Chronic Infections Undergoing Hemodialysis. Infection and Immunity 1998; 66:2782-2790.
64. Sexton AC, Good RT, Hansen DS, D'Ombrain MC, Buckingham L, Simpson K, et al. Transcriptional profiling reveals suppressed erythropoiesis, up-regulated glycolysis, and interferon-associated responses in murine malaria. J Infect Dis 2004; 189:1245-1256.
65. Libregts SF, Gutierrez L, de Bruin AM, Wensveen FM, Papadopoulos P, van Ijcken W, et al. Chronic IFN-gamma production in mice induces anemia by reducing erythrocyte life span and inhibiting erythropoiesis through an IRF-1/PU.1 axis. Blood 2011; 118:2578-2588.
66. Rekhtman N, Radparvar F, Evans T, Skoultchi AI. Direct interaction of hematopoietic transcription factors PU.1 and GATA-1: functional antagonism in erythroid cells. Genes & Development 1999; 13:1398-1411.
67. Thawani N, Tam M, Bellemare MJ, Bohle DS, Olivier M, de Souza JB, et al. *Plasmodium* products contribute to severe malarial anemia by inhibiting erythropoietin-induced proliferation of erythroid precursors. J Infect Dis 2013.
68. Chang KH, Stevenson MM. Malarial anaemia: mechanisms and implications of insufficient erythropoiesis during blood-stage malaria. Int J Parasitol 2004; 34:1501-1516.

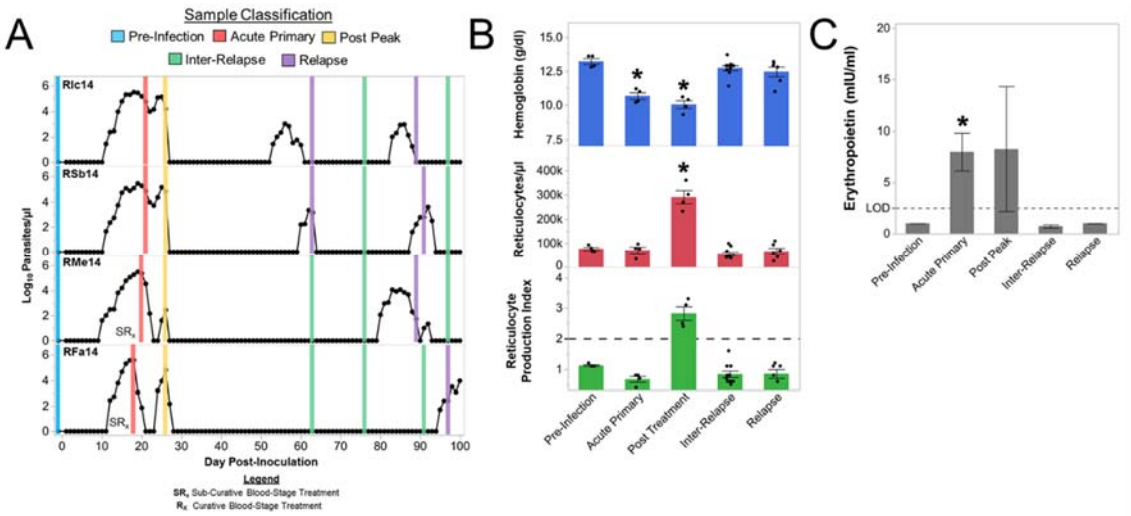

Figure 1. The bone marrow does not compensate for anemia during acute cynomolgi malaria despite increased EPO levels. (A) Parasitemia kinetics for the four animals are shown. Bone marrow sample collection times in relation to parasite kinetics are indicated by a vertical bar; the color of the bar indicates the infection point classification of the sample. (B) Hemoglobin levels, peripheral reticulocyte numbers, and the reticulocyte production index for each infection stage are shown. Statistical significance relative to pre-infection was assessed where relevant using a linear mixed-model with Tukey-Kramer post-hoc analysis. (C) Mean erythropoietin levels during each infection stage are indicated. Dashed line indicates the limit of detection of the assay. Statistical significance was assessed using a paired T-test relative to pre-infection levels. Error bars indicate standard error for Panels B and C. Asterisk indicates $p < 0.05$.

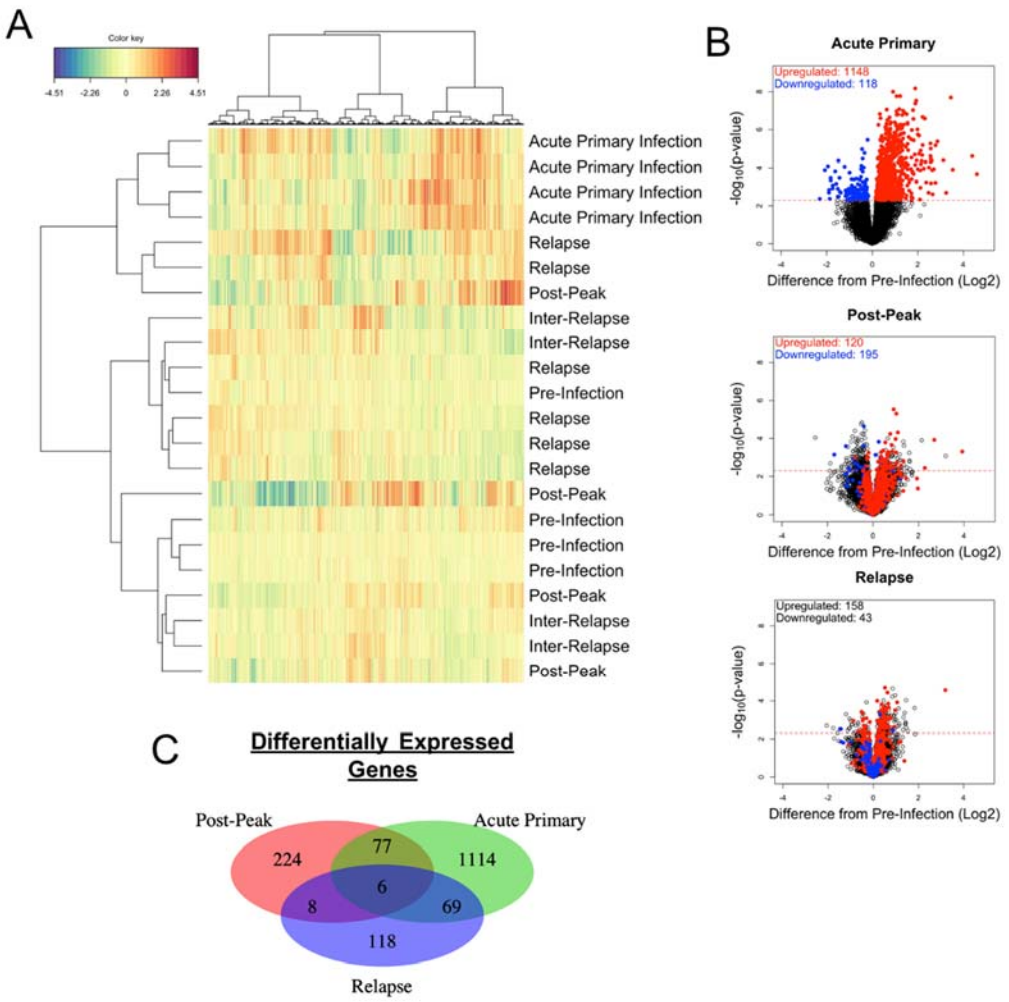

Figure 2. Acute malaria but not malaria relapse causes substantial changes in the bone marrow transcriptome. (A) Clustered heatmap of the BM transcriptome, with infection points of samples indicated. Four samples from acute primary infection form a cluster separated from other infection points. Another cluster captures more mild infection responses, including four out of six relapse time points. Colors indicate z-score normalized expression values. (B) Volcano plots of differentially expressed host genes in the BM at acute primary infection, post-peak, and relapse compared to pre-infection. The y axis is the negative logarithm base 10 of the P-value. The x axis is the log2 difference in expression values between pre-infection and the infection point of a given plot. The red dotted horizontal line represents FDR = 0.05. Thus, the right arm of dots

above the threshold line corresponds to genes significantly upregulated compared to pre-infection; the left arm of dots above the threshold line corresponds to downregulated genes. Red and blue dots for all three plots represent genes upregulated or downregulated (respectively) at acute primary infection, visualizing the fact that few genes differentially expressed at primary infection are differentially expressed during post-peak and relapse, with many genes not even trending in the same direction between the two infection points. (C) Venn diagram showing the overlap of differentially expressed genes at acute primary infection, post-peak and relapses.

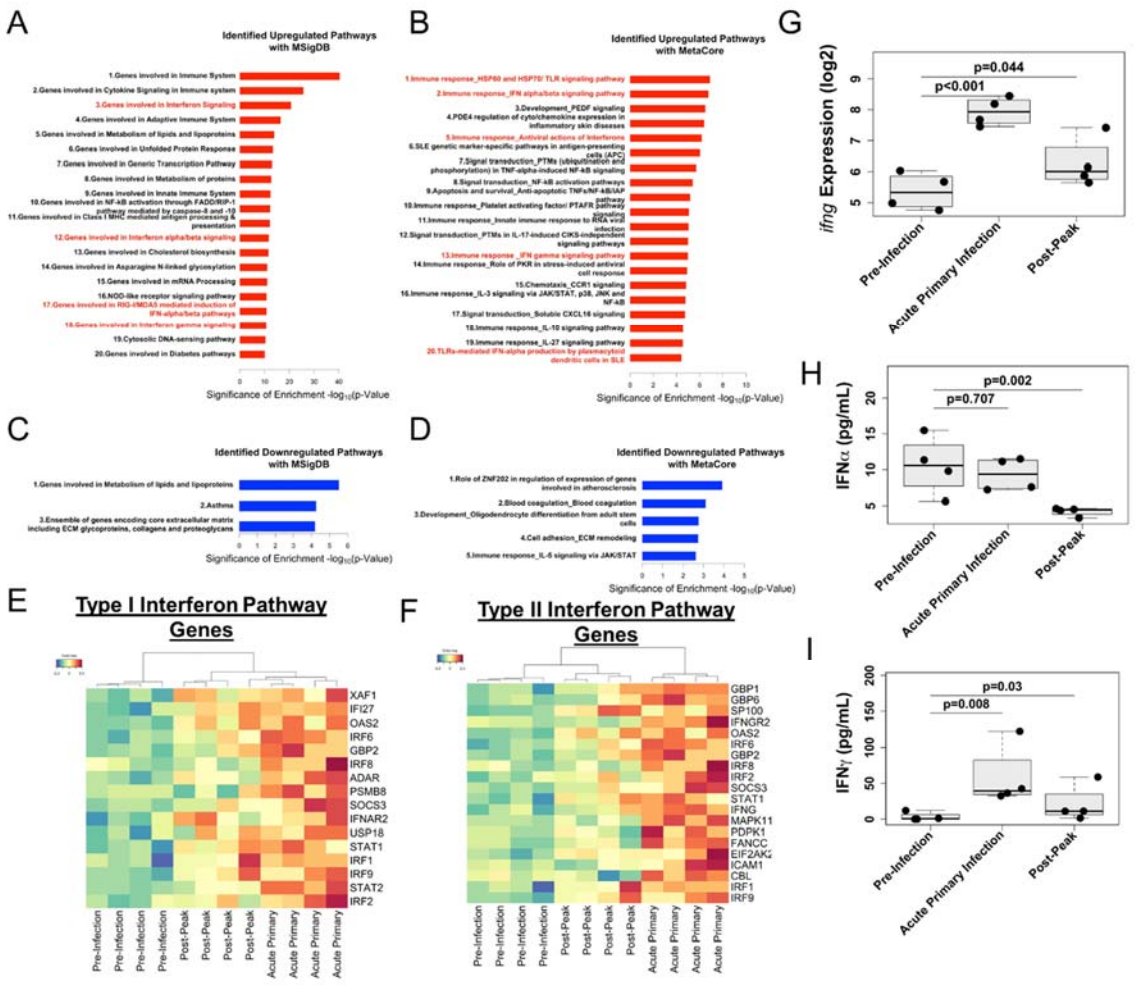

Figure 3. Type I and Type II interferon transcriptional signatures are enriched in the bone marrow during acute malaria. (A) Pathways enriched with upregulated genes using GSEA. Pathways associated with interferons are highlighted in red. Bars indicate the negative logarithm base 10 of the p-value of the enrichment for a given gene set. (B)Pathways enriched with upregulated genes using MetaCore. Pathways associated with interferons are highlighted in red. (C)Pathways enriched with downregulated genes using GSEA. (D)Pathways enriched with downregulated genes using MetaCore. (E)Clustered heatmap of transcriptional profiles of Type I IFN signature genes. Colors indicate z-score normalized expression values. (F)Clustered heatmap

of transcriptional profiles of Type II IFN signature genes. (G) *ifnγ* BM expression levels. (H) IFNα serum concentrations. (I) IFNγ serum concentrations.

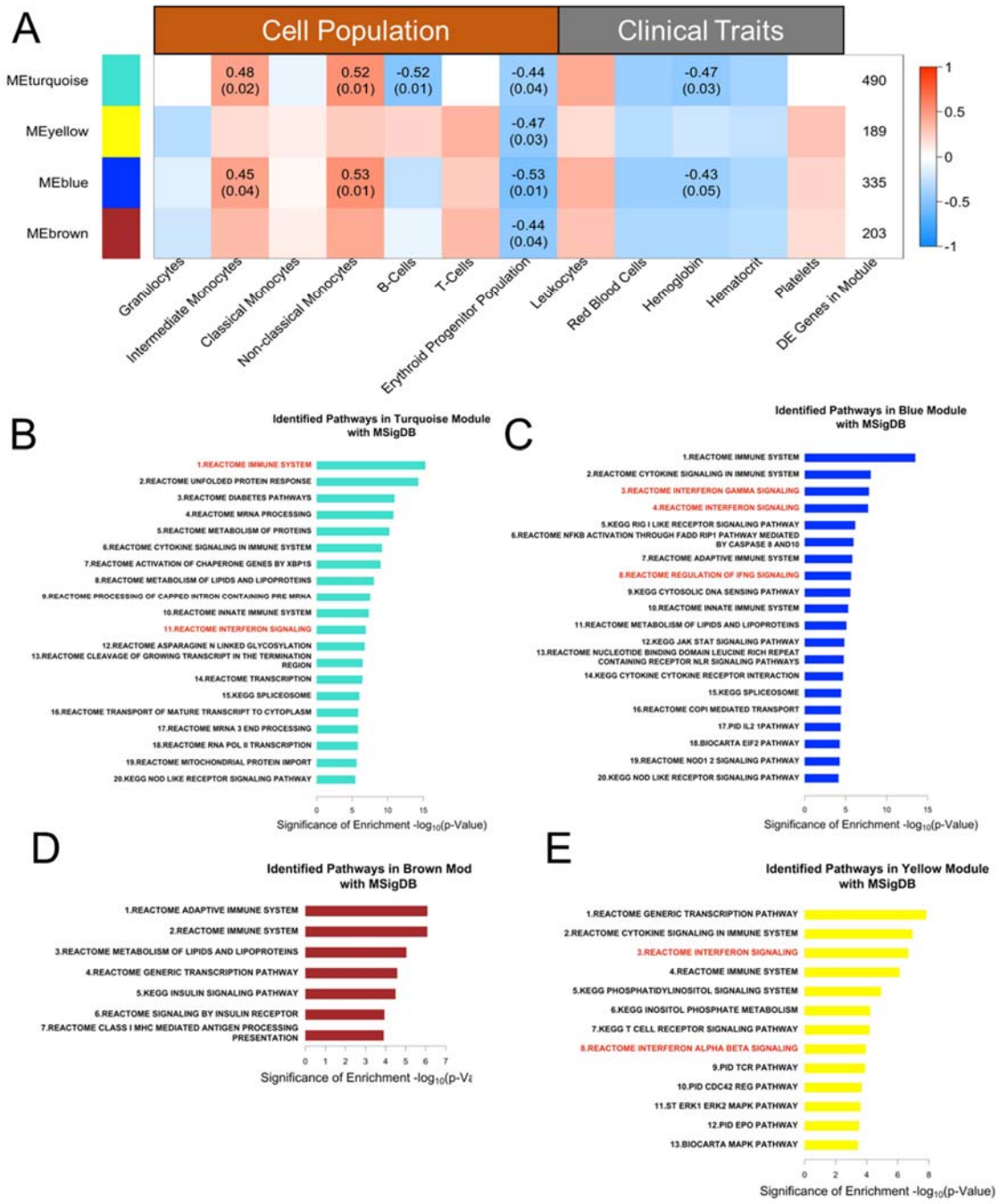

Figure 4. Intermediate and non-classical monocytes in the bone marrow are correlated with gene modules that may negatively impact the erythroid lineage. (A) Correlation of gene modules with cell population measurements and clinical traits based on WGNCA analysis of the BM transcriptome. Rows contain different transcriptional modules identified by WGCNA, with the

color in a given column indicating the degree of correlation of that module with cell population or clinical trait measurements. The top number in each entry is the Spearman correlation coefficient for any correlation with $p < 0.05$, and the bottom number is the p-value significance of the correlation coefficient. The last column indicates the number of genes in each module. (B-E) Significantly enriched pathways in the turquoise, blue, brown, and yellow modules based on analysis using MSigDB. Bars indicate the negative logarithm base 10 of the p-value of the enrichment for a given gene set.

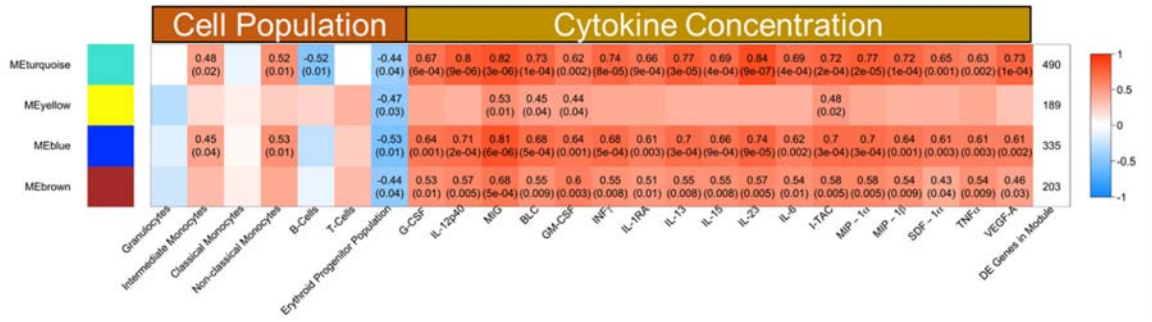

Figure 5. Systemic cytokines are positively associated with transcriptional modules that are negatively associated with erythroid progenitors but positively correlated with intermediate and non-classical monocytes. The correlation of gene modules with cell population measurements and cytokine concentrations based on WGNCA analysis of the BM transcriptome is shown. Cytokine measurements were performed using a multiplex assay with plasma collected after isolation of bone marrow mononuclear cells collected for RNA-Seq analysis. Rows contain different transcriptional modules identified by WGCNA, with the color in a given column indicating the degree of correlation of that module with cell population or cytokine measurements. The top number in each entry is the Spearman correlation coefficient for any correlation with $p < 0.05$, and the bottom number is the p-value significance of the correlation coefficient. The last column indicates the number of genes in each module.

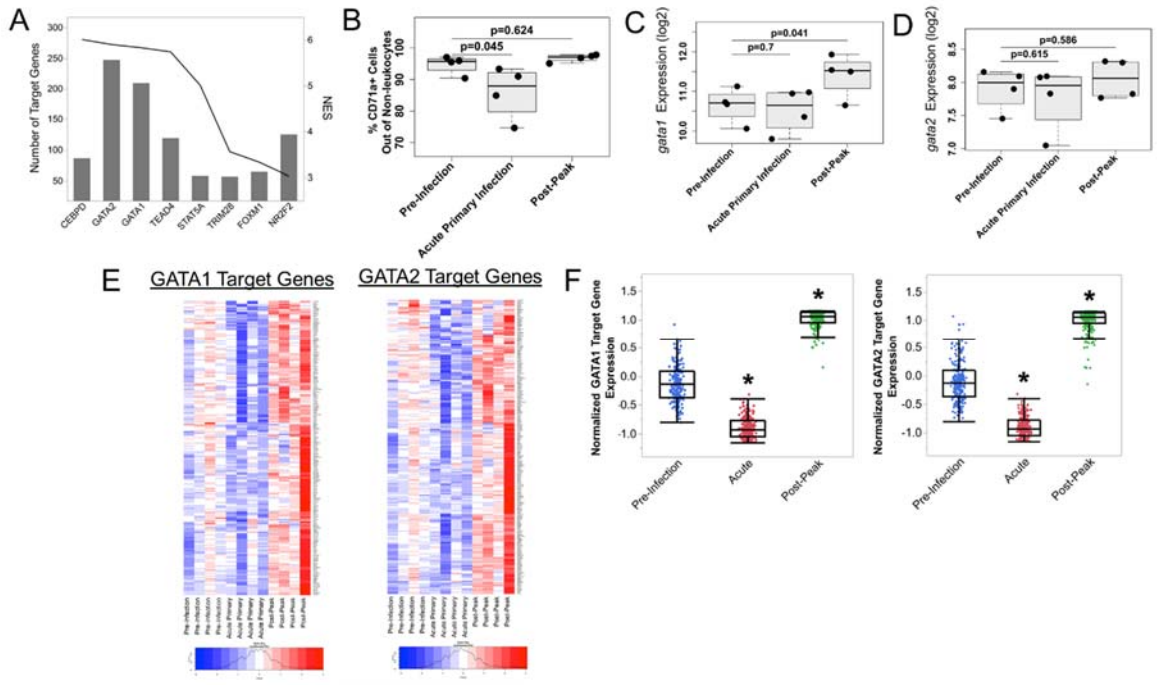

Figure 6. Disruption of GATA1 and GATA2 in erythroid progenitor cells may contribute to the decrease in erythroid progenitors and inefficient erythropoietic output during acute malaria. (A) Transcription factor analysis identified eight transcription factors (NES>3) associated with the cluster of genes positively correlated with reticulocyte levels. The line plot indicates the NES score, while the bar plot indicates the number of genes in the set containing a binding site for each transcription factor. (B) Frequency of erythroid progenitors in the bone marrow during different infection periods as determined by flow cytometry. There is a small but statistically significant decrease at acute primary infection. (C and D) Transcriptional expression levels of GATA1 and GATA2 in BM. Expression of GATA1 was upregulated at post-peak, but not at acute primary infection, while GATA2 levels were not significantly changed. (E) Heatmap of gene expression levels of the GATA1 and GATA2 transcriptional regulatory network; samples are in chronological order, while genes are hierarchically clustered. Most pathway members were downregulated at acute primary infection and upregulated at the post-peak infection point. (F) Gene expression of GATA1/2 targets was downregulated at acute primary and upregulated at

post-peak compared to pre-infection. Gene measurements were averaged across animals for each infection point, and paired t-tests were used to assess statistical significance (* significant at $p < 0.01$).

Additional Data

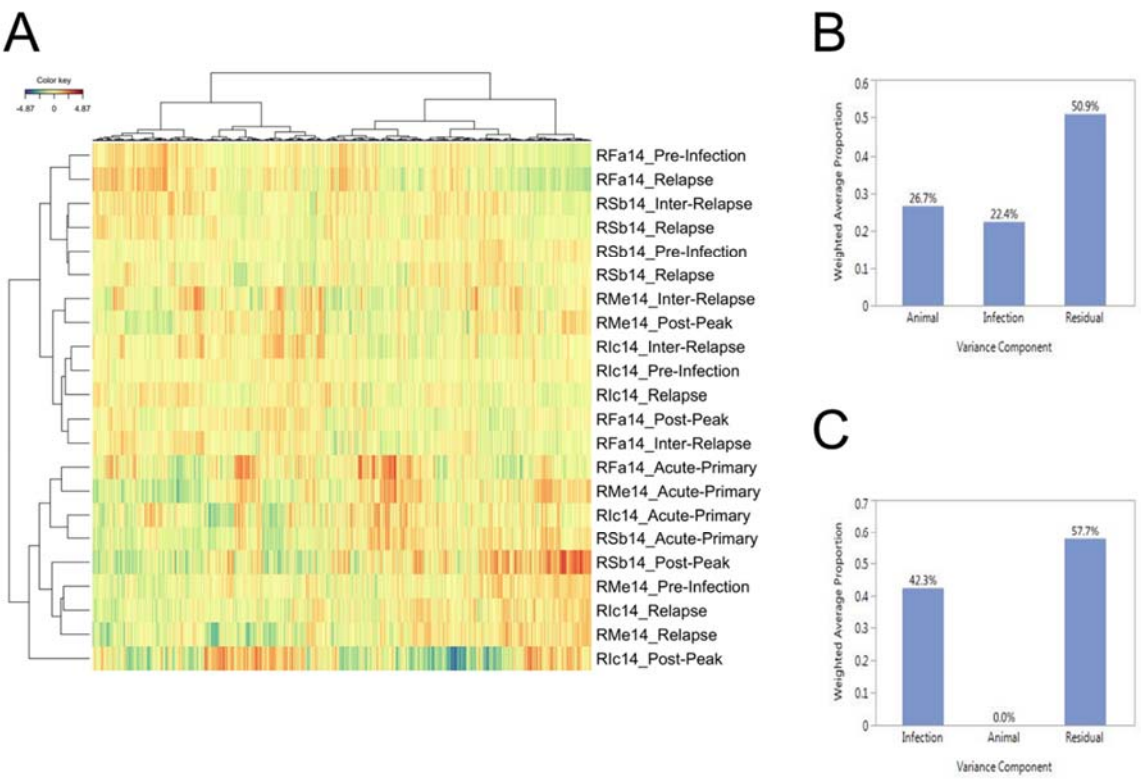

Additional File 1. Overview of the BM transcriptome prior to SNM transformation. (A) Clustered heatmap of the BM transcriptome before animal effects were removed. Four samples of acute primary infection form a cluster separated from other infection points. Other infection points do not form unique or separated clusters, with many of the most closely related samples coming from the same animals, suggesting that individual effects may confound the ability to identify the effect of infection points on gene expression profiles. Colors indicate z-score normalized expression values. (B) Variance Component Analysis showing that individual animal effects originally explain 26.7% of the gene expression variance, while infection points explain 22.4% of the gene expression variance. (C) After removing individual effects by SNM, infection points explain 42.3% of the gene expression variance.

Additional File 2. Gene ontology processes that are altered in the bone marrow during acute *P. cynomolgi* infections of rhesus macaques.						
	ID	**GO Process**	**pValue**	**FDR B&H**	**Genes from Input**	**Genes in Annotation**
1	GO:0006396	RNA processing	6.20E-14	4.37E-10	119	914
2	GO:0006397	mRNA processing	2.16E-10	7.60E-07	69	480
3	GO:0016071	mRNA metabolic process	3.25E-10	7.62E-07	86	665
4	GO:0006986	response to unfolded protein	1.21E-09	2.13E-06	35	174
5	GO:0035966	response to topologically incorrect protein	1.56E-09	2.19E-06	36	184
6	GO:0034341	response to interferon-gamma	3.02E-09	3.55E-06	33	163
7	GO:0008380	RNA splicing	5.79E-09	5.82E-06	58	403
8	GO:0070647	protein modification by small protein conjugation or removal	3.07E-08	2.71E-05	111	1026
9	GO:0030968	endoplasmic reticulum unfolded protein response	4.62E-08	2.84E-05	27	130
10	GO:0044403	symbiosis, encompassing mutualism through parasitism	4.82E-08	2.84E-05	92	808
11	GO:0044419	interspecies interaction between organisms	4.82E-08	2.84E-05	92	808
12	GO:0034976	response to endoplasmic reticulum stress	4.84E-08	2.84E-05	42	265
13	GO:0071346	cellular response to interferon-gamma	6.15E-08	3.15E-05	28	140
14	GO:0060333	interferon-gamma-mediated signaling pathway	6.26E-08	3.15E-05	21	85
15	GO:0035967	cellular response to topologically incorrect protein	7.21E-08	3.35E-05	28	141
16	GO:0034620	cellular response to unfolded protein	7.62E-08	3.35E-05	27	133
17	GO:0080134	regulation of response to stress	8.25E-08	3.42E-05	154	1585
18	GO:0032446	protein modification by small protein conjugation	3.34E-07	1.24E-04	97	903
19	GO:0009615	response to virus	3.34E-07	1.24E-04	56	430

20	GO:0071345	cellular response to cytokine stimulus	1.30E-06	4.44E-04	79	713
21	GO:0044764	multi-organism cellular process	1.32E-06	4.44E-04	84	773
22	GO:0034097	response to cytokine	1.60E-06	5.13E-04	88	825
23	GO:0006952	defense response	1.85E-06	5.66E-04	153	1655
24	GO:0000377	RNA splicing, via transesterification reactions with bulged adenosine as nucleophile	2.55E-06	7.18E-04	42	306
25	GO:0000398	mRNA splicing, via spliceosome	2.55E-06	7.18E-04	42	306
26	GO:0044248	cellular catabolic process	2.94E-06	7.96E-04	165	1828
27	GO:0051707	response to other organism	3.28E-06	8.25E-04	100	988
28	GO:0043207	response to external biotic stimulus	3.28E-06	8.25E-04	100	988
29	GO:0046165	alcohol biosynthetic process	3.49E-06	8.36E-04	27	160
30	GO:0000375	RNA splicing, via transesterification reactions	3.56E-06	8.36E-04	42	310
31	GO:0016567	protein ubiquitination	3.68E-06	8.36E-04	83	781
32	GO:0009607	response to biotic stimulus	3.97E-06	8.74E-04	103	1030
33	GO:0016032	viral process	4.12E-06	8.79E-04	81	759
34	GO:1902582	single-organism intracellular transport	4.40E-06	9.12E-04	166	1854
35	GO:0032606	type I interferon production	6.08E-06	1.22E-03	22	119
36	GO:0019221	cytokine-mediated signaling pathway	6.40E-06	1.25E-03	63	553
37	GO:0034340	response to type I interferon	7.01E-06	1.33E-03	18	86

Additional File 3. Complete list of gene sets that are upregulated in the bone marrow during acute *P. cynomolgi* infections of rhesus macaques using the GSEA database.

Gene Set Name	Description	FDR q-value
REACTOME_IMMUNE_SYSTEM	Genes involved in Immune System	6.99E-38
REACTOME_CYTOKINE_SIGNALING_IN_IMMUNE_SYSTEM	Genes involved in Cytokine Signaling in Immune system	1.50E-23
REACTOME_INTERFERON_SIGNALING	Genes involved in Interferon Signaling	9.22E-19
REACTOME_ADAPTIVE_IMMUNE_SYSTEM	Genes involved in Adaptive Immune System	1.22E-14
REACTOME_METABOLISM_OF_LIPIDS_AND_LIPOPROTEINS	Genes involved in Metabolism of lipids and lipoproteins	3.20E-12
REACTOME_UNFOLDED_PROTEIN_RESPONSE	Genes involved in Unfolded Protein Response	1.02E-11
REACTOME_GENERIC_TRANSCRIPTION_PATHWAY	Genes involved in Generic Transcription Pathway	1.83E-11
REACTOME_METABOLISM_OF_PROTEINS	Genes involved in Metabolism of proteins	3.51E-11
REACTOME_INNATE_IMMUNE_SYSTEM	Genes involved in Innate Immune System	6.17E-11
REACTOME_NFKB_ACTIVATION_THROUGH_FADD_RIP1_PATHWAY_MEDIATED_BY_CASPASE_8_AND10	Genes involved in NF-kB activation through FADD/RIP-1 pathway mediated by caspase-8 and -10	7.36E-11
REACTOME_CLASS_I_MHC_MEDIATED_ANTIGEN_PROCESSING_PRESENTATION	Genes involved in Class I MHC mediated antigen processing & presentation	9.30E-11
REACTOME_INTERFERON_ALPHA_BETA_SIGNALING	Genes involved in Interferon alpha/beta signaling	2.17E-10
REACTOME_CHOLESTEROL_BIOSYNTHESIS	Genes involved in Cholesterol biosynthesis	2.95E-10
REACTOME_ASPARAGINE_N_LINKED_GLYCOSYLATION	Genes involved in Asparagine N-linked glycosylation	8.05E-10
REACTOME_MRNA_PROCESSING	Genes involved in mRNA Processing	8.05E-10
KEGG_NOD_LIKE_RECEPTOR_SIGNALING_PATHWAY	NOD-like receptor signaling pathway	1.34E-09

REACTOME_RIG_I_MDA5_MEDIATED_INDUCTION_OF_IFN_ALPHA_BETA_PATHWAYS	Genes involved in RIG-I/MDA5 mediated induction of IFN-alpha/beta pathways	1.35E-09
REACTOME_INTERFERON_GAMMA_SIGNALING	Genes involved in Interferon gamma signaling	1.53E-09
KEGG_CYTOSOLIC_DNA_SENSING_PATHWAY	Cytosolic DNA-sensing pathway	3.31E-09
REACTOME_DIABETES_PATHWAYS	Genes involved in Diabetes pathways	5.25E-09
KEGG_T_CELL_RECEPTOR_SIGNALING_PATHWAY	T cell receptor signaling pathway	7.68E-09
KEGG_RIG_I_LIKE_RECEPTOR_SIGNALING_PATHWAY	RIG-I-like receptor signaling pathway	7.82E-09
REACTOME_ACTIVATION_OF_CHAPERONE_GENES_BY_XBP1S	Genes involved in Activation of Chaperone Genes by XBP1(S)	3.88E-08
REACTOME_ANTIVIRAL_MECHANISM_BY_IFN_STIMULATED_GENES	Genes involved in Antiviral mechanism by IFN-stimulated genes	3.04E-07
REACTOME_SIGNALING_BY_ILS	Genes involved in Signaling by Interleukins	3.51E-07
REACTOME_POST_TRANSLATIONAL_PROTEIN_MODIFICATION	Genes involved in Post-translational protein modification	3.58E-07
REACTOME_PROCESSING_OF_CAPPED_INTRON_CONTAINING_PRE_MRNA	Genes involved in Processing of Capped Intron-Containing Pre-mRNA	4.43E-07
REACTOME_NUCLEOTIDE_BINDING_DOMAIN_LEUCINE_RICH_REPEAT_CONTAINING_RECEPTOR_NLR_SIGNALING_PATHWAYS	Genes involved in Nucleotide-binding domain, leucine rich repeat containing receptor (NLR) signaling pathways	4.50E-07
KEGG_SPLICEOSOME	Spliceosome	6.47E-07
REACTOME_TRAF6_MEDIATED_NFKB_ACTIVATION	Genes involved in TRAF6 mediated NF-kB activation	7.65E-07
BIOCARTA_MAPK_PATHWAY	MAPKinase Signaling Pathway	9.45E-07
REACTOME_NOD1_2_SIGNALING_PATHWAY	Genes involved in NOD1/2 Signaling Pathway	9.91E-07
KEGG_TOLL_LIKE_RECEPTOR_SIGNALING_PATHWAY	Toll-like receptor signaling pathway	9.91E-07

KEGG_PHOSPHATIDYLINOSITOL_SIGNALING_SYSTEM	Phosphatidylinositol signaling system	1.28E-06
REACTOME_NEGATIVE_REGULATORS_OF_RIG_I_MDA5_SIGNALING	Genes involved in Negative regulators of RIG-I/MDA5 signaling	1.28E-06
KEGG_INOSITOL_PHOSPHATE_METABOLISM	Inositol phosphate metabolism	2.08E-06
REACTOME_ANTIGEN_PROCESSING_UBIQUITINATION_PROTEASOME_DEGRADATION	Genes involved in Antigen processing: Ubiquitination & Proteasome degradation	2.08E-06
KEGG_STEROID_BIOSYNTHESIS	Steroid biosynthesis	2.57E-06
PID_FAS_PATHWAY	FAS (CD95) signaling pathway	7.96E-06
REACTOME_RNA_POL_II_TRANSCRIPTION	Genes involved in RNA Polymerase II Transcription	8.32E-06
REACTOME_BIOSYNTHESIS_OF_THE_N_GLYCAN_PRECURSOR_DOLICHOL_LIPID_LINKED_OLIGOSACCHARIDE_LLO_AND_TRANSFER_TO_A_NASCENT_PROTEIN	Genes involved in Biosynthesis of the N-glycan precursor (dolichol lipid-linked oligosaccharide, LLO) and transfer to a nascent protein	9.94E-06
REACTOME_PHOSPHOLIPID_METABOLISM	Genes involved in Phospholipid metabolism	1.27E-05
PID_TCR_PATHWAY	TCR signaling in naïve CD4+ T cells	1.52E-05
PID_IL2_1PATHWAY	IL2-mediated signaling events	2.12E-05
REACTOME_FATTY_ACID_TRIACYLGLYCEROL_AND_KETONE_BODY_METABOLISM	Genes involved in Fatty acid, triacylglycerol, and ketone body metabolism	2.27E-05
REACTOME_CLEAVAGE_OF_GROWING_TRANSCRIPT_IN_THE_TERMINATION_REGION_	Genes involved in Cleavage of Growing Transcript in the Termination Region	2.58E-05
KEGG_CHEMOKINE_SIGNALING_PATHWAY	Chemokine signaling pathway	2.73E-05
REACTOME_TRANSCRIPTION	Genes involved in Transcription	2.73E-05
PID_EPO_PATHWAY	EPO signaling pathway	3.16E-05
KEGG_LEISHMANIA_INFECTION	Leishmania infection	3.22E-05
KEGG_JAK_STAT_SIGNALING_PATHWAY	Jak-STAT signaling pathway	3.22E-05
REACTOME_MRNA_3_END_PROCESSING	Genes involved in mRNA 3'-end processing	3.78E-05

REACTOME_SIGNALLING_TO_ERKS	Genes involved in Signalling to ERKs	4.67E-05
PID_IL23_PATHWAY	IL23-mediated signaling events	5.59E-05
ST_P38_MAPK_PATHWAY	p38 MAPK Pathway	5.59E-05
KEGG_NEUROTROPHIN_SIGNALING_PATHWAY	Neurotrophin signaling pathway	5.59E-05
REACTOME_MRNA_SPLICING	Genes involved in mRNA Splicing	6.93E-05
REACTOME_MEMBRANE_TRAFFICKING	Genes involved in Membrane Trafficking	7.15E-05
PID_IFNG_PATHWAY	IFN-gamma pathway	9.68E-05
BIOCARTA_VEGF_PATHWAY	VEGF, Hypoxia, and Angiogenesis	9.68E-05
ST_TUMOR_NECROSIS_FACTOR_PATHWAY	Tumor Necrosis Factor Pathway.	9.68E-05
KEGG_AMYOTROPHIC_LATERAL_SCLEROSIS_ALS	Amyotrophic lateral sclerosis (ALS)	9.68E-05
PID_CD8_TCR_PATHWAY	TCR signaling in naïve CD8+ T cells	9.68E-05
KEGG_EPITHELIAL_CELL_SIGNALING_IN_HELICOBACTER_PYLORI_INFECTION	Epithelial cell signaling in Helicobacter pylori infection	1.09E-04
REACTOME_TRANSPORT_OF_MATURE_TRANSCRIPT_TO_CYTOPLASM	Genes involved in Transport of Mature Transcript to Cytoplasm	1.10E-04
REACTOME_TRAF6_MEDIATED_IRF7_ACTIVATION	Genes involved in TRAF6 mediated IRF7 activation	1.18E-04
REACTOME_TRNA_AMINOACYLATION	Genes involved in tRNA Aminoacylation	1.27E-04
KEGG_UBIQUITIN_MEDIATED_PROTEOLYSIS	Ubiquitin mediated proteolysis	1.35E-04
REACTOME_ANTIGEN_PRESENTATION_FOLDING_ASSEMBLY_AND_PEPTIDE_LOADING_OF_CLASS_I_MHC	Genes involved in Antigen Presentation: Folding, assembly and peptide loading of class I MHC	1.49E-04
KEGG_APOPTOSIS	Apoptosis	1.72E-04
KEGG_CYTOKINE_CYTOKINE_RECEPTOR_INTERACTION	Cytokine-cytokine receptor interaction	1.74E-04
REACTOME_MITOCHONDRIAL_PROTEIN_IMPORT	Genes involved in Mitochondrial Protein Import	1.83E-04
KEGG_RNA_DEGRADATION	RNA degradation	2.07E-04

BIOCARTA_DEATH_PATHWAY	Induction of apoptosis through DR3 and DR4/5 Death Receptors	2.07E-04
BIOCARTA_KERATINOCYTE_PATHWAY	Keratinocyte Differentiation	2.27E-04
PID_TNF_PATHWAY	TNF receptor signaling pathway	2.27E-04
BIOCARTA_RANKL_PATHWAY	Bone Remodelling	2.30E-04
REACTOME_TRAF3_DEPENDENT_IRF_ACTIVATION_PATHWAY	Genes involved in TRAF3-dependent IRF activation pathway	2.30E-04
BIOCARTA_NFKB_PATHWAY	NF-kB Signaling Pathway	2.30E-04
PID_NFKAPPAB_CANONICAL_PATHWAY	Canonical NF-kappaB pathway	2.30E-04
SIG_CD40PATHWAYMAP	Genes related to CD40 signaling	2.33E-04
REACTOME_ANTIGEN_PROCESSING_CROSS_PRESENTATION	Genes involved in Antigen processing-Cross presentation	2.35E-04
REACTOME_ER_PHAGOSOME_PATHWAY	Genes involved in ER-Phagosome pathway	2.42E-04
PID_IL6_7_PATHWAY	IL6-mediated signaling events	2.42E-04
PID_HIV_NEF_PATHWAY	HIV-1 Nef: Negative effector of Fas and TNF-alpha	2.72E-04
BIOCARTA_NTHI_PATHWAY	NFkB activation by Nontypeable Hemophilus influenzae	2.79E-04
KEGG_TERPENOID_BACKBONE_BIOSYNTHESIS	Terpenoid backbone biosynthesis	3.04E-04
BIOCARTA_STRESS_PATHWAY	TNF/Stress Related Signaling	3.52E-04
PID_BCR_5PATHWAY	BCR signaling pathway	3.82E-04
BIOCARTA_RELA_PATHWAY	Acetylation and Deacetylation of RelA in The Nucleus	4.19E-04
PID_IL27_PATHWAY	IL27-mediated signaling events	4.30E-04
REACTOME_NGF_SIGNALLING_VIA_TRKA_FROM_THE_PLASMA_MEMBRANE	Genes involved in NGF signalling via TRKA from the plasma membrane	4.30E-04
BIOCARTA_IL2RB_PATHWAY	IL-2 Receptor Beta Chain in T cell Activation	4.39E-04
KEGG_ADIPOCYTOKINE_SIGNALING_PATHWAY	Adipocytokine signaling pathway	4.61E-04

PID_KIT_PATHWAY	Signaling events mediated by Stem cell factor receptor (c-Kit)	4.61E-04
REACTOME_SIGNALLING_TO_RAS	Genes involved in Signalling to RAS	5.17E-04
BIOCARTA_41BB_PATHWAY	The 4-1BB-dependent immune response	5.34E-04
BIOCARTA_IL10_PATHWAY	IL-10 Anti-inflammatory Signaling Pathway	5.34E-04
REACTOME_RIP_MEDIATED_NFKB_ACTIVATION_VIA_DAI	Genes involved in RIP-mediated NFkB activation via DAI	7.18E-04
REACTOME_GLYCOLYSIS	Genes involved in Glycolysis	7.57E-04

Additional File 4. Complete list of pathways that are upregulated in the bone marrow during acute *P. cynomolgi* infections of rhesus macaques using the Metacore database.

#	Maps	Genes in Pathway	Genes In Data	FDR p-value
1	Immune response_HSP60 and HSP70/ TLR signaling pathway	54	13	6.81E-05
2	Immune response_IFN alpha/beta signaling pathway	24	9	6.81E-05
3	Development_PEDF signaling	49	12	7.99E-05
4	PDE4 regulation of cyto/chemokine expression in inflammatory skin diseases	50	12	7.99E-05
5	Immune response_Antiviral actions of Interferons	52	12	1.01E-04
6	SLE genetic marker-specific pathways in antigen-presenting cells (APC)	84	15	1.19E-04
7	Signal transduction_PTMs (ubiquitination and phosphorylation) in TNF-alpha-induced NF-kB signaling	39	10	2.22E-04
8	Signal transduction_NF-kB activation pathways	51	11	3.79E-04
9	Apoptosis and survival_Anti-apoptotic TNFs/NF-kB/IAP pathway	27	8	5.75E-04
10	Immune response_Platelet activating factor/ PTAFR pathway signaling	55	11	6.09E-04
11	Immune response_Innate immune response to RNA viral infection	28	8	6.09E-04
12	Signal transduction_PTMs in IL-17-induced CIKS-independent signaling pathways	46	10	6.09E-04
13	Immune response _IFN gamma signaling pathway	56	11	6.09E-04
14	Immune response_Role of PKR in stress-induced antiviral cell response	57	11	6.77E-04
15	Chemotaxis_CCR1 signaling	48	10	7.75E-04
16	Immune response_IL-3 signaling via JAK/STAT, p38, JNK and NF-kB	93	14	8.12E-04
17	Signal transduction_Soluble CXCL16 signaling	49	10	8.29E-04
18	Immune response_IL-10 signaling pathway	62	11	1.17E-03
19	Immune response_IL-27 signaling pathway	24	7	1.17E-03
20	TLRs-mediated IFN-alpha production by plasmacytoid dendritic cells in SLE	53	10	1.45E-03
21	Development_Cross-talk between VEGF and Angiopoietin 1 signaling pathways	26	7	1.88E-03
22	Immune response_IL-9 signaling pathway	36	8	2.24E-03
23	Immune response_Role of HMGB1 in dendritic cell maturation and migration	27	7	2.24E-03

24	Immune response_IL-5 signaling via JAK/STAT	57	10	2.32E-03
25	Immune response_Antigen presentation by MHC class I	28	7	2.65E-03
26	Immune response_TLR5, TLR7, TLR8 and TLR9 signaling pathways	48	9	2.87E-03
27	Development_EGFR signaling pathway	71	11	2.95E-03
28	Development_G-CSF signaling	49	9	3.15E-03
29	Development_c-Kit ligand signaling pathway during hemopoiesis	61	10	3.48E-03
30	Development_IGF-1 receptor signaling	52	9	4.74E-03
31	Immune response_IL-12 signaling pathway	23	6	5.40E-03
32	Immune response_CD40 signaling	65	10	5.43E-03
33	Apoptosis and survival_TNFR1 signaling pathway	43	8	5.85E-03
34	Apoptosis and survival_Endoplasmic reticulum stress response pathway	55	9	6.32E-03
35	Immune response_Fc epsilon RI pathway	55	9	6.32E-03
36	Immune response_IL-1 signaling pathway	44	8	6.33E-03
37	Immune response_Inflammasome in inflammatory response	34	7	6.62E-03
38	Immune response_CD28 signaling	56	9	6.62E-03
39	Immune response_IL-4 signaling pathway	94	12	6.62E-03
40	Immune response_TLR2 and TLR4 signaling pathways	57	9	6.96E-03
41	Development_Growth hormone signaling via STATs and PLC/IP3	35	7	6.96E-03
42	DeltaF508-CFTR traffic / ER-to-Golgi in CF	17	5	6.96E-03
43	wtCFTR traffic / ER-to-Golgi (normal)	17	5	6.96E-03
44	Immune response_Naive CD4+ T cell differentiation	46	8	6.96E-03
45	Immune response_Inhibitory action of Lipoxins on pro-inflammatory TNF-alpha signaling	46	8	6.96E-03
46	Development_Prolactin receptor signaling	58	9	7.25E-03
47	Immune response_Oncostatin M signaling via JAK-Stat in mouse cells	18	5	8.81E-03
48	Transcription_Role of Akt in hypoxia induced HIF1 activation	27	6	8.81E-03
49	Immune response_IL-18 signaling	60	9	8.81E-03
50	Immune response_Bacterial infections in normal airways	49	8	9.46E-03
51	Signal transduction_mTORC1 downstream signaling	61	9	9.46E-03
52	Substance P-mediated inflammation and pain in Sickle cell disease	38	7	9.46E-03
53	SLE genetic marker-specific pathways in T cells	101	12	9.46E-03

54	Development_Role of CNTF and LIF in regulation of oligodendrocyte development	28	6	9.77E-03
55	Signal transduction_mTORC1 upstream signaling	62	9	1.00E-02
56	Immune response_Lectin induced complement pathway	50	8	1.00E-02
57	Development_ERBB-family signaling	39	7	1.02E-02
58	Translation _Regulation of EIF2 activity	39	7	1.02E-02
59	Cholesterol Biosynthesis	103	12	1.02E-02
60	IL-6 signaling in multiple myeloma	51	8	1.07E-02
61	Apoptosis and survival_NGF activation of NF-kB	40	7	1.12E-02
62	Transcription_Sirtuin6 regulation and functions	64	9	1.12E-02
63	Immune response_Oncostatin M signaling via JAK-Stat in human cells	20	5	1.12E-02
64	Main growth factor signaling cascades in multiple myeloma cells	41	7	1.26E-02
65	Immune response_Classical complement pathway	53	8	1.26E-02
66	Immune response_T cell receptor signaling pathway	53	8	1.26E-02
67	Translation_Insulin regulation of translation	42	7	1.37E-02
68	B cell signaling in hematological malignancies	80	10	1.37E-02
69	Development_FGFR signaling pathway	54	8	1.37E-02
70	Development_VEGF signaling and activation	43	7	1.54E-02
71	Development_Angiotensin signaling via STATs	32	6	1.54E-02
72	Development_Thrombopoetin signaling via JAK-STAT pathway	22	5	1.54E-02
73	Cell cycle_Role of 14-3-3 proteins in cell cycle regulation	22	5	1.54E-02
74	Apoptosis and survival_FAS signaling cascades	44	7	1.68E-02
75	Development_Cytokine-mediated regulation of megakaryopoiesis	57	8	1.78E-02
76	Cytoskeleton remodeling_FAK signaling	57	8	1.78E-02
77	Development_VEGF signaling via VEGFR2 - generic cascades	84	10	1.78E-02
78	Immune response_TNF-R2 signaling pathways	45	7	1.82E-02
79	Apoptosis and survival_Caspase cascade	34	6	1.88E-02
80	Chemotaxis_CXCR4 signaling pathway	34	6	1.88E-02
81	Immune response_IL-22 signaling pathway	34	6	1.88E-02
82	Immune response_CXCR4 signaling via second messenger	34	6	1.88E-02
83	Immune response_MIF-induced cell adhesion, migration and angiogenesis	46	7	1.94E-02
84	Immune response_T regulatory cell-mediated modulation of antigen-presenting cell functions	72	9	1.94E-02

85	SLE genetic marker-specific pathways in B cells	101	11	1.98E-02
86	CFTR folding and maturation (normal and CF)	24	5	1.98E-02
87	Development_EPO-induced Jak-STAT pathway	35	6	2.02E-02
88	NALP3 inflammasome activation in age-related macular degeneration (AMD)	35	6	2.02E-02
89	Development_Angiopoietin - Tie2 signaling	35	6	2.02E-02
90	Apoptosis and survival_Role of nuclear PI3K in NGF/ TrkA signaling	25	5	2.24E-02
91	Development_Leptin signaling via JAK/STAT and MAPK cascades	25	5	2.24E-02
92	Immune response_Histamine H1 receptor signaling in immune response	48	7	2.24E-02
93	Immune response_HMGB1/TLR signaling pathway	36	6	2.24E-02
94	Chemotaxis_Leukocyte chemotaxis	75	9	2.31E-02
95	Immune response_BCR pathway	62	8	2.44E-02
96	PDE4 regulation of cyto/chemokine expression in arthritis	49	7	2.44E-02
97	HCV-dependent regulation of membrane receptors signaling in HCC	27	5	3.01E-02
98	Inflammatory factors-induced expression of mucins in normal and asthmatic epithelium	51	7	3.01E-02
99	Development_Role of IL-8 in angiogenesis	65	8	3.04E-02
100	Immune response_Th17, Th22 and Th9 cell differentiation	39	6	3.04E-02
101	Immune response_TSLP signalling	39	6	3.04E-02
102	Role of tumor microenvironment in plexiform neurofibroma formation in neurofibromatosis type 1	39	6	3.04E-02
103	Apoptosis and survival_APRIL and BAFF signaling	39	6	3.04E-02
104	Immune response_HMGB1 release from the cell	39	6	3.04E-02
105	Immune response_TCR and CD28 co-stimulation in activation of NF-kB	40	6	3.34E-02
106	Apoptosis and survival_Role of PKR in stress-induced apoptosis	53	7	3.34E-02
107	Translation_Regulation of EIF4F activity	53	7	3.34E-02
108	Immune response_Inhibitory PD-1 signaling in T cells	53	7	3.34E-02
109	Immune response_HMGB1/RAGE signaling pathway	53	7	3.34E-02
110	Signal transduction_Additional pathways of NF-kB activation (in the cytoplasm)	53	7	3.34E-02
111	Schema: Initiation of T cell recruitment in allergic contact dermatitis	18	4	3.36E-02
112	Immune response_CD137 signaling in immune cell	29	5	3.54E-02

113	TLR2-induced platelet activation	41	6	3.54E-02
114	Signal transduction_PTMs (phosphorylation) in TNF-alpha-induced NF-kB signaling	41	6	3.54E-02
115	Th17 cells in CF	54	7	3.54E-02
116	Translation_Non-genomic (rapid) action of Androgen Receptor	42	6	3.88E-02
117	Apoptosis and survival_Anti-apoptotic TNFs/NF-kB/Bcl-2 pathway	42	6	3.88E-02
118	Signal transduction_JNK pathway	42	6	3.88E-02
119	DNA damage_Brca1 as a transcription regulator	30	5	3.88E-02
120	Signal transduction_Additional pathways of NF-kB activation (in the nucleus)	30	5	3.88E-02
121	Inter-cellular relations in COPD (general schema)	30	5	3.88E-02
122	Chemotaxis_CCL2-induced chemotaxis	56	7	4.09E-02
123	Immune response_IL-7 signaling in B lymphocytes	43	6	4.10E-02
124	Signal transduction_PTMs in BAFF-induced canonical NF-kB signaling	43	6	4.10E-02
125	Signal transduction_AKT signaling	43	6	4.10E-02
126	Regulation of Tissue factor signaling in cancer	43	6	4.10E-02
127	Apoptosis and survival_Role of IAP-proteins in apoptosis	31	5	4.20E-02
128	Signal transduction_PTMs in IL-23 signaling pathway	31	5	4.20E-02
129	Alternative complement cascade disruption in age-related macular degeneration	31	5	4.20E-02
130	Immune response_TLR3 and TLR4 induced TICAM1-specific signaling pathway	20	4	4.27E-02
131	Immune response_PGE2 in immune and neuroendocrine system interactions	44	6	4.35E-02
132	Development_Flt3 signaling	44	6	4.35E-02
133	Nociception_Expression and role of Nociceptin in immune system	44	6	4.35E-02
134	Immune response_IL-6 signaling pathway via JAK/STAT	72	8	4.36E-02
135	DNA damage_ATM/ATR regulation of G1/S checkpoint	32	5	4.54E-02
136	Development_PDGF signaling via STATs and NF-kB	32	5	4.54E-02
137	Signal transduction_PTMs in IL-17-induced CIKS-dependent MAPK signaling pathways	32	5	4.54E-02
138	Immune response_TREM1 signaling pathway	59	7	4.77E-02
139	Immune response_Immunological synapse formation	59	7	4.77E-02
140	Cell adhesion_Integrin inside-out signaling in T cells	74	8	4.91E-02

Additional File 5. Complete list of gene sets that are downregulated in the bone marrow during acute *P. cynomolgi* infections of rhesus macaques using the GSEA database.

Gene Set Name	Description	FDR q-value
REACTOME_METABOLISM_OF_LIPIDS_AND_LIPOPROTEINS	Genes involved in Metabolism of lipids and lipoproteins	4.03E-03
KEGG_ASTHMA	Asthma	2.85E-02
NABA_CORE_MATRISOME	Ensemble of genes encoding core extracellular matrix including ECM glycoproteins, collagens and proteoglycans	2.85E-02

Additional File 6. Complete list of pathways that are downregulated in the bone marrow during acute *P. cynomolgi* infections of rhesus macaques using the Metacore database.

#	Maps	Genes in Pathway	Genes in Data	FDR p-value
1	Role of ZNF202 in regulation of expression of genes involved in atherosclerosis	21	3	1.81E-02
2	Blood coagulation_Blood coagulation	39	3	5.87E-02
3	Development_Oligodendrocyte differentiation from adult stem cells	51	3	6.80E-02
4	Cell adhesion_ECM remodeling	52	3	6.80E-02
5	Immune response_IL-5 signaling via JAK/STAT	57	3	7.09E-02

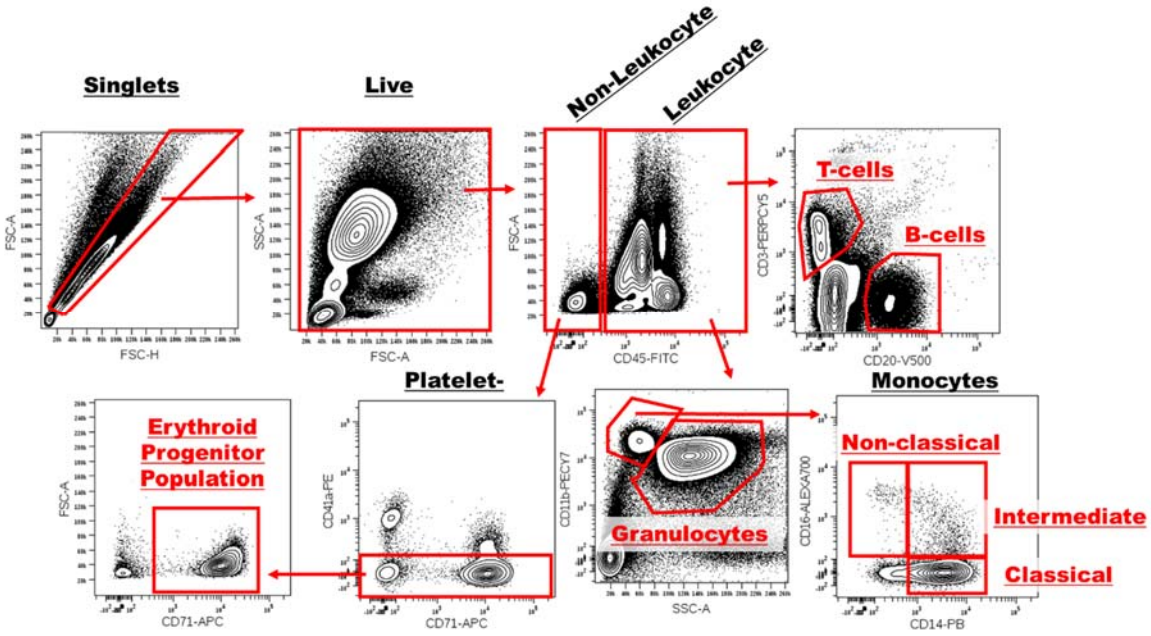

Additional File 7. Flow cytometry gating strategy to monitor cellular subset in the bone marrow of rhesus macaques with malaria. A representative gating strategy for determining the frequency of various immune cell subsets in bone marrow aspirate collected from rhesus macaques during *P. cynomolgi* infection. This representative plot is from a pre-infection time-point.

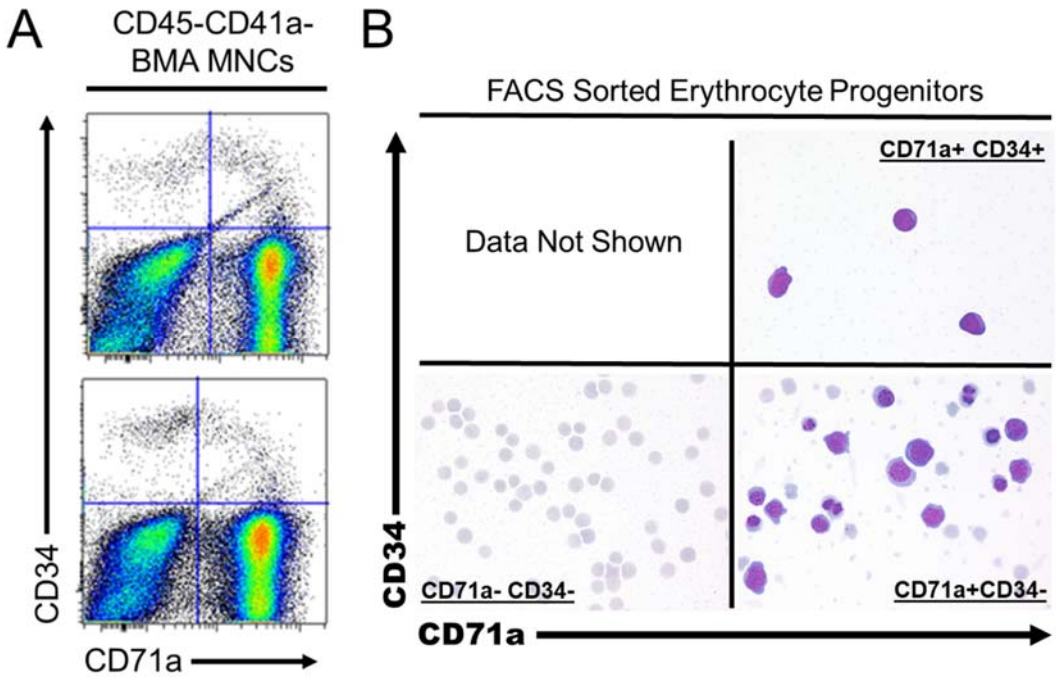

Additional File 8. Characterization of the cellular subsets constituting the erythroid progenitor cell population. (A) FACS profiles corresponding to (B). (B) Cells consistent with the cell surface phenotype of erythroid progenitors were identified based on CD34 and CD71a surface staining.

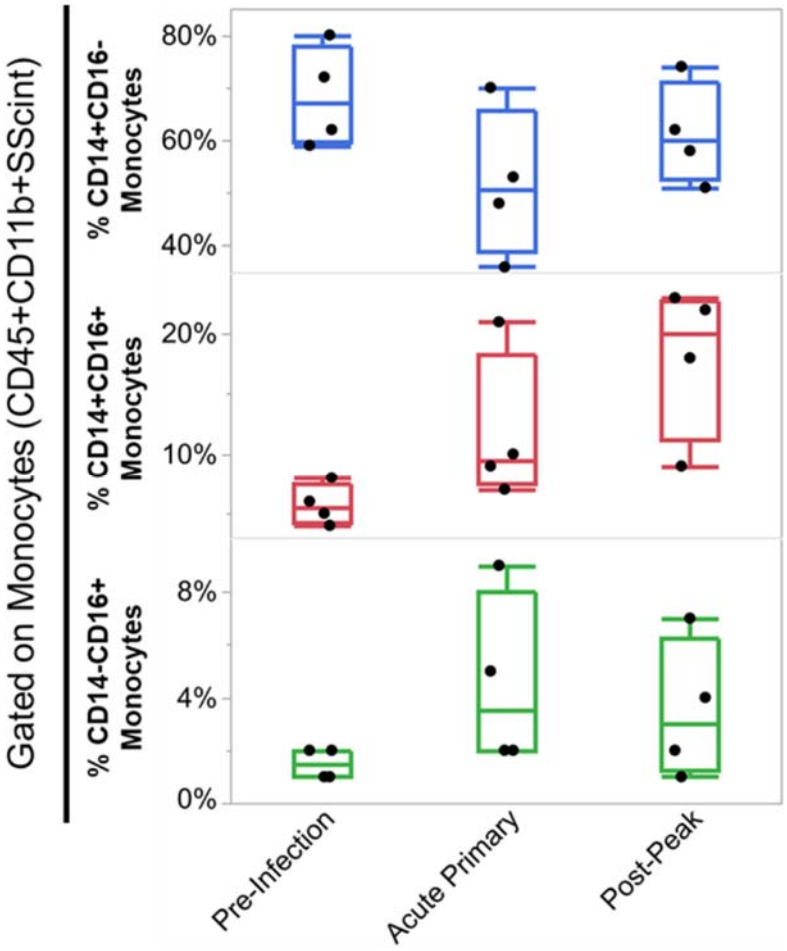

Additional File 9. Changes in monocyte subsets in the bone marrow during an initial blood-stage *P. cynomolgi* infection. The percentage of classical (CD14+CD16-), intermediate (CD14+CD16+), and non-classical (CD14-CD16+) monocytes out of the monocyte compartment are shown before infection, during the acute primary infection, and after the peak of infection.

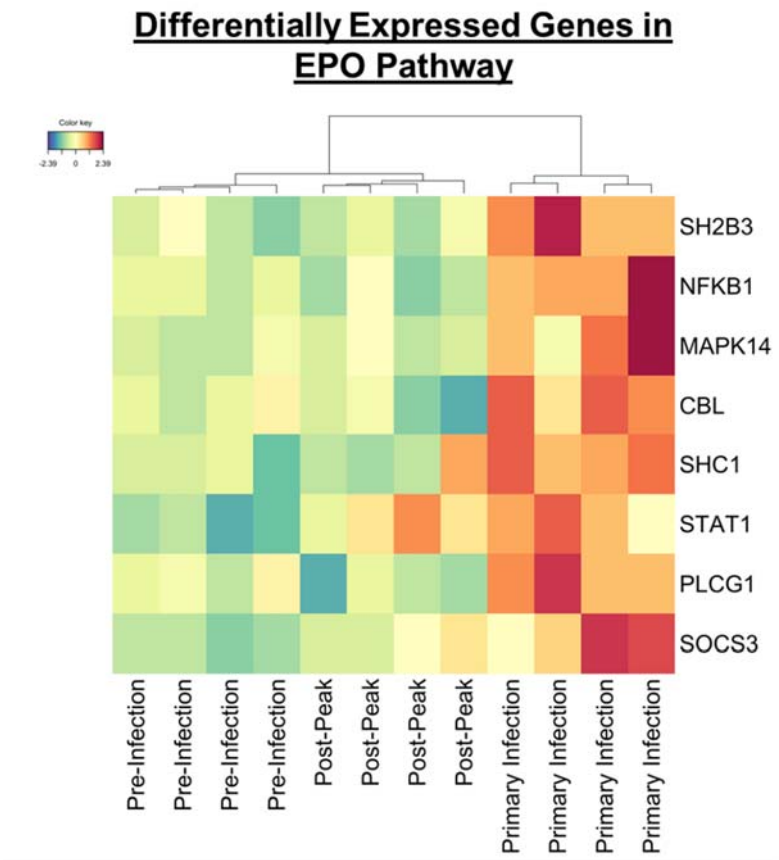

Additional File 10. Transcriptional profiles of genes in the EPO pathway before, during, and immediately after acute malaria. The genes in the erythropoietin pathway identified as differentially expressed in the bone marrow RNA-Seq data set are shown. Samples are hierarchically clustered. Colors indicate z-score normalized expression values.

Additional File 11. List of genes identified as significantly positively correlated with the frequency of the erythroid progenitor population in the BM.	
HostGene	**Correlation Coefficient**
EPN2	9.44E-01
TOX2	9.37E-01
CEP63	9.23E-01
FAHD1	9.23E-01
FAM210B	9.16E-01
AP5S1	9.02E-01
ARL2BP	8.95E-01
CR1L	8.95E-01
RNF152	8.95E-01
GCLC	8.88E-01
TMCC2	8.88E-01
FBXO7	8.81E-01
FECH	8.81E-01
GPSM2	8.81E-01
MPST	8.81E-01
RBBP8	8.81E-01
RBM38	8.81E-01
SLC4A1	8.81E-01
ZER1	8.81E-01
ITSN1	8.74E-01
NET1	8.74E-01
PRR5	8.74E-01
ADD1	8.67E-01
C5orf4	8.67E-01
CENPB	8.67E-01
FN3K	8.67E-01
RASGRP3	8.67E-01
SLFN14	8.67E-01
NDC80	8.60E-01
BSG	8.53E-01
GDE1	8.53E-01
LDOC1L	8.53E-01
MXI1	8.53E-01
PSMD9	8.53E-01
TSKU	8.53E-01
TUBB2B	8.53E-01
WDTC1	8.53E-01
FOXO3	8.46E-01

MAP1LC3B2	8.46E-01
MFSD12	8.46E-01
SSBP3	8.46E-01
STK24	8.46E-01
TMOD1	8.46E-01
ZNF324	8.46E-01
CDKN2C	8.39E-01
DCK	8.39E-01
FOXO4	8.39E-01
FZD1	8.39E-01
LAMA3	8.39E-01
RFC3	8.39E-01
SPECC1	8.39E-01
TRAK2	8.39E-01
ACSL6	8.32E-01
ARRDC2	8.32E-01
FKBP8	8.32E-01
ISCA1	8.32E-01
LY6G6D	8.32E-01
PIP5K1B	8.32E-01
SLC25A39	8.32E-01
AGFG2	8.25E-01
BCL2L1	8.25E-01
GTPBP1	8.25E-01
NEDD4L	8.25E-01
NEK2	8.25E-01
NUDT4	8.25E-01
RUNX1T1	8.25E-01
SLC2A1	8.25E-01
SLC45A3	8.25E-01
TFDP2	8.25E-01
WIF1	8.25E-01
ABL1	8.18E-01
ARHGAP23	8.18E-01
CA1	8.18E-01
CCDC167	8.18E-01
DARC	8.18E-01
GUCD1	8.18E-01
HEMGN	8.18E-01
PIGQ	8.18E-01
BPGM	8.11E-01

C17orf58	8.11E-01
EIF2AK1	8.11E-01
HDHD3	8.11E-01
HNRNPUL1	8.11E-01
PARP16	8.11E-01
PGA4	8.11E-01
RHBDD1	8.11E-01
SIRT2	8.11E-01
TMEM129	8.11E-01
ACP1	8.04E-01
ACSM3	8.04E-01
BEND7	8.04E-01
E2F2	8.04E-01
EPOR	8.04E-01
GFOD2	8.04E-01
ICAM4	8.04E-01
KIAA0101	8.04E-01
PHOSPHO1	8.04E-01
SLC22A16	8.04E-01
SNCA	8.04E-01
SNX15	8.04E-01
SOX6	8.04E-01
TST	8.04E-01
WIPI1	8.04E-01
ZNF526	8.04E-01
AP1M1	7.97E-01
ARL4A	7.97E-01
ASH2L	7.97E-01
DNAI2	7.97E-01
EPHB4	7.97E-01
FAM214B	7.97E-01
FSCN1	7.97E-01
HEY1	7.97E-01
NOSIP	7.97E-01
RNF182	7.97E-01
TMPRSS9	7.97E-01
TSPO2	7.97E-01
ZNF212	7.97E-01
C17orf99	7.90E-01
C7orf50	7.90E-01
CRAT	7.90E-01

DENND2A	7.90E-01
8-Mar	7.90E-01
MOSPD1	7.90E-01
PINK1	7.90E-01
SELENBP1	7.90E-01
STRADB	7.90E-01
UBXN11	7.90E-01
UROS	7.90E-01
BRPF3	7.83E-01
CLEC16A	7.83E-01
F8A1	7.83E-01
FGB	7.83E-01
GPKOW	7.83E-01
JOSD2	7.83E-01
NAT6	7.83E-01
NMNAT3	7.83E-01
SLC16A1	7.83E-01
SLC44A2	7.83E-01
BNIP3L	7.76E-01
GID8	7.76E-01
HEY2	7.76E-01
IGFBP4	7.76E-01
KANK2	7.76E-01
NT5M	7.76E-01
NUPL2	7.76E-01
REPS2	7.76E-01
SMOX	7.76E-01
SORBS2	7.76E-01
ASF1B	7.69E-01
COL4A6	7.69E-01
FAM57A	7.69E-01
FIS1	7.69E-01
IBA57	7.69E-01
KEAP1	7.69E-01
MAEA	7.69E-01
PLCD3	7.69E-01
PMVK	7.69E-01
RPS6KA1	7.69E-01
SKA3	7.69E-01
ST8SIA2	7.69E-01
UBALD1	7.69E-01

DSP	7.62E-01
FZR1	7.62E-01
GMPR	7.62E-01
MRP63	7.62E-01
NBL1	7.62E-01
PLXNA1	7.62E-01
RMND5B	7.62E-01
SLC25A11	7.62E-01
SPTA1	7.62E-01
TAB3	7.62E-01
TTC23L	7.62E-01
ZSCAN16	7.62E-01
C5orf30	7.55E-01
CDKN3	7.55E-01
CTSD	7.55E-01
DET1	7.55E-01
FAM117A	7.55E-01
GPC4	7.55E-01
GPX1	7.55E-01
ISCA2	7.55E-01
LRRC20	7.55E-01
NDE1	7.55E-01
PLEK2	7.55E-01
RFESD	7.55E-01
SLC14A1	7.55E-01
XYLT2	7.55E-01
AQP1	7.48E-01
C17orf103	7.48E-01
GLTPD1	7.48E-01
HBQ1	7.48E-01
HIPK1	7.48E-01
HMGB3	7.48E-01
NFIX	7.48E-01
PC	7.48E-01
SLC25A38	7.48E-01
SRI	7.48E-01
CLPX	7.41E-01
CTSE	7.41E-01
HBM	7.41E-01
NOSTRIN	7.41E-01
NOTCH3	7.41E-01

PCMT1	7.41E-01
PPAPDC3	7.41E-01
PVRL1	7.41E-01
SFXN5	7.41E-01
UBXN6	7.41E-01
VEZT	7.41E-01
ZFPM1	7.41E-01
ACTN4	7.34E-01
AGTPBP1	7.34E-01
ARHGEF12	7.34E-01
BACE2	7.34E-01
C7orf73	7.34E-01
CDCA4	7.34E-01
MOB2	7.34E-01
MPC1	7.34E-01
NARF	7.34E-01
NASP	7.34E-01
PAQR9	7.34E-01
PIK3R2	7.34E-01
PRKAB1	7.34E-01
TRIM59	7.34E-01
TTLL11	7.34E-01
CCDC135	7.27E-01
CDC34	7.27E-01
FLT4	7.27E-01
HYAL3	7.27E-01
MAP2K3	7.27E-01
MFHAS1	7.27E-01
MRPL55	7.27E-01
PUF60	7.27E-01
RTF1	7.27E-01
SLC22A4	7.27E-01
TCN1	7.27E-01
ZFAND3	7.27E-01
ABCB10	7.20E-01
ABCB6	7.20E-01
ALOX15	7.20E-01
ANAPC11	7.20E-01
CYB5R3	7.20E-01
DCAF6	7.20E-01
FAR2	7.20E-01

GSK3A	7.20E-01
IFIT1B	7.20E-01
KLHL21	7.20E-01
MGAT5	7.20E-01
MXRA5	7.20E-01
NCEH1	7.20E-01
PRDX2	7.20E-01
RGCC	7.20E-01
RMDN2	7.20E-01
STRA13	7.20E-01
ZCCHC24	7.20E-01
ZNF165	7.20E-01
ANKRD6	7.13E-01
ATG2A	7.13E-01
CAT	7.13E-01
DHRS3	7.13E-01
HDGFRP3	7.13E-01
HSPG2	7.13E-01
KAT5	7.13E-01
LGR4	7.13E-01
PLVAP	7.13E-01
RNF123	7.13E-01
TALDO1	7.13E-01
TIGD5	7.13E-01
TSC22D4	7.13E-01
TSN	7.13E-01
CCDC124	7.06E-01
CCDC71	7.06E-01
CDC42EP4	7.06E-01
ELAC1	7.06E-01
FEM1A	7.06E-01
FRMD4A	7.06E-01
GLRX5	7.06E-01
LIG1	7.06E-01
MEST	7.06E-01
NUP54	7.06E-01
PLS1	7.06E-01
PYGB	7.06E-01
REEP4	7.06E-01
SEMA3F	7.06E-01
SLC25A10	7.06E-01

TUBB4B	7.06E-01
AK9	6.99E-01
ALAD	6.99E-01
ANKH	6.99E-01
BTBD8	6.99E-01
CHMP4B	6.99E-01
CXXC5	6.99E-01
GSTCD	6.99E-01
MPP2	6.99E-01
NID1	6.99E-01
NUF2	6.99E-01
RABL6	6.99E-01
RANBP10	6.99E-01
RBX1	6.99E-01
RSC1A1	6.99E-01
ALAS2	6.92E-01
CDH5	6.92E-01
EPB42	6.92E-01
FZD5	6.92E-01
GLIPR2	6.92E-01
LCMT1	6.92E-01
MAP2K7	6.92E-01
MFSD2B	6.92E-01
PRELID2	6.92E-01
RAB40B	6.92E-01
WBP2	6.92E-01
ARF5	6.85E-01
ARHGAP42	6.85E-01
ASCC2	6.85E-01
BLVRB	6.85E-01
CARHSP1	6.85E-01
CDKN2D	6.85E-01
DAAM1	6.85E-01
DEPDC1B	6.85E-01
FAM127C	6.85E-01
FAM98C	6.85E-01
FDXR	6.85E-01
MAMLD1	6.85E-01
MED22	6.85E-01
MZT1	6.85E-01
NPR1	6.85E-01

RNF103-CHMP3	6.85E-01
STK11	6.85E-01
STUB1	6.85E-01
ADIPOR1	6.78E-01
AP5B1	6.78E-01
C9orf89	6.78E-01
CACFD1	6.78E-01
CCNF	6.78E-01
COL4A5	6.78E-01
DDA1	6.78E-01
EFHA1	6.78E-01
EFNB2	6.78E-01
FSTL1	6.78E-01
LCA5	6.78E-01
LYRM9	6.78E-01
SGOL2	6.78E-01
SH3D19	6.78E-01
SLC2A8	6.78E-01
SLC44A4	6.78E-01
UBE2G2	6.78E-01
ACADS	6.71E-01
BABAM1	6.71E-01
FAM98B	6.71E-01
FLRT1	6.71E-01
FOXRED2	6.71E-01
HIRIP3	6.71E-01
HIST1H2BI	6.71E-01
KIF15	6.71E-01
KIF22	6.71E-01
MAP4K5	6.71E-01
MXRA7	6.71E-01
PDZD8	6.71E-01
PSKH1	6.71E-01
PTGR1	6.71E-01
PTGS1	6.71E-01
RPE65	6.71E-01
SPHK2	6.71E-01
SPTB	6.71E-01
STOML1	6.71E-01
B3GNT2	6.64E-01
CXCL12	6.64E-01

ENDOG	6.64E-01
IFRD2	6.64E-01
KIF18A	6.64E-01
LRRC42	6.64E-01
LRRC8A	6.64E-01
MED29	6.64E-01
PPM1A	6.64E-01
RABGAP1L	6.64E-01
REEP6	6.64E-01
SERPINE2	6.64E-01
TESC	6.64E-01
TUBGCP2	6.64E-01
ZNF777	6.64E-01
ZNRF3	6.64E-01
ADD2	6.57E-01
C19orf24	6.57E-01
C9orf78	6.57E-01
EGFL7	6.57E-01
KIF4A	6.57E-01
LEPROT	6.57E-01
LGALSL	6.57E-01
MED25	6.57E-01
MPC2	6.57E-01
PAGR1	6.57E-01
PLCL2	6.57E-01
PSMF1	6.57E-01
RPS6KA2	6.57E-01
SCUBE1	6.57E-01
SORBS1	6.57E-01
TBC1D22A	6.57E-01
TMEM201	6.57E-01
TUBA4A	6.57E-01
VWA1	6.57E-01
ZDHHC12	6.57E-01
ZNF417	6.57E-01
ZNF423	6.57E-01
ARHGEF37	6.50E-01
ATP5D	6.50E-01
BLVRA	6.50E-01
C5orf42	6.50E-01
CCNDBP1	6.50E-01

EFCAB6	6.50E-01
FXN	6.50E-01
MICAL3	6.50E-01
PAK4	6.50E-01
PCIF1	6.50E-01
PHC2	6.50E-01
R3HDM4	6.50E-01
SFR1	6.50E-01
SMIM1	6.50E-01
TMEM56	6.50E-01
C16orf86	6.43E-01
CBR1	6.43E-01
COL14A1	6.43E-01
DCAF11	6.43E-01
EMC9	6.43E-01
FUOM	6.43E-01
KIAA1586	6.43E-01
MMRN2	6.43E-01
MYO1D	6.43E-01
PPP1R13L	6.43E-01
PRPF18	6.43E-01
PTS	6.43E-01
RAB25	6.43E-01
SEC22C	6.43E-01
TFRC	6.43E-01
WDR81	6.43E-01
ZNF17	6.43E-01
ALOX5	6.36E-01
AP2A1	6.36E-01
ARL6IP6	6.36E-01
ASF1A	6.36E-01
ATG4D	6.36E-01
C2orf15	6.36E-01
COPE	6.36E-01
HIC2	6.36E-01
JMJD4	6.36E-01
PIR	6.36E-01
PKIA	6.36E-01
RAB11B	6.36E-01
S100A16	6.36E-01
SMTN	6.36E-01

ST6GALNAC4	6.36E-01
TEK	6.36E-01
TINF2	6.36E-01
XRCC1	6.36E-01
A4GALT	6.29E-01
ERMAP	6.29E-01
GLYCTK	6.29E-01
HARBI1	6.29E-01
KIF23	6.29E-01
LMNA	6.29E-01
MLST8	6.29E-01
MOB1B	6.29E-01
PPAP2B	6.29E-01
PPP1R15A	6.29E-01
RNF26	6.29E-01
SLC6A9	6.29E-01
SRPX	6.29E-01
STK40	6.29E-01
TMEM203	6.29E-01
WLS	6.29E-01
YPEL4	6.29E-01
ANKLE1	6.22E-01
ARMC7	6.22E-01
BAG6	6.22E-01
BCOR	6.22E-01
C10orf12	6.22E-01
CD101	6.22E-01
CDK19	6.22E-01
COX8A	6.22E-01
CRIM1	6.22E-01
CYB5R1	6.22E-01
DCAF12	6.22E-01
DGCR2	6.22E-01
DNAJC4	6.22E-01
ENDOV	6.22E-01
EPHB6	6.22E-01
FAM131A	6.22E-01
GRINA	6.22E-01
KIAA1143	6.22E-01
PKMYT1	6.22E-01
PLK1	6.22E-01

TOR2A	6.22E-01
TPRA1	6.22E-01
TTC39A	6.22E-01
TTPAL	6.22E-01
ACER3	6.15E-01
ANK1	6.15E-01
ARHGAP19	6.15E-01
ATPIF1	6.15E-01
C19orf47	6.15E-01
CMIP	6.15E-01
EMP2	6.15E-01
GSTO1	6.15E-01
LBR	6.15E-01
MAN1B1	6.15E-01
MYL4	6.15E-01
NUDT8	6.15E-01
PEX19	6.15E-01
POP7	6.15E-01
RFX2	6.15E-01
RPTOR	6.15E-01
SUZ12	6.15E-01
TAL1	6.15E-01
TMEM242	6.15E-01
TSPAN33	6.15E-01
TTC30B	6.15E-01
UBALD2	6.15E-01
B4GALT2	6.08E-01
C21orf33	6.08E-01
CC2D1A	6.08E-01
GRN	6.08E-01
IGFBP3	6.08E-01
KIAA1715	6.08E-01
RHCE	6.08E-01
TP53I11	6.08E-01
ZSCAN2	6.08E-01
ABT1	6.01E-01
BAD	6.01E-01
BCL7B	6.01E-01
BOLA1	6.01E-01
CAAP1	6.01E-01
GAB1	6.01E-01

GMDS	6.01E-01
INPP5K	6.01E-01
ITGB3BP	6.01E-01
LRP10	6.01E-01
MAF1	6.01E-01
MPHOSPH6	6.01E-01
NDUFAF3	6.01E-01
PARPBP	6.01E-01
PRMT6	6.01E-01
PRPF31	6.01E-01
SF3A2	6.01E-01
SLC43A1	6.01E-01
TRAPPC6A	6.01E-01
UBL7	6.01E-01
VAMP4	6.01E-01
WDR18	6.01E-01
ZFAT	6.01E-01

Chapter V

Malaria relapses expand B-cell memory that provides strain-specific protection against reinfection

Chester J. Joyner[1], Cristiana F. A. Brito[2], Stacey A. Lapp[1], Celia L. Saney[1], Shuya Kyu[3], Monica Cabrera-Mora[1], the MaHPIC Consortium[1], Frances Eun-Hyung Lee[3*], Tracey J. Lamb[4]*, and Mary R. Galinski[5]*

*Authors contributed equally to this work.

[1]Malaria Host–Pathogen Interaction Center, Emory Vaccine Center, Yerkes National Primate Research Center, Emory University, Atlanta, GA, USA

[2]Laboratory of Malaria, Centro de Pesquisa René Rachou – Fiocruz Minas

[3] Division of Pulmonary, Allergy, Critical Care, & Sleep Medicine, Department of Medicine, Emory University, Atlanta, GA, USA

[4]Department of Pathology, University of Utah, Salt Lake City, UT, USA

[5]Division of Infectious Diseases, Department of Medicine, Emory University, Atlanta, GA, USA

Introductory Paragraph

Relapses are responsible for a significant portion of blood-stage *Plasmodium vivax* infections and provide repeated opportunities for transmission and clinical attacks. Without understanding the factors that influence relapse infection biology, effective elimination strategies for *P. vivax* and other relapsing malaria parasites will be a distant goal. Studying relapses using patient samples is challenging because distinguishing relapses from new or recrudescing infection is difficult. Here, the *Plasmodium cynomolgi* - *Macaca mulatta* nonhuman primate model of relapsing malaria is used to overcome these limitations. We show that relapses are asymptomatic and self-resolving. This clinical, but non-sterilizing immunity, is associated with a robust humoral immune response that is characterized by an increase in parasite-specific IgG in addition to expansion of unswitched and switched memory B-cells. Interestingly, reinfection with the same strain of *P. cynomolgi* resulted in an asymptomatic infection that self-resolved like a relapse with similar humoral immune responses. Contrastingly, challenge with a heterologous strain resulted in similar parasite burden and clinical presentation as the initial infection. Critically, these experiments suggest that most symptomatic vivax malaria cases may be due to exposures to new parasite variants and not relapses or homologous reinfections in endemic areas.

Main Text

Plasmodium vivax is the predominant malaria parasite outside of sub-Saharan Africa, causes significant morbidity each year, and poses unique challenges to malaria eradication [1-3]. Undoubtedly, the most formidable obstacle posed by *P. vivax* is its ability to form hypnozoites, dormant forms of the parasite that reside in the liver [4]. Hypnozoites can activate and cause repeat blood-stage infections, known as relapses [5, 6]. While relapses are thought to be responsible for the majority of *P. vivax* blood-stage infections, it remains unclear if they are responsible for significant illness, or if new infections with genetically similar or distinct parasites are responsible for most disease in endemic areas [7-9]. Here, we utilized the *P. cynomolgi* – *Macaca mulatta* (rhesus macaque) model of vivax malaria to evaluate the propensity of relapses, homologous reinfections, and heterologous infections to cause disease and understand the associated host immune responses.

Six rhesus macaques were infected with *P. cynomolgi* M/B strain sporozoites and monitored for 100 days. Parasitemia and complete blood counts were analyzed daily to evaluate each animal clinically and to determine when criteria for blood collections were met to evaluate ongoing immune responses (Fig. 1A). Relapses did not cause anemia, thrombocytopenia, or fever (Fig 1D; Supplementary Fig 1). In agreement with the clinical presentation, cytokine responses were significantly subdued during a relapse in comparison to the initial infection (Fig. 1E). The lack of inflammation and illness was likely due to a significant reduction in parasitemia in comparison with the initial infection (Figs. 1B-C). Together, as noted in our previous study, these data showed that relapses did not result in illness, likely through the establishment of immunity after a primary infection [10].

We hypothesized that B-cell and antibody responses were responsible for suppressing parasitemia and ameliorating disease during relapses. To test this hypothesis, the total and parasite-specific IgM and IgG kinetics were measured during initial infections and relapses. Total IgM was significantly increased during the initial infection, and parasite-specific IgM was

significantly increased during acute infection, albeit at low levels (Fig. 2A; Supplementary Figure 2A). The minimal increase in parasite-specific IgM during acute infection was due to the ability of the detectable IgM to recognize proteins from both uninfected and infected erythrocytes (Supplementary Fig. 3). This result suggested that IgM directed against RBC proteins may inhibit parasite growth during an initial infection. Indeed, auto-antibodies during malaria have been previously reported, but their role in parasite control has remained unclear [11-14]. In contrast, parasite-specific IgG was significantly increased after the peak of parasitemia even though it did not appear to reduce parasitemia (Fig. 2B). However during a relapse, parasite-specific IgG was rapidly produced in much higher quantities than the initial infection and peaked whenever a relapse was resolving (Fig. 2B). Together, these results suggested that relapse parasitemias were suppressed by a parasite-specific IgG response.

The lack of increase in total IgM and increased IgG response against the parasite during a relapse versus a naïve infection suggested that a memory B-cell response was responsible for suppressing parasite growth and preventing disease during relapses. To further evaluate this hypothesis, we developed, optimized, and validated a flow cytometry assay for monitoring B-cell subsets in the peripheral blood of macaques based on an immunophenotyping strategy commonly used in humans (Supplementary Fig. 4; [15]). Specifically, we optimized the panels to monitor the frequency and absolute numbers of four B-cell subsets based on surface expression of IgD and CD27 (Supplementary Fig. 4). To ensure that this strategy was comparable between humans and macaques, the strategy was validated by surface immunoglobulin staining for IgG and IgM (Supplementary Fig. 4). As expected, IgG surface staining was not observed in naïve (IgD+CD27-) and unswitched memory (IgD+CD27+) B-cell populations but was present in the double negative (IgD-CD27-) and switched memory (IgD-CD27+) populations (Supplementary Fig.4). Surface IgM was present in all subsets as previously reported in humans, albeit at low frequencies in the switched memory compartment (Supplementary Fig 4; [15]).

Unswitched and switched memory B-cells significantly increased during relapses, and the expansion of these subsets was associated with the resolution of parasitemia (Fig 2D). The switched memory B-cells that expanded were IgG+ in agreement with the parasite-specific IgG responses (Fig 2F). Notably, we did not observe an increase in the absolute number of double negative or naïve B-cells during relapses, suggesting that these subsets were not involved in the response (Supplementary Fig. 5A). The antibody and cellular B-cell responses supported a model where humoral immunity was established after an initial infection and persisted to reduce parasitemia, and thus illness, through the production of parasite-specific IgG via a memory B-cell response during a relapse.

After studying relapses in the cohort, a radical cure regimen consisting of artemether and primaquine was administered to each animal to eliminate blood and liver-stage parasites, including hypnozoites [10, 16]. Approximately 60 days after radical cure, five out of six of the animals were re-challenged with *P. cynomolgi* M/B strain sporozoites to determine if a reinfection would cause illness; one animal was removed from the cohort for reasons unrelated to malaria. A homologous reinfection did not induce anemia, thrombocytopenia, or fever, and in fact, hematological values, parasite load, and inflammatory responses were virtually indistinguishable from relapses (Figs 3A-E; Supplementary Fig. 7). Importantly, there was no evidence that this protection was directed against the liver or sporozoite stages of the parasite since the days to patency of the blood-stage infections were similar between the initial and homologous reinfections (Supplementary Fig. 6). These experiments demonstrated that, as with the relapses, homologous reinfections did not result in clinical illness.

Next, we evaluated if the humoral immunity was responsible for the protection observed during a homologous reinfection, as shown for the relapses. Indeed, the total and parasite-specific IgM and IgG kinetics were indistinguishable between the two infections (Figs 3F-G). The cellular B-cell response was similar to relapses, and was predominated by an expansion of IgG+ switched memory B-cells (Figs 3H-J). Notably, switched memory B-cells did not expand during a

homologous reinfection although the reason underlying this result is unclear (Fig 3H). These results demonstrate humoral immunity provided protection against illness during the homologous reinfections, comparable to relapses.

We then hypothesized that an infection with a different strain of *P. cynomolgi* would result in disease. To test this hypothesis, all but one animal was administered radical cure as described above and re-challenged with *P. cynomolgi* Ceylon strain sporozoites approximately 30 days later (Fig. 4B). One animal was removed from the study after challenge due to a treatment failure (Fig 4B). The heterologous challenge resulted in restored parasite burden, anemia, thrombocytopenia, and inflammatory cytokine responses similar to the initial infections (Figs. 4A-E; Supplementary Fig. 8). Additionally, the B-cell kinetics were similar to the initial infections (Fig. 4F; Supplementary Fig. 5C).

The antibody responses during the heterologous infections were similar to the initial infection except for the lack of an increase in parasite-specific IgM (Fig 4G). A significant increase in total or parasite-specific IgM was not detected during the heterologous infection (Fig. 4G). Parasite-specific IgG peaked after the peak of infection and was capable of recognizing both *P. cynomolgi* strains (Fig. 4H). However, these antibodies were ineffective at neutralizing *P. cynomolgi* Ceylon based on parasitemia kinetics (Figs. 4B-C). These data indicate that the established humoral immunity was strain-specific.

Overall, these results do not support that all *P. vivax* relapses are responsible for significant disease. Instead, our study supports the view that new parasite variants are responsible for clinical vivax malaria in endemic areas, at least in temperate climates where relapses are routinely observed 30 – 60 days after an initial infection, for example in Papua New Guinea [17]. Recent investigations have highlighted that *P. vivax* is extremely genetically diverse at a population level, and individuals in areas in high endemicity are likely infected with genetically distinct parasites frequently [18-21]. Future studies should aim to evaluate how the clonality and frequency of relapses influence the humoral immune response and development of disease,

especially since it is thought that most relapses are composed of multiple strains of the parasite [17, 20, 22]. Notably, relapses with diverse parasites may result in clinical illness, and such aspects can be methodically explored using the established NHP malaria model system presented here. Overall, this study awakens the study of *Plasmodium* relapse immunobiology in longitudinal infections using NHP models and stresses the potential of such research in informing *P. vivax* epidemiology and control efforts.

Methods

Animal use. Nonhuman primate cohort infections were carried out at the Yerkes National Primate Research Center (YNPRC) at Emory University, an Association for Assessment and Accreditation of Laboratory Animal Care (AAALAC) international-certified institution. Sporozoites were generated for each infection using additional rhesus monkeys at the Centers for Disease Control and Prevention (CDC). All procedures including blood collections, infections with malaria parasites, clinical interventions, etc. were reviewed and approved by Emory University's and/or CDC's Institutional Animal Care and Use Committees. During the experimental procedures at YNPRC, the animals were housed socially in pairs in compliance with Animal Welfare Act regulations as well as the Guide for the Care and Use of Laboratory Animals. All male animals were used for experiments to eliminate the contributing factor of the loss of blood during the female menstrual cycle to the degree of anemia observed in any of the individuals.

Sample collections. Blood and bone marrow aspirates were collected in EDTA at pre-defined time points as indicated in the experimental schematics in Figures 1A, 3A, and 4A. Parasitemia and hematological parameters were evaluated daily by light microscopy and complete blood counts (CBC) analysis, respectively. For the daily parasitemia and CBC assays, blood was collected into a pediatric capillary tube using a standardized ear-prick procedure as previously reported in Joyner et al. (…). Pilot studies indicated that the ear pricks yielded similar CBC readings, parasitemias, and reticulocyte counts as venous blood draws. Plasma was collected from each time point prior to isolation of PBMCs for flow cytometry analysis as described below. Bone marrow samples were not utilized for the experiments presented here.

Parasite enumeration. Daily parasitemia was determined as reported in Joyner et al. 2016 [10]. Briefly, thick and thin blood film preparations from capillary or venous blood were prepared and allowed to dry. Thin films were fixed with 100% methanol, and thick films left unfixed. The thick and thin films were then stained using a Wright's-Gurr stain. For thick film preparations,

parasites were enumerated by determining the number of parasites that were observed within 500-2000 white blood cells (WBCs) depending on the parasite density. The number of parasites per the number of WBCs was then calculated and multiplied with the leukocyte count as determined by the CBC to yield parasites per microliter. For days where parasitemia was too high to enumerate using thick blood films, the thin blood film was used; this was typically when parasitemia was greater than 1%. The number of parasites out of 1000 – 2000 RBCs were determined and the percent parasitemia calculated by dividing the number of parasites counted by the number of total RBCs counted and multiplying by 100. The percentage of infected RBCs was then multiplied against the RBC concentration as determined by the CBC analysis to determine parasites/µl. Parasitemia was determined by two expert microscopists independently through the course of each infection. If discrepancies were observed between the two readers, a third, independent microscopist counted the slides. The two most similar values were then averaged to determine the parasitemia at any point during the infection.

Complete blood count analysis. Complete blood counts were performed prior to infections and daily after inoculation using capillary and/or venous blood. If values from the CBC were considered abnormal (e.g. low platelet counts or observation of nucleated RBCs), the values obtained by the hematology analyzer were either confirmed or adjusted based on a manual differential or manual platelet count. For manual differentials, the phenotype (e.g. monocyte, neutrophil, nucleated RBC, etc.) was determined, and the percentage of each subset calculated. If there was a discrepancy with the CBC based on the differential, the percentage of monocytes, lymphocytes, and granulocytes was adjusted to ensure accuracy. If nucleated RBCs were present, the number of nucleated RBCs was determined and subtracted from the leukocyte count and added to the RBC count.

Multiplex cytokine analysis. A custom, nonhuman primate multiplex cytokine assay was designed and purchased from eBioscience/Affymetrix, which is now a part of Theromofisher. These kits were performed according to the manufacturer's suggested protocol except for one

modification. Instead of diluting plasma 1:1 with sample dilution buffer as the protocol suggests, the samples were not diluted prior to running the assay. This was altered after initial experiments demonstrated that many analytes were not within the dynamic range of the standard curves if additional dilutions were performed. Samples were fully randomized prior to performing the multiplex kit to minimize plate- and well-specific effects. All multiplex data was analyzed using the ProcartaPlex Analyst software available through Thermofisher. Concentrations of cytokines in the plasma were determined and used for downstream analyses.

Total IgG and IgM ELISAs. Total IgM and IgG plasma concentrations were evaluated using a commercially-available kit designed for nonhuman primates. The manufacturer's suggested protocol was followed. The optimal dilutions of plasma were 1:80,000 and 1:40,000 for IgG and IgM, respectively. Samples were fully randomized prior to performing the ELISA to minimize plate and well-specific effects.

***In vitro* maturation and isolation of *P. cynomolgi* schizonts.** Rhesus macaques were inoculated with cryopreserved, blood-stage *P. cynomolgi* parasites of each strain to generate schizonts for lysate preps described below. Briefly, a vial of cryopreserved, blood-stage parasites were removed from the liquid nitrogen and quickly thawed in a 37°C water bath. After thawing, concentrations of different salines were added to slowly change the osmotic pressure to prevent the RBCs from lysing. The number of ring-stage parasites were then enumerated using light microscopy as described above and inoculated intravenously into a rhesus macaque. The infections were followed daily for each monkey until parasitemia reached 3-10% ring-stage parasites. At this time, blood containing predominantly rings was collected in sodium heparin, washed, and depleted of leukocytes and platelets by passing over a glass bead column and through a Plasmodipur filter. The parasites were then matured *ex vivo* to 3-8 nucleated schizonts under blood-gas conditions (5%:5%:90%;O2:CO2:N2) in RPMI supplemented with L-glutamine, supplemented with 0.25% sodium bicarbonate, 50 μg/ml hypoxanthine, 7.2 mg/ml HEPES, 2 mg/ml glucose, and 10 – 20 % Human AB+ serum. When mature, the schizonts were isolated by

a 1.093 g/ml Percoll density gradient. The parasite layer was then isolated and washed 4 times in sterile RPMI, aliquoted, and stored in vapor phase liquid nitrogen until needed.

Infected and uninfected RBC lysate preparation. Aliquots of parasite or uninfected RBC pellets were removed from liquid nitrogen storage, thawed quickly in a 37°C water bath and placed back into the liquid nitrogen tank for ten minutes. This procedure was repeated three more times. After the final thaw, 1 volume of PBS was added followed by vigorous vortexing for 1-2 minutes. The aliquot was then centrifuged at 3,000 × g for 10 minutes at 4°C. The supernatant was then removed and placed into another sterile tube and the pellet discarded. This process was repeated three more times. After the final centrifugation, the protein concentration was determined using a Pierce BCA assay according to the manufacturer's protocols. The lysates were then diluted to optimal concentrations for ELISAs in PBS, aliquoted, and stored at -80°C until needed.

Parasite-specific antibody ELISAs. Corning® high-binding microtiter plates were coated with schizont lysate or uninfected RBC lysate diluted in ELISA coating buffer (Abcam) to 5 ug/ml. The plate was incubated overnight at 4°C followed by washing four times with PBS containing 0.05% Tween-20 (PBS-T). After the final wash, the plate was blotted dry and blocked serum-free Sea Block (Abcam) for two hours at RT followed by four washes in PBS-T. Plasma samples from the different infection points were diluted 1:100 in 33% serum-free Sea Block and then added to each well. The plate was then incubated at RT for 2 h followed by washing four times with PBS-T. After blotting dry, horseradish-peroxidase (HRP) conjugated anti-IgG (Jackson Immunoresearch) or HRP-conjugated anti-IgM (Jackson Immunoresearch) diluted 1:40,000 or 1:20,000 in 33% Sea Block in PBS, respectively, were added to each well and incubated for 1 h at RT in the dark. After incubating, the plate was washed four times with PBS-T and 100 µl of High Sensitivity TMB Substrate (Abcam) was added to each well and allowed to develop for 3-5 minutes. One hundred microliters of Stop Solution (Abcam) was then added to stop the reaction. The absorbance of each well was then measured at 450 nm, and iRBC or uRBC-specific antibody

concentrations were calculated based on a 4-PL standard curve using purified IgG or IgM calibrators from Abcam's Monkey Total IgG and IgM ELISA kits mentioned above. Concentration of specific IgG and IgM was used for downstream analyses.

PBMC isolation. Plasma was isolated prior to performing the PBMC isolation by centrifuging the blood samples at 400 × g followed by pipetting off the plasma. After removing the plasma, the blood pellet was resuspended in two times the original volume of blood that was received to perform the manufacturer's suggested protocol. This modification of the procedure did not appear to alter the viability or yield of PBMCs. After each isolation, each monkey's PBMCs were washed two times in sterile PBS followed by enumeration on a Countess II fluorescent cell counter. The viability of the PBMCs was simultaneously assessed by Trypan Blue exclusion assay. PBMC viability was always ≥ 90%.

Flow cytometry. 5×10^5 - 2×10^6 PBMCs were aliquoted into flow cytometry tubes for staining with fluorescently conjugated antibodies. The variation in number of PBMCs used for each staining procedure was due to leukopenia that developed during the acute, symptomatic infections. After aliquoting into individual FACS tubes, cells were washed once more in PBS prior to re-suspending in antibody cocktails comprised of the antibodies indicated in Tables 1-4, which was dependent on the infection.

All staining procedures were two-step. For surface IgG staining, the IgG was prepared in a separate cocktail and added first, followed by a 30-minute incubation, washing PBS by centrifugation at 400 × g, and then resuspending in a cocktail that contained the other antibodies in the panels.

For intracellular staining, cells were initially surface-stained with the cocktail followed by incubation in eBioscience FoxP3 fix perm buffer overnight at 4°C for intracellular markers. After fixing overnight, the cells were washed according to the manufacturer's procedure and then incubated for 45 minutes at 4°C with antibodies against intracellular markers. After incubating, the cells were washed twice in the fix/perm buffer provided by the kit and resuspended in 100 -

200 µl of PBS depending upon cell yield. All samples were acquired on an LSR-II flow cytometer using standardized acquisition templates and rainbow calibration particles. New compensation samples were run for each separate acquisition. Data was analyzed in Cytobank before exporting statistics for statistical assessment.

Determining absolute cell counts with flow cytometry data. Absolute numbers for each B-cell subset was determined by calculating the percentage of each subset out of the mononuclear cells in the sample and multiplying the percentage against the mononuclear cells per microliter value obtained from the CBC analysis at each time point. The mononuclear cells/µl value was obtained by adding the lymphocyte/µl value to the monocyte/µl value.

Statistical analyses. All statistical analyses were performed using a linear mixed-effect model with Tukey-Kramer HSD post-hoc analysis. For the statistical model, each animal was treated as a random effect with time points nested within infection and set as fixed effects. All data were transformed as necessary to ensure the best model fit. Typically, the best model fits were obtained with a $\log_{10}$, $\log_2$, or arcsin transformation. **Data management and release.** All data went through rigorous validation protocols and are publicly deposited in different public repositories depending on the data type. Flow cytometry, multiplex cytokine assay, and ELISA data have been submitted to ImmPort for public release. All clinical data associated with the experiment have been publicly release on PlasmoDB.

Author Contributions

Conceived and designed the experiments: C.J.J, M.R.G., T.J.L., F.E.L. Performed the experiments: C.J.J., C.F.A., S.A.L., C.L.S., S.K., M.C.M., Analyzed the results: C.J.J, C.F.B., S.K., Provided analytical guidance: M.R.G., F.E.L, T.J.L., Developed the figures and wrote the manuscript: C.J.J., Edited the manuscript: M.R.G., F.E.L., T.J.L., C.F.B. All author's read an approved the final manuscript.

Acknowledgements

The authors would like to the following individuals for their contributions to the content of this manuscript: Dr. John Barnwell for helpful discussion regarding the design and execution of these experiments, Dr. Ignacio Sanz for helpful discussion regarding approaches to phenotype B-cells in macaques, Dr. Alberto Moreno for assistance with monitoring the clinical outcomes of the infections, Dr. Jennifer S. Wood for consultations on the clinical phenotypes of the macaques in the cohort, Yerkes National Primate Research Center Staff for assisting with all nonhuman primate procedures, and the Children's Healthcare of Atlanta Flow Cytometry Core for maintaining the flow cytometers during these experiments.

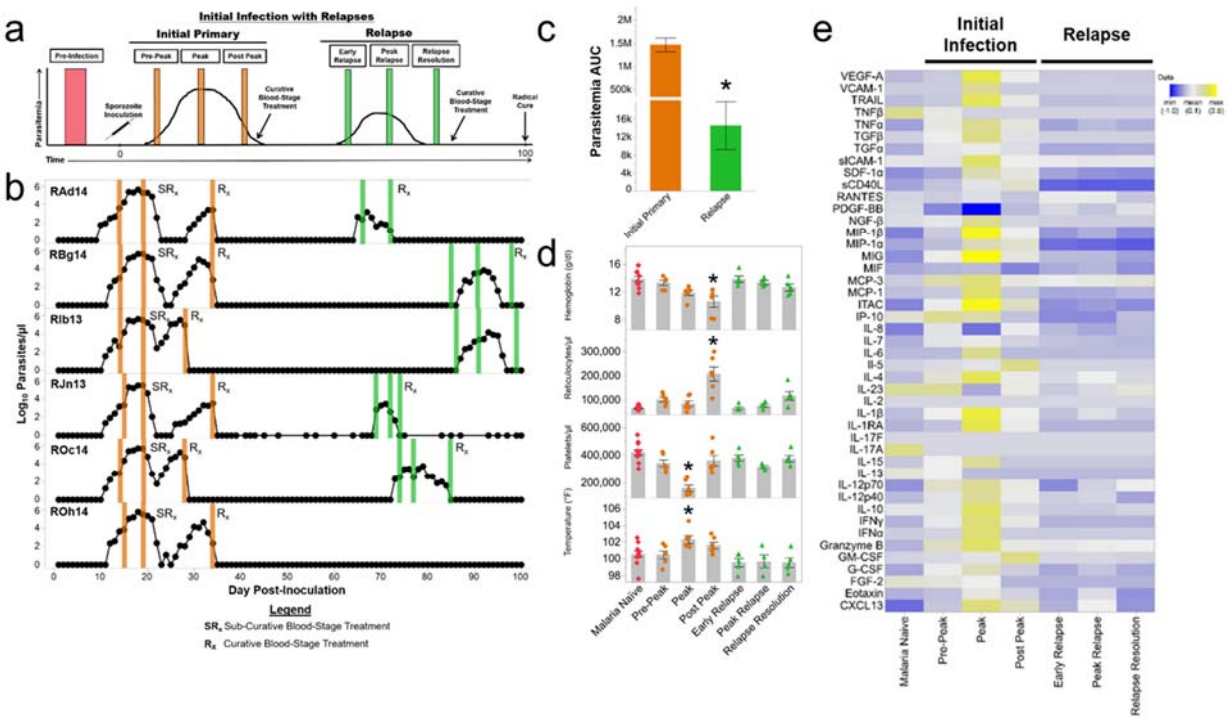

Figure 1. Malaria relapses do not cause disease and are self-resolving in macaques infected with *P. cynomolgi*. (a) Experimental schematic for studying relapse pathogenesis and immunology in rhesus macaques infected with *P. cynomolgi* B strain (b) Parasitemia kinetics over a 100-day *P. cynomolgi* B strain infection in rhesus macaques. Each row represents a different individual as indicated by the unique five letter identifier on the graph. Colored bars indicate when sample collections were performed during initial infections (orange) or relapses (green) to assess host responses. These collections correspond from left to right with the idealized experimental schematic in panel a (c) Mean parasitemia area under the curve during initial infections and relapses for the animals indicated in panel b. Error Bars = SEM (d) Mean hemoglobin levels, reticulocyte numbers, platelet concentrations, and temperature prior to infection (pink diamonds), during the initial infections (orange circles) and during relapses (green triangles). Gray bars are the mean of all data points shown. Error Bars = SEM (e) Cytokine responses at different points during initial and relapse infections. Cytokine values were z-scored normalized prior to visualization by the heatmap. Higher z-scores are indicated in yellow whereas lower values are

blue. Statistical significance was assessed by a linear mixed effect model using a Tukey-Kramer HSD post-hoc analysis when relevant. Asterisks indicate p-value < 0.05 in comparison to the malaria naïve condition unless otherwise noted.

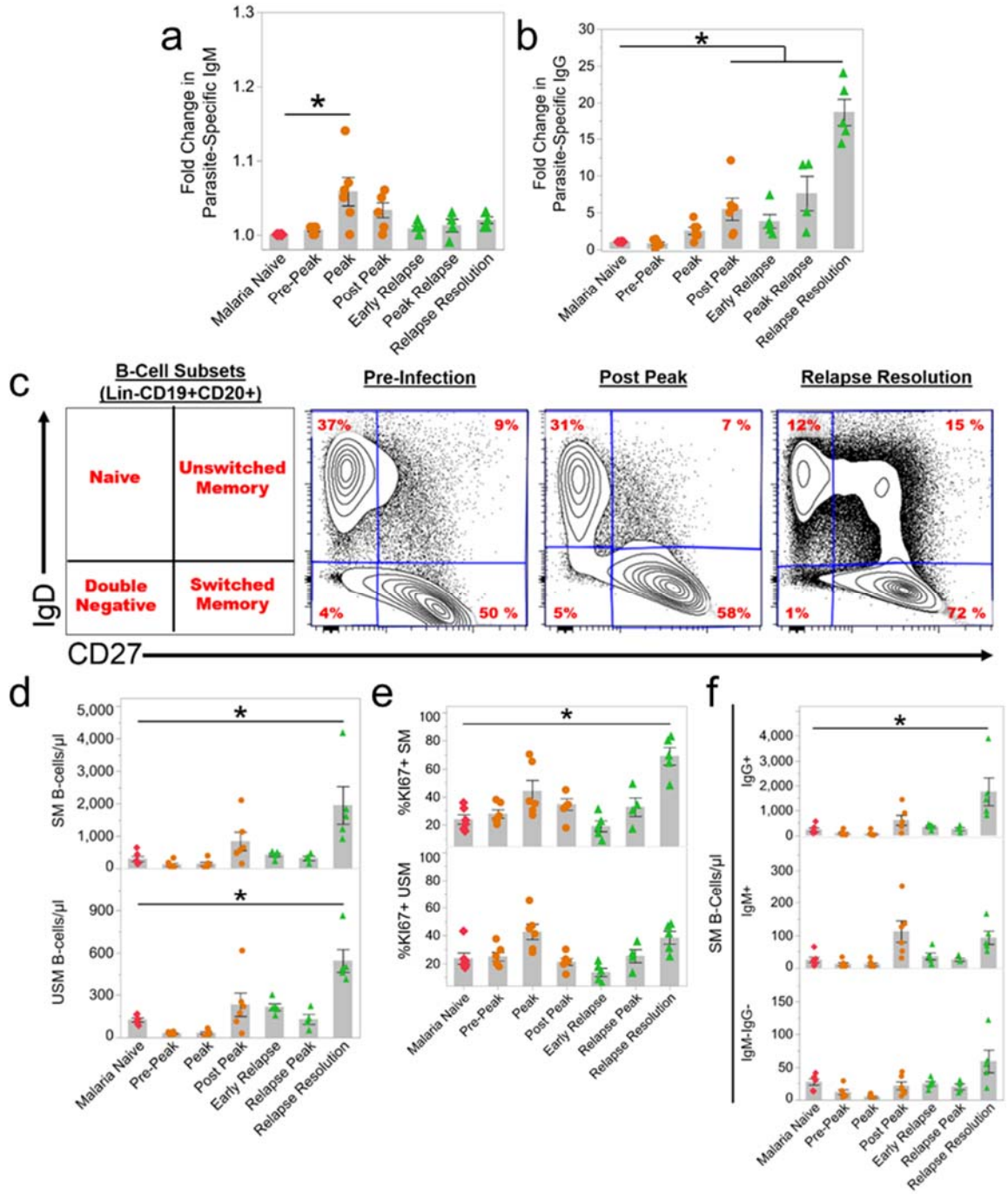

Figure 2. Parasitemia during *P. cynomolgi* relapses is suppressed by a memory B-cell response via the production of parasite-specific IgG antibodies. (a) Fold increase in parasite-specific IgM antibodies as measured by ELISA. All values were normalized to pre-infection values. Pink diamonds = naïve condition, orange circles = initial infection, and green triangles = relapse infections. Gray bars indicate the mean of the data points shown; Error Bars = SEM.

Experiments were repeated two times. (b) Fold increase in parasite-specific IgG antibodies as measured by ELISA. All values were normalized to pre-infection values. Pink diamonds = naïve condition, orange circles = initial infection, and green triangles = relapse infections. Gray bars indicate the mean of the data points shown; Error Bars = SEM. Experiments were repeated two times. (c) The frequencies of four peripheral blood B-cell subsets in rhesus macaques as determined by flow cytometry prior to infection, after the peak of parasitemia during the initial infection (Post Peak), and during the resolution of a relapse (Relapse Resolution). The far left panel indicates the B-cell subset in each quadrant based on the gating strategy in Supplementary Figure 4. Red numbers in each quadrants indicate the percentage of each subset out of CD19+CD20+ B-cells at the indicated infection point. (d) Absolute numbers of switched and unswitched memory B-cells at each infection point. Pink diamonds = naïve condition, orange circles = initial infection, and green triangles = relapse infections. Gray bars indicate the mean of the data points shown; Error Bars = SEM. (e) The percentage of KI67+ switched and unswitched memory B-cells at during initial infections and relapses. Pink diamonds = naïve condition, orange circles = initial infection, and green triangles = relapse infections. Gray bars indicate the mean of the data points shown; Error Bars = SEM. SM= Switched memory; USM = unswitched memory. (f) The absolute number of IgG+, IgM+, and IgG-IgM- switched memory B-cells during initial infections and relapses. Pink diamonds = naïve condition, orange circles = initial infection, and green triangles = relapse infections. Gray bars indicate the mean of the data points shown; Error Bars = SEM. SM= Switched memory. For all panels, statistical significance was assessed by a linear mixed effect model using a Tukey-Kramer HSD post-hoc analysis. Asterisks indicate a p-value < 0.05.

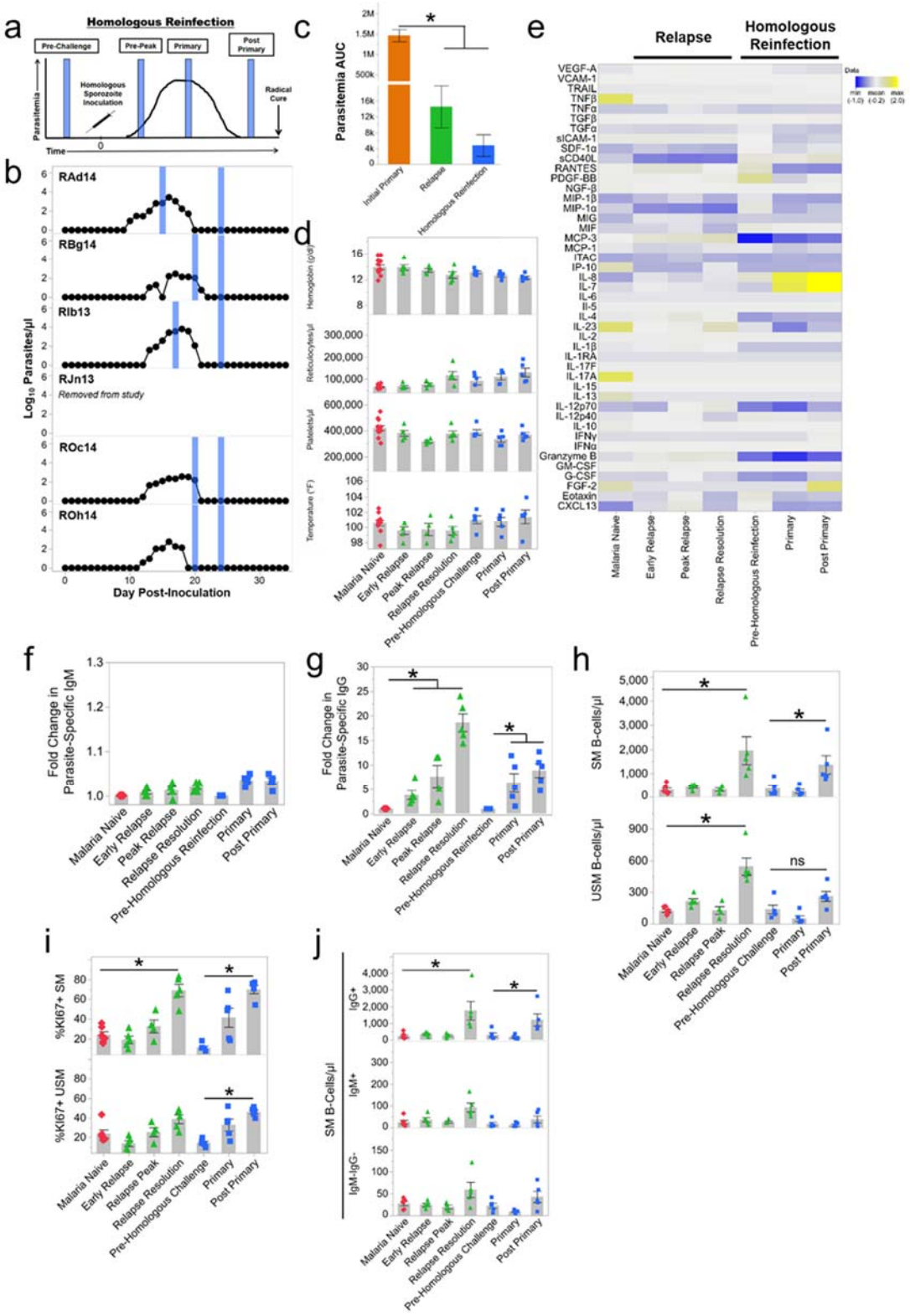
a
Homologous Reinfection
Pre-Challenge
Pre-Peak
Primary
Post Primary
Parasitemia
Homologous Sporozoite Inoculation
Radical Cure
Time
0
b
RAd14
RBg14
RIb13
RJn13
Removed from study
ROc14
ROh14
Log10 Parasites/µl
Day Post-Inoculation
c
Parasitemia AUC
Initial Primary
Relapse
Homologous Reinfection
d
Hemoglobin (g/dl)
Reticulocytes/µl
Platelets/µl
Temperature (°F)
Malaria Naive
Early Relapse
Peak Relapse
Relapse Resolution
Pre-Homologous Challenge
Primary
Post Primary
e
Relapse
Homologous Reinfection
VEGF-A
VCAM-1
TRAIL
TNFβ
TNFα
TGFβ
TGFα
sICAM-1
SDF-1α
sCD40L
RANTES
PDGF-BB
NGF-β
MIP-1β
MIP-1α
MIG
MIF
MCP-3
MCP-1
ITAC
IP-10
IL-8
IL-7
IL-6
Il-5
IL-4
IL-23
IL-2
IL-1β
IL-1RA
IL-17F
IL-17A
IL-15
IL-13
IL-12p70
IL-12p40
IL-10
IFNγ
IFNα
Granzyme B
GM-CSF
G-CSF
FGF-2
Eotaxin
CXCL13
Malaria Naive
Early Relapse
Peak Relapse
Relapse Resolution
Pre-Homologous Reinfection
Primary
Post Primary
f
Fold Change in Parasite-Specific IgM
Malaria Naive
Early Relapse
Peak Relapse
Relapse Resolution
Pre-Homologous Reinfection
Primary
Post Primary
g
Fold Change in Parasite-Specific IgG
Malaria Naive
Early Relapse
Peak Relapse
Relapse Resolution
Pre-Homologous Reinfection
Primary
Post Primary
h
SM B-cells/µl
USM B-cells/µl
ns
Malaria Naive
Early Relapse
Relapse Peak
Relapse Resolution
Pre-Homologous Challenge
Primary
Post Primary
i
%Ki67+ SM
%Ki67+ USM
Malaria Naive
Early Relapse
Relapse Peak
Relapse Resolution
Pre-Homologous Challenge
Primary
Post Primary
j
SM B-Cells/µl
IgG+
IgM+
IgM-IgG-
Malaria Naive
Early Relapse
Relapse Peak
Relapse Resolution
Pre-Homologous Challenge
Primary
Post Primary

Figure 3. Homologous reinfections, like relapses, are controlled through a robust humoral immune response that ameliorates disease. (a) Experimental schematic for homologous reinfections of rhesus macaques with *P. cynomolgi* B strain sporozoites 60 days after radical cure (b) Parasitemia kinetics during a homologous reinfection. Blue bars indicate when samples to assess host responses were taken in relation to parasitemia. Notably, the anticipated pre-peak time point was not captured from the idealized infection schematic in panel a (c) Mean parasitemia area under the curve during initial infections, relapses, and homologous reinfections for the animals indicated in panel b. Error Bars = SEM (d) Mean hemoglobin levels, reticulocyte numbers, platelet concentrations, and temperature prior to infection (pink diamonds), during relapses (green triangles), and during homologous reinfections (blue squares). Gray bars are the mean of all data points shown; Error Bars = SEM (e) Cytokine responses prior to malaria, during relapses, and during homologous reinfections. Cytokine values were z-scored normalized prior to visualization by the heatmap. Higher z-scores are indicated in yellow whereas lower values are blue. (f) Fold increase in parasite-specific IgM antibodies as measured by ELISA. All values were normalized to pre-infection values. Pink diamonds = naïve condition, green triangles = relapses, blue squares = homologous reinfections. Gray bars indicate the mean of the data points shown; error bars = SEM. Experiments were repeated two times. (g) Fold increase in parasite-specific IgG antibodies as measured by ELISA. All values were normalized to pre-infection values. Pink diamonds = naïve condition, green triangles = relapses, blue squares = homologous reinfections. Gray bars indicate the mean of the data points shown; error bars = SEM. Experiments were repeated two times. (h) Absolute numbers of switched and unswitched memory B-cells at each infection point. Pink diamonds = naïve condition, green triangles = relapse infections, blue squares = homologous reinfections. Gray bars indicate the mean of the data points shown; error bars = SEM. (i) The percentage of KI67+ switched and unswitched memory B-cells at during relapses and homologous reinfections. Pink diamonds = naïve condition, orange circles = initial infection, and green triangles = relapse infections. Gray bars indicate the mean of the data points

shown; error bars = SEM. SM= Switched memory; USM = unswitched memory (j) The absolute number of IgG+, IgM+, and IgG-IgM- switched memory B-cells during initial infections and relapses. Pink diamonds = naïve condition, orange circles = initial infection, and green triangles = relapse infections. Gray bars indicate the mean of the data points shown; error bars = SEM. SM= Switched memory. For all panels, statistical significance was assessed by a linear mixed effect model using a Tukey-Kramer HSD post-hoc analysis. Asterisks indicated $p < 0.05$ between the infection points indicated.

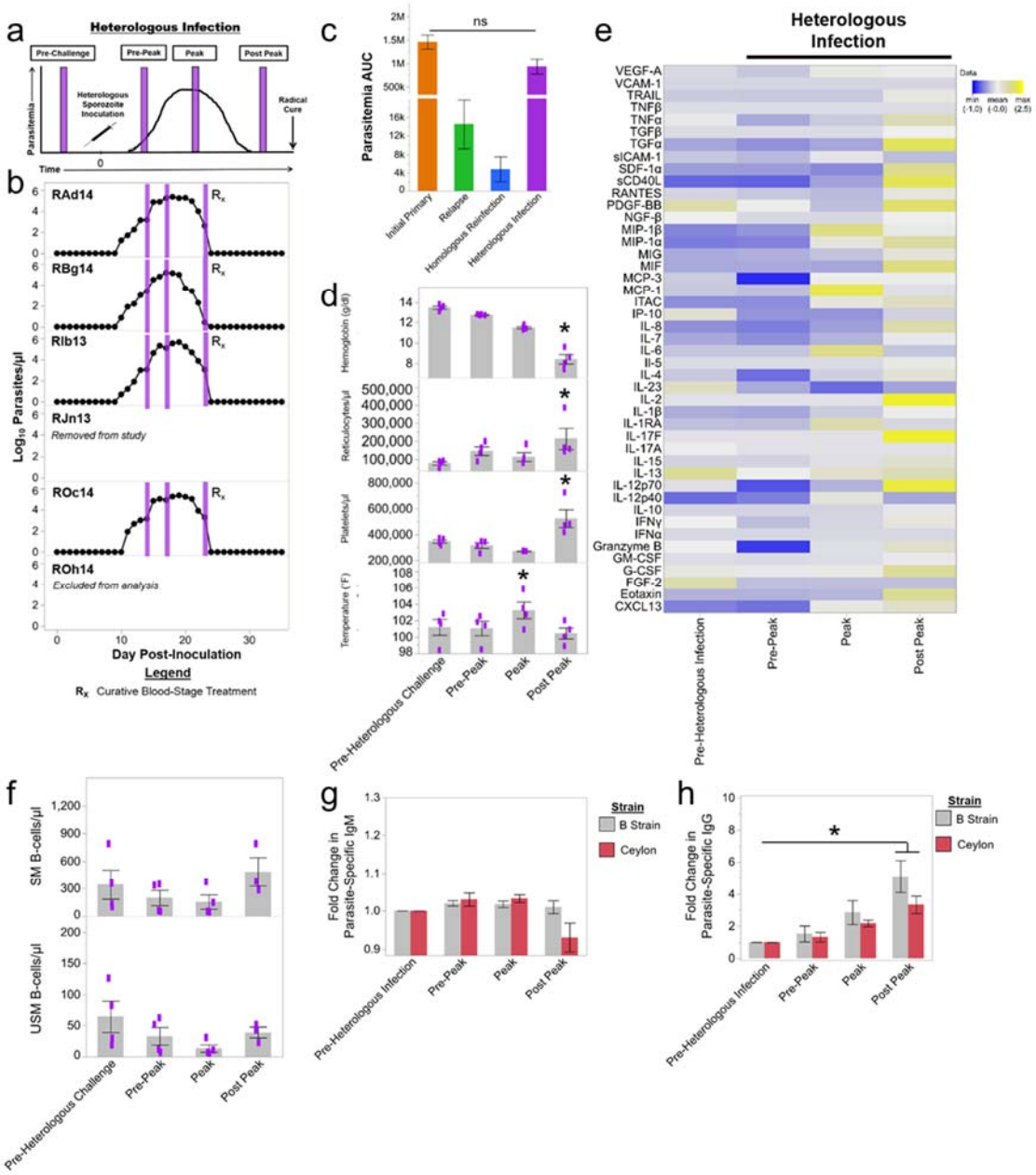

Figure 4. Heterologous infections result in illness and similar antibody responses as an initial infection. (a) Experimental schematic for heterologous infections of rhesus macaques with *P. cynomolgi* Ceylon strain sporozoites 30 days after radical cure (b) Parasitemia kinetics during heterologous infections. Purple bars indicate when samples to assess host responses were taken in

relation to parasitemia (c) Mean parasitemia area under the curve during initial infections, relapses, homologous reinfections, and heterologous infections for the animals indicated in panel b. Error Bars = SEM (d) Mean hemoglobin levels, reticulocyte numbers, platelet concentrations, and temperature prior to the heterologous challenge and during infection. Gray bars are the mean of all data points shown; Error Bars = SEM (e) Cytokine responses prior to and during heterologous infections. Cytokine values were z-scored normalized prior to visualization by the heatmap. Higher z-scores are indicated in yellow whereas lower values are blue. (f) Absolute numbers of switched and unswitched memory B-cells prior to during heterologous reinfections. Gray bars indicate the mean of the data points shown; Error Bars = SEM (g) Fold increase in parasite-specific IgM antibodies as measured by ELISA when normalized to pre-heterologous infection values. Gray bars indicate the mean of the data points shown; Error Bars = SEM. Experiments were repeated two times. (h) Fold increase in parasite-specific IgG antibodies as measured by ELISA when normalized to pre-heterologous infection values. Gray bars indicate the mean of the data points shown; Error Bars = SEM. Experiment was repeated two times. For all panels, statistical significance was assessed by a linear mixed-effect model using a Tukey-Kramer HSD post-hoc analysis. Asterisks indicated $p < 0.05$ between the infection points indicated.

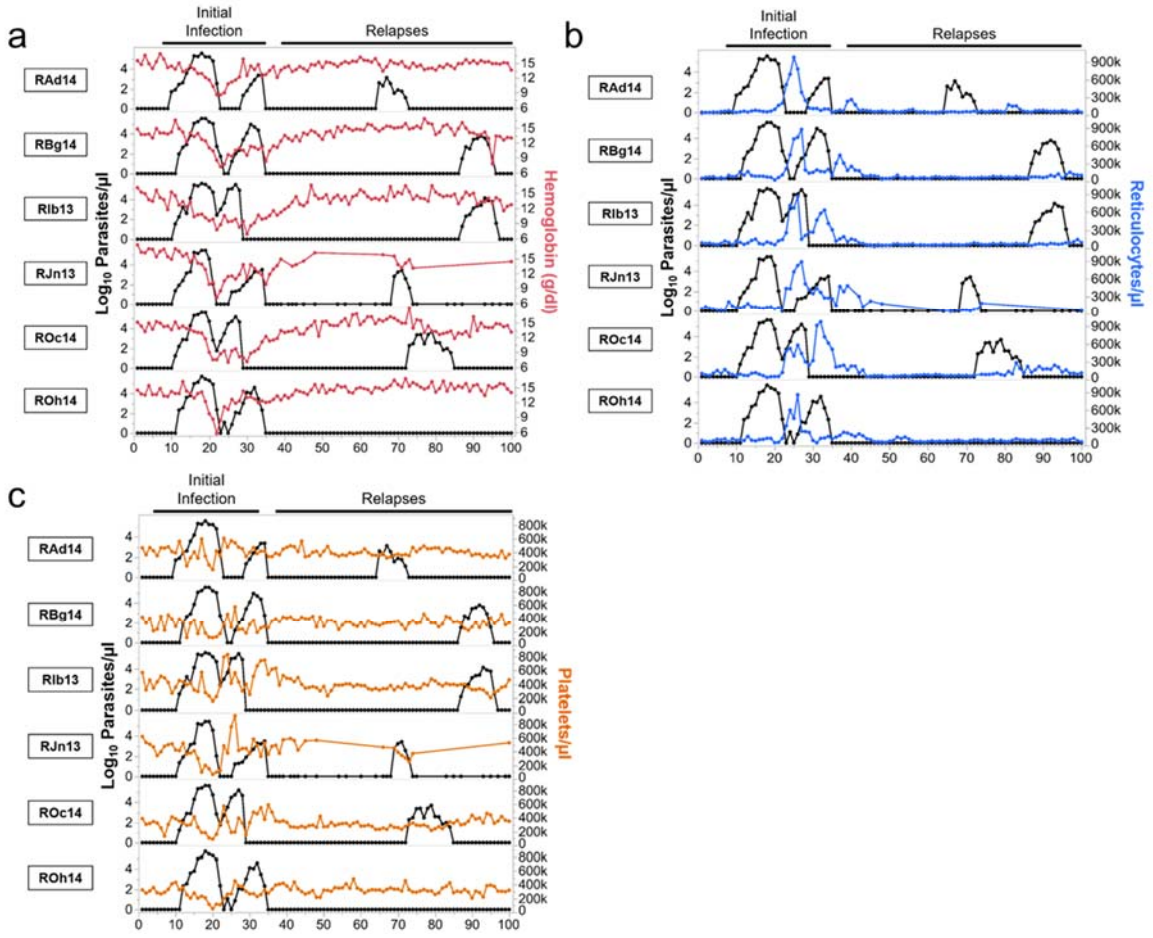

Supplementary Figure 1. Hemoglobin, platelet, and reticulocyte kinetics with parasitemia during an initial and relapse *P. cynomolgi* infection. Daily hemoglobin levels (a), reticulocyte counts (b), and platelet numbers (c) during initial and relapse infections with *P. cynomolgi* B strain. The five letter code on the lefthand side of each graph indicates a different individual. k = multiple number by 1,000.

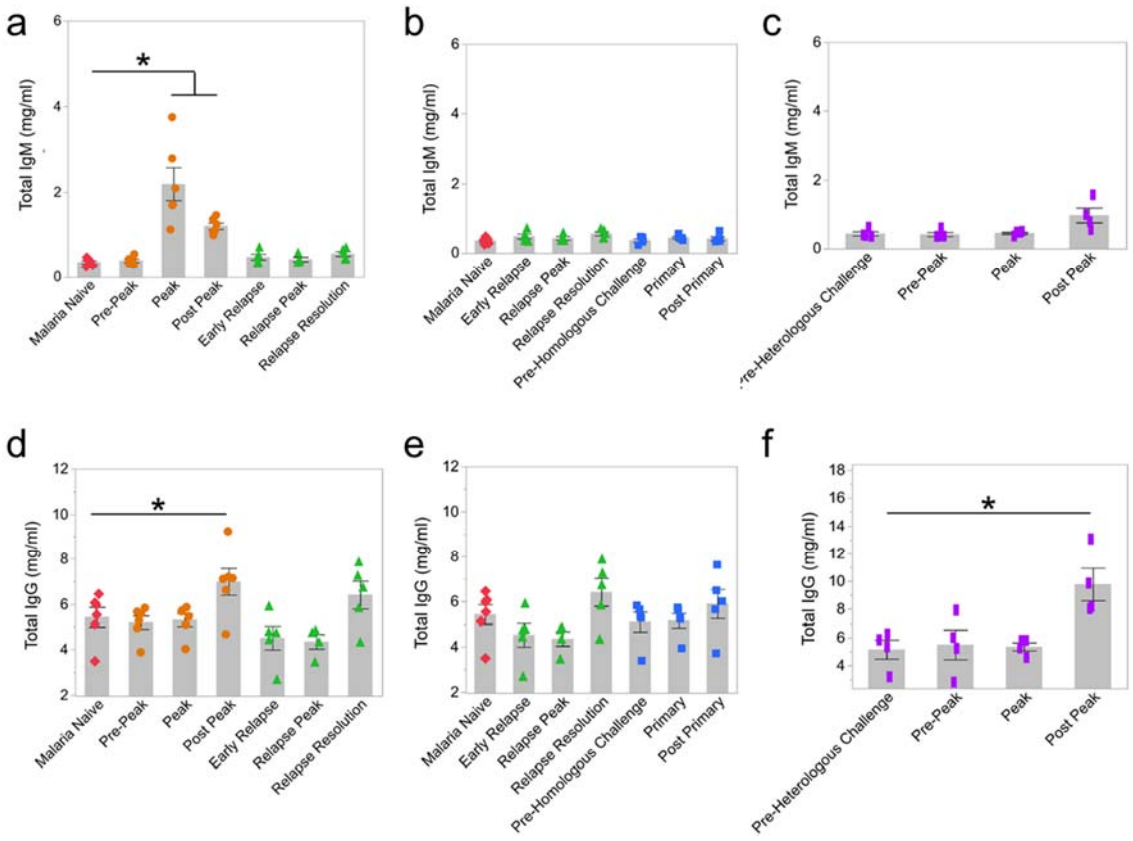

Supplementary Figure 2. Total IgM and IgG kinetics during initial infections, relapses, homologous reinfections, and heterologous infection in rhesus macaques infected with *P. cynomolgi*. (a-c) Total IgM concentrations during initial infections (a), relapses (a), homologous reinfections (b), and heterologous infections (c). (d-f) Total IgG concentrations during initial infections (d), relapses (d), homologous reinfections (e), and heterologous infections (f). For all panels, different infection stages are indicated by a symbol and color. Pink diamonds = malaria naïve, orange circles = infection points during initial infections, green triangles = infection points during relapses, blue squares = infection points during homologous reinfections, purple rectangles = infection points during heterologous reinfections. Statistical significance was assessed using a

linear mixed model with Tukey-Kramer post-hoc analysis. * = $p < 0.05$. Gray bars are the mean of the displayed data points; error bars = SEM.

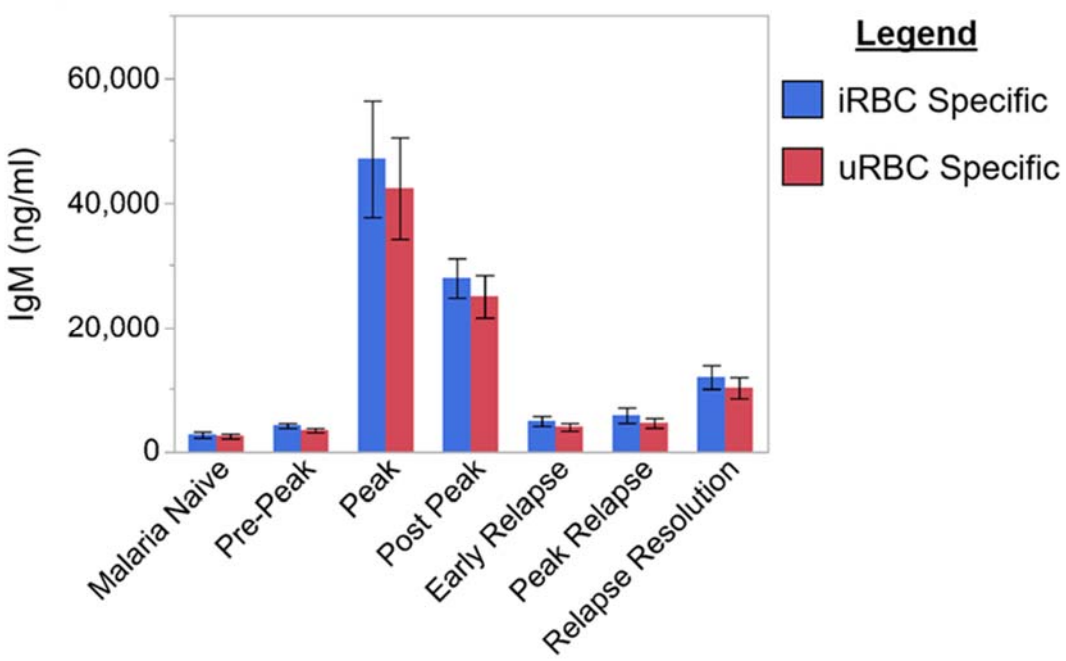

Supplementary Figure 3. IgM reactivity with uninfected and infected RBC lysates during initial infections and relapses. The mean concentration of IgM that reacts with uninfected and infected RBC during initial infections and relapses as measured by ELISA. Error bars = SEM.

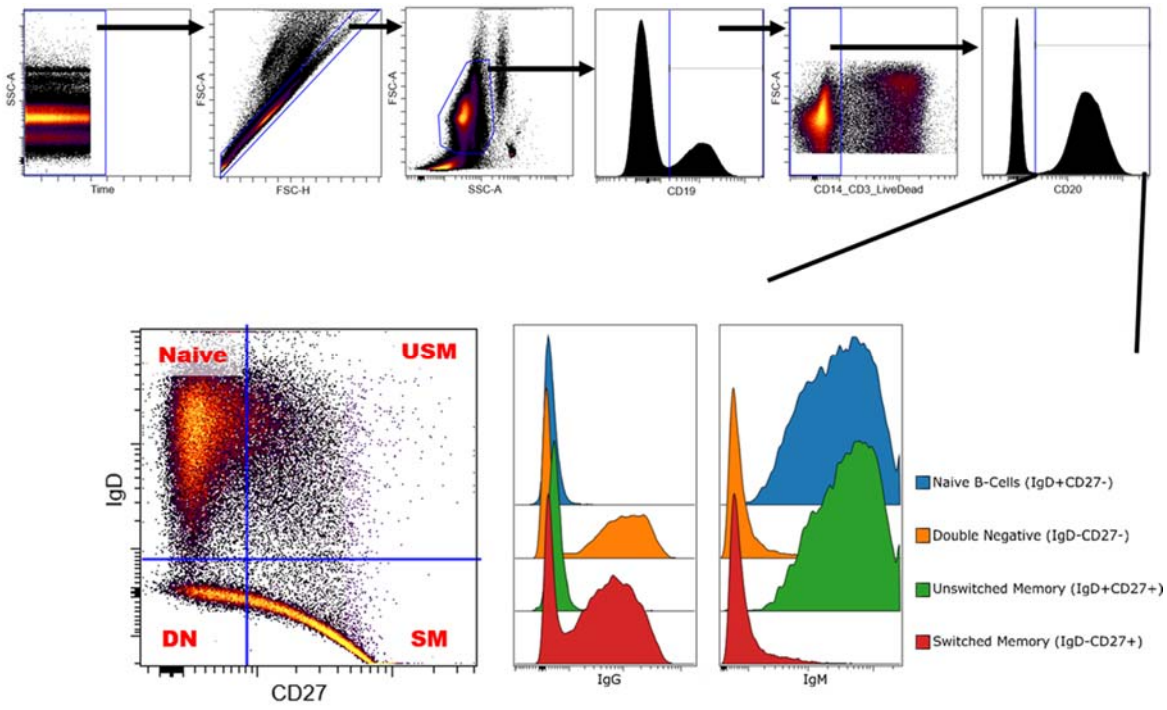

Supplementary Figure 4. Gating strategy and IgG/IgM surface profiles of four B-cell subsets in the peripheral blood of rhesus macaques. A representative flow cytometry plot for monitoring peripheral rhesus macaque B-cell subsets is shown. Histograms indicated different surface IgM and IgG profiles of the four different subsets being monitored. USM = Unswitched Memory, DN = Double-Negative, SM = Switched Memory.

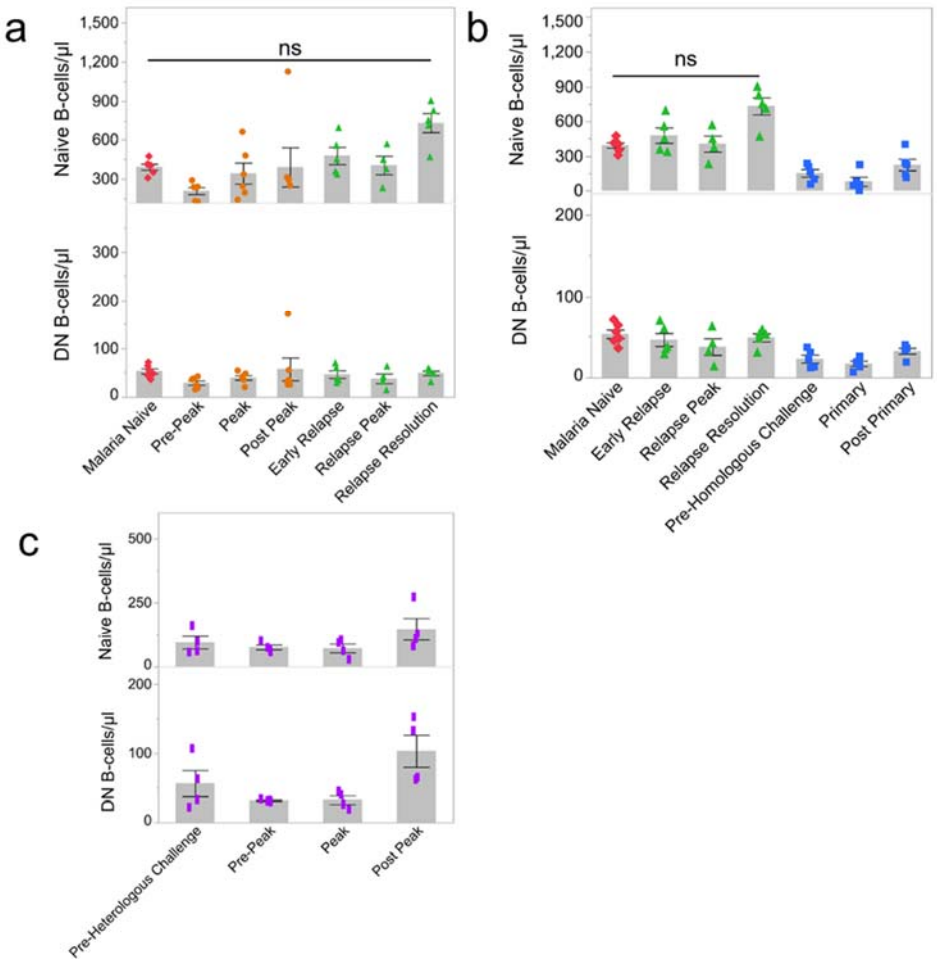

Supplementary Figure 5. Double-negative and naïve B-cell kinetics during an initial and relapse *P. cynomolgi* M/B strain infection. Absolute numbers of Naïve and DN B-cells are shown during initial inffections (a), relapses (a), homologous reinfections (b), and heterologous infections (c). Different infection stages are indicated by a symbol and color. Pink diamonds = malaria naïve, orange circles = infection points during initial infections, green triangles = infection points during relapses, blue squares = infection points during homologous reinfections, purple rectangles = infection points during heterologous reinfections. Statistical significance was assessed using a linear mixed model with Tukey-Kramer post-hoc analysis. Gray bars indicated the mean of the shown data points. Error bars = SEM.

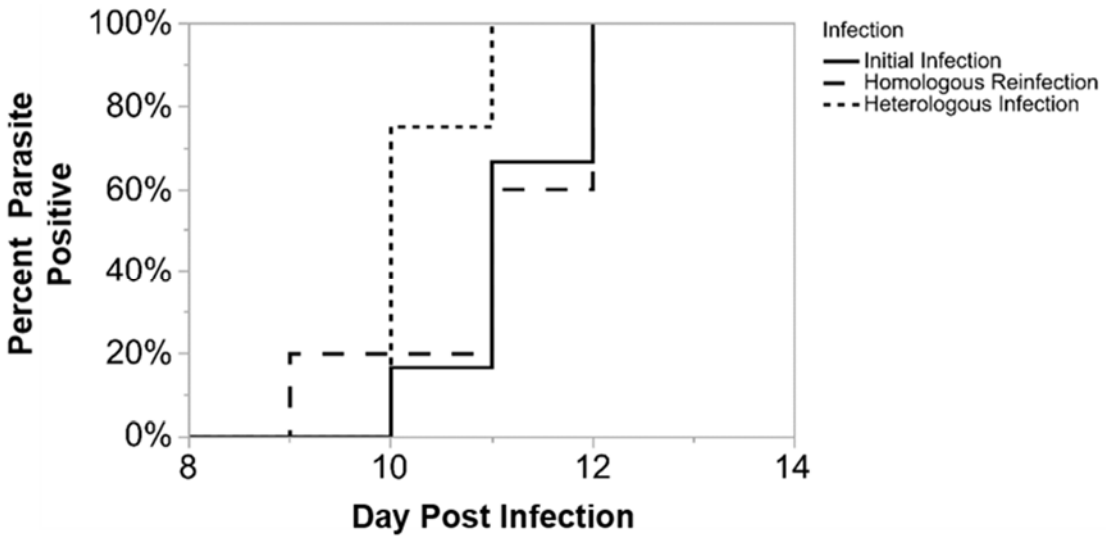

Supplementary Figure 6. Pre-existing immunity does not change day-to-patency during homologous or heterologous infections. The day to patency for the initial infection, homologous reinfection, and heterologous infection is shown. Statistical significance was assessed by a Wilcoxon test.

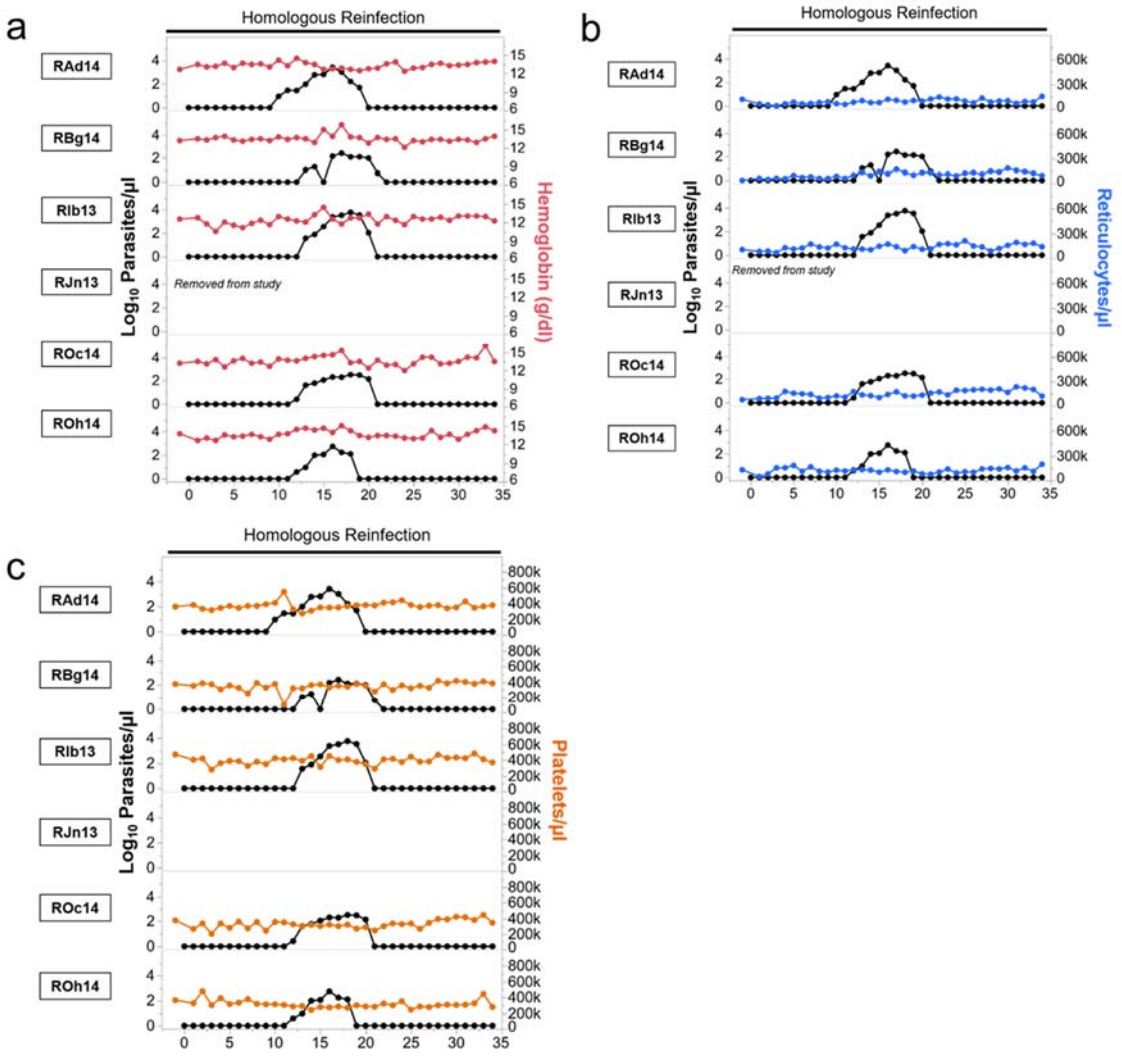

Supplementary Figure 7. Hemoglobin, platelet, and reticulocyte kinetics with parasitemia during homologous reinfection with *P. cynomolgi* B strain. Daily hemoglobin levels (a), reticulocyte counts (b), and platelet numbers (c) during a homologous reinfection with *P. cynomolgi* B strain are shown. The five letter code on the left-hand side of each graph indicates a different individual. k = multiple number by 1,000.

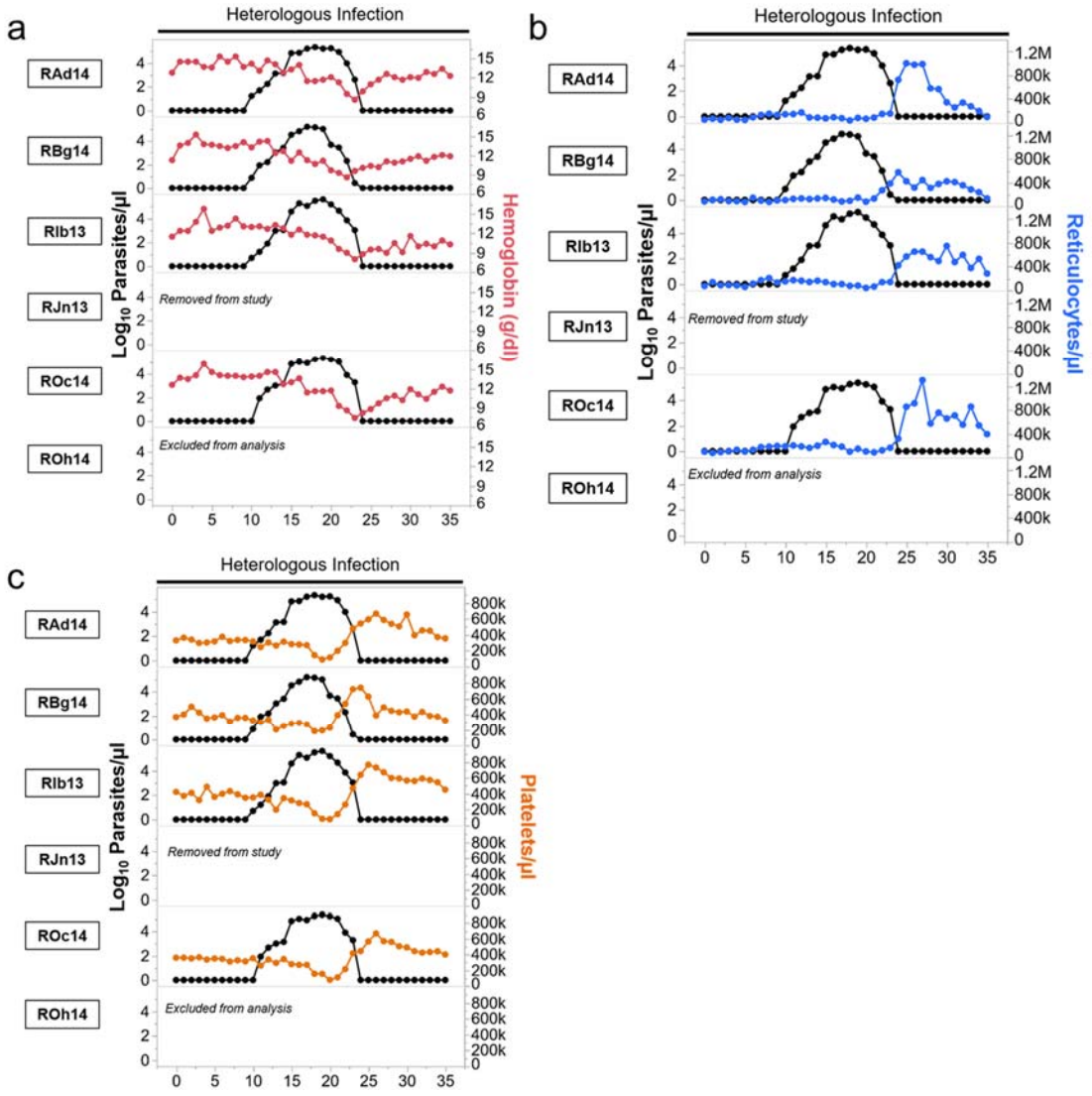

Supplementary Figure 8. Hemoglobin, platelet, and reticulocyte kinetics with parasitemia during heterologous infections with *P. cynomolgi* Ceylon. Daily hemoglobin levels (a), reticulocyte counts (b), and platelet numbers (c) during a heterologous infection is shown. The five letter code on the left-hand side of each graph indicates a different individual. k = multiple number by 1,000.

Table 1. B-cell phenotyping panel utilized for evaluating B-cell subset kinetics and surface immunoglobulin expression during initial and relapse infections.

Antibody	**Fluorophore**	**Clone**	**Company**
LiveDead Fixable Yellow	n/a	n/a	Life Technologies
CD14	BV605	M5E2	Biolegend
CD3	BV605	SP-34-2	BD
CD20	BV650	2H7	Biolegend
IgM	Alexa488	2020-30	Southern Biotech
CD138	PerCP-Cy5.5	M115	BD
IgD	PE	2030-02	Southern Biotech
CD21	PE-CF594	B-LY4	BD
CD27	PE-Cy7	M-T271	Biolegend
IgG	Alexa647	4700-31	Southern Biotech
CD19	APC-Alexa700	J3-119	Beckman Coulter
CD45	APC-Cy7	D058-1283	BD
PD1	BV421	EH12.1	BD

Table 2. B-cell phenotyping panel utilized for evaluating B-cell subset kinetics and intracellular markers during initial and relapse infections.

Antibody	**Fluorophore**	**Clone**	**Company**
LiveDead Fixable Yellow	n/a	n/a	Life Technologies
CD14	BV605	M5E2	Biolegend
CD3	BV605	SP-34-2	BD
CD20	BV650	2H7	Biolegend
CD38	FITC	AT-1	Stem Cell Technologies
CD138	PerCP-Cy5.5	M115	BD
IgD	PE	2030-02	Southern Biotech
CD21	PE-CF94	B-LY4	BD
CD27	PE-Cy7	M-T271	BD
CD19	APC-Alexa700	J3-119	Beckman Coulter
CD45	APC-Cy7	D058-1283	BD
KI67	BV421	B56	BD
Caspase-3	Alexa647	C92-605	BD

Table 3. B-cell phenotyping panel utilized for evaluating B-cell subset kinetics and surface immunoglobulin expression during homologous reinfections and heterologous infections.

Antibody	**Fluorophore**	**Clone**	**Company**
LiveDead Fixable Yellow	n/a	n/a	Life Technologies
CD14	Pac Blue	M5E2	BD
CD20	BV650	2H7	Biolegend
IgM	Alexa488	2020-30	Southern Biotech
CD3	PerCP-Cy5.5	SP-34-2	BD
IgD	PE	2030-02	Southern Biotech
CD21	PE-CF594	B-LY4	BD
CD27	PE-Cy7	M-T271	Biolegend
CD19	APC-Alexa700	J3-119	Beckman Coulter
CD45	APC-Cy7	D058-1283	BD
IgG	Alexa647	4700-31	Southern Biotech

Table 4. B-cell phenotyping panel utilized for evaluating B-cell subset kinetics and intracellular markers during homologous reinfections and heterologous infections.

Antibody	**Fluorophore**	**Clone**	**Company**
LiveDead Fixable Yellow	n/a	n/a	Life Technologies
CD14	BV605	M5E2	Biolegend
CD20	BV650	2H7	Biolegend
CD38	FITC	AT-1	Stem Cell Technologies
CD3	PerCp-Cy5.5	SP-34-2	BD
IgD	PE	2030-02	Southern Biotech
CD21	PE-CF594	B-LY4	BD
CD27	PE-Cy7	M-T271	BD
CD19	APC-Alexa700	J3-119	Beckman Coulter
CD45	APC-Cy7	D058-1283	BD
KI67	BV421	B56	BD
Caspase-3	Alexa647	C92-605	BD

References

1. Howes RE, Battle KE, Mendis KN, Smith DL, Cibulskis RE, Baird JK, et al. Global Epidemiology of *Plasmodium vivax*. Am J Trop Med Hyg 2016.
2. Bassat Q, Velarde M, Mueller I, Lin J, Leslie T, Wongsrichanalai C, et al. Key Knowledge Gaps for *Plasmodium vivax* Control and Elimination. Am J Trop Med Hyg 2016; 95:62-71.
3. Organization WH: *World Malaria Report 2016*.2016.
4. Krotoski WA, Collins WE, Bray RS, Garnham PC, Cogswell FB, Gwadz RW, et al. Demonstration of hypnozoites in sporozoite-transmitted *Plasmodium vivax* infection. Am J Trop Med Hyg 1982; 31:1291-1293.
5. Dembele L, Franetich JF, Lorthiois A, Gego A, Zeeman AM, Kocken CH, et al. Persistence and activation of malaria hypnozoites in long-term primary hepatocyte cultures. Nat Med 2014; 20:307-312.
6. White NJ, Imwong M. Relapse. Adv Parasitol 2012; 80:113-150.
7. Adekunle AI, Pinkevych M, McGready R, Luxemburger C, White LJ, Nosten F, et al. Modeling the Dynamics of *Plasmodium vivax* Infection and Hypnozoite Reactivation In Vivo. PLoS Negl Trop Dis 2015; 9:e0003595.
8. White MT, Karl S, Battle KE, Hay SI, Mueller I, Ghani AC. Modelling the contribution of the hypnozoite reservoir to *Plasmodium vivax* transmission. Elife 2014; 3.
9. Betuela I, Rosanas-Urgell A, Kiniboro B, Stanisic DI, Samol L, de Lazzari E, et al. Relapses contribute significantly to the risk of *Plasmodium vivax* infection and disease in Papua New Guinean children 1-5 years of age. J Infect Dis 2012; 206:1771-1780.
10. Joyner C, Moreno A, Meyer EVS, Cabrera-Mora M, Kissinger JC, Barnwell JW, et al. *Plasmodium cynomolgi* infections in rhesus macaques display clinical and parasitological features pertinent to modelling vivax malaria pathology and relapse infections. Malaria Journal 2016; 15:1-18.
11. Berzins K, Wahlgren M, Perlmann P. Studies on the specificity of anti-erythrocyte antibodies in the serum of patients with malaria. Clinical and Experimental Immunology 1983; 54:313-318.
12. Mourao LC, Roma PM, Sultane Aboobacar Jda S, Medeiros CM, de Almeida ZB, Fontes CJ, et al. Anti-erythrocyte antibodies may contribute to anaemia in *Plasmodium vivax* malaria by decreasing red blood cell deformability and increasing erythrophagocytosis. Malar J 2016; 15:397.
13. Ravindran B, Satapathy AK, Das MK. Naturally-occurring anti-alpha-galactosyl antibodies in human *Plasmodium falciparum* infections--a possible role for autoantibodies in malaria. Immunol Lett 1988; 19:137-141.
14. Fernandez-Arias C, Rivera-Correa J, Gallego-Delgado J, Rudlaff R, Fernandez C, Roussel C, et al. Anti-Self Phosphatidylserine Antibodies Recognize Uninfected Erythrocytes Promoting Malarial Anemia. Cell Host Microbe 2016; 19:194-203.
15. Kaminski DA, Wei C, Qian Y, Rosenberg AF, Sanz I. Advances in human B cell phenotypic profiling. Front Immunol 2012; 3:302.
16. Schmidt LH. Compatibility of relapse patterns of *Plasmodium cynomolgi* infections in rhesus monkeys with continuous cyclical development and hypnozoite concepts of relapse. Am J Trop Med Hyg 1986; 35:1077-1099.
17. Ross A, Koepfli C, Schoepflin S, Timinao L, Siba P, Smith T, et al. The Incidence and Differential Seasonal Patterns of *Plasmodium vivax* Primary Infections and Relapses in a Cohort of Children in Papua New Guinea. PLOS Neglected Tropical Diseases 2016; 10:e0004582.

18. Arnott A, Barnadas C, Senn N, Siba P, Mueller I, Reeder JC, et al. High Genetic Diversity of *Plasmodium vivax* on the North Coast of Papua New Guinea. Am J Trop Med Hyg 2013.
19. Bruce MC, Galinski MR, Barnwell JW, Donnelly CA, Walmsley M, Alpers MP, et al. Genetic diversity and dynamics of *plasmodium falciparum* and *P. vivax* populations in multiply infected children with asymptomatic malaria infections in Papua New Guinea. Parasitology 2000; 121 (Pt 3):257-272.
20. de Souza AM, de Araujo FC, Fontes CJ, Carvalho LH, de Brito CF, de Sousa TN. Multiple-clone infections of *Plasmodium vivax*: definition of a panel of markers for molecular epidemiology. Malar J 2015; 14:330.
21. Neafsey DE, Galinsky K, Jiang RHY, Young L, Sykes SM, Saif S, et al. The malaria parasite *Plasmodium vivax* exhibits greater genetic diversity than Plasmodium falciparum. Nature genetics 2012; 44:1046-1050.
22. Imwong M, Snounou G, Pukrittayakamee S, Tanomsing N, Kim JR, Nandy A, et al. Relapses of *Plasmodium vivax* infection usually result from activation of heterologous hypnozoites. J Infect Dis 2007; 195:927-933.

Discussion

The *Plasmodium cynomolgi* – rhesus macaque model is an excellent animal model for vivax malaria

The rhesus macaque – *Plasmodium cynomolgi* model of vivax malaria has historically been utilized to circumvent the challenges of working with *P. vivax* directly. The main goals of these studies have been to utilize the model for hypnozoite drug discovery, basic parasite biology, and testing malaria vaccine candidates [1-5]. It is unclear why this model was never developed in-depth for immunological or pathogenesis-related experiments, given its ability to recapitulate key aspects of *P. vivax* infections like relapses [6-8]. The scarcity of information on the host response during infection has likely played a role, however, and such characterizations, albeit largely descriptive, are critical before targeted, hypothesis-driven experiment can be performed. The studies presented in this dissertation have provided the most comprehensive characterization of the host response during *P. cynomolgi* infection of rhesus macaques and provide to date and provide clear evidence of the relevance of this model for *P. vivax* research.

An initial focus of the studies carried out in this dissertation was to characterize clinical aspects of disease caused by *P. cynomolgi* and, thus, *P. vivax*. This led to a main focus on the development of anemia in the rhesus – *P. cynomolgi* model to compare and contrast these dynamics with malarial anemia caused by *P. vivax* infections in patients [9]. In Chapters 2 and 5, daily hematological measurements composed of complete blood count analysis, reticulocyte enumeration, etc., were determined and described. Similar to studies on *P. vivax* in humans, the data indicated that insufficient erythropoiesis occurs during acute infection and coincides with the initial decline in hemoglobin levels [10]. After the acute phase of the infection, bone marrow function is restored. Despite the restoration of compensatory erythropoiesis by the bone marrow, hemoglobin levels continue to decrease. Indeed, malaria chemotherapy patients infected with *P. vivax* had similar hemoglobin kinetics during infection as was observed here, suggesting that

similar pathophysiological mechanisms are involved between the two species [11]. Future studies should aim to investigate the processes that contribute to anemia after bone marrow function is restored since it is clear that RBCs lost to parasitism are not able to account for the continuing decrease in hemoglobin levels in this model or in individuals infected with *P. vivax* [11].

The development of thrombocytopenia was also examined for comparison of pathogenesis with this model and vivax malaria in humans. Similar to previous reports with *P. vivax*, thrombocytopenia, defined as a platelet count of ≤ 150,000 per microliter of blood, developed in all animals during the acute infection of an initial or heterologous infection. Interestingly, thrombocytopenia did not seem to correlate with disease severity since all animals developed this condition irrespective of their clinical presentation described in Chapter 3. Thus, it does not appear that thrombocytopenia is predictive of the development of severe disease, but it may be useful to consider in tandem with other clinical criteria such as anemia. A similar conclusion has been reached based on patient outcomes in individuals infected with *P. falciparum* [12]. One of the most intriguing findings, and relatively novel discoveries related to thrombocytopenia to emerge here is that platelet levels increase whenever compensatory erythropoiesis is restored after an acute infection. This results suggests that platelet production may be compromised and contribute to the overall decrease in platelet numbers in addition to other reported mechanisms such as platelet phagocytosis [13]. Due to the cross-sectional nature of most *P. vivax* pathogenesis studies, to our knowledge, this phenomenon has not been noted previously. Indeed, dysplastic megakaryocytes have been reported in the marrow of individuals who have succumbed to *P. vivax* infection, suggesting that megakaryocyte function may be compromised during vivax malaria, as observed here [10, 14].

The first comprehensive histopathological study on a rhesus macaque that succumbed to cynomolgi malaria was performed here and reported in Chapter 2. Previous studies have mentioned that macaques infected with *P. cynomolgi* can succumb to infection, but no formal assessment of

the tissues after such an event had been published. Thus, the need to sacrifice this animal due to clinical complications provided a unique opportunity to further demonstrate the relevance of this model to vivax malaria in humans. The histopathology of the euthanized animal was strikingly similar to autopsy studies of individuals that were infected with *P. vivax* at time of death [10, 14, 15]. For example, there were dysplastic megakaryocytes and expansion of the erythroid lineage in the bone marrow as well as evidence of lung complications, which is common during *P. vivax* infections [15-17]. Ultimately, the histopathology demonstrated that acute tubular necrosis was responsible for the animal's irreversible kidney failure, and these lesions have also been linked to vivax malaria [18-20].

Overall, the studies and data presented in this dissertation provide the most comprehensive characterization and validation of the *P. cynomolgi* – rhesus macaque model as a robust model of *P. vivax* malaria to date, with in-depth inquiry into the host response during infection. Combining the information related to pathogenesis obtained here with the previous literature on the similarities between *P. cynomolgi* and *P. vivax* biology and genetics demonstrate the clear relevance of this model for *P. vivax* research [6]. Future studies can benefit from the comprehensive data that has been collected here and move research on vivax malaria pathogenesis and immunological research forward.

Inflammation and disruption of GATA1/GATA2 transcriptional programs contribute to inefficient erythropoiesis during acute cynomolgi malaria in macaques

One of the most common complications of vivax malaria is anemia, and severe malarial anemia characterizes a large proportion of severe vivax malaria cases, especially in infants [21]. In addition to severe disease, anemia caused by *P. vivax* also has negative socioeconomic impacts in endemic areas such as cognitive impairment [22]. These factors make understanding the processes underlying vivax malaria anemia imperative, but understanding the mechanisms that contribute to the development of anemia has been difficult from cross-sectional studies relying on patient samples and rodent models that have different erythropoietic processes than primates [23, 24].

The hematological data collected during the *P. cynomolgi* infections demonstrated that there was significant overlap of the vivax malarial anemia in patients and cynomolgi malaria anemia in macaques. One of the phenotypes that was of particular interest for further investigation using this model was the evidence for inadequate erythropoiesis during acute infection despite increased levels of erythropoietin. This phenomenon has been reported previously with *P. vivax* infected individuals and thought to be a critical mediator of malarial anemia in patients [10]. Thus, as reported in Chapter 3, RNA-Seq, flow cytometry, and multiplex cytokine assays were performed on bone marrow aspirates collected longitudinally during the infection and a series of analyses conducted to determine the changes in the bone marrow that may influence inefficient erythropoiesis during acute malaria.

Acute malaria induced significant changes in the bone marrow transcriptome. These changes were largely related to ongoing inflammatory responses that were largely dominated by a Type I and Type II interferon signature although other pathways such as IL-10 and IL-27 were also enriched in the bone marrow at that time. Thus, it appeared that inflammation in the bone marrow was potentially responsible for the lack of compensatory erythropoiesis, and indeed, inflammation is known to cause anemia in a variety of other diseases [25]. Further experimentation suggested

that IFNγ was central to this process since other cytokines such as IFNα were not upregulated on the protein levels. IFNγ levels were inversely correlated with hemoglobin levels and the percentage of erythroid progenitors in bone marrow, and this cytokine has also been demonstrated to inhibit erythropoiesis *in vitro* and be involved in disruption of erythropoiesis in rodent malaria models [26-28]. Therefore, it appeared that IFNγ, which is required for parasite control, was also mediating the disruption of erythropoiesis during acute malaria in macaques infected with *P. cynomolgi*.

Although a role for Type I IFNs for suppressing erythropoiesis was not clear from the current studies, these molecules should not be discounted. One explanation for why Type I IFN gene signatures were present, but we could not confirm this with transcriptional or protein data, could be due to timing. Type I IFNs are tightly regulated on a transcriptional and translational level, and thus, these molecules could initiate the suppression of erythropoiesis between days 12-16 during the blood-stage infection. Indeed, reticulocyte kinetics would suggest that some event occurs during this period that suppresses the compensatory response of the bone marrow. Future studies should acquire samples earlier to evaluate if these proteins can be identified in the plasma and/or if they are involved, especially since these molecules can suppress erythropoiesis in response to erythropoietin *in vitro* [29].

The leukocyte subsets that are responsible for disrupting the bone marrow during malaria are poorly characterized; thus, these studies aimed to improve our understanding of what cell types were involved in the inflammation *in vivo* by integrating flow cytometry and transcriptome data collected from the same samples using Weighted Gene Coexpression Network Analysis (WGCNA) [30]. Interestingly, the analysis demonstrated that intermediate and non-classical monocytes were potentially involved in the disruption of erythropoiesis in the marrow during acute infection. The involvement of monocytes in suppressing erythropoiesis *in vitro* via the production of inflammatory cytokines after stimulation with infected RBCs has been reported previously [31,

32]. However, there has been little information available on the subsets of monocytes that may mediate such inhibition *in vivo*.

The identification of these monocyte subsets as potentially mediating this effect was unexpected since these monocyte subsets are not classically "pro-inflammatory". Perhaps, malaria induces these subsets to produce cytokines that they have not classically been associated with. Importantly, it should be noted that non-classical and intermediate monocytes are critical for the control of parasitemia, and thus, it is interesting to speculate that these cells may control parasite growth but contribute to anemia by producing cytokines that affect erythropoiesis [33, 34]. Future studies should closely examine monocytes isolated from the blood and bone marrow of rhesus macaques infected with *P. cynomolgi* to understand their propensity to produce cytokines locally or systemically that may influence bone marrow suppression.

The molecular mechanisms that underlie the disruption of compensatory erythropoiesis during malaria are poorly understood. It is clear from the study presented in Chapter 4 in addition to studies in humans, NHPs and rodents that this is not due to the lack of erythropoietin production [35-37]. Instead, it appears that the erythropoiesis is potentially suppressed in the marrow during acute malaria, perhaps by ongoing local or systemic inflammatory responses. Using the transcriptomics and flow cytometry data, this study identified that the function of two master regulators of erythropoiesis, GATA1 and GATA2, were potentially disrupted during acute malaria [38, 39]. Interestingly, a previous study in rodent malaria models also arrived at a similar conclusion although the transcriptional levels were downregulated in that study [40]. Here, the gene expression of GATA1 and GATA2 was not changed during acute infection. Instead, the genes that were regulated by these two proteins were downregulated during acute infection, which suggests that the function of these proteins is modified during acute malaria. Indeed, previous studies have demonstrated that some of the inflammatory molecules identified here that were correlated with the decrease in erythroid progenitors can antagonize GATA1 [41]. The most notable example

would be IFNγ, which has been demonstrated to antagonize the function of GATA1, and was also identified in our analysis as being a potential key mediator of inflammation in the marrow.

The study of the bone marrow in rhesus macaques infected with *P. cynomolgi* suggests that monocyte-driven inflammation caused by IFNγ is responsible for disrupting compensatory erythropoiesis during acute malaria via disruption of GATA1/GATA2 transcriptional networks. Indeed, such findings are supported by studies utilizing rodent malaria models [28, 40]. Future studies should isolate the erythroid progenitors directly and better understand the factors that may be antagonizing GATA1/GATA2 since these could serve as targets of new interventions to serve as adjunctive therapies with malarial anemia. However if molecules such as Type I and Type II IFNs are involved, it may be difficult to rectify the disruption using immunotherapies or small molecules since both of these proteins are imperative for parasite control during malaria. Nonetheless, this study provides a clear pathway forward with a validated model of *P. vivax* malaria for studying the effects of malaria on the bone marrow and erythropoiesis.

Heterologous infections, and not relapses, may be responsible for clinical disease in endemic areas

Initially, based on the literature and rising concerns about relapses being the cause of millions of cases of vivax malaria illness, it was anticipated that relapses would result in clinical attacks in the rhesus infected with *P. cynomolgi* [42-44]. Surprisingly, the data in Chapters 2 and 5 clearly demonstrate that relapses do not necessarily result in illness, and in fact, the macaques infected with *P. cynomolgi* were able to control and suppress relapse infections without intervention. These results called into question if relapses are responsible for significant disease in endemic areas.

Most of the studies that have concluded that relapses cause significant disease and morbidity in *P. vivax* endemic areas have notable caveats when examined closely. Perhaps the most crippling is a sampling bias to individuals that seek medical attention. This strategy for collecting human samples, albeit more practical and less expensive than longitudinal sampling, has biased the literature to studies on symptomatic relapses. Thus, current interpretation on relapse pathogenesis must be assessed keeping this aspect in mind. The second caveat that is common is that much of the current conclusions regarding relapses are based off of epidemiological and mathematical modelling experiments of mass drug administration at a population level, or patient data [45, 46]. Although these studies are useful and undoubtedly informative for guiding future inquiry, they are not based on empirical evidence and inherently require assumptions that may be incorrect, which leads to the incorrect interpretation of available data. Overall, the relapse literature is biased to the biology of symptomatic relapses, and also modelling results, while carefully designed validation experiments have not been carried out.

The realization of the bias of the literature to symptomatic relapses and the evidence presented in these studies led to the question, “If relapses are not causing significant disease in endemic areas, then what is?” A longitudinal study was designed to assess this question in the

context of three distinct infection scenarios, namely initial infections, relapses, homologous reinfections, and heterologous infections. These experiments demonstrated that the lack of symptomology during a relapse was reproducible in the rhesus – *P. cynomolgi* model. Furthermore, there was also significant protection approximately 60 days after an animal was cured, suggesting that the clinical protection was able to persist in the short-term. A heterologous infection resulted in similar disease as an initial malaria infection in a naïve individual demonstrating the strain-specificity of the immunity that is suppressing the clinical attacks. Indeed, similar results for all of these infection scenarios have been previously reported in *P. vivax*, and thus, this pointing to the relevance and potential of the NHP animal model utilized here [47-50].

Combined with the historical malaria chemotherapy studies carried out with *P. vivax*, these experiments supported a model where infections with new parasite variants were potentially responsible for a larger portion of symptomatic *P. vivax* infections in endemic areas than previously appreciated. Such results have major implications for vivax elimination strategies. Recent studies have highlighted the significant biodiversity of *P. vivax* within an endemic area, and thus, it seems reasonable that an individual may encounter genetically distinct parasites frequently [51, 52]. Such evidence supports the findings from the experiments using this monkey model. Future studies should focus on understanding the different genes and proteins within different parasite variants that are critical for conferring strain-specific immunity. Such knowledge could pave the way for determining approaches to induce strain-transcending immune responses, which is difficult to achieve in both natural infection and vaccination scenarios. The rhesus – *P. cynomolgi* challenge model is well-suited for such undertakings, especially given a variety of diverse *P. cynomolgi* strains that have been characterized and stored for future research as cryopreserved stocks [53-55].

Although the data presented here suggests that relapses may not be as important for clinical vivax malaria as previously thought, much remains to be explored in the field with regards to relapse biology, clinical implications, pathogenesis and transmission. In particular, more work is

needed to examine the many different situations that may augment the pathogenesis of malaria relapses. Future endeavors using the rhesus - *P. cynomolgi* model could evaluate the effects of primary infection length, drug prophylaxis or treatment, clonality of relapses, and relapse periodicity on the pathogenesis of relapse infections. Indeed, there is suggestive evidence and conjectures that these factors may play a role in influencing vivax malaria disease severity and clinical presentations [8, 56]. Overall, the future is bright for understanding immunobiology and pathogenesis of vivax malaria and relapse infections, and the studies in this body of work provide a glimpse into the many different facets of relapse biology that remain incompletely understood.

Memory B-cells mediate clinical protection during relapses and homologous reinfections

The immunology of malaria relapses is virtually unstudied beyond measuring parasite burden [6, 57]. This gap in knowledge has been critical to fill since understanding the immune responses during relapses could provide insight into pathogenesis and aid vaccine development to limit and/or eliminate relapses. Such a vaccine would have major implications for vivax malaria control and ultimately eradication [58]. The lack of knowledge related to the immune response during relapses has been due to the difficulty of collecting '*bona fide*' relapse samples from endemic areas and not fully capitalizing on the rhesus – *P. cynomolgi* model of *P. vivax* infection. In the studies carried out in Chapters 2 and 5, these challenges were overcome, and it became apparent that the asymptomatic nature of relapses and homologous reinfections was due to a significant reduction in parasite burden. Thus, a major focus of this work became to understand the immune responses that may be critical for suppressing parasitemia and, thus, preventing the development of disease.

Humoral immunity is critical for mediating anti-parasite and anti-disease immunity during both *P. falciparum* and *P. vivax* infections [59-61]. In this work, the antibody and B-cell kinetics during relapses and homologous reinfections demonstrated that a memory B-cell response was responsible for conferring clinical immunity via the production of parasite-specific IgG. Importantly, the parasite-specific IgG titers waned quickly, typically within 60 days after a blood-stage infection, confirming that the immunity was predominantly mediated by a memory B-cell response versus a long-lived serological response mediated by plasma cells in the bone marrow. Similar results have been reported using samples collected from individuals that have been infected with *P. vivax* although these studies have not been able to assess if the B-cell memory that persists for up to 7 years was capable of conferring protection as demonstrated here [62].

The control of a relapse through a memory B-cell response after a single infection was not necessarily expected since the ability of *Plasmodium* infections to induce B-cell mediated

immunological memory has been controversial. Some investigations have concluded that such memory can form after infection whereas others have concluded that B-cells become dysfunctional, which prevents the establishment of effective B-cell memory [61-63]. In these studies, it was shown that clinically protective B-cell memory responses can form after a single blood-stage infection and can persist for up to 60 days. This is in direct contrast to previous literature that suggests the formation of protective B-cell memory does not form. Future studies using the rhesus – *P. cynomolgi* model should determine if this memory is able to persist longer than 60 days and assess its ability to provide protection upon subsequent challenges. Such studies when combined with the molecular analysis of antigen-specific B-cell subsets through the development of B-cell tetramers for *P. cynomolgi* would provide an unprecedented opportunity to better understand the development of humoral immunity against malaria parasites.

Although B-cell mediated immunological memory was formed and clinically protective, the established humoral immunity was unable to protect against a challenge with a heterologous *P. cynomolgi* strain. Indeed, strain-specific immunity has been previously noted for *P. vivax* infections [47]. This finding was critical because it provided an immunological basis for why heterologous infections resulted in disease whereas homologous relapses and reinfections did not. Future studies using this challenge model should aim to better understand the mechanisms that influence the strain-specificity of the immunity formed against malaria parasites, and this model is now poised for such investigations. Indeed, better understanding the strain-specificity of immunity against *Plasmodium* will be critical for malaria vaccines.

Future investigations should also evaluate the impact of a heterologous infection on the pre-existing clinically immunity against another strain. In an area with high endemicity, it would not be uncommon for individuals to routinely encounter the same or different parasite-variants, and thus, understanding how the pre-existing immunity against one parasites variant is impacted after being infected with a new variant is likely critical for understanding the development of strain-

transcending immunity. The challenge model developed here coupled with the availability of an multiple strains of *P. cynomolgi* make this model appropriate for addressing such questions in the future [53, 54]. Undoubtedly, the B-cell methods developed here for phenotyping rhesus macaque B-cells will also be useful when coupled with next generation sequencing technology to understand the clonality of the response and how the memory B-cell response is matured over time with each subsequent infection. Although the efforts outlined in this paper would support a model where a memory B-cell response is matured to recognize parasite proteins of both strains, this question remains to be directly addressed but would have significant impact on understanding the development and maintenance of B-cell mediated immunity against *Plasmodium*.

Overall, these studies have demonstrated the importance of humoral immunity in providing clinical immunity during relapses and homologous reinfections and have also provided an immunological basis for observations made almost 80 years ago in individuals undergoing malaria chemotherapy with *P. vivax* [64, 65]. Furthermore, these data emphasize that an effective vaccination strategy to reduce morbidity against *P. vivax* would have to induce strain-transcending humoral immunity, particularly when considering that most blood-stage infections multi-clonal. Indeed, the evidence provided here suggests that achieving such goals is possible at least in places where relapses and reinfections occur within 60 days. Future work should continue to dissect B-cell responses using the developed rhesus macaque – *P. cynomolgi* challenge model system.

Summary

The studies carried out in this dissertation have informed the current understanding of the immunology and pathogenesis of acute and relapsing vivax malaria using the rhesus macaque – *P. cynomolgi* model of *P. vivax* infection. The wealth of data generated here will help to guide future hypothesis-driven studies and should allow for the utilization of this model with greater ease. This comes with the benefit of all Standard Operating Procedures and data sets being released to the public by the MaHPIC. This NHP model can help to address the many outstanding questions related to relapses and malaria immunology to inform *P. vivax* epidemiology, vaccine development, drug discovery, diagnostics, and control strategies to ultimately lead to improved control and elimination programs. In conclusion, this body of work can serve as the foundation to continue to answer burning questions at the forefront of *P. vivax* research.

References

1. Galinski MR, Barnwell JW: Non-human Primate Models for Human Malaria Research. In *Nonhuman Primates in Biomedical Research: Diseases.* Elsevier, Inc.; 2012: 299-323
2. Deye GA, Gettayacamin M, Hansukjariya P, Im-erbsin R, Sattabongkot J, Rothstein Y, et al. Use of a rhesus *Plasmodium cynomolgi* model to screen for anti-hypnozoite activity of pharmaceutical substances. Am J Trop Med Hyg 2012; 86:931-935.
3. Akinyi S, Hanssen E, Meyer EV, Jiang J, Korir CC, Singh B, et al. A 95 kDa protein of *Plasmodium vivax* and *P. cynomolgi* visualized by three-dimensional tomography in the caveola-vesicle complexes (Schuffner's dots) of infected erythrocytes is a member of the PHIST family. Mol Microbiol 2012; 84:816-831.
4. Tachibana S, Sullivan SA, Kawai S, Nakamura S, Kim HR, Goto N, et al. *Plasmodium cynomolgi* genome sequences provide insight into *Plasmodium vivax* and the monkey malaria clade. Nat Genet 2012; 44:1051-1055.
5. Wijayalath W, Cheesman S, Tanabe K, Handunnetti S, Carter R, Pathirana S. Strain-specific protective effect of the immunity induced by live malarial sporozoites under chloroquine cover. PLoS One 2012; 7:e45861.
6. Coatney GR, Collins, W.E., Warren M., Contacos, P.G.: *Primate Malarias.* Washington DC: U. S. Dept. of Health, Education and Welfare; 1971.
7. Krotoski WA, Garnham PC, Bray RS, Krotoski DM, Killick-Kendrick R, Draper CC, et al. Observations on early and late post-sporozoite tissue stages in primate malaria. I. Discovery of a new latent form of *Plasmodium cynomolgi* (the hypnozoite), and failure to detect hepatic forms within the first 24 hours after infection. Am J Trop Med Hyg 1982; 31:24-35.
8. White NJ. Why do some primate malarias relapse? Trends Parasitol 2016.
9. Douglas NM, Anstey NM, Buffet PA, Poespoprodjo JR, Yeo TW, White NJ, et al. The anaemia of *Plasmodium vivax* malaria. Malaria Journal 2012; 11:1-14.
10. Wickramasinghe SN, Looareesuwan S, Nagachinta B, White NJ. Dyserythropoiesis and ineffective erythropoiesis in *Plasmodium vivax* malaria. Br J Haematol 1989; 72:91-99.
11. Collins WE, Jeffery GM, Roberts JM. A retrospective examination of reinfection of humans with *Plasmodium vivax*. Am J Trop Med Hyg 2004; 70.
12. Hanson J, Phu NH, Hasan MU, Charunwatthana P, Plewes K, Maude RJ, et al. The clinical implications of thrombocytopenia in adults with severe falciparum malaria: a retrospective analysis. BMC Med 2015; 13:97.
13. Coelho HC, Lopes SC, Pimentel JP, Nogueira PA, Costa FT, Siqueira AM, et al. Thrombocytopenia in *Plasmodium vivax* Malaria Is Related to Platelets Phagocytosis. PLoS One 2013; 8:e63410.
14. Wickramasinghe SN, Abdalla SH. Blood and bone marrow changes in malaria. Baillieres Best Pract Res Clin Haematol 2000; 13:277-299.
15. Lacerda MV, Fragoso SC, Alecrim MG, Alexandre MA, Magalhaes BM, Siqueira AM, et al. Postmortem characterization of patients with clinical diagnosis of *Plasmodium vivax* malaria: to what extent does this parasite kill? Clin Infect Dis 2012; 55:e67-74.
16. Anstey NM, Russell B, Yeo TW, Price RN. The pathophysiology of vivax malaria. Trends Parasitol 2009; 25.
17. Anstey NM, Handojo T, Pain MCF, Kenangalem E, Tjitra E, Price RN, et al. Lung injury in vivax malaria: pathophysiological evidence for pulmonary vascular sequestration and posttreatment alveolar-capillary inflammation. J Infect Dis 2007; 195.
18. Nayak KC, Kumar S, Gupta BK, Kumar S, Gupta A, Prakash P, et al. Clinical and histopathological profile of acute renal failure caused by falciparum and vivax

monoinfection: an observational study from Bikaner, northwest zone of Rajasthan, India. J Vector Borne Dis 2014; 51:40-46.
19. Shukla VS, Singh RG, Rathore SS, Usha. Outcome of malaria-associated acute kidney injury: a prospective study from a single center. Ren Fail 2013; 35:801-805.
20. Kute VB, Vanikar AV, Ghuge PP, Goswami JG, Patel MP, Patel HV, et al. Renal cortical necrosis and acute kidney injury associated with *Plasmodium vivax*: a neglected human malaria parasite. Parasitol Res 2012; 111:2213-2216.
21. Kenangalem E, Karyana M, Burdarm L, Yeung S, Simpson JA, Tjitra E, et al. *Plasmodium vivax* infection: a major determinant of severe anaemia in infancy. Malaria Journal 2016; 15:321.
22. Douglas NM, Anstey NM, Buffet PA, Poespoprodjo JR, Yeo TW, White NJ, et al. The anaemia of *Plasmodium vivax* malaria. Malar J 2012; 11:135.
23. Pishesha N, Thiru P, Shi J, Eng JC, Sankaran VG, Lodish HF. Transcriptional divergence and conservation of human and mouse erythropoiesis. Proceedings of the National Academy of Sciences of the United States of America 2014; 111:4103-4108.
24. An X, Schulz VP, Mohandas N, Gallagher PG. Human and murine erythropoiesis. Curr Opin Hematol 2015; 22:206-211.
25. Fraenkel PG. Anemia of Inflammation: A Review. Med Clin North Am 2017; 101:285-296.
26. Mamus SW, Beck-Schroeder S, Zanjani ED. Suppression of normal human erythropoiesis by gamma interferon in vitro. Role of monocytes and T lymphocytes. Journal of Clinical Investigation 1985; 75:1496-1503.
27. Means RT, Jr., Krantz SB. Inhibition of human erythroid colony-forming units by gamma interferon can be corrected by recombinant human erythropoietin. Blood 1991; 78:2564-2567.
28. Thawani N, Tam M, Stevenson MM. STAT6-mediated suppression of erythropoiesis in an experimental model of malarial anemia. Haematologica 2009; 94:195-204.
29. Means RT, Jr., Krantz SB. Inhibition of human erythroid colony-forming units by interferons alpha and beta: differing mechanisms despite shared receptor. Exp Hematol 1996; 24:204-208.
30. Langfelder P, Horvath S. WGCNA: an R package for weighted correlation network analysis. BMC Bioinformatics 2008; 9:559.
31. Pichyangkul S, Saengkrai P, Webster HK. *Plasmodium falciparum* pigment induces monocytes to release high levels of tumor necrosis factor-alpha and interleukin-1 beta. Am J Trop Med Hyg 1994; 51:430-435.
32. Perkins DJ, Were T, Davenport GC, Kempaiah P, Hittner JB, Ong'echa JM. Severe malarial anemia: innate immunity and pathogenesis. Int J Biol Sci 2011; 7:1427-1442.
33. Zhou J, Feng G, Beeson J, Hogarth PM, Rogerson SJ, Yan Y, et al. CD14(hi)CD16+ monocytes phagocytose antibody-opsonised *Plasmodium falciparum* infected erythrocytes more efficiently than other monocyte subsets, and require CD16 and complement to do so. BMC Med 2015; 13:154.
34. Hirako IC, Gallego-Marin C, Ataide MA, Andrade WA, Gravina H, Rocha BC, et al. DNA-Containing Immunocomplexes Promote Inflammasome Assembly and Release of Pyrogenic Cytokines by CD14+ CD16+ CD64high CD32low Inflammatory Monocytes from Malaria Patients. MBio 2015; 6:e01605-01615.
35. Chang KH, Stevenson MM. Malarial anaemia: mechanisms and implications of insufficient erythropoiesis during blood-stage malaria. Int J Parasitol 2004; 34:1501-1516.
36. Thawani N, Tam M, Bellemare MJ, Bohle DS, Olivier M, de Souza JB, et al. *Plasmodium* products contribute to severe malarial anemia by inhibiting erythropoietin-induced proliferation of erythroid precursors. J Infect Dis 2013.

37. Burchard GD, Radloff P, Philipps J, Nkeyi M, Knobloch J, Kremsner PG. Increased erythropoietin production in children with severe malarial anemia. Am J Trop Med Hyg 1995; 53:547-551.
38. Liang R, Ghaffari S. Advances in understanding the mechanisms of erythropoiesis in homeostasis and disease. Br J Haematol 2016; 174:661-673.
39. Moriguchi T, Yamamoto M. A regulatory network governing Gata1 and Gata2 gene transcription orchestrates erythroid lineage differentiation. Int J Hematol 2014; 100:417-424.
40. Sexton AC, Good RT, Hansen DS, Ombrain MCD, Buckingham L, Simpson K, et al. Transcriptional Profiling Reveals Suppressed Erythropoiesis, Up-Regulated Glycolysis, and Interferon-Associated Responses in Murine Malaria. The Journal of Infectious Diseases 2004; 189:1245-1256.
41. Bibikova E, Youn MY, Danilova N, Ono-Uruga Y, Konto-Ghiorghi Y, Ochoa R, et al. TNF-mediated inflammation represses GATA1 and activates p38 MAP kinase in RPS19-deficient hematopoietic progenitors. Blood 2014; 124:3791-3798.
42. Howes RE, Battle KE, Mendis KN, Smith DL, Cibulskis RE, Baird JK, et al. Global Epidemiology of *Plasmodium vivax*. Am J Trop Med Hyg 2016.
43. Bassat Q, Velarde M, Mueller I, Lin J, Leslie T, Wongsrichanalai C, et al. Key Knowledge Gaps for *Plasmodium vivax* Control and Elimination. Am J Trop Med Hyg 2016; 95:62-71.
44. Ingram RJH, Crenna-Darusallam C, Soebianto S, Noviyanti R, Baird JK. The clinical and public health problem of relapse despite primaquine therapy: case review of repeated relapses of *Plasmodium vivax* acquired in Papua New Guinea. Malar J 2014; 13.
45. Adekunle AI, Pinkevych M, McGready R, Luxemburger C, White LJ, Nosten F, et al. Modeling the Dynamics of *Plasmodium vivax* Infection and Hypnozoite Reactivation In Vivo. PLoS Negl Trop Dis 2015; 9:e0003595.
46. Betuela I, Rosanas-Urgell A, Kiniboro B, Stanisic DI, Samol L, de Lazzari E, et al. Relapses contribute significantly to the risk of *Plasmodium vivax* infection and disease in Papua New Guinean children 1-5 years of age. J Infect Dis 2012; 206:1771-1780.
47. Boyd MF. A review of studies on immunity to vivax malaria. J Natl Malar Soc 1947; 6.
48. Boyd MF. Criteria of immunity and susceptibility in naturally induced vivax malaria infections. Am J Trop Med 1942; s1-22.
49. Boyd MF, Matthews CB. Further observations on the duration of immunity to the homologous strain of *Plasmodium vivax*. Am J Trop Med Hyg 1939; 19.
50. Boyd MF, Kupper WH, Matthews CB. A deficient homologous immunity following simultaneous inoculation with two strains of *Plasmodium vivax*. Am J Trop Med 1938; s1-18.
51. Neafsey DE, Galinsky K, Jiang RHY, Young L, Sykes SM, Saif S, et al. The malaria parasite *Plasmodium vivax* exhibits greater genetic diversity than *Plasmodium falciparum*. Nat Genet 2012; 44:1046-1050.
52. Cui L, Escalante AA, Imwong M, Snounou G. The genetic diversity of *Plasmodium vivax* populations. Trends in Parasitology; 19:220-226.
53. Galinski MR, Arnot DE, Cochrane AH, Barnwell JW, Nussenzweig RS, Enea V. The circumsporozoite gene of the *Plasmodium cynomolgi* complex. Cell 1987; 48:311-319.
54. Galinski MR, Barnwell JW: Chapter 5 - Nonhuman Primate Models for Human Malaria Research. In *Nonhuman Primates in Biomedical Research (Second Edition)*. Edited by Morris CRAMT. Boston: Academic Press; 2012: 299-323
55. Joyner CJ, Barnwell JW, Galinski MR. No More Monkeying Around: Primate Malaria Model Systems are Key to Understanding *Plasmodium vivax* Liver-Stage Biology, Hypnozoites, and Relapses. Frontiers in Microbiology 2015; 6.

56. Mueller I, Schoepflin S, Smith TA, Benton KL, Bretscher MT, Lin E, et al. Force of infection is key to understanding the epidemiology of *Plasmodium falciparum* malaria in Papua New Guinean children. Proceedings of the National Academy of Sciences 2012; 109:10030-10035.
57. Schmidt LH. Compatibility of relapse patterns of *Plasmodium cynomolgi* infections in Rhesus monkeys with continuous cyclical development and hypnozoite concepts of relapse. Am J Trop Med Hyg 1986; 35.
58. White M, Amino R, Mueller I. Theoretical Implications of a Pre-Erythrocytic *Plasmodium vivax* Vaccine for Preventing Relapses. Trends in Parasitology; 33:260-263.
59. Boyle MJ, Reiling L, Osier FH, Fowkes FJI. Recent insights into humoral immunity targeting *Plasmodium falciparum* and *Plasmodium vivax* malaria. International Journal for Parasitology 2017; 47:99-104.
60. Cohen S, Mc GI, Carrington S. Gamma-globulin and acquired immunity to human malaria. Nature 1961; 192:733-737.
61. Portugal S, Pierce SK, Crompton PD. Young Lives Lost as B Cells Falter: What We're Learning about Antibody Responses in Malaria. Journal of immunology (Baltimore, Md : 1950) 2013; 190:3039-3046.
62. Wipasa J, Suphavilai C, Okell LC, Cook J, Corran PH, Thaikla K, et al. Long-lived antibody and B Cell memory responses to the human malaria parasites, *Plasmodium falciparum* and *Plasmodium vivax*. PLoS Pathog 2010; 6:e1000770.
63. Weiss GE, Crompton PD, Li S, Walsh LA, Moir S, Traore B, et al. Atypical memory B cells are greatly expanded in individuals living in a malaria-endemic area. J Immunol 2009; 183:2176-2182.
64. Boyd MF, Kitchen SF. On the efficiency of the homologous properties of acquired immunity to *Plasmodium vivax*. Am J Trop Med 1936; s1-16.
65. Boyd MF, Stratman-Thomas WK, Kitchen SF. On the duration of homologous immunity to *Plasmodium vivax*. Am J Trop Med 1936; 21.